Characterization of mercury (Hg) chemical species and biological ligands produced by phytoplankton

Javier García Calleja

THÈSE

UNIVERSITE DE PAU ET DES PAYS DE L'ADOUR

École doctorale des sciences exactes et de leurs applications

Présentée et soutenue le 1 juillet 2022

par Javier GARCÍA CALLEJA

pour obtenir le grade de docteur
de l'Université de Pau et des Pays de l'Adour
Spécialité : Chimie Analytique et de l´Environnement

CARACTÉRISATION DES FORMES CHIMIQUES DU MERCURE (Hg) ET DE LIGANDS BIOLOGIQUES PRODUITS PAR LE PHYTOPLANCTON

Characterization of mercury (Hg) chemical species and biological ligands produced by phytoplankton

MEMBRES DU JURY

RAPPORTEURS

• Claudia Cosio	Professeure / Université de Reims, France
• Erik Björn	Professeur / University of Umeå, Sweden
• Rosa C. Rodríguez Martín-Doimeadios	Professeure / University of Castilla-La Mancha, Spain

EXAMINATEURS

• Laurent Ouerdane	Maître de conférence / Université de Pau et des Pays de l´Adour
• Vera I. Slaveykova	Professeure / Université de Genève, Suisse

DIRECTEURS

• David Amouroux	Directeur de recherche CNRS / Université de Pau et des Pays de l´Adour
• Zoyne Pedrero Zayas	Chargée de recherche CNRS / Université de Pau et des Pays de l´Adour

UNIVERSITÉ DE PAU ET DES PAYS DE L'ADOUR

Characterization of mercury (Hg) chemical species and biological ligands produced by phytoplankton.

This doctoral work was performed in collaboration with three laboratories:

Institut des sciences analytiques et de physico-chimie pour l'environnement et les matériaux (IPREM)

UMR 5254, CNRS-Université de Pau et Pays de l'Adour, France

Département F.-A. Forel des sciences de l'environnement et de l'eau

Université de Genève, Suisse

Department of Physical and Analytical Chemistry, Faculty of Chemistry

University of Oviedo, Spain

Thanks to the financial and logistical support of:

Agence National de la Recherche (ANR) (Project ANR-17-CE34-0014) and the Swiss National Foundation (SNF) (Project N-175721) in the framework of PHYTAMBA project (PRCI ANR/SNSF)

Remerciements/ Acknowledgements

First of all, I would like to thank my director and co-director of thesis, David Amouroux and Zoyne Pedrero for your support, advices and patience, I really learnt a lot from both of you during these three years and half.

Zoyne, muchísimas gracias por haber confiado en mí desde el principio. Por tus consejos, por hacerme madurar como persona y como científico, por contagiarme tu alegría y sacarme una sonrisa en momentos claves de mi doctorado.

David, merci pour m'avoir appris toutes vos connaissances sur le mercure, merci pour vos critiques constructives, vos corrections et vos conseils. Science appart, vous m'avez fait évoluer en tant que chercheur et en tant que personne, vous m'avez rendu plus fort, plus indépendant et plus mature.

Un grand merci á Emmanuel Tessier, merci pour m´avoir appris à travailler avec le mercure, pour ta patience au début du doctorat et tes conseils.

Thank you, Vera, Joao, Thibaut and Isa for hosting me in Geneva, making feel comfortable since the very beginning and teaching me all your knowledge about phytoplankton microbial ecotoxicology. Particularly Joao, thanks for your support and our numerous talks about science and life. Working with you was an unforgettable experience!

Thank you Séverine Le Faucheur, Bahia Khalfaoui and Marisol Goni for teaching part of your knowledge in our small talks during my PhD. I appreciate it a lot! Merci Sylvain de m'avoir accueilli à Zurich. C'était une expérience très enrichissante.

I would also like to thank all my colleagues (those who left and those who are still there) at the IPREM: Khouloud, Sebastiano, Edith, MariAngels, Fran, Iago, Gema, Naomi, Oceane, Bastien, Jeremy, Thiago, Maricarmen, Lucile, Elaheh, Domenico, Diogo and Eleftheria. Especially Alina, Nang and Jinping, I really enjoyed our random scientific talks about whatever the topic (mercury biogeochemistry in oceans, role of DOM in freshwaters, iron speciation in anaerobic bacteria among others).

I had also the opportunity of meeting amazing people outside the IPREM these years such as the Erasmus crew (1st year of PhD): Sergio, Sergio Little, Andres, Elena, Maria, Julia, Mariana, Othman, Sara and Victor. Por nuestras noches en Conemara, barbacoas en el río, viajes a

Hossegor y Burdeos, partidillos de futbol y las bachas interminables en la cocina de la residencia.

During my second year of PhD, COVID-19 arrived but Miguel “el filósofo”, Victor “el brasileño”, Victor “el carbayón” and Markel made this period also special for me. Chavales, muchas gracias por nuestras tardes de cerveceo en el río, noches inolvidables por Pau, viajes a Santander, Biarritz, Saint-Malo. Charlotte merci aussi de nous avoir accueillis dans votre maison, le voyage en Bretagne a été l'un des plus beaux que j'ai fait dans ma vie.

También quería dar las gracias a Claudia, Yaidel, Rosana, Mikel y Silvia. Habéis sido un gran apoyo dentro y fuera del IPREM estos dos últimos años y me va a dar mucha pena despedirme de vosotros. Estos dos últimos meses he echado mucho de menos nuestras cervecitas en el Bondi, fiestas en Baracuba y cenas varias. Os tengo en muy alta estima.

Je voulais aussi remercier à mes colocataires de m'avoir soutenu pendant tout ce temps. Abder, Alice, Annabelle, Hypolite, Nico et, en particulier Donald. Merci beaucoup pour ton soutien mon ami.

Por último, quería agradecer a mis padres y a mi hermano todo el apoyo recibido durante este tiempo. Siempre habéis estado ahí en los buenos y en los malos momentos. Sois lo mejor que tengo en esta vida. Os quiero mucho.

Resumé

Les micro-organismes vivants (ex. phytoplancton, bactéries) dans les écosystèmes aquatiques sont fortement affectés par plusieurs polluants globaux tels que le mercure (Hg), par le biais des dépôts atmosphériques et des rejets directs des activités humaines. Contrairement aux travaux approfondis réalisés sur les bactéries méthylantes, le rôle du phytoplancton dans le cycle aquatique du Hg n'est pas bien documenté. Le phytoplancton représente le principal point d'entrée dans le réseau trophique aquatique, où la diversité et l'abondance des différents micro-organismes phytoplanctoniques (par exemple, les cyanobactéries, les diatomées, les algues vertes, entre autres) déterminent la bioaccumulation et la bioamplification potentielles du Hg dans la chaîne alimentaire. En outre, il est suggéré que le phytoplancton affecte directement (biotique) et/ou indirectement (abiotique) les transformations des composés du Hg, tels que le mercure inorganique (Hg(II), Hg(0)) et le méthylmercure (MeHg), par l'excrétion de bioligands ayant une forte affinité avec le Hg. Par conséquent, le phytoplancton devrait jouer un rôle important dans le cycle du Hg des environnements aquatiques. Les principaux objectifs de ce travail de doctorat sont : (1) le développement d'approches de chimie analytique utilisant les isotopes stables du Hg pour aborder les transformations potentielles des composés du Hg dans des expériences d'incubation biologique et (2) la caractérisation moléculaire des principaux bioligands impliqués dans la spéciation et le devenir du Hg dans le phytoplancton. Le premier objectif implique un développement méthodologique basé sur l'incubation de composés du Hg enrichis en isotopes (Hg(II) et MeHg) et une approche mathématique basée sur la déconvolution des signatures isotopiques. La méthodologie proposée a été appliquée avec succès pour la détermination des composés du Hg nouvellement formés pendant le processus d'incubation et des potentiels de transformation spécifiques aux composés dans différentes matrices environnementales telles que les biofilms, les sédiments et les eaux, mais aussi dans les cultures cellulaires de phytoplancton. Le deuxième objectif implique une procédure expérimentale basée sur le fractionnement des cellules de trois différents micro-organismes photosynthétiques modèles (*Synechocystis* sp. PCC 6803 ; *Cyclotella meneghiniana* ; *Chlamydomonas reinhardtii*). Ces expérimentations ont permis d'effectuer la caractérisation des principaux bioligands intracellulaires liant le Hg et impliqués dans la prise en charge intracellulaire du Hg en utilisant des techniques combinées basées sur la spectrométrie de masse élémentaire et moléculaire. Les informations combinées obtenues à partir de la quantification des composés de Hg dans les différentes fractions cellulaires et subcellulaires, les changements dans les fractions de taille moléculaire de Hg(II) et MeHg intracellulaires et l'identification des

bioligands spécifiques de faible poids moléculaire ont fourni des informations précieuses sur le rôle des espèces phytoplanctoniques étudiées, dans la spéciation du Hg et particulièrement dans la prise en charge intracellulaire du Hg. Les différents résultats obtenus permettent d'améliorer les approches expérimentales et analytiques pour étudier la compréhension des interactions Hg-phytoplancton, et de mieux comprendre le rôle spécifique de chaque espèce photosynthétique dans le devenir du Hg présent dans les milieux aquatiques.

Keywords : mercure, phytoplancton, déconvolution des signatures isotopiques, prise en charge intracellulaire du Hg.

Abstract

Living microorganisms (e.g phytoplankton, bacteria) in aquatic ecosystems are highly impacted by several worldwide pollutants such as mercury (Hg), through the atmospheric deposition and direct discharges of industrial wastes. Contrary to the extensive work carried out in methylating-bacteria, the role of phytoplankton in the aquatic Hg cycle is not well documented. Phytoplankton represents the main entry point in the aquatic food web where the diversity and abundance of different phytoplankton microorganisms (e.g., cyanobacteria, diatom, green algae among others) determine the potential Hg bioaccumulation and biomagnification through the trophic chain. Furthermore, phytoplankton is thought to affect directly (biotic) /or indirectly (abiotic) Hg compounds transformations (Hg(II), Hg(0) and MeHg) through the excretion of bioligands with strong Hg affinity. Therefore, phytoplankton is expected to have a relevant role in Hg cycle of aquatic environments. The main objectives of this doctoral work are: (1) the development of analytical approaches using isotopically enriched Hg isotopes to address the potential Hg compounds transformations in Hg incubation experiments, and (2) the molecular characterization of the major bioligands involved in Hg speciation in phytoplankton. The first objective involves a methodological development based on the incubation of isotopically enriched Hg compounds (Hg(II) and MeHg) and a mathematical approach based on the deconvolution of isotopic patterns. The proposed methodology have been successfully applied for the determination of newly-formed Hg compounds during the incubation process and compounds-specific transformations potentials in different environmental matrices such as biofilms, sediments and freshwaters but also, in phytoplankton cell cultures. The second objective involves an experimental procedure based on cells fractionation in three different model photosynthetic microorganisms (*Synechocystis* sp. PCC 6803; *Cyclotella meneghiniana* ; *Chlamydomonas reinhardtii*). This experimental approach allowed to the characterization of the major Hg binding intracellular bioligands involved in Hg intracellular handling using hyphenated techniques based on elemental and molecular mass spectrometry. The combined information obtained from the quantification of Hg compounds and localization in the different cellular and sub-cellular fractions, the changes in the intracellular size fractions containing Hg(II) and MeHg binding intracellular bioligands, and the identification of LMW bioligands provided valuable information about the role of three different model phytoplankton species in Hg speciation and particularly, Hg intracellular handling. The different results obtained allow improving the experimental and analytical approaches for studying Hg-phytoplankton

interactions and better understand the specific role of each photosynthetic microorganism in the Hg fate in aquatic environments.

Keywords: mercury, phytoplankton, isotope pattern deconvolution, Hg intracellular handling.

Table of contents.

List of Figures.

Chapter 1.

Chapter 2.

Annexes C.2

Chapter 3.

Annexes C.3.

List of Tables.

Chapter 1.

Chapter 2.

Annexes C.2.

Chapter 3.

Annexes C.3.

Chapter 1

General introduction

Chapter 1: General Introduction.

1. Global context: Hg as a global pollutant.

1.1. Fundamental Hg chemistry.

Mercury (Hg) is an element of the group 12 of the periodic table and it has seven stable isotopes with different natural abundances: ^{196}Hg (0.15%), ^{198}Hg (9.97%), ^{199}Hg (16.87%), ^{200}Hg (23.10%), ^{201}Hg (13.18%), ^{202}Hg (29.86%), ^{204}Hg (6.87%). Hg is a transition element with an atomic number of 80 and atomic weight of 200.59 u. It is a heavy, silvery-white liquid metal at room temperature with a freezing point of – 38.83 ^{o}C and a boiling point of 356.73 ^{o}C (IUPAC, Third Edition, 2006). The electronic configuration responsible for its chemical properties is $1s^2$… $5d^{10}$, $4f^{14}$, $\mathbf{6s^2}$. Because of this ground state configuration, Hg has a high ionization potential (10.4 eV) due to the difficulty of removing an electron from the shell valence (Gaffney & Marley, 2014).

Hg can exist in three oxidation states: elemental mercury (Hg(0), Hg^0), mercurous mercury, which exists as a dimeric cation (Hg(I), (Hg_2^{2+})), and divalent inorganic mercury (Hg(II), Hg^{2+}) where Hg_2^{2+} is rapidly disproportionated to give Hg^0 and Hg^{2+} (Eq.1.1)

$$Hg_2^{2+} \leftrightarrow Hg^{2+} + Hg^0 \quad (1.1)$$

The standard reduction potentials (E^0) of Hg redox states are:

$$Hg_2^{2+} + 2e = 2Hg^0 \quad E^0 = 0.796\ V \quad (1.2)$$

$$2Hg^{2+} + 2e = Hg_2^{2+} \quad E^0 = 0.911\ V \quad (1.3)$$

$$Hg^{2+} + 2e = Hg^0 \quad E^0 = 0.854\ V \quad (1.4)$$

In fact, only oxidizing compounds with potentials between – 0.8 V and – 0.85 V are capable to oxidize Hg^0 to Hg_2^{2+}. Since no natural oxidizing compounds are found in this range in the environment, the oxidation of Hg^0 forms Hg^{2+} (Gaffney & Marley, 2014).

Hg(II) can form organometallic Hg compounds through covalent bonds with carbon atoms. The most common environmental forms of organometallic Hg compounds in natural waters are monomethylmercury (CH_3-Hg^+, MeHg) and dimethylmercury (CH_3-Hg-CH_3, DMeHg). MeHg is soluble in water, while DMeHg is a volatile compound with chemical properties similar to Hg(0). Although both organometallic Hg compounds are stable to atmospheric oxidation and hydrolysis, they can be degraded due to the exposure to light or heat. Others organometallic Hg compounds found in natural waters are ethyl-mercury (EtHg and phenyl-mercury (Ph-Hg). On

the other hand, sulphur (S) and selenium (Se), with electronic configuration of $1s^2 \ldots 3s^2$, $\mathbf{3p^4}$ and $1s^2 \ldots 4s^2$,$\mathbf{4p^4}$, respectively, can also form covalent bonds with Hg ($1s^2 \ldots 5d^{10}$, $4f^{14}$,$\mathbf{6s^2}$). In the environment, mercury sulphide ($HgS_{(s)}$) and mercury selenide ($HgSe_{(s)}$) are found in mineralised form. They are characterized by a low reactivity and high stability in comparison with other Hg chemical compounds (Craig et al. 1986).

In solution, Hg(II) and MeHg are not in a free ion form, they form variety of complexes with other ligands containing halides, oxygen, sulphur, selenium, nitrogen or phosphorus which their stability and binding affinity is characterized by:

- Nature of the ligand.
- Chelating effect.
- Resonance effect.
- Steric effects.
- Ionic strength.
- Temperature.
- pH.

All these parameters will determine the physico-chemical speciation of Hg in natural waters (**2.1. Hg physicochemical speciation in surface waters**.).

1.2. Hg pollution, toxicological effects and sources to aquatic systems.

Hg occurs naturally in the earth crust, however, anthropogenic activities have led to widespread pollution (Sundseth et al., 2017). Hg is released into the environment through natural and anthropogenic sources (Pirrone et al., 2010). The contribution of natural sources to the global Hg budget takes into account the contribution from volcanic activity, geothermal sources, and the re-emissions and re-mobilization processes coming from the aquatic and terrestrial ecosystems (e.g. biomass burning) (Amos et al., 2013). Indeed, the main natural sources of Hg^0 emitted into the atmosphere are from re-emission processes from aquatic systems (61%), and soil and vegetation (18%) (UNEP, 2018). On the other hand, Hg inputs from anthropogenic sources (human activities) have demonstrated to disturb the natural Hg biogeochemical cycle (**Figure 1.1**). Whereas the 80% of anthropogenic Hg is released into the atmosphere, 20% is discharged in terrestrial and aquatic ecosystems (UNEP, 2018). The main anthropogenic sources contributing to the global Hg budget are: artisanal and small-scale gold mining (37%),

coal burning, other fossil fuels, and heat production in industrial plants (25%) (Sundseth et al., 2017).

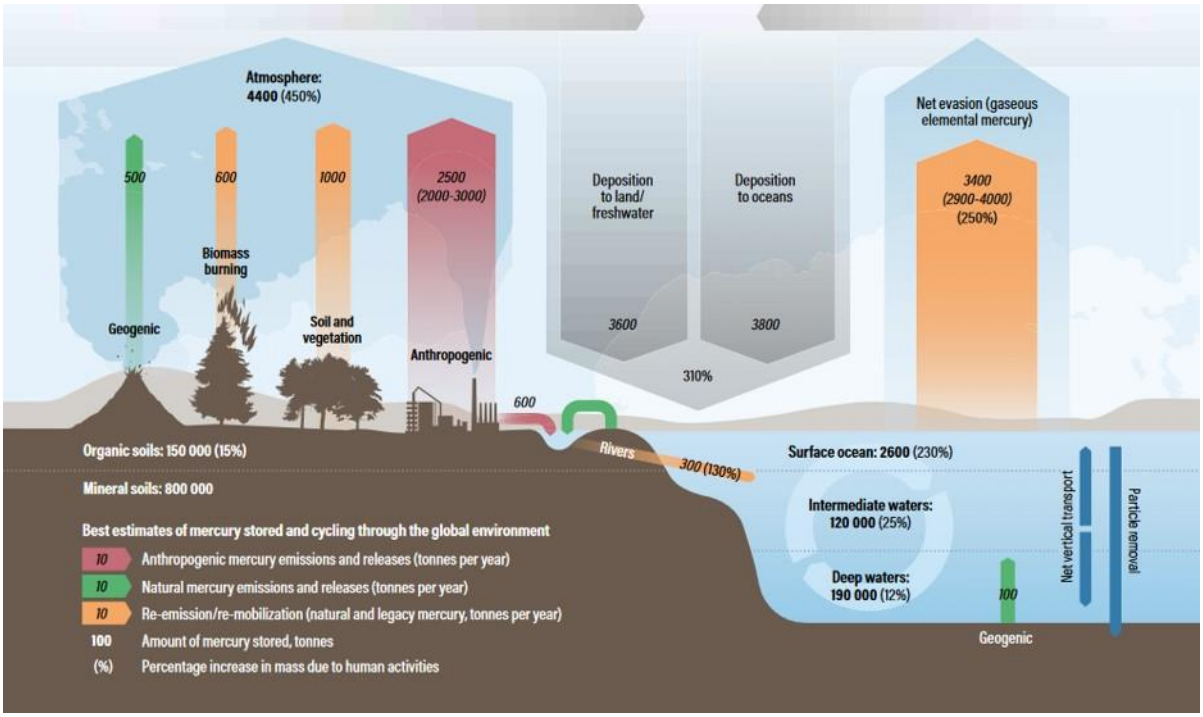

Figure 1.1. Updated global mercury budget from the global mercury assessment 2018 report (UNEP, 2018).

Hg is considered as a persistent, bioaccumulative, toxic pollutant due to the toxicological effects observed on human and wildlife (Clarkson & Magos, 2006). In wildlife, behavioural, neurochemical, and reproductive changes have been addressed due to MeHg exposure (Scheuhammer et al., 2007). A recent review highlighted that MeHg exposure is mainly determined by ecological factors such as dietary intake and habitat specific feeding, combined with the physiological processes that govern Hg compounds assimilation, transformations and elimination (Chételat et al., 2020). As a result, risk assessments are needed to examine what precautions must be taken and prevent such toxicological effects in wildlife (Tan et al., 2009). Concerning human exposure, Hg toxicological impacts related to fish consumption were, for first time, addressed in 1956 (Harada, 1995). Fishermen and their families from Minamata Bay, Japan witnessed the first known large-scale disaster of Hg poisoning by the discharge of Hg in the wastewater from a processing plant. The harmful effects on the local population, via seafood consumption, principally affected the neurological system with symptoms such as mental retardation, primitive reflex, and cerebellar ataxia. This accident caused more than 1043 deaths over 36 years due to the consumption of contaminated fish and seafood. More than 2 million people were diagnosed as suffering the “Minamata disease”. Nowadays, the impact of the

disaster is still under investigation with the purpose of studying the MeHg long-term exposure on the population of Minamata (Yorifuji et al., 2011). In order to design a global strategy to protect human health and provide environmental risk assessment from the adverse effects of Hg, on 11th October 2013 the European Union and 86 countries signed the Minamata convention, named after the catastrophic accident, at the Diplomatic Conference in Kumamoto (Japan). Nowadays, 127 parties constitute the Minamata convention where the main requirement of these countries is to reduce and/or eliminate the release of Hg from artisanal and small-scale gold mining (ASGM) and the manufacturing of products that contain Hg (UNEP, 2018).

Hg enters into the aquatic systems by atmospheric deposition or point sources discharges (Mason et al., 2012). Atmospheric deposition is the main source of Hg to most aquatic ecosystems (Holmes et al., 2010; Selin, 2009) where the Hg atmospheric residence time is between 0.5 and 1 year before it is deposited in aquatic ecosystems via dry or wet deposition (Zhang et al., 2009). Other important Hg inputs into the aquatic systems are coming from the remobilisation of sediments, direct discharge of industrial, and mining wastes or naturally mercury minerals. Furthermore, melting ice, snow and permafrost have shown to represent important Hg inputs in polar regions (Lamborg et al., 2014).

2. Hg biogeochemical cycle in aquatic ecosystems.

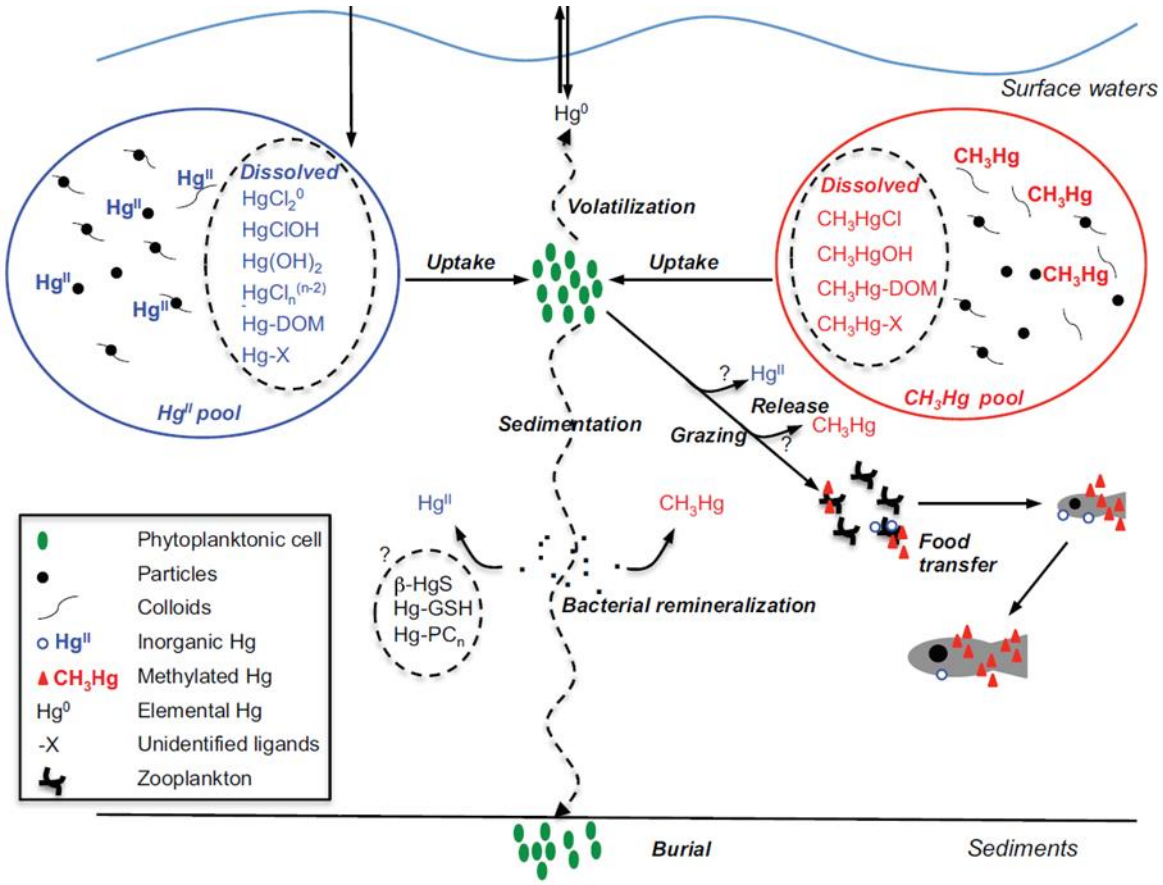

Figure 1.2. Hg cycle in natural waters from Le Faucheur et al., 2014.

2.1. Hg physicochemical speciation in surface waters.

In the aquatic systems, three predominant Hg compounds (Hg(0), Hg(II) and MeHg) govern the Hg physicochemical speciation (Fitzgerald et al., 2007). Hg(II) and MeHg concentrations range from 1 to 100 and 0.001 to 10 ng L^{-1}, respectively (Bank, M.S., 2012). Both Hg(II) and MeHg are distributed in the dissolved and solid/adsorbed pool, forming complexes with inorganic and organic ligands (**Figure 1.2**). In surface waters and in the absence of significant chelators, Hg(II) and MeHg form complexes with inorganic ligands such as chloride (Cl^-) and hydroxide anions (OH^-), where the chemical speciation is mostly dependent on the pH and chlorine concentration (Morel et al., 1998). For example, $HgCl_2$ can be hydrolysed in aqueous solution, but also dissociated into other highly soluble complexes forming an equilibrium. In seawaters, the main dissociated complex is $HgCl_4^{2-}$, whereas $HgCl_4^{2-}$, $HgCl_3^-$ and $HgCl_2$ compose the main Hg species in freshwaters (**Table 1.1**). Under low [Cl-], the chemical

speciation is dominated by OH^- forming HgClOH, $Hg(OH)_2$ and MeHgOH. In anoxic waters, the speciation of dissolved Hg(II) is completely governed by sulphide complexes (HgS_2H, HgS_2H^- and HgS_2^{2-}) (Morel et al., 1998).

Organic ligands such as dissolved organic matter (DOM) among others are the main ligands governing Hg speciation and Hg bioavailability in the dissolved pool (Ravichandran, 2004). DOM consists of a mixture of chemical compounds of unknown structure containing potential reduced thiol functional groups (RS-H) and carboxylic acids (R-COO-H), which are characterized by a high binding affinity towards Hg compounds (**Table 1.1**). (Liem-Nguyen et al., 2017; Song et al., 2018). DOM can come either from terrestrial or microbial sources in which the Hg physicochemical speciation is strongly dependent on the DOM concentration and size; varying from 200 to 2000 kDa (Bravo et al., 2017). DOM has multiple roles in the transport and fate of Hg compounds. Although DOM can inhibit Hg uptake by aquatic microorganisms by forming insoluble complexes, DOM can also facilitate the Hg delivery to membrane transport sites, or even enter directly inside the cells when DOM is required as a carbon or energy source by anaerobic microorganisms (Schaefer et al., 2011). DOM also promotes the dissolution of Hg and inhibits the precipitation of insoluble cinnabar (β-$HgS_{(s)}$) in deep waters (Graham et al., 2013). In addition, the complex physicochemical properties of DOM could vary under different redox conditions; making the investigation of its role in Hg biogeochemistry challenging for the scientific community (Branfireun et al., 2020).

On the other hand, low molecular weight (LMW) thiol compounds (LMW-R-SH) are expected to play an essential role in Hg physicochemical speciation in natural waters due to their high thermodynamic stability constants (**Table 1.1**) (Song et al., 2020). LMW thiol compounds are referring to a specific set of thiol compounds with a molecular mass up to glutathione (GSH-307Da) (Bouchet & Björn, 2014). So far, LMW thiols compounds concentrations have been determined in several freshwater and seawater compartments, ranging from nM to µM levels (Bouchet et al., 2018; Liem-Nguyen et al., 2015, 2019; J. Zhang et al., 2004). LMW thiol compounds are mainly exported from aquatic microorganisms with concentrations high enough to control Hg speciation (Adediran et al., 2019). Although relevant information can be obtained by correlating LMW thiol compounds concentration with Hg compounds concentration (Liem-Nguyen et al., 2021), the characterization and determination of LMW thiol Hg-complexes will provide a better understanding of the role of LMW thiol compounds in Hg speciation and Hg bioavailability. So far, only one study reported the quantification LMW thiol-MeHg complexes, ranging from 12 to 530 pM, in the extracellular fraction of the methylating bacterium,

Geobacter sulfurreducens PCA (Liem-Nguyen et al., 2020). Nevertheless, the *in-situ* quantification of LMW thiol-Hg complexes have never been reported in natural waters.

Table 1.1. Logarithmic thermodynamic formation constants for Hg(II) and MeHg species affinities of the main Hg-complexes. Number of each component gives the stoichiometry of the reaction with positive number representing reactants and negative numbers products obtained from Liem-Nguyen et al., 2017.

Hg species	**Components**									
	Log Kf	**H_2O**	**H^+**	**Hg (II)**	**Cl^-**	**H_2S**	**S^0**	**LMW-RS^- (aq)**	**$MeHg^+$**	**DOM-RS-(aq)**
$HgOH^+$	3.4	1	-1	1						
$Hg(OH)_2$	-6.2	2	-2	1						
$HgCl^+$	7.1			1	1					
$HgCl_2$	13.8			1	2					
$HgCl_3^-$	14.7			1	3					
$HgCl_4^-$	15.4			1	4					
HgOHCl	4.3	1	-1	1	1					
$HgSH^+$	13.0		-1	1		1				
HgS_2H^-	18.2		-3	1		2				
HgS_2^{2-}	8.9		-4	1		2				
$Hg(SH)_2$	24.6		-2	1		2				
HgS_nSH^-(n=4-6)	18.6		-3	1		2	3-5			
$Hg(S_n)_2^{2-}$ (n=4-6)	11.1		-4	1		2	3-5			
HgOHSH	9.4	1	-2	1		1				
HgClSH	18.9		-1	1	1	1				
HgS(s)	30.3		-2	1		1				
LMM-RSH	9.1		1							
NOM-RSH(aq)	9.0		1							
NOM-RSH(ads)	9.0		1							
$Hg(LMW\text{-}RS)_2$	**40.1**							**2**		
$Hg(DOM\text{-}RS)_2$ (aq)	**41.0**			**1**						**2**
MeHgOH	-4.5	1	-1						1	
MeHgCl	5.4				1				1	
MeHgSH	7.6		-1			1			1	
$MeHgS^-$	0.12		-2			1			1	
$S(MeHg)_2$	16.4		-2			1			2	
MeHgSR-LMM	**17.5**					**1**		**1**	**1**	
MeHgSR-DOM(aq)	**17.5**					**1**			**1**	**1**

2.2. Hg compounds transformations in aquatic systems.

Hg compounds can undergo different biotic and abiotic processes in the aquatic environment such as oxidation/ reduction and methylation/ demethylation. Biotic Hg compounds transformations are mediated by aquatic organisms (e.g., bacteria and phytoplankton) due to the interaction with the cell surface or internalization within the cells. On the other hand, abiotic transformations can occur in the aquatic environment due to the combination of solar radiation with non-biogenic or biogenic species such reactive oxygen species (ROS), inorganic ligands, or organic ligands such as DOM, extracellular polymeric substances (EPS), LMW thiol compounds among others. Overall, the extent of these transformations is determined by the environmental factors, physicochemical parameters, and biological activity of aquatic microorganisms (Blum et al., 2014).

2.2.1. Reduction/ oxidation.

Abiotic.

Abiotic redox reactions regulate the exchange of Hg between the atmosphere and the hydrosphere (air/water) (Soerensen et al., 2014). Since Hg(II) is the main substrate for methylation, the oxidation of Hg(0) is an important process regulating the MeHg levels in aquatic ecosystems (Lalonde et al., 2001). A recent review in photochemical behaviours of Hg compounds highlighted that the photo-oxidation of Hg(0) is mainly mediated by ROS (Luo et al., 2020). Although aquatic microorganisms can generate ROS in the intracellular fraction, the free radicals and ROS generation can also occur by the absorption of ultraviolet-B radiation by DOM (Latch & McNeill, 2006). On the other hand, the Hg redox cycle in oxic surface waters is mainly dominated by the photochemical Hg(II) reduction (Amyot et al., 1997). Normally, high dissolved gaseous mercury (DGM) production is correlated with the high concentration of dissolved organic carbon (DOC), which refers to the mass of carbon of DOM. In laboratory experiments, the study of DOM functional groups position on the ring benzene, and the presence of thioglycolic acid and alkanethiols, which represent thiols binding sites of DOM humic substances, was proved to have a great impact on Hg photoreduction (He et al., 2012; Si & Ariya, 2011, 2015). In phytoplankton, only one study showed that biogenic DOM produced by the marine diatom *Chaetoceros* sp. was involved the photoreduction of Hg(II) (Lanzillotta et al., 2004).

Biotic.

Although photochemical redox processes are the main mechanisms responsible for the air-water Hg exchanges in surface waters, biotic reduction and oxidation processes can be triggered by aquatic microorganisms (Grégoire & Poulain, 2014; Mason et al. 1995). Biotic reduction can be carried out by phototrophic organisms, while both reduction and oxidation processes have been observed in chemotrophic microorganisms (Colombo et al., 2014). Nowadays, it is well known that bacteria, that carry *mer* operon genes (merA), are involved in Hg reduction under anaerobic conditions via activity of the enzyme mercury reductase (Wiatrowski et al., 2006). MerA encodes a group of cytosolic proteins in the detection, transport and Hg(II) reduction. On the other hand, a little information is available about the mechanisms involving Hg(0) bio-oxidation by chemotrophic microorganisms.

Phototrophic reduction of Hg(II) also contributes to the Hg redox cycling in aquatic systems (Grégoire & Poulain, 2014). Often, the formation of DGM is correlated with phytoplankton dynamics and blooms (Poulain et al., 2004). However, it is unclear whether phototrophs are directly involved in DGM production or Hg(II) reduction is indirectly mediated by the release of biogenic organic ligands. Consequently, laboratory experiments with pure phytoplankton cell cultures demonstrated that phototrophic microorganisms are able to produce DGM (Morelli et al., 2009; Oh et al., 2011), but the mechanisms in eukaryotic alga remains unknown. Although Hg(II) reduction is thought to be a detoxification mechanism against Hg toxicity, a recent study in phototrophic bacteria showed that phototrophic cells might use Hg(II) as an electron acceptor reducing and controlling the Hg(II) intracellular levels and redox homeostasis (Grégoire & Poulain, 2016). Studies in phototrophic bacterium *Synechocystis* sp. PCC 6803 showed that, Hg(II) reduction is mediated by the glutaredoxin-pathway thanks to the characterization of MerA-like enzymes (Boyd & Barkay, 2012; Marteyn et al., 2013; Singh et al., 2019).

2.2.2. Methylation/ demethylation.

Abiotic methylation.

Hg(II) methylation was always considered to be biologically mediated, however, some studies suggested that this process cannot account for all MeHg found in the aquatic ecosystems (Cossa et al., 2009). Abiotic Hg(II) methylation demands suitable methyl-donor compounds in the water column and sediments such as methylcobalamin (MeCo) (Chen et al., 2007). Particularly, MeCo is a coenzyme of vitamin B12 and is considered as the main environmental compound

involved in abiotic Hg(II) methylation in aquatic environments (Ullrich et al., 2001). Furthermore, abiotic Hg(II) methylation was reported in presence of the solar radiation and DOM (Siciliano et al., 2005). However, the contribution of the abiotic methylation in natural waters is expected to be negligible.

Biotic methylation.

It is well established that aquatic heterotrophic microorganisms are mainly responsible for the biotic methylation of Hg(II) (Regnell & Watras, 2019). The discovery of the hgcAB gene cluster needed for Hg(II) methylation (Parks et al., 2013) in sulfate reducing bacteria (SRB) could help to identify a large range of methylating microbes such as iron reducers, fermenters and methanogens as potentially equally relevant (Hamelin et al., 2011; Jones et al., 2019). In the aquatic environment, biotic Hg(II) methylation is mainly correlated with the biological activity of methylators (Gilmour et al., 1992). Although there is no evidences that phototrophic microorganisms can methylate Hg itself, several studies highlighted the importance of algae in MeHg production (Lázaro et al., 2019). For example, phytoplankton is known to produce a high content of biogenic organic matter making these micro-environments beneficial for microorganisms capable of Hg methylation (Gascón Díez et al., 2016; Lázaro et al., 2013; Lei et al., 2021). Particularly, higher abundance of cyanobacteria in periphyton was correlated with higher MeHg production (Lázaro et al., 2019). Furthermore, high Hg methylation yields in benthic biofilms and periphyton were correlated with high content of EPS in Lake Titicaca (Bouchet et al., 2018). In Lake Geneva, higher methylation yields were found in settling particles sinking through the oxic water column than in the surface sediments (Gascón Díez et al., 2016). It was evidenced that DOM enhanced in MeHg production in boreal lakes (Bravo et al., 2017). Furthermore, DOM promoted Hg(II) methylation under sulfidic conditions (Graham et al., 2012, 2013). The complexation of LMW thiol compounds binding Hg(II) with cysteine (Cys) or glutathione (GSH) was demonstrated to enhance (Cys) and inhibit (GSH) the Hg(II) uptake and therefore, Hg(II) methylation in anaerobic bacteria (Schaefer et al., 2011). However, it is still unclear the role of organic ligands in the biotic MeHg production in aquatic systems.

Abiotic demethylation.

MeHg demethylation can be transformed into Hg(II) or Hg(0). MeHg photodemethylation is the main process responsible for MeHg degradation in surface waters (Barkay & Gu, 2021). The extent of MeHg photodemethylation is mainly influenced by the type of solar radiation (UV-A, UV-B and visible light) and DOM concentration and structure (Luo et al., 2020).

Indeed, laboratory experiments demonstrated that compounds containing both thiols and aromatic moieties increase MeHg photodegradation (Qian et al., 2014). The central role of humic-like DOM in MeHg photodegradation was evidenced by the different DOM concentration and molecular weight, as well as, UV-light, pH, and co-existing ions such as NO^{3-} and Fe^{3+} (Zhang et al., 2017). Furthermore, a recent study evidenced the MeHg demethylation by 6 marine microalga due to the release of EPS (Li et al., 2022).

Biotic demethylation.

Biotic MeHg demethylation should normally overcome abiotic demethylation at depth water columns due to the attenuation of radiation (Alanoca et al., 2016; Gascón Díez et al., 2016; Sharif et al., 2014). In bottom waters, anaerobic microorganisms are capable of performing either reductive demethylation forming Hg^0 and methane (CH_4) as products, and /or oxidative demethylation forming Hg (II), CO_2 and CH_4 of the microbial degradation (Barkay & Wagner-Döbler, 2005). This process consists of a first demethylation of MeHg by an enzyme (merB, organomercurial lyase) resulting in Hg(II) that is then further reduced within the bacterial cell by another enzyme (merA) (Barkay & Gu, 2021). Although reductive demethylation seems to be dominant at high Hg(II) concentrations, oxidative demethylation is suggested to be the main mechanism at lower Hg(II) concentrations ($100 < ng\ g^{-1}$) under anaerobic conditions (Marvin-DiPasquale et al., 2000). Laboratory experiments indicate that most of the methylating SRB are also capable of demethylating MeHg (Bridou et al., 2011; Pedrero et al., 2012). Although little information is available on biotic demethylation of MeHg by phototrophic microorganisms, so far only one study reported the oxidative demethylation ([MeHg] = 4 nM / 802 ng L^{-1}) in the green algae *Chlamydomonas reinhardtii* (Bravo et al., 2014). In field experiments, a positive correlation was found between the percentage of MeHg demethylated and the abundance of diatoms in pico-nanoplankton (Cossart et al., 2021).

2.3. Hg compounds bioaccumulation and biomagnification in phytoplankton.

Phytoplankton represent an important ecological part for all aquatic life living in the surface layer (euphotic zone) since they compose the base of marine and freshwater food web. Phytoplankton assimilate light, carbon dioxide and nutrients, releasing oxygen and dissolved organic matter through the photosynthesis. Phytoplankton is also affected by the anthropogenic perturbations such as pollution by organic chemicals and heavy metals. Also, changes in temperature, vertical stratification of water column and supply of nutrients among others (light

radiation, salinity, pH, seasonal variations, etc) modify the phytoplankton composition, abundance, and productivity in a particular aquatic ecosystem and therefore, the speciation of Hg compounds and their potential bioaccumulation and biomagnification through the trophic chain (Reynolds, 2006).

The concentration of Hg in phytoplankton is normally 10^4–10^5 higher than the surrounding waters representing the largest relative difference in concentration in comparison with any point of the trophic chain (Le Faucheur et al., 2014). So far, it is well known that phytoplankton preferentially accumulates MeHg in the intracellular fraction, while Hg(II) is mainly attached to the membrane (**Figure 1 3**) (Morel et al., 1998). Because of this, higher MeHg assimilation efficiencies are normally observed in zooplankton (Gosnell et al., 2021). For example, MeHg concentration increased by a factor 2 between the first (phytoplankton) and second trophic level (zooplankton) (Hammerschmidt & Fitzgerald, 2006b). Also, alga quality and ambient phytoplankton density influence the MeHg biomagnification (Karimi et al., 2007; Pickhardt et al., 2005). In fact, the development of a MeHg bioaccumulation model at the base of the marine food web showed that diatoms and synechococcus are the two most important phytoplanktonic species for transferring MeHg from water to zooplankton (Zhang et al., 2020). Also, rapid growth of phytoplankton reduce MeHg concentrations within the cell since the MeHg concentration per cell (biodilution) is lower (Chen & Folt, 2005; Karimi et al., 2007). However, the interaction of Hg compounds with phytoplankton at the cellular level are still under investigation.

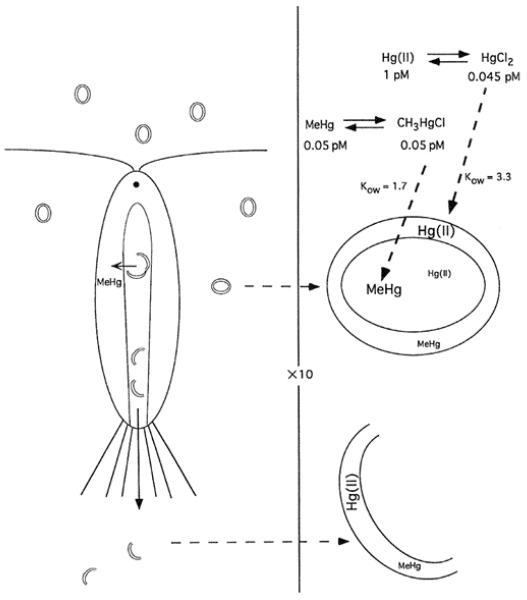

Figure 1 3. Assimilation of Hg(II) and MeHg at the first stages of the trophic levels obtained from Morel et al., 1998.

3. Hg-phytoplankton interactions at the cellular scale.

Phytoplankton communities are composed by several species involving unicellular eukaryotic microalgae (e.g. green alga, diatom among others) and cyanobacteria (prokaryotes) (Sunda & Huntsman, 1998). Phytoplankton species vary from one specie to another in terms of cellular wall, intracellular structure, and metabolic activity (Reynolds, 2006). The cell wall composition is usually composed by cellulose in green algae, peptidoglycan in cyanobacteria, and silica frustule in diatoms (Dranguet et al., 2014). Although cyanobacteria and eukaryotic microalga are both photosynthetic microorganisms, they have different intracellular compartments to perform the photosynthesis. In fact, eukaryotic microalga contains one or more chloroplasts in the intracellular fraction, whereas cyanobacteria perform the photosynthesis in the thylakoids. Therefore, Hg compounds internalization, intracellular complexation and reactivity, and impact on the metabolic activity is specific from each type of phytoplankton specie. A conceptual view about the potential Hg-interactions with eukaryotic alga is observed in **Figure 1.4**.

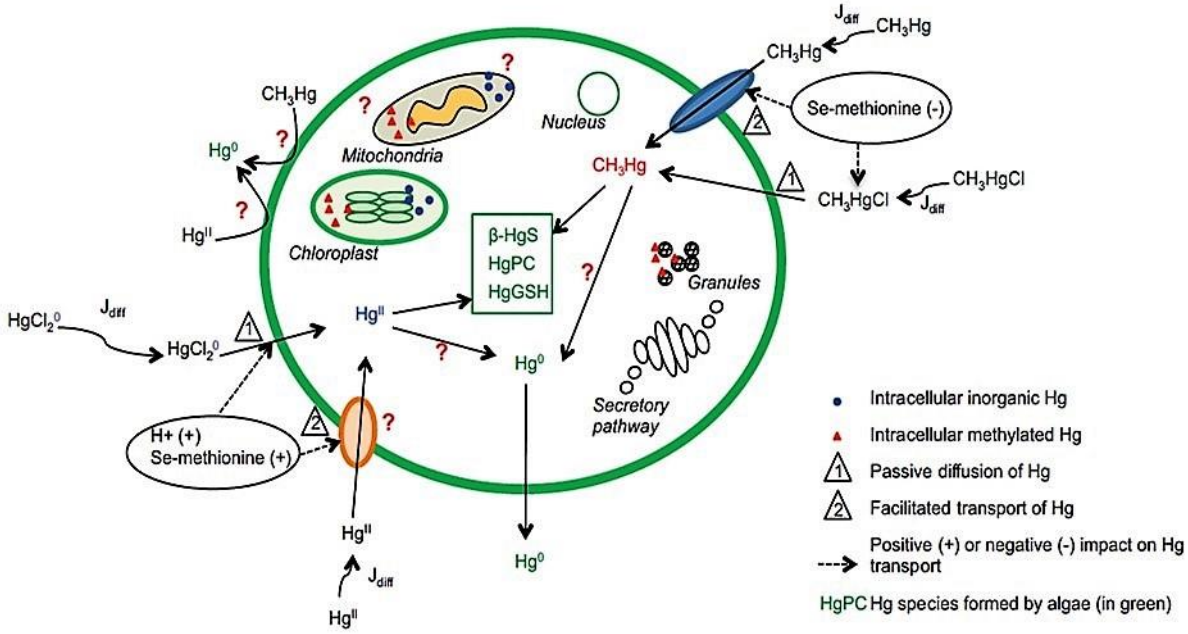

Figure 1.4. Conceptual view about Hg-phytoplankton interactions at the cellular level obtained from Le Faucheur et al., 2014.

After a careful revision of the literature concerning the Hg exposure in pure phytoplankton cell cultures, studies carried out so far were focused on studying Hg uptake mechanisms and Hg intracellular handling. In addition, the main factors affecting the Hg-phytoplankton interactions were: (***i***) the concentration of Hg compounds, (***ii***) cell density, (***iii***) the type of exposure medium

and (***iv***) type of phytoplankton strain. Concerning the studies focused on Hg uptake mechanisms, the green alga *Selenastrum Capricornutum* was exposed to 1 ng L^{-1} of Hg (II) and MeHg with a cell density of $4x10^3$ cell mL^{-1} resulting in 1.2 amol $cell^{-1}$ (Gorski et al., 2008). Furthermore, Skrobonja et al., 2019 exposed 300 ng L^{-1} of MeHg to the green alga *Selenastrum Capricornutum* (cell density: $4x10^6$ cell mL^{-1}) in which the MeHg exposure per cell was 0.5 amol $cell^{-1}$. A recent work exposed 2 and 0.2 ng L^{-1} of Hg(II) and MeHg, respectively in which the Hg concentration per cell was between 0.3–1.6 and 0.03–0.1 amol $cell^{-1}$, respectively (Li et al., 2022). Regarding the medium where the cells were exposed, almost all the previous cited studies used filtered natural waters (0.22 µm) as exposure medium, except for Skrobonja et al., 2019. The choice of the exposure medium might have two major effects on the outcomes observed for the study of Hg-phytoplankton interactions. Firstly, the use of filtered natural waters is known to decrease the bioavailability of Hg compounds to be taken up by cells (Klapstein & O'Driscoll, 2018). In fact, the presence of LMW thiol compounds and non-colloid DOM among others influence Hg compounds delivery to the phytoplanktonic cells (Bravo et al., 2017; Schaefer et al., 2011), but also, they can promote abiotic Hg compounds transformations (Luo et al., 2020). Second, the potential nutrients containing in filtered natural waters can affect the metabolic activity of phytoplankton. Indeed, the toxicity induced by Hg compounds decrease in filtered natural waters in comparison with artificial exposure media (Gorski et al., 2008; Le Faucheur et al., 2011; Val et al., 2016). In addition, the pre-exposure of Hg in phytoplankton was shown to lead to an acclimation of the phytoplankton microorganism (Wu & Wang, 2013).

On the other hand, studies focusing on the potential physiological responses and Hg intracellular handling reported Hg compounds concentrations ranging from 10 to 22000 amol $cell^{-1}$(Morelli et al., 2009; Wu et al., 2012; Wu & Wang, 2012, 2013, 2014). In some cases, the cell density was not even determined but Hg compounds concentration ranged between 100-200 µg L^{-1} (Kelly et al., 2006; Lefebvre et al., 2007). The cited studies carried out the experiments in artificial exposure mediums. In this doctoral dissertation, the initial Hg amol per cell in *Synechocystis*, *C.meneghiniana*, and *C.reinhardtii* was 0.9, 3 and 0.04 for Hg (II), and 0.09, 0.3 and 0.004 amol $cell^{-1}$ for MeHg, respectively in an exposure medium based on major cations (**Table 1.2**).

Table 1.2 Hg(II) and MeHg concentrations in phytoplanktonic species, including the type of phytoplanktonic specie, exposure medium composition, Hg exposure concentration (amol cell^{-1}), intracellular concentration (amol cell^{-1}) and cell fractionation procedure. (*) In these cases, we took for the calculations the cell density in the beginning of the Hg exposure since the cell density was increasing over time. No determined (N.D) means that it was not reported.

References	Phytoplanktonic specie	Exposure medium composition	Hg exposure per cell (amol cell^{-1})	Hg exposure concentration (ng L^{-1})	Cell fractionation procedure
Zhong et al. 2009	*Diatom (Thalassiosira Pseudonana)*	Filtered Seawater (0.22 µm)	[^{203}Hg(II)] = 6.6 [^{203}MeHg] = 3.3	[^{203}Hg(II)] = 400 [^{203}MeHg] = 200	No fractionation
Luengen et al. 2012	*Diatom (Cyclotella meneghiniana)*	Freshwater river	[^{203}MeHg] = 10-20	[^{203}MeHg] = 80-150	ND
Le Faucheur et al. 2011	*Green alga (Chlamydomonas reinhardtii)*	Simplified exposure solution (major ions)	[^{203}Hg(II)] = 500-2000	[^{203}Hg(II)] = 10000-16000	No fractionation
Lee and Fisher et al. 2016	*Diatom (Thalassiosira Pseudonana)* *Chlorophyte (Dunaliella tertiolecta)* *Cryptophyte (Rhodomonas salina)* *Dinoflagellate (Prorocentrum minimum)* *Coccolithophore (Emiliania huxleyi)* *Cyanobacterium (Synechococcus bacillaris)*	Filtered surface seawater	*[^{203}MeHg] = 66	[^{203}MeHg] = 50-80	No fractionation
Kim et al. 2014	*Diatom (Stephanopyxis palmeriana)* *Diatom (Odontella regia)* *Diatom (Ditylum brightwellii)* *Diatom (Chaetoceros curvisetus)* *Cyanobacterium (Chroococcus minutus)*	Filtered surface seawater	*[^{203}MeHg] = 4-415	[^{203}MeHg] = 4-500	No fractionation
Gorski et al. 2008	*Green alga (Selenastrum capricornutum)*	Filtered river-lake water	[^{201}Hg(II)] = 1.2 [^{199}MeHg] = 1.2	[^{201}Hg(II)] = 1 [^{199}MeHg] = 1	No fractionation
Mason et al. 1996	*Diatom (Thalassiosira Pseudonana)*	Filtered surface seawater	[Hg(II)] = 15-25 [MeHg] = 15-25	[Hg(II)] = 5-50 [MeHg] = 2-30	Cell sonication
Pickhardt and Fisher 2007	*Diatom (Cyclotella meneghiniana)* *Green alga (Chlamydomonas reinhardtii)* *Cryptophyte (Cryptomonas ozolini)* *Cyanobacterium (Synechocystis sp.)*	Filtered river water	*[^{203}Hg(II)] = 700-1000 *[^{203}MeHg] = 650-700	*[^{203}Hg(II)] = 150-325 *[^{203}MeHg] = 120-150	Cell sonication
Skrobonja et al. 2019	*Green alga (Selenastrum capricornutum)*	BBM medium (just major cations)	[MeHg] = 0.5	[MeHg] = 300	Cell disruption
Moye et al. 2002	*Green alga (Selenastrum capricornutum)* *Green alga (Cosmarium botrytis)* *Diatom (Thalassiosira Pseudonana)* *Blue-green alga (Schizothrix calcicola)*	Allen's media (Phosphate buffer)	*[MeHg] = 10-2000 *[MeHg] = 10 *[MeHg] = 10 *[MeHg] = 10	[MeHg] = 400-80000 [MeHg] = 400 [MeHg] = 400 [MeHg] = 400	N.D
Bravo et al. 2017	*Green alga (Chlamydomonas reinhardtii)*	Exposure medium (just major cations)	N.D	[^{199}Hg(II)] = 4-800[1] [^{201}MeHg] = 0.1-20	N.D
Our work	*Cyanobacterium (Synechocystis sp.)* *Green alga (Chlamydomonas reinhardtii)* *Diatom (Cyclotella meneghiniana)*	Exposure medium (just major cations)	Syn [^{199}Hg(II)] = 0.9 [^{201}MeHg] = 9 x 10^{-2} Chla [^{199}Hg(II)] = 4.2 x 10^{-2} [^{201}MeHg] = 4.2 x 10^{-3} Cyclo [^{199}Hg(II)] = 3 [^{201}MeHg] = 0.3	Syn [^{199}Hg(II)] = 600 [^{201}MeHg] = 60 Chla [^{199}Hg(II)] = 600 [^{201}MeHg] = 60 Cyclo [^{199}Hg(II)] = 600 [^{201}MeHg] = 60	Ultrasonication

References	*Phytoplanktonic specie*	*Exposure medium composition*	*Hg exposure concentration (amol cell^{-1})*	*Hg exposure concentration (ng L^{-1})*	*Cell fractionation procedure*
Wu and Wang et al. 2012	*Diatom (Thalassiosira weissflogii)*	Exposure medium (only major cations)	[Hg(II)] = 840-22000 [MeHg] = 10-500	[^{203}Hg(II)] = 840-222000 [^{203}MeHg] = 100-8400	No fractionation
Wu and Wang et al. 2014	*Diatom (Thalassiosira weissflogii)* *Flagellate (Isocrystis galbana)* *Green alga (Chlorella autotrophica)*	Exposure medium (only major cations)	[Hg(II)] = 0-6900	[^{203}Hg(II)] = 0-180000	N.D
Wu and Wang et al. 2011	*Diatom (Thalassiosira weissflogii)* *Flagellate (Isocrystis galbana)* *Green alga (Chlorella autotrophica)*	Exposure medium (only major cations)	[Hg(II)] = 0-6900 [MeHg] = 0-100	[^{203}Hg(II)] =0-100000 [^{203}MeHg] = 0-1580	No fractionation
Wu and Wang et al. 2013	*Diatom (Thalassiosira weissflogii)*	Exposure medium (only major cations)	[Hg(II)] = 8-800 [MeHg] = 5-70	[^{203}Hg(II)] = 500-5000 [^{203}MeHg] = 20-400	Cell ultrasonication Lavoie et al. 2009
Morelli et al. 2009	*Diatom (Thalassiosira weissflogii)*	Exposure medium (only major cations)	[Hg(II)] = 5-70	[Hg(II)] = 1000-25000	N.D
Kelly et al. 2006	*Green alga (Selenastrum capricornutum)* *Green alga (Chlorella fusca)* *Diatom (Navicula pelliculosa)*	Exposure medium (only major cations)	N.D	[Hg(II)] = 100000-200000	N.D
Kelly et al. 2006b	*Green alga (Selenastrum capricornutum)* *Cyanobacterium (Limnothrix planctonica)*	Exposure medium (only major cations)	N.D	[Hg(II)] = 100000-200000	N.D
Lefebre et al. 2007	*Cyanobacterium (Limnothrix planctonica)* *Cyanobacterium (Synechococcus leopoldiensis)* *Cyanobacterium (Phormidium limnetica)*	Exposure medium (only major cations)	N.D	[Hg(II)] = 100000-200000	N.D

3.1. Hg uptake.

Several models have been developed to elucidate the different Hg uptake mechanisms by phytoplankton such as the free metal ion activity model or the biotic ligand model (Campbell et al., 2002). Most of the Hg-complexes are polar and hydrophilic in the extracellular environment and algae membranes are constituted by hydrophobic bilayers. Since the cellular uptake of Hg by phytoplankton has not been elucidated yet, these uptake mechanisms might involve: (***i***) the diffusion of neutral Hg-complexes through the cell wall (passive uptake), (***ii***) the Hg compounds binding to active protein transporters found in extracellular medium and/or (***iii***) the Hg compounds binding to reactive specific spots encountered on the cell wall or membrane followed by a posterior internalization (Le Faucheur et al., 2014). Mason et al., 1996 proposed that MeHg uptake is mainly governed by passive diffusion of uncharged lipophilic chloride complexes in the diatom *Thalassiosira weissflogii* in artificial seawater. Furthermore, another study supported this previous finding affirming that, MeHg passive uptake is related to the surface area of diverse phytoplankton cells (Lee & Fisher, 2016). In contrast, studies in kinetics suggested that, Hg compounds uptake is mainly active (Luengen et al., 2012; Pickhardt & Fisher, 2007). In the cited studies, Hg(II) and MeHg uptake experiments were carried out by comparing living phytoplankton cells with heat killed cells. Both studies suggested that Hg uptake is energy dependent considering that, Hg(II) and MeHg were completely associated to the cell surface in heat killed cells, while Hg compounds were bioaccumulated in living cells in most phytoplankton species.

Inorganic/ organic ligands along with pH have a major impact on Hg compounds uptake. Theoretically, Hg uptake should decrease with low pH values due to the metal-proton competition at the transporter binding sites (active uptake) and changes in cell membrane permeability (Lavoie et al., 2012). However, the enhancement of Hg uptake at low pH (5.5) was reported in the green algae *Chlamydomonas reinhardtii*; being not possible to well explain this unexpected result (Le Faucheur et al., 2011). The role of DOM in Hg compounds uptake is also quite controversial. Whereas high dissolved organic carbon (DOC) concentrations were reported to reduce Hg compounds uptake in marine diatom (Lee & Fisher, 2016), another study documented that Hg compounds internalization was enhanced by an increase of DOC concentrations (Pickhardt & Fisher, 2007). On the other hand, Hg uptake demonstrated to be strongly dependent on the type of LMW thiol compounds. For example, the complexation with Cys enhanced MeHg uptake in *Escherichia coli*, while lowest MeHg uptake was observed in

presence of GSH (Ndu et al., 2012). In agreement with this previous study carried out in bacteria, freshwater green microalga was showed to promote higher MeHg uptake when it was complexed with Cys rather than GSH (Skrobonja et al., 2019); being coherent with the investigation performed in iron reducing bacteria for Hg(II) (Adediran et al., 2019). All studies suggested that simple smaller thiols chemical structure (e.g. Cys) have a greater impact on Hg uptake than large size thiol compounds (e.g. GSH).

3.2. Hg within the phytoplanktonic cells.

Hg(II) and MeHg can be found in different intracellular fractions such as granules, organelles (e.g. mitochondria, chloroplasts), heat denatured proteins (e.g. enzymes) and/ or heat stable proteins (e.g. glutathione and phytochelatins), which represent the four predominant sub-fractions within the cell (Wu & Wang, 2014). The internalization of Hg compounds induce oxidative stress by binding to the sensitive spots into the organelles or heat-denatured proteins (Hg sensitive fraction), whereas the granules and heat stable proteins are the fractions involved in cellular protection (**Figure 1.5**) (Dranguet et al., 2014; Le Faucheur et al., 2014).

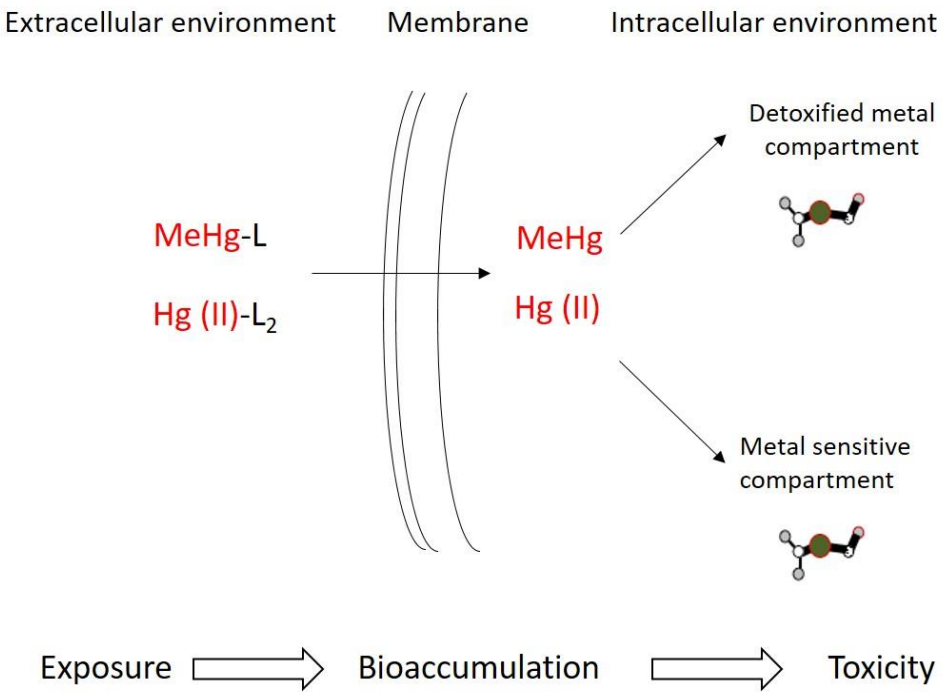

Figure 1.5. Schematic illustration showing the links between Hg exposure, bioaccumulation, toxicity (metal-sensitive compartment) and detoxification (detoxified metal compartment).

3.2.1. Hg induce oxidative stress.

Hg compounds induce oxidative stress within the cell by blocking the functional groups (thiol groups, S-H) of essential biomolecules involved in fundamental cellular processes (Beauvais-Flück et al., 2018). Particularly, the internalization of Hg compounds in chloroplasts or mitochondria and subsequent inhibition of the biomolecules function generate a high content of ROS in these specific organelles (Van Breusegem et al., 2008). In eukaryotic cells, chloroplast are the main ROS production sites due to the functioning of the photosynthetic electron transport chains and high oxygen (O_2) concentration (Gechev et al., 2006). Since cyanobacteria do not contain chloroplasts, the major site of ROS formation is expected to occur in the thylakoids.

Oxidative damage within the cell can be promoted by Hg compounds damage or ROS induced by Hg compounds. The most vulnerable fundamental biomolecules are proteins, DNA, and lipids (Nowicka, 2022). In proteins, Hg compounds can displace essential elements, whereas ROS can oxidize the thiol groups of the cysteine residues of proteins (-SH) into sulfenic (-SOH), disulfides (-S-S-), sulfinic acids ($-SO_2H$) or sulfonic acids ($-SO_3H$) (Cassier-Chauvat, 2014; Imlay, 2013). Disulfide bonds might be formed with two cysteine residues from the same protein or different proteins, leading to the inactivation of the biomolecule function by changing the tertiary or quaternary structure. In DNA, Hg compounds and ROS can induce modification of the nitrogenous bases and sugar residues (Ugya et al., 2020). Furthermore, chloroplasts and mitochondria, where the majority of ROS are generated, enclose their own genetic material making it even more available for DNA oxidative damage.

Earlier studies addressed the toxicological effects of Hg(II) and MeHg by observing the cell morphology, cell growth rate, and photosynthesis activity in phytoplankton microorganisms (Sunda & Huntsman, 1998; Mason et al.1995). Cell growth inhibition was observed when cells were exposed to 10 nM (2 µg L^{-1}) of Hg (II), whereas cells grew properly at 2 nM (0.4 µg L^{-1}). On the other hand, MeHg concentrations above 80 pM (16 ng L^{-1}) was observed to cause a reduction in the growth rate (Mason et al., 1996). Furthermore, different toxicological effects were shown between Hg(II) and MeHg in terms of cell morphology, population growth and photosynthetic activity (Wu et al., 2012). In this previous study, Hg(II) was mainly involved in the inhibition of the photosynthetic activity by blocking the electron transport chain, while MeHg had different intracellular targets. A recent study carried out at Hg compounds subnanomolar concentrations in *Chlamydomonas reinhardtii* revealed that, the reduction of the division rate was promoted by MeHg exposure but not Hg(II) exposure (Beauvais-Flück et al.,

2016). Recently, metabolic responses were assessed for first time in *Chlamydomonas reinhardtii* in order to provide the physiological state of at 50 nM / 10 µg L^{-1} and 5 nM / 1 µg L^{-1} Hg(II) and MeHg concentrations (Slaveykova et al., 2021). In this previous study, Hg(II) exposure showed a faster metabolic response to Hg compounds exposure than alga physiology.

3.2.2. Phytoplankton detoxification strategies to Hg exposure.

Overall, heavy metal detoxification mechanisms in phytoplankton might cover a wide range of strategies. Complexation to detoxifying metal binding biomolecules with thiol groups; formation of high molecular weight (HMW) and LMW insoluble sulphide compounds; excretion of metal binding ligands with EPS; secretion of vesicles containing metals; control of the metal efflux across the membrane, synthesis of enzymatic and non-enzymatic antioxidants to counteract the negative effects of heavy metal induced ROS or the synthesis of polyphosphate granules (PolyP) (**Figure 1.6**).

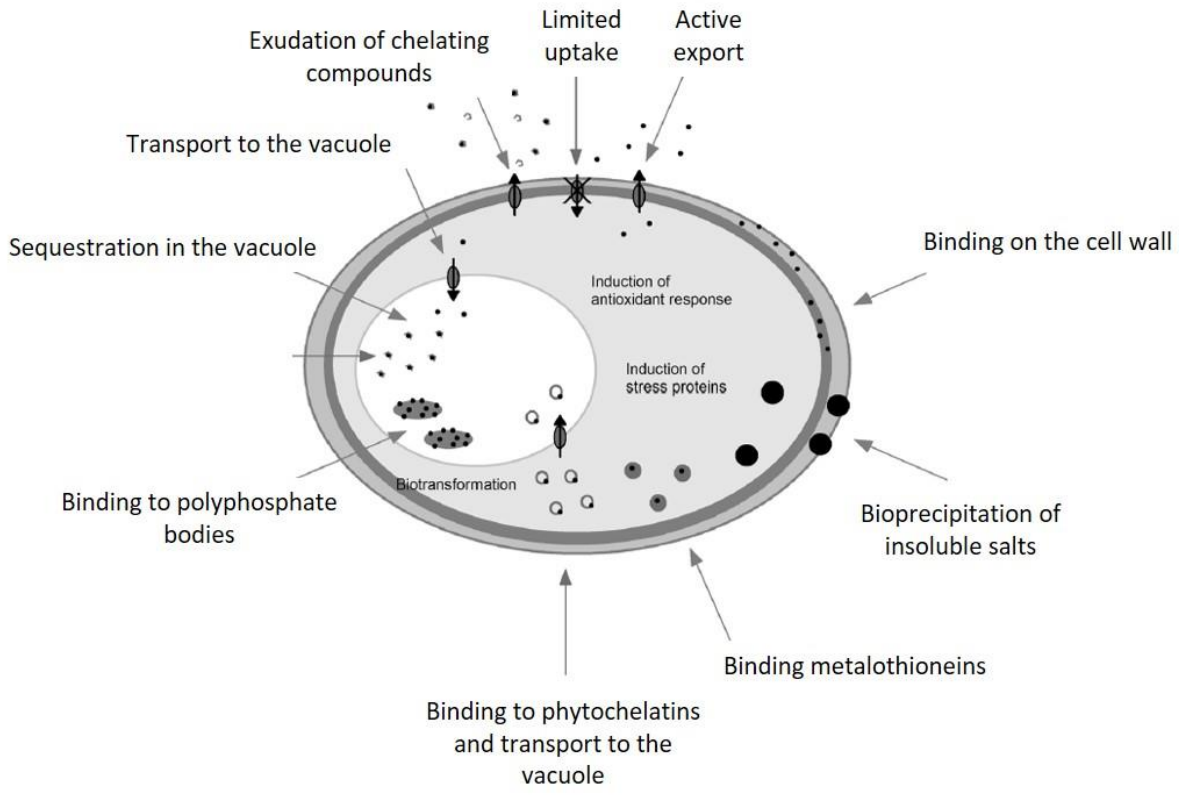

Figure 1.6. Major mechanisms of heavy metal detoxification in algae. In some species, heavy metals are sequestrated not in the vacuole, but in plastid or mitochondria. Figure modified from Nowicka, 2022.

Release / excretion of heavy metals.

Cells control the uptake rate of both toxic and essential metals to maintain their metal intracellular concentrations at the optimal level in function of the inputs needed for the growth and metabolic activities. The secretion of EPS, as extracellular barriers, has been identified to prevent the uptake and toxicity of several heavy metals in phytoplankton and bacteria among others (**Figure 1.7**) (Cassier-Chauvat, 2014; Sunda & Huntsman, 1998). EPS encompasses a wide range of components, such as polysaccharides, proteins, nucleic acids, lipids and humic substances, in which EPS production and composition are highly dependent on the toxicity induced (Naveed et al., 2019). It is known that many alga release into the extracellular medium large amount of EPS containing spots to bind heavy metals (Freire-Nordi et al., 2005). However, the release / excretion of EPS or other LMW thiol compounds containing Hg compounds as detoxification mechanism has not been evidenced yet in phytoplankton.

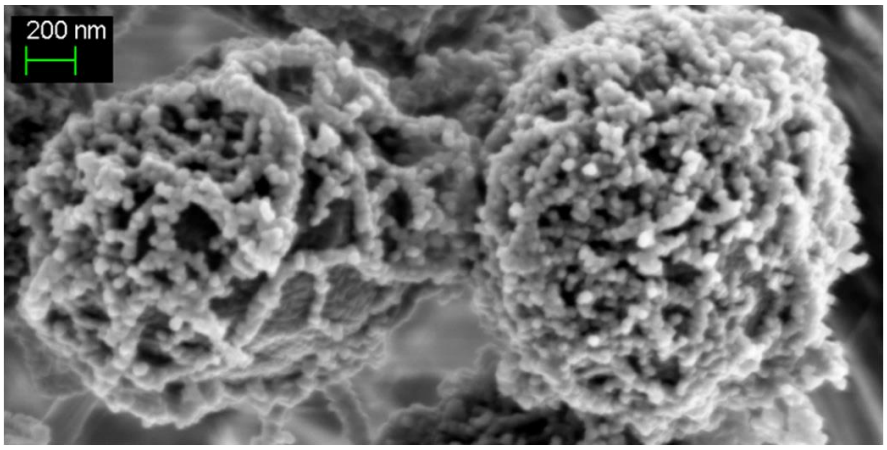

Figure 1.7. SEM (scanning electron microscopy) image of the cyanobacterium Synechocystis sp. PCC 6803 showing the thick mantle of EPS surrounding the cells. Image obtained from Cassier-Chauvat, 2014.

Induction of the antioxidant activity.

In most cases, the responses of phytoplankton to the oxidative stress induced by high Hg concentrations are accompanied by the increase of the activity of antioxidant enzymes (Ugya et al., 2020). Enzymatic antioxidant, such as superoxide dismutases (SODs) are a group of metallo-enzymes (Cu/ZnSOD, MnSOD, FeSOD, and NiSOD) involved in ROS detoxification in both cyanobacteria and eukaryotic algae (Nowicka, 2022). Several studies reported the increase of the enzymatic activity of SODs, APX and catalase (CAT) at micromolar Hg (II) exposure concentration in green algae *Chlamydomonas reinhardtii* (Elbaz et al., 2010) and *Coccomyxa subellipsoidea* (Kováčik et al., 2017). Nevertheless, no changes in the antioxidant enzymatic activity have been addressed under environmental relevant Hg concentrations.

LMW thiol compounds sequestration within the cells.

GSH is present in the cytosol and several sub-cellular compartments between µM–nM concentrations in both prokaryotes and eukaryotes phytoplankton (Ahner et al., 2002; Meister Alton, 1983; Narainsamy et al., 2013, 2016). It represents the major pool of non-protein reduced thiols and can be present in the reduced form (SH) or oxidized form (GS-SG). GSH regeneration is mediated by the enzyme glutathione reductase and it is considered a precursor of phytochelatins (PCs) synthesis, which can be activated due to the Hg exposure (Meister Alton, 1983).

The synthesis of LMW thiol compounds and peptides capable of binding heavy metals is considered the preferential detoxification mechanism against Hg exposure controlling the intracellular Hg speciation (Bellini et al., 2020). For example, an increase of the reduced GSH and PCs content was observed in the marine diatom *Thalassiosira weissflogii* when it was exposed to sub-toxic Hg(II) concentrations (20–160 nM / 4–32 µg L^{-1}) (Morelli et al., 2009). MeHg (25 nM/5 µg L^{-1}) exposure was also shown to induce synthesis of GSH in *Thalassiosira weissflogii*, but it was at higher Hg(II) concentrations (40–1110 nM/ 8–222 µg L^{-1}) that contributed to higher levels of other thiol compounds such as cysteine and PCs (Wu & Wang, 2012, 2013). The comparison of *Thalassiosira weissflogii* with other phytoplantonic species (green algae *Chlorella autotrophica* and flagellate *Isochrysis galbana*) revealed that the biological responses, in terms of PCs induction, were highly dependent on the phytoplanktonic specie. Whereas important biological responses were observed in *Thalassiosira weissflogii,* low PCs induction was observed for the most tolerant specie *Chlorella autotrophica* (Wu & Wang, 2014). The sequestration of Hg(II) binding PCs was identified in the microalga *Chlorella sorokiniana* exposed to 0.5,1,5 and 10 mg L^{-1} of Hg(II) (Gómez-Jacinto et al., 2015). Other studies investigated the potential biotransformations of Hg(II)) into β-HgS and Hg-PCs. Results showed that all algae tested (green algae *Chlorella autotrophica,* flagellate *Isochrysis galbana* and marine diatom *Thalassiosira weissflogii*) could transform Hg(II) into cinnabar (β-HgS) and Hg-PCs complexes (Wu & Wang, 2014). The formation of insoluble β-HgS was suggested to occur in three different cyanobacteria (*Limnothrix planctonica, Synechococcus leopoldiensis* and *Phormidium limnetica*) and four different eukaryotic algae (*Selenastrum minutum, Navicula pelliculosa, Galdieria sulphuraria and Chlorella fusca var. fusca*) under toxic Hg(II) exposure concentrations (100–200 µg L^{-1} / 500–1000 nM) (Kelly et al., 2006; Lefebvre et al., 2007). Both prokaryotic and phytoplankton species were thought to produce, intracellularly, β-HgS to a greater or lesser extent. Overall, phytoplankton might sequester high quantities of Hg

compounds as a detoxification strategy without apparent harmful effects. The tolerance to Hg compounds toxicity has been related to the capacity of the phytoplanktonic cells to capture Hg in subcellular compartments such as vacuoles, which serve as a sink in a mineralize form or bound to LMW thiol compounds. Nevertheless, no information has been ever provided at environmental relevant concentrations.

Polyphosphate granules formation.

Studies using electron and light microscopy have reported the sequestration of heavy metals in mineralized accumulations. Such insoluble structures have a variety of names, but the term of granules is widely accepted. Granules structures are extremely variable in terms of cellular location, structure and chemical composition. Chemical analysis revealed that granules contain high quantities of sulphur suggesting that might be related to reduce thiol groups capable of binding metals. Several studies reported the synthesis of granular polyphosphate bodies as a response of Cd exposure by electron microscopy in *Chlamydomonas reinhardtii* (Aguilera & Amils, 2005). In phytoplankton, granules formation is thought to have a sequestration/ excretion function; however, the formation of granules as Hg detoxification mechanism is still unknown (Lavoie et al., 2016).

4. Chemical speciation methods based on mass spectrometry to understand Hg-phytoplankton interactions.

4.1. Determination of Hg(II) and MeHg using isotope dilution analysis.

Nowadays, the simultaneous determination of Hg(II) and MeHg is usually based on a chromatographic separation (e.g. gas chromatography (GC) coupled to an elemental ionization source (e.g. inductively coupled plasma (ICP)) and mass spectrometer (e.g. quadrupole (MS)). ICP-MS is the most suitable technique for an accurate determination of Hg compounds since it provides detection limits at trace and ultra-trace levels (Clémens et al., 2012; Leopold et al., 2010). Furthermore, its application has been proven in a wide range of matrices and it can be coupled online to either gas chromatography (GC) or liquid chromatography (LC) being useful for elemental speciation analysis (Pröfrock & Prange, 2012). Normally, the analysis of Hg(II) and MeHg by GC-ICP-MS (**Figure 1.8**) requires a derivatization step in which Hg compounds are usually propylated or ethylated and subsequently transferred in organic solvent before the injection into the GC port. This sample preparation may lead to Hg compounds degradation or losses due to incomplete recoveries during the derivatization step. Although the quantification of the Hg compounds can be carried out through several methodological calibration such as external calibration, standards addition and internal standards, only the use of isotopically enriched Hg compounds standards allows the correction of Hg compounds losses during the sample preparation (Rodríguez-González, et al., 2005).

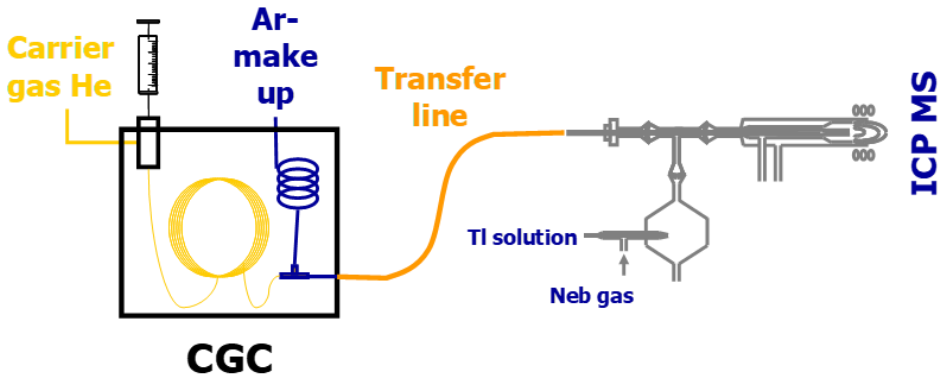

Figure 1.8. Gas chromatography coupled to inductively coupled plasma instrumentation (GC-ICP-MS).

4.1.1. Concept of isotope dilution analysis.

In 1895, C.G.J. Petersen published an article about the estimation of fish population by labelling and returning a part of them to the aquatic ecosystem. After waiting for a period where he

assumed that the labelled fishes were well equilibrated (mixed) with the non-labelled ones, he recaptured a group of them. Knowing the proportion between the labelled and non-labelled fishes in the aliquot collected, he could estimate the total population of fishes in the studied ecosystem, well known as capture-recapture methods (Petersen, 1895). This approach is illustrated in **Figure 1.9** where an unknown number of blue fishes are contained inside a fishbowl. In order to quantify the number of blue fishes, a known number of red fishes is added to the close system. After waiting for the equilibration between both types of fishes, an aliquot is collected where the proportion of red and blue fishes will be equivalent to the total fishes in the fishbowl. Then, isotope dilution analysis (IDA) consist in modifying the isotopic composition of an element or compound inside a sample by the addition of this compound or element enriched in one of its isotopes (Alonso & Rodriguez-González, 2013). The enriched compound added is called tracer or spike.

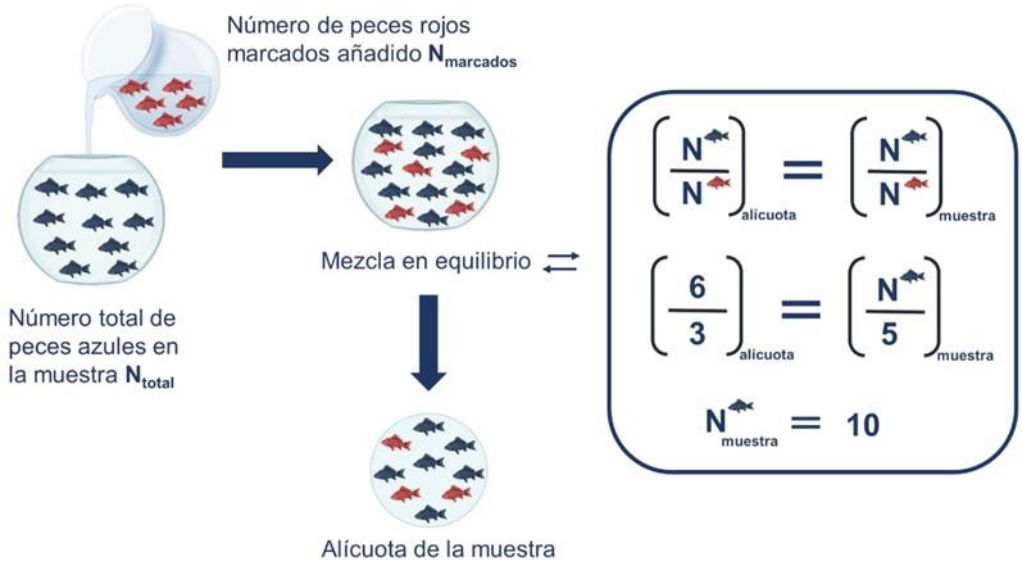

Figure 1.9. Principle of isotope dilution analysis illustrated with labelled and non-labelled fishes (Abad, 2019).

4.1.2. IDA and mass spectrometry: Advantages and requirements.

IDMS is an alternative way of measurement in analytical chemistry that does not require a methodological calibration graph. It is a primary measurement method as it is directly traceable to the international system of units (high metrological quality) used for the certification of reference materials and in the validation of analytical methods. IDMS provides several advantages in comparison with other methodological calibration (e.g. external calibration, standards additions) (Rodríguez-González & García Alonso, 2010):

- Any variation in sensitivity due to instrumental instabilities will have no influence on the final concentration of Hg compounds in the sample.

- Once the isotope equilibration is achieved between the natural and enriched spike (spike means enriched in one isotope), any loss of sample will not affect the final results.

On the other hand, there are several **requirements** that must be taken into consideration:

- Any loss of the analyte from the natural sample or enriched spike before the isotopic equilibration will be an important source of error.

- Once the isotopic equilibration is achieved, the enriched Hg compound must behave identically to the natural throughout the whole analytical process (sample preparation).

- The measurement of the isotopic peak areas in the ICP-MS must be free of spectral interferences.

- An exhaustive control of blanks must be carried out due to a contamination will lead to erroneous results.

- The amount of the enriched compound added must be within a certain range comparing to the natural compound.

4.1.3. Hg compounds transformation during the sample preparation.

The determination of Hg(II) and MeHg has been problematic due to non-quantitative recoveries. Nevertheless, the use of multiple isotopically enriched stable isotopes allowed an accurate and precise quantification of the corrected Hg(II) and MeHg concentrations, the correction of the Hg compounds losses, and the calculation of the Hg compounds interconversion reactions (**Figure 1.10**) during the sample preparation (Castillo et al., 2010). Then, the application of IDMS led to a huge enhancement in terms of data quality in Hg speciation analysis (Björn et al., 2007; Lambertsson et al., 2001; Pablo Rodrıguez-Gonzalez et al., 2006; Rodriguez-Gonzalez et al., 2013; Rodríguez Martín-Doimeadios et al., 2004).

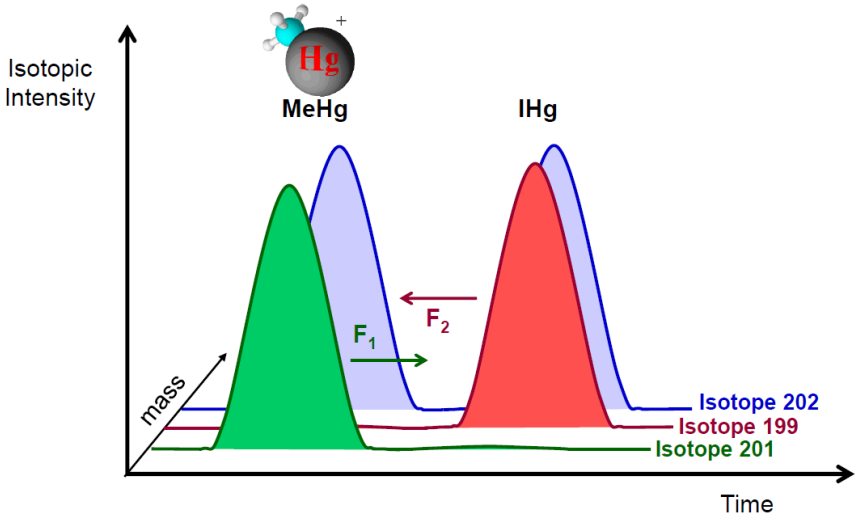

Figure 1.10. F_1 and F_2 correspond to the demethylation of ^{201}MeHg and methylation of ^{199}Hg(II) (IHg) occurred during the sample preparation.

Hg(II) and MeHg quantification by IDA can be carried out by adding both Hg compounds labelled in the same isotope (single compounds-specific spiking) or in different isotopes (multiple compounds-specific spiking). Single compounds-specific has the traditional advantage of isotope dilution analysis. Meaning that, it allows to correct any losses occurred during the sample preparation such as incomplete recoveries. However, these losses can be corrected only when there is no generation of newly formed Hg(II) coming from the original MeHg or MeHg coming from the original Hg(II). In other words, single compounds-specific does not allow correcting interconversion reactions (methylation/demethylation) during the sample preparation. For this purpose, it is necessary to add multiple labelled isotopes for each Hg compound (Castillo et al., 2010; Rodríguez-González et al., 2007; Rodríguez-González & García Alonso, 2010). The first work using multiple compounds-specific for the determination of Hg(II) and MeHg was presented by Hintelmann & Evans, 1997.

Principle based on the mass balance.

The principle of IDA is based on a mass balance of the different Hg compounds present in the mixture (Alonso & Rodriguez-González, 2013). For the simple determination of natural Hg(II) and MeHg, three isotopes are followed. The natural isotope chosen for both Hg compounds is normally ^{202}Hg since it is the most abundant (29.86%). After, the Hg(II) quantification tracer can be labelled in isotope 199 and MeHg is labelled in isotope 201, however different isotopes have been used in different research groups. When both quantification tracers are added to the sample containing the natural Hg compounds, a mass balance can be obtained as seen in Eq. 1.5 and 1.6:

$$N_m^{Hg(II)} = N_{nat}^{Hg(II)} + N_{199}^{Hg(II)} + N_{201}^{Hg(II)} \quad (1.5)$$

$$N_m^{MeHg} = N_{nat}^{MeHg} + N_{201}^{MeHg} + N_{199}^{MeHg} \quad (1.6)$$

Where,

- $N_{199}^{Hg(II)}$ and N_{201}^{MeHg} correspond to the number of moles added from each Hg compound, while $N_{201}^{Hg(II)}$ and N_{199}^{MeHg} are the potential impurities of each Hg compound respectively.

- $N_{nat}^{Hg(II)}$ and N_{nat}^{MeHg} correspond to the number of moles that we want to quantify.

- $N_m^{Hg(II)}$ and N_m^{MeHg} correspond to total amount moles from each Hg compound.

The quantification of $N_{nat}^{Hg(II)}$ and N_{nat}^{MeHg} requires knowing the concentration, isotopic abundances and impurities of each quantification tracer. Once the isotopic equilibration is achieved, different interconversion reactions might occur during the sample preparation. Here, the ^{199}Hg(II) methylation into ^{199}MeHg is called F1,whereas the demethylation of ^{201}MeHg forming ^{201}Hg (II) is called F2. Then, the number of moles of each Hg compound interconverted can be taken into account by rewriting the equation 1.5 and 1.6 as:

$$N_m^{Hg(II)} = \left(N_{nat}^{Hg(II)} + N_{199}^{Hg(II)} + N_{201}^{Hg(II)}\right) \times (1 - F2) + \left(N_{nat}^{MeHg} + N_{201}^{MeHg} + N_{199}^{MeHg}\right) \times F1 \quad (1.7)$$

$$N_m^{MeHg} = \left(N_{nat}^{MeHg} + N_{201}^{MeHg} + N_{199}^{MeHg}\right) \times (1 - F1) + \left(N_{nat}^{Hg(II)} + N_{199}^{Hg(II)} + N_{201}^{Hg(II)}\right) \times F2 \quad (1.8)$$

In order to solve these mass balances (Eq.1.7 and Eq.1.8) and obtain the amount of moles for each natural Hg compound in turns with F1 and F2, several mathematical models have been developed in the past applying this principle to Hg and other chemical species such as tin (Sn) or chromium (Cr) for example (Hintelmann & Evans, 1997; Huo & H.M. Kingston, 2000; Meija et al., 2006; Monperrus et al., 2008; Ouerdane et al., 2009; Rahman & Kingston, 2004; Rodríguez-González et al., 2007; Rodríguez-González, Rodríguez-Cea, et al., 2005; Rodıguez-Gonzalez et al., 2004).

Rodríguez-González et al., 2007 compared four different mathematical models for Sn speciation analysis based on (**1**) the first work reporting on multiple spiking compounds-specific developed by Hintelmann and Evans in 1997 (Hintelmann & Evans, 1997) called "Calculation of Stable Isotope Concentrations ", (**2**) the work developed by Kingston and co-workers called "Speciated Isotope dilution analysis" able to correct the bidirectional

degradation of Cr(III) and Cr(VI) (Huo & H.M. Kingston, 2000), later applied for Hg(II) and MeHg (Rahman & Kingston, 2004), (**3**) the equations developed by Ruiz Encinar et al., 2002 for the determination of butyltin compounds, and (**4**) the application of isotope pattern deconvolution (IPD) developed by Meija and co-workers (Meija et al., 2006). Results revealed that the four methodologies provided the same corrected concentrations of Sn compounds and similar transformation factors, however, the matrix model based on isotope pattern deconvolution (IPD) was the most valuable tool based on the analytical figures of merit, lower mathematical complexity, and the ability of extension to a higher number of species and isotopes.

4.1.4. Isotopically enriched Hg compounds as biological and environmental tracers.

Although isotopically enriched Hg compounds have been mainly used as analytical tracers to correct Hg losses during the sample preparation, the use of enriched Hg compounds as incubation tracers for environmental and biological studies has grown over the last two decades. The incubation of isotopically enriched Hg compounds allows determining the potential methylation and demethylation yields in environmental or biological samples. Hintelmann and co-workers carried out the first study that combined the use of enriched Hg stable isotopes as environmental tracers with GC-ICP-MS instrumentation in 1995 (H.Hintelmann et al., 1995). Hg methylation yields were determined by adding enriched ^{199}Hg (II) to sediments slurries and the ^{199}MeHg produced was calculated by measuring the isotopic ratios. Once the enriched ^{199}Hg(II) was added to a sediment, the isotopic ratio between the ^{199}Hg and ^{202}Hg (reference isotope) was modified from the natural ratio to a higher value. Later, the simultaneous incubation of isotopically enriched Hg(II) and MeHg was used for determining the potential methylation and demethylation yields simultaneously using different enriched isotopes for each Hg compound (Hintelmann et al., 2000; Hintelmann & Evans, 1997). Here, the demethylation yields were measured based on the loss of MeHg instead of determining the newly-produced Hg(II). In addition to this, they could not provide the distinction of the Hg compounds interconversion processes during the analytical procedure and incubation process. For this purpose, Lamberson and coworkers proposed an alternative way to correct the both Hg compounds (Hg(II) and MeHg) transformations (incubation and analytical) by adding two enriched environmental tracers and two analytical tracers for Hg(II) and MeHg respectively (Drott et al., 2008a; Lambertsson et al., 2001). Here, the mathematical approach used required an isotopic enrichment higher than 99 % in order to avoid contributions coming from other isotopic sources, but also, they could not discriminate between MeHg demethylation into Hg(0)

or into Hg(II). The quantification of MeHg and newly-formed Hg(II) was, for first time, achieved by applying the deconvolution of isotopic patterns (IPD) in coastal waters and surface sediments (Rodriguez-Gonzalez et al., 2013). In this previous work, natural Hg standards were used as analytical tracers (single compounds-specific) and it was assumed, under previous optimized conditions, the non-existence of any analytical transformation/degradation during the sample preparation.

Nowadays, many studies have provided the Hg(II) methylation and MeHg demethylation potentials through the incubation of isotopically enriched Hg compounds in several environmental compartments (Achá et al., 2012; Bouchet et al., 2013, 2018; Cossart et al., 2021; Gascón Díez et al., 2016; Hamelin et al., 2015; Monperrus et al., 2007; Ranchou-Peyruse et al., 2009; Sharif et al., 2014), bacteria and phytoplankton cell cultures (Bravo et al., 2014; Bridou et al., 2011; Li et al., 2022; Pedrero, et al., 2012). Indeed, the use of four isotopically enriched compounds during field incubations (^{199}Hg(II) and ^{201}MeHg as incubation tracers and ^{198}Hg(II) and ^{202}MeHg as quantification tracers) have been recently published by Bouchet et al., 2018, 2022 applying IPD. However, the distinction between methylation and demethylation yields during the incubation process and sample preparation have never been provided.

The main limitation of working with isotopically enriched Hg compounds is based on the assumption that the exogenous isotopically enriched Hg compounds incubated will behave identically during the incubation process as the endogenous natural abundance Hg compounds present already in the sample. Indeed, a recent study suggested that isotope exchange took place between Hg(II) chloride and Hg(II) bound to minerals and thiolate ligands (Zhang et al., 2021). The concepts of "isotope exchange" between endogenous (natural/ambient) and exogenous (enriched) Hg compounds is important for determining environmental reactivity before reaching the isotopic equilibration of both pools. In the aqueous phase, endogenous Hg compounds are already complexed with ligands occurring in the environmental matrix, while exogenous Hg compounds are externally added to the system. Furthermore, the addition of exogenous Hg compounds may influence the biogeochemical reactivity of endogenous Hg compounds already "equilibrated" in the system (Zhang et al., 2021). Furthermore, the addition of isotopically enriched or natural abundance Hg compounds may also promote artificial specific transformations such as reduction, methylation or demethylation until a steady-state (chemical equilibrium) is reached (Graham et al., 2012; Rodriguez-Gonzalez et al., 2013; Wang et al., 2020). However, the pre-equilibration of the Hg compounds should minimize these non-desirable reactions and better mimic the behaviour of both endogenous and exogenous Hg

compounds as shown in Rodriguez-Gonzalez et al., 2013. The importance of pre-equilibrated or non-prequilibrated the exogenous Hg compounds before the addition to the matrix is a critical step that would also depend on the hypothesis/question to be tested. For example, Jonsson et al., 2014 carried out a model water-sediments mesocosm using five different isotopically enriched Hg isotopes. In sediments, isotopically enriched Hg(II) and MeHg compounds were pre-complexed with natural organic matter (NOM) and cinnabar ($HgS_{(s)}$), while labile $HgCl^{+}$ and MeHgCl were added simulating new Hg inputs to the aqueous phase. The main aim of this study was to investigate the MeHg formation and bioaccumulation in sediments in function of the Hg compounds-specific availability in different geochemical pools. In laboratory experiments, isotopically enriched Hg compounds have also been used to study Hg bioaccumulation and transformations in plants (Strickman & Mitchell, 2017), phytoplankton (Bravo et al., 2014; Garcia-Calleja et al., 2021) and bacteria (Bridou et al., 2011; Pedrero, et al., 2012) however, cell culture experiments are always based on external additions.

4.2. Determination of Hg(II) and MeHg binding bioligands using liquid chromatography coupled to mass spectrometry techniques.

The determination of Hg binding bioligands (e.g., proteins, metabolites, enzymes and LMW thiol compounds) is of interest in studies of (1) uptake and bioavailability of Hg, (2) Hg bioaccumulation, distribution and localization and (3) defence mechanisms against oxidative stress induced by Hg, and the alteration of metabolic pathways triggered by overexpression of biomolecules involved in Hg handling or inhibition of essential biomolecules involved in the cell metabolism. For these aims, the physico-chemical forms of Hg-complexes requires the applicability of chromatography techniques for the separation of Hg-biocomplexes and specific detection/identification. Consequently, liquid chromatography (LC) coupled to ICP-MS is considered the most popular technique since it has the capability to separate soluble Hg-biocomplexes and isotope monitoring by ICP-MS (Lobinski et al., 2010).

Several analytical approaches have been applied for determining Hg-biocomplexes in living organisms (**Table 1.3**). For example, size exclusion chromatography (SEC-ICP-MS) has demonstrated to be a useful tool to investigate the distribution of different size ranges of Hg binding biomolecules; maintaining the physiological conditions and reducing the potential Hg binding biomolecule decomplexation. It allows the fractionation of metal binding biomolecules as a function of size prior detection. Although SEC does not have the resolution to separate biomolecules of similar sizes; it is probably the first approach to study the speciation and size

distribution of Hg binding biomolecules (Pedrero et al., 2012; Pedrero et al., 2011; Pedrero et al., 2014). For example, this technique allowed to detect changes in the screening of Hg binding bioligands during the exposure periods of a mouse liver and kidney (García-Sevillano et al., 2014). Results revealed that Hg interacted with biomolecules containing Cu and Zn affecting negatively to the homeostasis of these essential metals. The screening of Hg binding biomolecules in the while-sited dolphin liver in combination with the quantification of Hg(II) and MeHg by IDA-GC-ICP-MS provided the percentage of MeHg and Hg (II) containing in size fractions (Pedrero et al., 2011). Similar approach was used in a methylating and non-methylating bacteria (Pedrero, et al., 2012). In this case, isotopically enriched Hg compounds (^{199}Hg(II) and ^{201}MeHg) were incubated in the bacteria cell culture and the screening of Hg binding bioligands in the cytoplasmic and extracellular fraction showed that the newly-formed ^{199}MeHg was mainly bound to bioligands between 70–17 kDa released by bacteria (**Figure 1.11**).

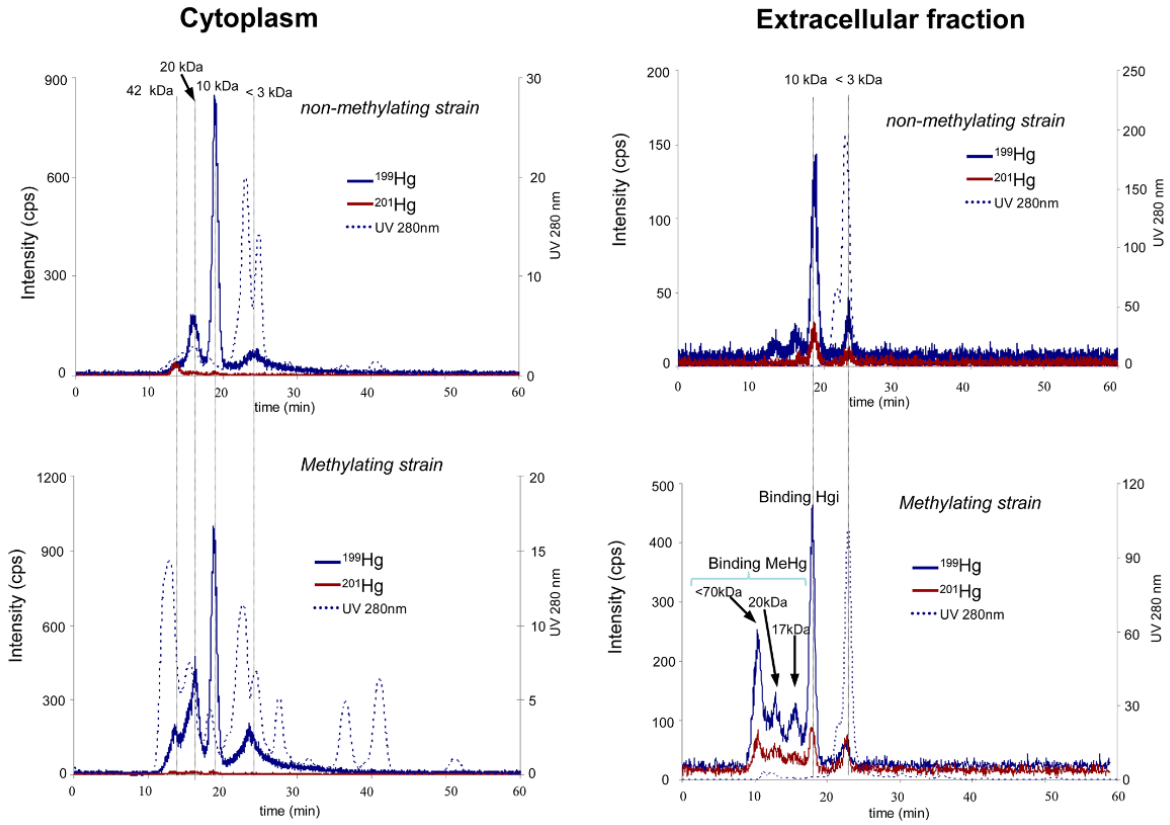

Figure 1.11. Typical size exclusion chromatograms corresponding to the UV (280 nm)/ICP-MS detection of different Hg isotopes (^{199}Hg and ^{201}Hg) in the cytoplasmic and extracellular fractions obtained from Pedrero, et al., 2012.

On the other hand, the molecular identification of Hg-biocomplexes by parallel detection in biological samples have been achieved though reverse phase (RP) LC-ICP/ESI-MS and HILIC-ICP/ESI-MS (**Table 1.3**). The identification of hemoglobin, as a major binding protein for

MeHg in dolphin liver, was achieved through the parallel detection of RPLC by ICP-MS and ESI-MS (Pedrero et al., 2014). Results revealed that cysteine residue on the dolphin hemoglobin β chain was the main MeHg binding site. Using the same approach, Hg-phytochelatin complexes were identified in plants that were exposed to high Hg(II) concentrations (Chen et al., 2009; Iglesia-Turiño et al., 2006; Krupp et al., 2009). In these previous studies, the findings showed evidences for the understanding of the detoxification mechanisms and accumulation of plants towards Hg exposure in which induced phytochelatins plays a fundamental role in Hg sequestration reducing the oxidative stress induced by Hg. Another study identified, for the first time, Hg binding metallothioneins in dolphin livers by HILIC-ICP/ESI-MS (Pedrero, et al., 2012). Nowadays, HILIC coupled to of ICP-MS and ESI-MS (parallel detection) seem to provide the best adequate methodology for the *in vivo* structural identification of LMW Hg-biocomplexes at nanomolar level. Since the identification of Hg binding HMW proteins requires several purification steps, so far, the identification has been limited to small polar biomolecules. For HILIC-ICP-MS/ESI-MS analysis, acetonitrile must be added to aqueous samples in order to precipitate of most proteins (>10 kDa) (AlChoubassi et al., 2018). As a result, the use of HILIC is mainly limited to small Hg-biocomplexes (<10 kDa).

The existing literature of Hg biocomplexes characterization in aquatic microorganisms is reduced in terms of molecular mass spectrometry characterization. X-ray absorption fine structure (EXAFS) spectroscopy analysis can also be used to elucidate the structural characterization of thiol functional groups among others (O/N) binding Hg(II) in bacteria (Song et al., 2020) and in freshwater ecosystems (Song et al., 2018). A recent study revealed that the molecular composition of Hg binding dissolved organic matter (DOM) released by phytoplankton (Mangal et al., 2019). This analytical approach is focused on the bonding environment of local functional groups rather than the identification of intact Hg-biocomplexes.

Table 1.3. Summary of the studies for the determination of Hg binding bioligands in living organisms using hyphenated techniques based on elemental and/or molecular mass spectrometry.

Hg species investigation	Matrix/Sample	Instrumentation	Reference
Size distribution of Hg(II) and MeHg binding biomolecules	Dolphin liver	SEC-ICP-MS (Superdex 200; Range: 10-600 kDa) GC-ICP-MS	Pedrero et al. 2010
Hg-metallothioneins	Dolphin liver	HILIC-ICP-MS HILIC-ESI-LTQ Orbitrap-MS/MS	Pedrero et al. 2012
MeHg- hemoglobin	Dolphin liver	RP-ICP-MS RP-ESI-LTQ Orbitrap-MS/MS	Pedrero et al. 2014
^{199}Hg (II) and ^{201}MeHg biocomplexes size distribution	Sulfate-reducing bacteria	SEC-ICP-MS (Superdex 75; Range : 3-70 kDa) GC-ICP-MS	Pedrero et al. 2012
Hg (II) binding biomolecules size distribution Hg-phytochelatins (Hg-PCs)	Mouse kindey,blood plasma and liver	SEC-ICP-MS (Superdex 75; Range : 3-70 kDa) DIMS	García Sevillano et al. 2014
Hg-phytochelatins (Hg-PCs)	Plants	RP-HPLC-ICP-MS RP-HPLC-ESI-MS	Krupp et al. 2009
Hg-PCs	Plants	RP-HPLC-ESI-MS/MS (QQQ)	Chen et al. 2009
MeHg-LMW thiols	Sulfate-reducing bacteria	HPLC-ESI-MS/MS (QQQ)	Liem-Nguyen et al. 2020

5. Objectives.

In the general introduction, the reactivity of Hg compounds using isotopically enriched Hg compounds have been observed to be a useful tool to address Hg compounds transformation potentials in different environmental compartments. However, there is still a lack of information about the calculation of Hg(II) methylation and MeHg demethylation yields between the incubation process and sample preparation. Based on the current knowledge, the **first objective** of the present doctoral work is:

(1) To develop, evaluate and provide the most adequate analytical methodologies to address Hg compounds transformations potentials in Hg incubation experiments with isotopically enriched Hg compounds.

To achieve the first objective (**Chapter 2**), the calculations of isotope dilution analysis based on IPD have been revisited for the development and evaluation of two mathematical models based on IPD. Furthermore, the application of the methodology was carried out in biofilms, sediments, freshwaters and phytoplankton cell cultures at different Hg concentration levels (from pg L^{-1} to µg L^{-1}). The final goal was to discriminate between the methylation and demethylation yields during the incubation process and sample preparation, but also, the distinction between MeHg demethylation potentials coming from the decrease of MeHg concentration and the formation of Hg(II) (**Chapter 2.1**). By taking advantage of isotope pattern deconvolution approach, the development of an additional methodology was carried out for the determination of simultaneous reduction pathways (Hg(II) reduction and reductive MeHg demethylation) leading to the formation of dissolved gaseous mercury (DGM) in unfiltered surface freshwater and seawater samples (**Chapter 2.2**). In the third part of chapter 2, we present an experimental design based on the double incubation of isotopically enriched Hg compounds in two consecutive 48 hours processes for the specific determination of the biotic MeHg demethylation in pure phytoplankton cell cultures (**Chapter 2.3**).

On the other hand, the general introduction highlighted that, no studies have ever investigated the Hg intracellular handling at non-toxic Hg exposure levels in pure phytoplankton cell cultures. Most studies were carried out under non-reliable Hg concentrations (**Table 1.2**). Based on this, the **second objective** of this doctoral work is:

(2) To investigate and characterize the major intracellular bioligands involved in Hg speciation in three different model phytoplankton organisms at low Hg exposure levels.

The second objective involved, at first, a methodological approach to collect the different fractions (extracellular medium, whole cells, cytosolic fraction, and membranes + cell debris) in three different cell culture phytoplankton microorganisms, and an analytical approach for the characterization of Hg binding intracellular bioligands and identification of Hg binding LMW bioligands (**Chapter 3.1**). Therefore, the role of the potential intracellular bioligands involved in Hg speciation and Hg intracellular handling was carried through: (***i***) the tracking of isotopically enriched Hg compounds between the different (sub-) cellular fractions over time, (***ii***) the changes in the screening of the size fractions containing Hg(II) and MeHg over time, and (***iii***) the identification of Hg compounds binding LMW bioligands in the intracellular fraction of the diatom, *Cyclotella meneghiniana* (**Chapter 3.2**) and the cyanobacterium, *Synechocystis* sp. PCC 6803 (**Chapter 3.3**). The comparison between the outcomes obtained for both phytoplankton species are shown in **Chapter 3.4**. Furthermore, the results obtained for the green alga *Chlamydomonas reinhardtii* (**Annexes C.3**). The conclusions and perspectives of this doctoral dissertation are presented in **Chapter 4**.

Chapter 2

Analytical and experimental approaches using isotopically enriched Hg compounds

Chapter 2: Analytical and experimental approaches using isotopically enriched Hg compounds.

Summary.

Isotopically enriched Hg isotopes have been used for the determination of Hg compounds transformations. However, the analytical methodologies applied for determining these transformations should be better clarified. The aim of this chapter is to provide reliable and tested analytical methodologies based on isotope pattern deconvolution (IPD) as tools to study the compounds-specific Hg compounds transformations potentials in natural samples with isotopically enriched Hg compounds (^{199}Hg(II) and ^{201}MeHg). The first part includes the development of two mathematical models based on isotopic pattern deconvolution (IPD) with the purpose of discriminating and determining the methylation and demethylation yields during both, the incubation process and sample preparation. The performance of this methodology is tested through three model incubation experiments, in which the ratio of incubation tracers (MeHg:Hg (II)) varied from ca. 1:1 up to 10:1. Finally, the methodology is applied for determining Hg(II) methylation and MeHg demethylation potentials in natural samples (biofilms, sediments, freshwaters and phytoplankton cell cultures assays) with Hg concentrations ranging from pg L^{-1} to µg L^{-1}. In the second part, IPD is used, in combination with an external calibration, to calculate the compounds-specific DGM formation coming from ^{199}Hg(II) and ^{201}MeHg. The final objective is to compare Hg(II) reduction and reductive MeHg potentials between selected unfiltered surface freshwater and seawater samples. The third part consists in a novel experimental design involving the incubation of isotopically enriched Hg compounds in two consecutive 48 hours processes. The main goal is to determine the biotic MeHg demethylation in pure phytoplankton cell cultures.

1. Simultaneous determination of Hg(II) methylation and MeHg demethylation yields in Hg incubation experiments.[1]

1.1. Introduction.

The toxicological impacts of mercury (Hg) have been addressed since the last century. However, the understanding of Hg reactivity in the environment still needs further studies. Although Hg reduction/oxidation are the main processes involved in Hg exchange within the three main environmental compartments (terrestrial, atmospheric and aquatic), inorganic mercury (Hg(II)) can also be transformed into methylmercury (MeHg) through several biotic and/or abiotic processes in aquatic ecosystems (Bishop et al., 2020; Gworek et al., 2020; Klapstein & O'Driscoll, 2018; Soerensen et al., 2014; Whalin et al., 2007). The study of Hg(II) and MeHg reactivity is a fundamental step towards an accurate reading of the correlated complex processes occurring in aquatic environment. Nowadays, isotopically enriched Hg tracers are being used for two main purposes: ***i***. to quantify accurately Hg compounds when interconversion reactions and/or incomplete recoveries occur during sample preparation (see more information in **page 27**) and ***ii***. to study the *in situ* Hg compounds reactivity in environmental matrices (Bouchet et al., 2018, 2022) and cell cultures experiments with aquatic microorganisms (e.g. bacteria, phytoplankton) (see more information in **page 30**). Nevertheless, no distinction of the methylation or demethylation yields between the incubation process and sample preparation have been ever proposed.

The main objective of this work was to provide a reliable and tested analytical methodology to study the methylation and demethylation processes in natural samples. For this reason, two mathematical models (a "step by step" model and a "direct determination" model) based on isotope pattern deconvolution (IPD) have been developed. Both models provided the same results, and allowed to determine simultaneously and accurately: **(1)** the endogenous (natural/ambient) and exogenous (enriched) Hg(II) and MeHg concentration (+ newly-formed) corrected from the unintentional interconversion processes occurring during the sample

[1] *(Manuscript in preparation)*

Authors: Javier Garcia-Calleja, Laura Suarez-Criado, João P. Santos, Sylvain Bouchet, Emmanuel Tesier, Pablo Rodríguez-González, Zoyne Pedrero Zayas, Vera I. Slaveykova, J.I. García Alonso, and David Amouroux.

Javier Garcia Calleja: Development of the mathematical equations of the quadruple tracer methodology and performance of three model incubation experiments and phytoplankton cell cultures incubation with enriched Hg compounds.

preparation and, **(2)** the Hg(II) methylation and MeHg demethylation yields during the sample preparation and the incubation process. The robustness of this quadruple tracer methodology (two isotopically enriched Hg compounds as incubation tracers and two as quantification tracers) was assessed through three model incubation experiments, in which a microwave (MW) digestion was used to stimulate the Hg(II) methylation and MeHg demethylation containing in the tetramethylammonium hydroxide (TMAH) solution. The final procedure was to apply the methodology in different Hg incubation experiments involving biofilms, sediments, freshwaters, and phytoplankton cell culture assays. The endogenous and exogenous Hg(II) and MeHg concentration in the natural samples ranged from pg L^{-1} to µg L^{-1}.

1.2. Material and methods.

1.2.1. Reagents and standards.

Model incubation experiments.

Isotopically enriched ^{202}Hg inorganic mercury and ^{201}Hg methylmercury were employed as incubation tracers (exogenous Hg compounds), while ^{198}Hg inorganic mercury and ^{199}Hg methylmercury were employed as quantification tracers. All these tracers were obtained from ISC-Sciences (Oviedo, Spain). Stock solutions of natural abundance Hg(II) and MeHg were also obtained from ISC-Sciences. All solutions were prepared using ultrapure water (18 MΩ cm, Millipore). All samples and standards were prepared with trace metal grade acid (Sigma-Aldrich). Working Hg(II) standard solutions were prepared daily by appropriate dilution of the stock standard solutions in 1% of ultrapure sub-boiled hydrochloric acid (HCl) in Milli-Q water and stored at 4 °C until use. Working MeHg standard solutions were diluted with 3:1 mixture of acetic acid (Merck, Darmstadt, Germany) and methanol (Sigma-Aldrich) and stored at –18°C until use. Hg compounds were digested in tetramethylammonium hydroxide (TMAH) (Sigma-Aldrich). Hg compounds were derivatized by using sodium (tetra-n-ethyl) borate 2% (w/v %) solution (LGC-Standards, Wesel, Germany). Hg compounds were extracted in hexane (Sigma-Aldrich). As a remainder, natural abundance Hg(II) and MeHg were used as "endogenous Hg compounds". Isotopically enriched ^{202}Hg(II) and ^{201}MeHg were employed as "exogenous Hg compounds" (incubation tracers) in the model incubation experiments. Hg isotopic composition of all tracers is given in **Table 2.1.**

Table 2.1. Isotope composition (at %) of natural abundance of mercury and the different tracers used for the model incubation experiments.

Isotope mass	Natural mercury	^{202}Hg enriched Hg(II)	^{201}Hg enriched MeHg	^{198}Hg enriched Hg(II)	^{199}Hg enriched MeHg
198	9.97	0.04	0.05	93.23	1.46
199	16.87	0.09	0.11	4.95	92.61
200	23.10	0.24	0.85	1.00	4.61
201	13.18	0.10	96.74	0.34	0.64
202	29.86	99.53	2.25	0.47	0.68

Natural samples.

Isotopically enriched ^{199}Hg inorganic mercury and ^{201}Hg methylmercury were obtained from ISC-Sciences (Oviedo, Spain) and employed as incubation tracers in biofilms, sediments, freshwaters and phytoplankton cell culture assays. On the other hand, enriched ^{198}Hg inorganic mercury and ^{202}Hg methylmercury were used as quantification tracers. Enriched isotopic abundances varied as a function of the isotopically enriched standards solution lots used at different periods (**Table 2.2** and **Table 2.3**). More information about the reagents and standards for biofilms, sediments and freshwaters incubation is provided in Bouchet et al., 2018, 2022.

Table 2.2. Isotope composition (at %) of natural abundance of mercury and the different tracers used for biofilms, sediments ande freshwaters.

Isotope mass	Natural mercury	^{202}Hg enriched MeHg	^{201}Hg enriched MeHg	^{198}Hg enriched Hg(II)	^{199}Hg enriched Hg(II)
198	9.97	2.36	0.00	90.38	1.56
199	16.87	2.46	0.46	5.15	91.90
200	23.10	2.39	0.52	1.20	4.86
201	13.18	2.98	97.37	0.45	0.73
202	29.86	89.80	1.66	2.78	0.95

Table 2.3. Isotope composition (at %) of natural abundance of mercury and the different tracers used for phytoplankton cell culture assays.

Isotope mass	Natural mercury	^{202}Hg enriched MeHg	^{201}Hg enriched MeHg	^{198}Hg enriched Hg(II)	^{199}Hg enriched Hg(II)
198	9.97	0.39	0.00	90.82	1.20
199	16.87	1.76	0.10	5.15	91.40
200	23.10	1.00	0.90	1.20	4.10
201	13.18	1.7	96.50	0.45	0.90
202	29.86	95.08	2.40	2.78	1.80

1.2.2. Instrumentation.

A gas chromatography model Agilent Technologies 7890A (Agilent Technologies, Tokyo, Japan) with a DB-5MS capillary column from Agilent J&W Scientific (cross-linked 5% diphenyl, 95% dimethylsiloxane, 30m x 0.53 mm i.d. x 1.0 μm) coupled to a quadrupole inductively coupled plasma mass spectrometer Agilent 7900 was employed for the quantification of endogenous and exogenous Hg compounds in the model incubation experiments. On the other hand, a Thermo Electron GC (Trace) coupled to a Thermo Electron ICP-MS (X7 X series) was used for the determination of endogenous and exogenous Hg (II) and MeHg compounds in natural samples. Although different columns have been used, the separation of Hg(II) and MeHg have been achieved in both cases. Sample digestions were performed with a focused microwave Explorer Hybrid from CEM Corporation (Matthews, NC) in the model incubation experiments.

Table 2.4. Operating parameters for Gas Chromatography coupled to Inductively Coupled Plasma Mass Spectrometry (GC-ICP-MS) analysis of endogenous and exogenous Hg compounds used for the model incubation experiments and natural samples.

Parameters	**GC-ICP-MS (Model incubation experiments)**	**GC-ICP-MS (Natural samples)**
Type of column	DB-5MS (5% diphenyl, 95% dimethylsiloxane, 30m x 0.53mm i.d. x 1μm)	R x 1-5ms Crossbond 5% diphenyl/ 95% polysiloxane (30m x 0.25mm x 0.25μm)
Injector Mode	Splitless	Splitless
Injector Temperature	250 ºC	250 ºC
Interphase Temperature	270 ºC	280 ºC
Injection volume	2μL	2μL
Carrier flow rate	5mL/min (He)	5mL/min (He)
Acquisition mode	Transient Time Resolved Analysis	Transient Time Resolved Analysis
Acquisition Time	300sec	300sec
Dwell Time	30ms	20ms
Isotopes measured	^{196}Hg, ^{198}Hg, ^{199}Hg, ^{200}Hg, ^{201}Hg, ^{202}Hg, ^{204}Hg, ^{203}Tl, ^{205}Tl	^{196}Hg, ^{198}Hg, ^{199}Hg, ^{200}Hg, ^{201}Hg, ^{202}Hg, ^{204}Hg, ^{203}Tl, ^{205}Tl

1.2.3. Experimental procedure.

Model incubation experiment.

The scheme for the model incubation experiments is shown in **Figure 2.1**. First, weighed amounts of natural abundance Hg(II) and MeHg were added to MW digestion vials containing 5 ml of TMAH (25 %), reaching constant concentrations between 0.3–0.7 mg L^{-1} in the sample. The addition of natural Hg compounds simulates the endogenous Hg compounds in an environmental matrix. Then, weighed amounts of exogenous Hg compounds, with concentrations ranging from 0.3 to 3 mg L^{-1} (Ratio ^{201}MeHg:^{202}Hg(II) 1:1. 3:1 and 10:1) were added to the same MW vial containing endogenous Hg compounds. Subsequently, the MW vial was subjected to MW irradiation (100 °C, 12 min, 150 W) to force the Hg(II) methylation (M_1) and MeHg demethylation (D_1) (each condition was performed in triplicate). After the first MW treatment, weighed amounts of ^{198}Hg(II) and ^{199}MeHg (quantification tracers), previously characterized in terms of isotopic abundances and concentration, were added to the same MW vial, and a second digestion process was carried out. In this second digestion, additional methylation (M_2) and demethylation (D_2) reactions could take place. Once the second MW treatment finished, 5 mL of an acetic acid/acetate buffer (0.1 M, pH 3.9) were aggregated to the vials.

From now on, the sample preparation was similar between the model incubation experiments and natural samples. First, the pH must be adjusted to 3.9 using additions of ultrapure NH_3 and/or HCl solutions (Optima Grade). After, the sample was derivatized using 70 µL of sodium (tetra-n-ethyl) borate 2% (w/v %) ($NaBrEt_4$) and 250–500 µL of GC organic solvent (hexane for the model incubation experiments and isooctane for the natural samples) were added. After an agitation step of 20 min using an elliptic table, the organic phase containing Hg compounds is recovered and transferred in a GC vial equipped with a 200 µL micro insert. Finally, derivatized samples were stored at -20 °C until analysis before injection in the GC-ICP-MS. The resulting organic extracts were injected in the GC-ICP-MS with the operating parameters detailed in **Table 2.4**. Integration of the chromatographic peaks was carried out by using the commercial software Agilent Mass Hunter for the model incubation experiments and Thermo PlasmaLab for the natural samples. A typical chromatogram obtained for the model incubation experiments is shown in **Figure 2.2**. The quantification of endogenous and exogenous Hg compounds and the determination of the different interconversion yields (methylation/demethylation) corresponding to the incubation process and analytical procedure

was carried out by applying isotope dilution analysis (IDA) based on isotope pattern deconvolution (IPD) described in the next section.

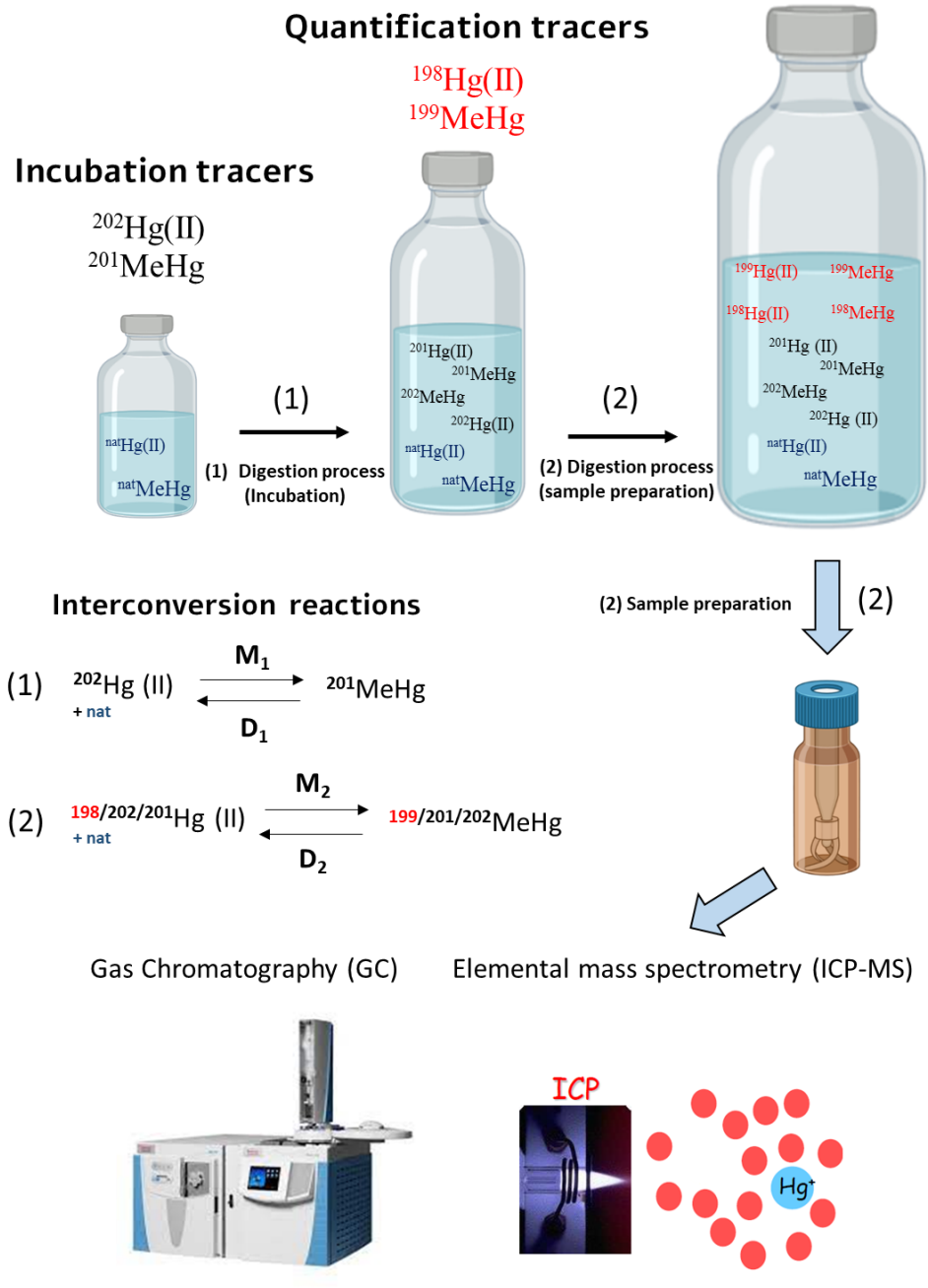

Figure 2.1. Schema for the model incubation experiments performed. M_1/D_1 refers to the methylation/demethylation processes during incubation while M_2/D_2 refers to methylation/demethylation processes during the sample preparation procedure that includes the second digestion. Incubation tracers, quantification tracers and natural Hg compounds are in black, red and blue, respectively.

Natural samples.

Sediments and biofilms. The detailed experimental set-up for the samples collection can be consulted in Bouchet et al., 2018. In brief, isotopically enriched ^{199}Hg(II) and ^{201}MeHg were added at concentrations close to the endogenous ones found (17–180 ng g^{-1} for Hg(II) and 1–10 ng g^{-1} for MeHg). Biofilms incubation were carried out over 36h, whereas sediments were incubated during 24h at *in situ* temperature and stopped by freezing. After, Hg(II) and MeHg compounds were extracted with 6N HNO_3 under a focused MW treatment (85°C, 5min) with a subsequent addition of the quantification tracers ^{198}Hg(II) and ^{202}MeHg. Then, the samples were derivatized in $NaBrEt_4$ and extracted in isooctane before injection in GC-ICP-MS.

Phytoplankton cell culture assays. Samples were obtained following the experimental procedure described in Chapter 3 (**Experimental approach.**). Here, the diatom *Cyclotella meneghiniana* was incubated over 96 hours with concentrations of 600 ng L^{-1} and 60 ng L^{-1} for ^{199}Hg(II) and ^{201}MeHg, respectively.

Freshwaters. Samples collection and incubation can be consulted in Bouchet et al., 2022. Concisely, the concentration of the isotopically enriched Hg compounds (199 & 201) were added within ambient concentration with concentrations of 0.8–1.6 ng L^{-1} for ^{199}Hg(II) and 0.1–0.2 ng L^{-1} for ^{201}MeHg. The incubation time was between 4–8 h and stopped by acidification.

Laboratory blanks were used for the calculation of the detection limits (D.L) for each type of sample. In biofilms and sediments, D.L was 0.03 ng L^{-1} for both Hg compounds (Bouchet et al., 2018). Hg(II) and MeHg DLs in freshwater were 15 pg L^{-1} and 3 pg L^{-1}, respectively. DLs in phytoplankton cell cultures were 0.05 ng L^{-1} for Hg(II), and 0.03 ng L^{-1} for MeHg.

Rational explanation of the experimental choices.

The addition of isotopically enriched Hg compounds is highly dependent on the matrices. After the addition of the enriched Hg compounds to the biofilms and sediments, the samples had to be homogenized to well distribute the Hg compounds all over the sample before freezing. Otherwise, the enriched Hg compounds would not have been well distributed into the samples if the biofilms and sediments samples had been frozen prior to the exogenous Hg compounds additions. Concerning water samples, t_0 samples were collected by acidifying prior to the exogenous Hg compounds additions. In all cases, t_0 samples were collected to check and eventually correct any unintentional methylation or demethylation reaction promoted by the addition of labile enriched Hg compounds. Enriched Hg compounds t_0 recoveries reported in

Bouchet et al., 2018 ranged from 93-101%. On the other hand, phytoplankton cell cultures samples were acidified after 5 minutes of the addition of enriched Hg compounds (see more information in Chapter 3).

1.2.4. Calculation of Hg compounds transformation yields.

Model incubation experiment.

The full description of the mathematical equations employed is described in the Annexes C.2 (**page** ¡Error! Marcador no definido.). In brief, the isotopic distribution observed in **Figure 2.2** for Hg(II) (A) and MeHg (B) arises from the contribution of several Hg sources such as, the natural abundance of endogenous Hg(II) and MeHg (s), the abundances of the exogenous Hg compounds (t1 and t2), and the abundances of the quantification tracers (t3 and t4). The contribution of the different sources to the overall isotopic distribution for Hg(II) and MeHg can be calculated by multiple linear regression applying IPD using Eq.2.1 and 2.2, where A_m^{xxx} is the isotopic distribution in the final mixture determined experimentally by GC-ICP-MS for both, Hg(II) (A, Eq.2.1) and MeHg (B, Eq.2.2). This isotopic distribution in the mixture is simply calculated by dividing the peak area obtained from an isotopic mass measured by the sum of all peak areas of all isotopic masses measured. More information about the previous steps for obtaining Eq.2.1 and 2.2 are shown in **¡Error! No se encuentra el origen de la referencia.**

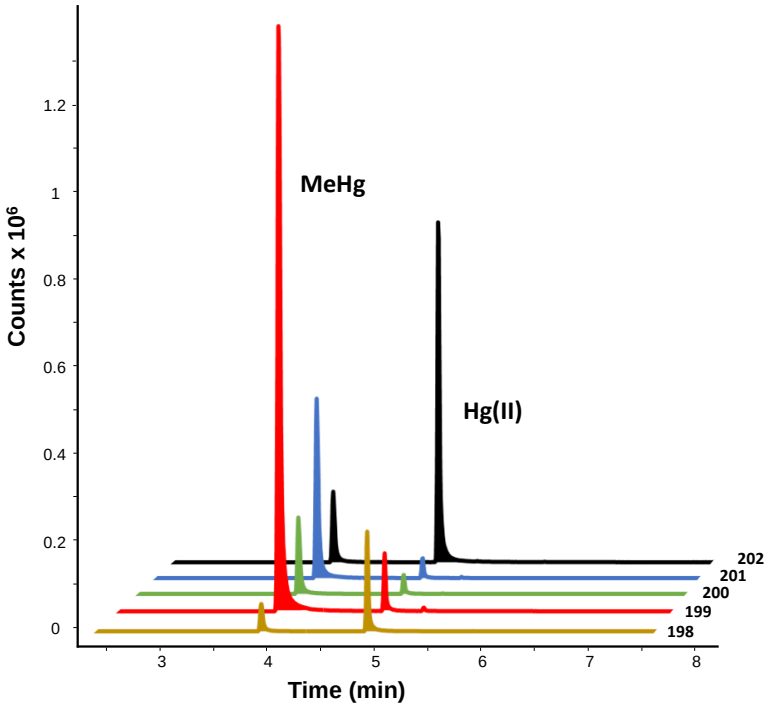

Figure 2.2. Separation of Hg (II) and MeHg in the gas chromatography column and the detection of the Hg isotopes in the ICP-MS in the model incubation experiments.

$$\begin{bmatrix} A_m^{198} \\ A_m^{199} \\ A_m^{200} \\ A_m^{201} \\ A_m^{202} \end{bmatrix} = \begin{bmatrix} A_s^{198} & A_{t1}^{198} & A_{t2}^{198} & A_{t3}^{198} & A_{t4}^{198} \\ A_s^{199} & A_{t1}^{199} & A_{t2}^{199} & A_{t3}^{199} & A_{t4}^{199} \\ A_s^{200} & A_{t1}^{200} & A_{t2}^{200} & A_{t3}^{200} & A_{t4}^{200} \\ A_s^{201} & A_{t1}^{201} & A_{t2}^{201} & A_{t3}^{201} & A_{t4}^{201} \\ A_s^{202} & A_{t1}^{202} & A_{t2}^{202} & A_{t3}^{202} & A_{t4}^{202} \end{bmatrix} \times \begin{bmatrix} x_s^A \\ x_{t1}^A \\ x_{t2}^A \\ x_{t3}^A \\ x_{t4}^A \end{bmatrix} \quad (2.1)$$

$$\begin{bmatrix} A_m^{198} \\ A_m^{199} \\ A_m^{200} \\ A_m^{201} \\ A_m^{202} \end{bmatrix} = \begin{bmatrix} A_s^{198} & A_{t1}^{198} & A_{t2}^{198} & A_{t3}^{198} & A_{t4}^{198} \\ A_s^{199} & A_{t1}^{199} & A_{t2}^{199} & A_{t3}^{199} & A_{t4}^{199} \\ A_s^{200} & A_{t1}^{200} & A_{t2}^{200} & A_{t3}^{200} & A_{t4}^{200} \\ A_s^{201} & A_{t1}^{201} & A_{t2}^{201} & A_{t3}^{201} & A_{t4}^{201} \\ A_s^{202} & A_{t1}^{202} & A_{t2}^{202} & A_{t3}^{202} & A_{t4}^{202} \end{bmatrix} \times \begin{bmatrix} x_s^B \\ x_{t1}^B \\ x_{t2}^B \\ x_{t3}^B \\ x_{t4}^B \end{bmatrix} \quad (2.2)$$

Where, **xxx** being a isotope,

- A^{xxx}_{mix} is obtained by dividing the peak area obtained at one particular isotope by the sum of all peak areas obtained for all isotopes measured in the sample.
- A^{xxx}_{s} corresponds to the natural distribution for each isotope.
- A^{xxx}_{t1} corresponds to the isotopic distribution of the **exogenous ^{202}Hg(II)**.
- A^{xxx}_{t2} corresponds to the isotopic distribution of the **exogenous ^{201}MeHg**.

- A^{xxx}_{t3} corresponds to the isotopic distribution of the isotopically enriched **quantification tracer ^{198}Hg(II)**.
- A^{xxx}_{t4} corresponds to the isotopic distribution of the isotopically enriched **quantification tracer ^{199}MeHg**.

After resolving the two multiple linear regressions, ten molar fractions are obtained. Five for each Hg compound (Hg(II) and MeHg). Using the molar fractions and the known amounts of quantification tracers weighted just before the second digestion process (sample preparation) (^{198}Hg(II)=N^{A}_{t3} and ^{199}MeHg=N^{B}_{t4}), the amount of moles corresponding to the newly-formed ^{199}Hg(II) and ^{198}MeHg during the sample preparation from the quantification tracers is calculated applying Eq.2.3 and 2.4.

$$N^{B}_{t3} = {}^{198}\text{MeHg formed by methylation} = N^{B}_{t4}\frac{x^{B}_{t3}}{x^{B}_{t4}} \qquad (2.3)$$

$$N^{A}_{t4} = {}^{199}\text{Hg (II) formed by demethylation} = N^{A}_{t3}\frac{x^{A}_{t4}}{x^{A}_{t3}} \qquad (2.4)$$

Since the quantification tracers were only affected by the interconversion processes during the analytical procedure (no incubation process), the methylation and demethylation yields during the sample preparation (M_2 and D_2) are calculated as Eq.2.5 and 2.6.

$$M_2 = \frac{N^{B}_{t3}}{N^{A}_{t3}} \qquad (2.5)$$

$$D_2 = \frac{N^{A}_{t4}}{N^{B}_{t4}} \qquad (2.6)$$

Where,

^{198}Hg(II)=N^{A}_{t3} and ^{199}MeHg=N^{B}_{t4} have been calculated from the weighted values before the sample preparation.

^{198}MeHg=N^{B}_{t3} and ^{199}Hg(II)=N^{A}_{t4} have been calculated.

Once the methylation and demethylation yields during the sample preparation have been calculated, we need, first, to correct and recalculate the amount of moles corresponding to the exogenous and endogenous Hg compounds that have been also affected likewise during the sample preparation. The recalculation is achieved applying a mass balance (see Annexes C.2, Eq.A18, A19, A20, A21). It is important to notice that the addition of the quantification tracers corrects automatically (no extra calculations) the Hg(II) and MeHg incomplete recoveries during the sample preparation but, **it does not correct automatically the interconversion**

processes. Therefore, the recalculation of Hg compounds moles amount through a mass balance is mandatory to correct interconversion processes during the sample preparation in both, model incubation experiments and real samples. In the results and discussion section, **uncorrected (NC)** and **corrected (CI)** Hg compounds concentration from the interconversion processes during the sample preparation are compared for the model incubation experiments and natural samples.

After performing the mass balance, we can calculate the methylation and demethylation yields (M_1 and D_1) during the incubation process by dividing the amount found for the corrected newly-formed methylated/demethylated exogenous tracers (${}^{c}N_{t2}^{A}$ and ${}^{c}N_{t1}^{B}$) by the total amount of that tracer found (the corrected original form (${}^{c}N_{t1}^{A}$ and ${}^{c}N_{t2}^{B}$) plus the corrected newly-formed methylated/demethylated form) as:

$$M_1 = \frac{{}^{c}N_{t1}^{B}}{({}^{c}N_{t1}^{A} + {}^{c}N_{t1}^{B})} \qquad (2.7)$$

$$D_1 = \frac{{}^{c}N_{t2}^{A}}{({}^{c}N_{t2}^{B} + {}^{c}N_{t2}^{A})} \qquad (2.8)$$

Note that the determination of the methylation and demethylation yields during the incubation process using equations 2.7 and 2.8 does not consider any possible Hg compounds losses such as Hg compounds reduction during the incubation process (first digestion) or any unintentional reaction promoted by the sudden spike addition and abiotic transformations of labile enriched isotopes. For these reasons, additional equations had to be applied for the determination of Hg(II) methylation and MeHg demethylation potentials in natural samples (more information in section below). More detailed information about the mathematical approach between both models developed in this work is provided in Annexes C.2 (Annexes Chapter 2.

Common equations for both mathematical **models and notation.**).

Natural samples.

In this work, we call oxidative MeHg demethylation (D_{ox} %) to the formation of Hg(II), whereas the reductive MeHg demethylation (D_{red} %) refers to the formation of Hg(0). On the other hand, MeHg loss involved the formation of Hg(II), Hg(0) and DMeHg from the initial MeHg (**Figure 2.3**). Since the quadruple tracer methodology does not allow to determine D_{red} %, we assumed that no ^{201}Hg(0) have been transformed into ^{201}Hg(II) during the sample storage or acidification. Then, the original and newly-formed Hg compounds concentrations corrected from the interconversion process during the sample preparation allowed to determine the Hg(II)

methylation, MeHg demethylation and MeHg loss potentials applying the equations 2.9, 2.10, and 2.11 in biofilms, sediments, freshwaters and phytoplankton.

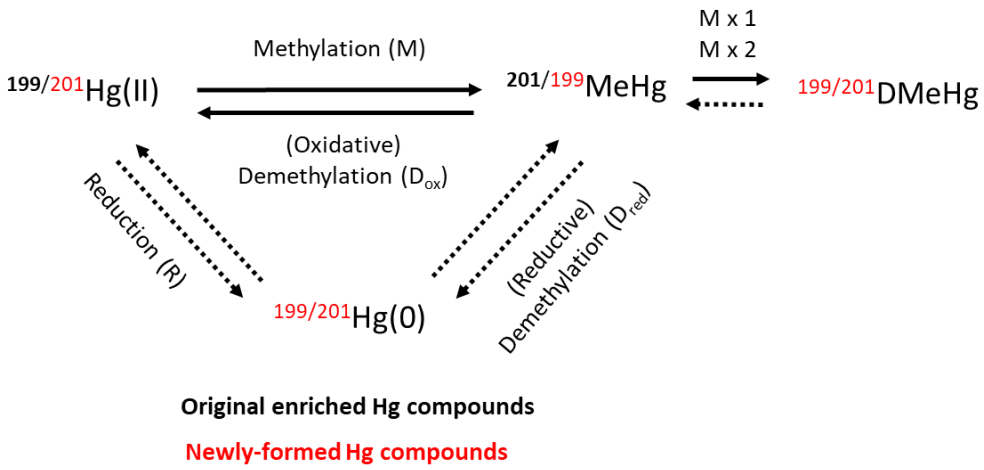

Figure 2.3. Reactivity model of Hg compounds. Solid arrows correspond to the specific reaction pathways that can be calculated with the quadruple tracer methodology and dotted arrows correspond the pathway that cannot be determined. MeHg loss is the sum of oxidative demethylation (D_{Ox}), reductive demethylation (D_{red}) and DMeHg formation coming from MeHg (Mx1).

Potential Hg(II) Methylation (M % h^{-1}):

$$M\ \% = \left(\frac{(^{199}MeHg_{tf} - {}^{199}MeHg_{t0})}{(^{199}MeHg_{t0} + {}^{199}Hg(II)_{t0})}\right) x \frac{1}{tf(h)} x\ 100 \qquad (2.9)$$

Potential MeHg demethylation (D_{ox} % h^{-1}):

$$D_{ox}\% = \left(\frac{(^{201}Hg(II)_{tf} - {}^{201}Hg(II)_{t0})}{(^{201}Hg(II)_{t0} + {}^{201}MeHg_{t0})}\right) x \frac{1}{tf(h)} x\ 100 \qquad (2.10)$$

Potential MeHg loss (% h^{-1}):

$$MeHg\ loss\ \% = \left(\frac{(^{201}MeHg_{t0} - {}^{201}MeHg_{tf})}{^{201}MeHg_{t0}}\right) x \frac{1}{tf(h)} x\ 100 \qquad (2.11)$$

Several studies have reported MeHg demethylation and Hg(II) methylation in the t_0 samples (Graham et al., 2012; Rodriguez-Gonzalez et al., 2013; Wang et al., 2020). Consequently, the

concentration of newly formed Hg compounds at the end of the incubation (t_f) must be corrected from t_0 in order to not overestimate the Hg(II) methylation and MeHg demethylation potentials during the incubation processes as shown in eq. 2.9 and 2.10. The main limitation is related to the differences in terms of Hg compounds concentration obtained from two different samples (t_0 and t_f). Since they are coming from different measurements, the determination of Hg compounds transformation potentials has a higher experimental variability. In most cases, the concentration of original and newly formed Hg compounds, and the standard deviations associated are obtained by performing several independent replicates. Then, the standard deviation of Hg(II) methylation, MeHg demethylation, and MeHg loss potentials is mostly coming from the environmental/experimental variability rather than the mathematical/analytical methodologies. In other words, equations 2.9, 2.10 and 2.11 are reliable equations to address Hg compounds transformations potentials but the values obtained are quite influenced by experimental uncertainties, experimental set-up, and the analytical performance. The main factors shown (Rodriguez-Gonzalez et al., 2013) to influence the Hg compounds transformations are:

- Incubation time: the incubation time should be established depending on the ability of the method to detect reliable transformations.

- Pre-equilibration of isotopically enriched Hg compounds added.

- Endogenous background of Hg compounds.

In this work, no detection limit could be provided for the Hg compounds transformation potentials since it does not exist an absolute value for all samples.

1.3. Results and discussion.

1.3.1. Evaluation of the quadruple tracer methodology in model incubation experiments.

Recoveries of the endogenous and exogenous Hg compounds.

The distinction of the uncorrected (**NC**) Hg compounds concentration from the interconversion processes during the sample preparation (before performing the mass balance) and corrected Hg compounds concentration (**CI**) (after performing the mass balance) were compared for the model incubation experiments and natural samples. The evaluation of the methodology performance have been carried out in mixtures with three different exogenous Hg compounds ratio (MeHg:Hg(II), 1:1, 3:1 and 10:1). In the laboratory, standards of endogenous and exogenous Hg compounds were weighted, and an accurate recovery of Hg compounds could be determined. In **Figure 2.4A** and **2.4B**, the recoveries of endogenous and exogenous Hg compounds corrected from interconversion processes (CI) during the sample preparation and uncorrected (NC) are presented for the three mixtures. Overall, better recoveries were obtained by correcting the Hg compounds interconversion processes during the sample preparation (**Figure 2.4A**). CI endogenous Hg(II) and MeHg recoveries for the three mixtures were 98.1–103.6% and 97.7–105.0%, respectively. In contrast, the recoveries of the NC endogenous Hg compounds ranged from 100.1 to 122.7% for Hg(II), and from 96.6 to 130.4% for MeHg (Figure 2.4B). Looking at the exogenous Hg compounds recoveries, no differences were observed between CI and NC. Recoveries of CI exogenous Hg compounds ranged between 94.0–103.2% for ^{202}Hg(II) and 90.1–101.6% for ^{201}MeHg, whereas the NC recoveries were between 89.4–101.7% for ^{202}Hg (II) and 88.9–95.2% for ^{201}MeHg.

In general terms, the overestimation of NC natural Hg(II) in the mixture 1:1 (Figure 2.4B) can be related to the high demethylation (28±12%) yield during the sample preparation (D_2, Figure 2.4C). Concerning the endogenous Hg compounds, the demethylation of MeHg contributed to the endogenous Hg(II) formation. However, it did not occur to the exogenous Hg compounds since they were labelled with different isotopes. Because of the high Hg(II) methylation (M_1=14.3±2.7% ,Figure 2.4C) in the mixture 1:10, differences in the recoveries were observed for ^{202}Hg(II) (CI ^{202}Hg(II): 101.8%; NC ^{202}Hg(II): 89.4%), however, the standards deviations associated did not allow to go any further. To sum up, better recoveries were obtained when low interconversion reactions took place in both, incubation process and sample preparation. However, the comparison of the original exogenous and endogenous Hg compounds recoveries did not seem to be a good approach to illustrate the importance of correcting the methylation

and demethylation yields during the sample preparation. Because of that, the differences between the NC and CI were investigating in the newly-formed ^{201}Hg(II) and ^{202}MeHg concentrations.

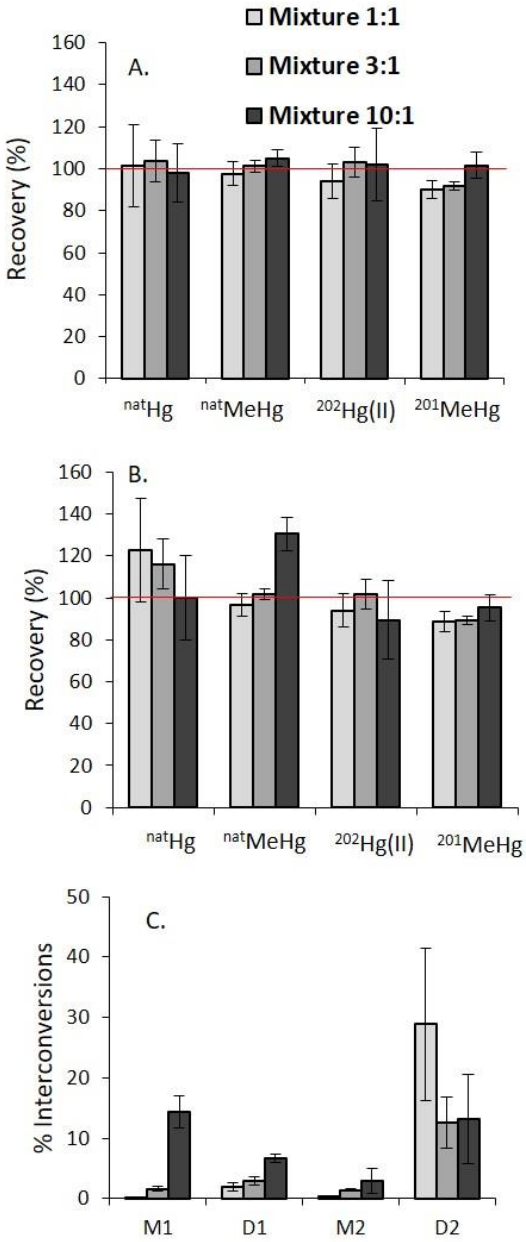

Figure 2.4. Recoveries (%) of the endogenous and exogenous Hg compounds from the weights (theoretical) added to the vial for the three mixtures (ratio MeHg: Hg (II) of 1:1, 3:1 and 10:1 in (A) after the correction of interconversion processes and (B) without correction of the interconversion processes during the sample preparation. (C) Methylation and demethylation yields corresponding to the sample preparation (M_2 and D_2) and incubation process (M_1 and D_1) for the three mixtures. Standard deviations correspond to triplicates for each condition (n=3).

Non-corrected and corrected newly-formed Hg compounds concentration.

Regarding the newly-formed Hg compounds, the NC and CI concentrations exhibited differences (¡Error! No se encuentra el origen de la referencia.). For the mixture 1:1, CI and NC ^{201}Hg(II) concentrations were 24.2±6.9 and 377.1±127.2 µg L^{-1}, respectively. Differences were also observed for the mixture 3:1 (CI: 70.0±18.2 µg L^{-1}, NC: 367.5±99.7 µg L^{-1}) and 10:1 (CI: 186.4±9.9 µg L^{-1}; NC: 541.8±183.9 µg L^{-1}) (Figure 2.5A). Such important differences were mainly influenced by high demethylation yields observed during the sample preparation for the three mixtures (D_2, Figure 2.4C). Regarding the formation ^{202}MeHg, NC ^{202}MeHg concentrations in the mixture 1:1, 3:1 and 10:1 were 9.0±7.3, 32.6±7.1 and 92.9±10.7 µg L^{-1}, respectively. In contrast, CI ^{202}MeHg concentration were 2.0±2.9 µg L^{-1} for the mixture 1:1, 16.5±4.6 µg L^{-1}for the mixture 3:1, and 78.4±3.8 µg L^{-1} for the mixture 10:1 (Figure 2.5B). The lower differences between CI and NC ^{202}MeHg concentration than those observed in ^{201}Hg(II) were due to the low methylation yields during the sample preparation (M_2 %, Figure 2.4C). In accordance with the newly-formed Hg compounds concentrations, similar trends were observed for the determination of methylation and demethylation yields during the incubation process (Figure 2.5C and 2.5D).

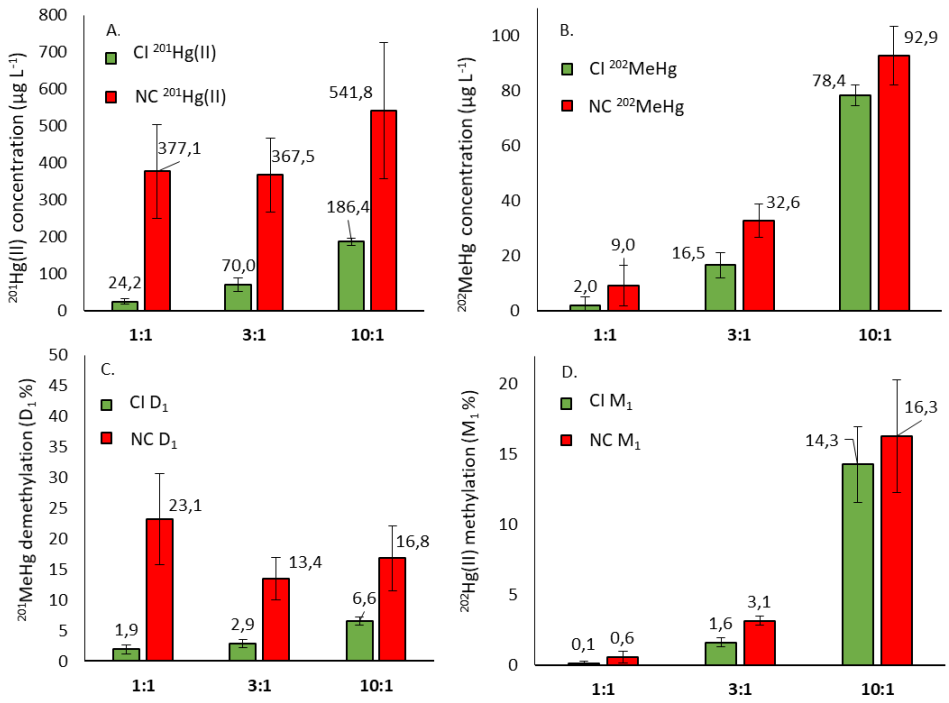

Figure 2.5. Corrected (CI) and non-corrected (NC) (A) ^{201}Hg(II) and (B) ^{202}MeHg concentration (µg L^{-1}) in the three mixtures (1:1, 3:1 and 10:1). Demethylation (C) and methylation (D) yields (D_1 % and M_1 %) corresponding to the incubation process calculated with the correted and non-corrected newly-formed compounds in the three mixtures (1:1, 3:1 and 10:1). Standards deviations corresponds to three independent replicates (n=3).

To conclude, larger corrections were shown in the model incubation experiments for the determination of ^{201}Hg(II) concentrations due to the high extent of MeHg demethylation (D_2) during the sample preparation. Indeed, the success of evaluating the quadruple tracer methodology performance relied on the discrimination of the interconversion reactions between the sample preparation and incubation process. The assessment of the quadruple tracer methodology demonstrated an accurate determination of endogenous and exogenous Hg compounds in mixtures with three different exogenous MeHg:Hg(II) ratios.

1.3.2. Application of the quadruple tracer methodology in natural samples Hg incubation experiments.

Non-corrected and corrected newly-formed Hg compounds concentration.

In ¡Error! No se encuentra el origen de la referencia., the CI and NC newly-formed ^{199}MeHg and ^{201}Hg(II) concentration are shown in biofilms and freshwaters under light (**l**) and dark (**d**) conditions, sediments under dark conditions (**d**), and phytoplankton. Hg(II) methylation was only found in biofilms and sediments, whereas MeHg demethylation was observed in biofilms, sediments, freshwaters and phytoplankton. Overall, no differences were observed between NC and CI ^{199}MeHg concentrations in biofilms (Figure 2.6A) and sediments (Figure 2.6B) because the methylation of Hg(II) during the sample preparation was negligible (see interconversions in Annexes C.2, **page 92**). On the other hand, Hg(II) demethylation during the sample preparation in all natural samples revealed differences between NC and CI newly-formed ^{201}Hg(II) concentration. In phytoplankton, CI ^{201}Hg(II) concentration at the beginning of the exposure (5min) was 0.2±0.2 ng L^{-1}, whereas the NC ^{201}Hg(II) concentration was higher (2.2±0.9 ng L^{-1}). (Figure 2.6C). In biofilms, NC and CI ^{201}Hg(II) concentration under dark and light conditions were similar, however, the NC ^{201}Hg(II) concentration in t_0 was greater (0.50±0.03 µg L^{-1}) than CI (0.07±0.01 µg L^{-1}). In freshwaters, NC ^{201}Hg(II) concentrations were higher in all types of samples (t_0, light and dark) in comparison with CI for each type of sample. To sum up, NC ^{201}Hg(II) concentrations were higher than CI to a greater or lesser extent in all natural samples (¡Error! No se encuentra el origen de la referencia.), however, NC and CI ^{199}MeHg concentrations were similar.

Non-corrected and corrected MeHg loss and MeHg demethylation potentials (% h^{-1}).

In **Figure 2.6,** NC and CI MeHg loss and MeHg demethylation potentials are shown for biofilms (light and dark), sediments (dark), freshwaters (light and dark) and phytoplankton. Similar MeHg loss potentials were observed in all samples (Figure 2.7A) since no differences were found between NC and CI ^{201}MeHg concentrations (Annexes C.2, **page 90**). In contrast, NC MeHg demethylation potentials in phytoplankton were lower (NC D_{ox}: 0.034±0.002 % h^{-1}) in comparison with CI (D_{ox}: 0.057±0.004 % h^{-1}). NC D_{ox} in sediments (NC D_{ox}: 0.51±0.21 % h^{-1}) was two folds higher than CI (D_{ox}: 1.05±0.28 % h^{-1}). In biofilms and freshwaters, no differences could be observed between CI and NC MeHg demethylation potentials. Although the correction of the Hg compounds concentration provided more accurate results in almost all natural samples (¡Error! No se encuentra el origen de la referencia.), the determination of MeHg loss and MeHg demethylation potentials (% h^{-1}) involved the subtraction between the t_f and t_0. This subtraction was of great importance for the determination of Hg compounds potentials since the bias between the NC and CI newly-formed Hg compounds concentration was automatically corrected in biofilms and freshwaters due to the similar methylation/demethylation yields during the sample preparation for t_f and t_0 samples (**Figure A2- 2** and **Figure A2- 3**).

Comparing the CI MeHg loss with the CI demethylation of MeHg into Hg(II), results in biofilms revealed that almost all MeHg loss (l: 0.46±0.04 % h^{-1}) came from the demethylation of MeHg (l: 0.44±0.11 % h^{-1}) under light conditions, whereas D_{ox} (d: 0.16±0.03% h^{-1}) under dark conditions contributed around 50% of the total MeHg loss (d: 0.28±0.08% h^{-1}). In freshwaters, around one third (≈1/3) of the total ^{201}MeHg loss (l: 1.9±0.3% h^{-1}) was originated from the ^{201}MeHg demethylation (0.63±0.05 % h^{-1}) under light conditions. In contrast, the contribution of MeHg demethylation to the MeHg loss under dark conditions was around 60%. In phytoplankton, MeHg demethylation (0.057±0.004 % h^{-1}) contributed more than 60% to the MeHg loss (0.088±0.004%).

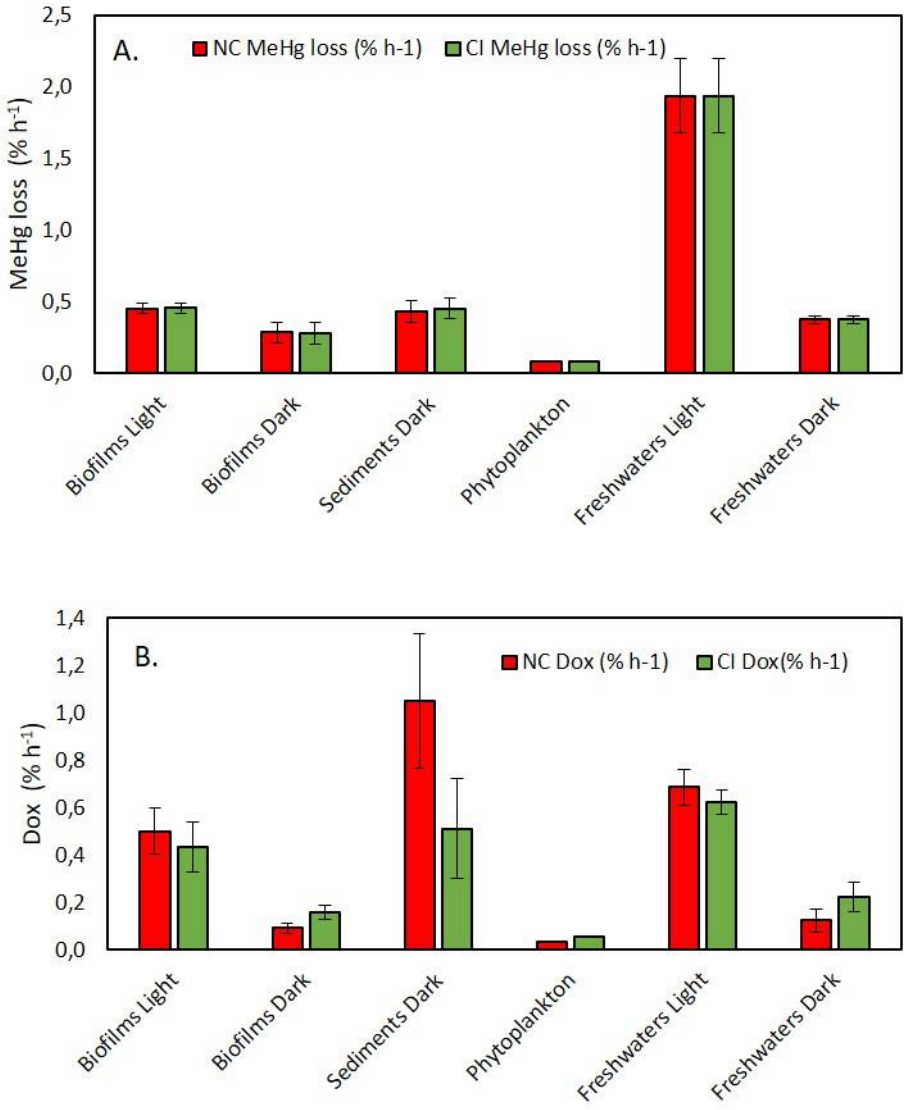

Figure 2.6. Corrected (Cl) and non-corrected (NC) of (A) MeHg loss and (B) MeHg demethylation (Dox) potentials in biofilms, sediments, phytoplankton and freshwaters under light and dark conditions. Standards deviations corresponds to two independent replicates (n=2).

Several studies have addressed the Hg(II) methylation potentials during the incubation process by tracking the MeHg formation (Achá et al., 2012; Gilmour et al., 2011, 2018; Hintelmann & Evans, 1997; Ranchou-Peyruse et al., 2009). In some cases, the quantification of newly formed MeHg was carried out by adding only one enriched MeHg as a quantification tracer. This approach is really useful to calculate Hg(II) methylation potentials only when there is no Hg(II) methylation during the sample preparation. Concerning MeHg demethylation, most studies measured the MeHg demethylation as MeHg loss, but not as the formation of Hg(II) (Drott et al., 2008b; Hintelmann et al., 2000; Li et al., 2022; Tjerngren et al., 2012; Zhu et al., 2018). In our work, MeHg loss was referred to the formation of Hg(II), Hg(0) and DMeHg from the initial MeHg added. Furthermore, studies reporting the MeHg demethylation potentials by measuring

the formation of Hg(II) using IPD did not mention the need of calculating and correcting Hg compounds interconversion reactions during the sample preparation (Bouchet et al., 2018, 2022; Bravo et al., 2014; Bridou et al., 2011; Gascón Díez et al., 2016; Hamelin et al., 2015; Pedrero, et al., 2012; Rodriguez-Gonzalez et al., 2013). In this work, the quadruple tracer methodology allowed to distinguish between the interconversion processes during the incubation process and sample preparation but also, the distinction between MeHg loss and MeHg demethylation potentials.

1.4. Conclusions.

In this work, the proposed methodology provided an accurate experimental assessment by determining the methylation and demethylation yields during the incubation process and sample preparation. Furthermore, important differences were observed between NC and CI newly formed Hg compounds concentration in the model incubations experiments demonstrating the importance of correcting the Hg interconversion processes during the sample preparation. The methodology presented also allowed to distinguish the MeHg loss and MeHg demethylation potentials in biofilms, sediments, freshwaters and phytoplankton. Furthermore, a more accurate detection was observed for the newly formed Hg(II) than the original MeHg concentration. In freshwaters and biofilms, the similarities found in CI and NC D_{ox} potentials were associated with the similar methylation and demethylation yields in the t_0 and t_f samples during the sample preparation. Overall, the quadruple tracer methodology developed have shown to be a promising tool for the determination of Hg compounds transformation potentials. However, further investigations will be needed to determine the minimum detectable Hg(II) methylation and MeHg demethylation for each type of matrix in order to well validate this methodology.

2. Isotope pattern deconvolution to determine simultaneous reduction pathways leading to the formation of dissolved gaseous mercury in Hg incubation experiments.[2]

2.1. Introduction.

Several volatile (elemental Hg (Hg^0) and dimethyl mercury (Me_2Hg)) and non-volatile (inorganic mercury (Hg(II)) and monomethyl mercury (MeHg)) mercury compounds are found in the hydrosphere and their distribution varies among the aquatic environment (Branfireun et al., 2020; Klapstein & O'Driscoll, 2018; Selin, 2009; Stein et al., 1996). In the surface, freshwater Hg compounds distribution is usually as Hg(II)>Hg(0)≈MeHg, whereas this proportion is Hg(II)>Hg(0)>MeHg>Me_2Hg in surface seawaters (Leopold et al., 2010). Hg(II) and MeHg form a variety of inorganic and organic complexes, which play a fundamental role in Hg compounds interconversions. Hg(II) can be reduced into Hg(0), but also methylated through abiotic and/or biotic mechanisms (Amyot et al., 1997; Poulain et al., 2004). On the other hand, MeHg can be re-methylated into DMeHg or demethylated forming Hg(II) (oxidative demethylation) or Hg(0) (reductive demethylation) (Barkay & Gu, 2021).

The determination of dissolved gaseous mercury (DGM=Hg(0)+DMeHg) through the incubation of isotopically enriched Hg(II) and MeHg have been carried out in several freshwater and seawater ecosystems, such as coastal waters, water column, or surface sediments (Monperrus et al., 2007; Rodríguez Martín-Doimeadios et al., 2004; Sharif et al., 2014). In all cases, the concentration of compounds-specific DGM formation was calculated by subtracting, manually, the intensity of the ^{202}Hg isotope (natural contribution) from the isotopes corresponding to the enriched Hg compounds added (^{199}Hg and ^{201}Hg). To go further to the cited studies, we have applied the mathematical approach based on isotope pattern deconvolution (IPD) with the purpose of extracting the isotopic patterns (or signatures) from the DGM produced. The final goal was to determine, simultaneously, the Hg(II) reduction and reductive MeHg demethylation potentials in incubated lake and seawater samples. This

---

[2] *(Manuscript in preparation)*

Authors: Javier Garcia-Calleja, Alina Kleindienst, Bastien Duval, Emmanuel Tessier, Zoyne Pedrero Zayas and David Amouroux.

Javier Garcia Calleja: Development of the analytical methodology for the calculation of the simultaneous Hg(II) reduction and MeHg reductive demethylation potentials in surface seawater and lakewaters samples.

approach shows the versatility of IPD for the determination of the Hg compounds transformation pathways leading to DGM formation.

2.2. Experimental approach.

2.2.1. Sampling.

The experimental approach presented in this section involved three field sampling campaigns and two different sites. The first sampling campaign was carried out in Marseille (October 2020, GMOS TRAIN project) and the other two campaigns were performed in Lake Gentau (October 2018 and June 2019, REPLIM project). Unfiltered seawater surface samples were collected from Marseille Endoume coastal Station (Sampling from continuously pumped seawater) and from a profile sample near Île-Riou (Marseille, Mediterranean Sea; 5 m depth, Trace metal clean sampling from GOFLO Bottles). On the other hand, unfiltered lake water surface samples were collected at 0.5 m depth in Lake Gentau (GOFLO samplers). Water samples were directly sampled into 125ml (lake waters) and 250mL (seawaters) PFA/FEP bottles without a head space, and subsequently incubated as soon as possible after the sampling. More information is provided in Duval, 2021 and in Kleindienst et al. (in prep).

2.2.2. Incubation of isotopically enriched Hg compounds in lake and seawater samples.

A known amount of isotopically enriched Hg compounds was added to the PFA/FEP bottles in order to obtain a final concentration of ~2 ng L^{-1} for $^{199}Hg(II)$ and ~0.2 ng L^{-1} for $^{201}MeHg$ in both seawater and lakewater samples; corresponding to about 5 to 10 folds of the natural concentrations observed in the studied ecosystems. The final Hg compounds concentration was chosen according to previous incubation experiments (Monperrus et al., 2007; Sharif et al., 2014). All incubation bottles were submerged at ambient temperature (water temperature ranged between 10 and 17°C). After 7 hours, the Teflon containers were collected, and the incubation processes were stopped by adding high-purity HCl (1 % v/v). Teflon containers were closed tightly and stored in double PE zip-lock bags in a portable cooler (5–10 °C), protected from light, and further transported and stored in the laboratory (5–10 °C).

Rational explanation of the experimental choices.

All surface water samples were incubated and exposed to sunlight or dark conditions. In seawaters, light incubations were conducted for 7 hours, while dark incubations were performed for 24 hours. In lake waters, both light and dark incubation were carried out between 7–9 hours.

All incubations were conducted in triplicates. In lake waters, t_0 samples were performed for lake water samples but not for seawater.

2.2.3. Analysis of newly-formed dissolved gaseous mercury (DGM).

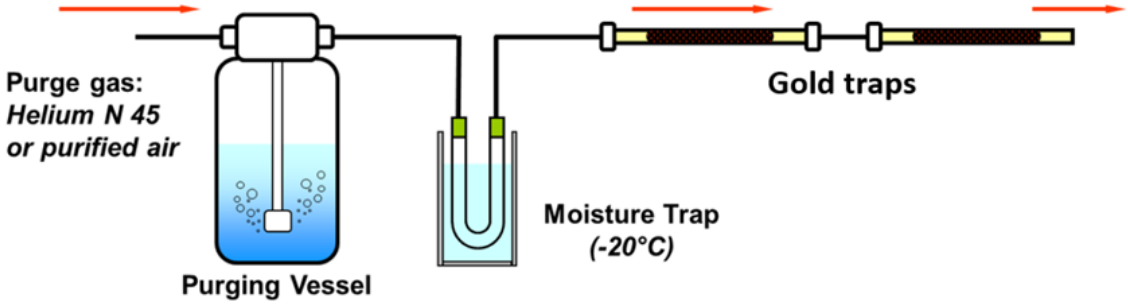

Figure 2.7. Purging system scheme on site used in Duval, 2021.

The following analytical procedure is set up for the determination of DGM, which include both the Hg(0) and the DMHg. The determination of MeHg concentration (being MeHg i.e., the sum of MMHg and DMHg) in purged and unpurged samples verified that DGM was mainly composed by Hg(0) (Duval, 2021). The elemental Hg (Hg(0)) was immediately recovered in gold coated sand traps by purging the water samples (**Figure 2.7**) and analysed by thermal desorption cryogenic trapping (CT) followed by GC-ICP-MS in less than 1 month after sampling (**Table 2.5**). The purge efficiency was assessed reaching 95±3% (n=12). The detection limit was calculated either with the results from a second analysis of a trap associated to the sample (sample blanks) or the results from the analysis of traps that were only transported during the sampling campaigns. DL for DGM ranged between 0.1–0.4 pg L^{-1}.

Table 2.5. Operating conditions of GC-ICP-MS for the determination of DGM.

Parameters	**GC-ICP-MS**
Type of column	Rxi-5ms Restek, 30m, ID 0.25mm, df 25µm
Injector Mode	Splitless
Injector Temperature	250 ºC
Interphase Temperature	270 ºC
Injection volume	2µL
Carrier flow rate	5mL/min (He)
Acquisition mode	Transient Time Resolved Analysis
Acquisition Time	550sec

Dwell Time	20ms
Isotopes measured	^{196}Hg, ^{198}Hg, ^{199}Hg, ^{200}Hg, ^{201}Hg, ^{202}Hg, ^{204}Hg, ^{203}Tl, ^{205}Tl

Quantification of compounds-specific DGM formation.

Enriched DGM concentrations were calculated by combining the IPD approach with an external calibration developed during this PhD. The external calibration was done using Hg(0) standards and injecting known quantities (syringe injections, Hamilton RN 25) through a septum into the system. Peak integration was done by Thermo PlasmaLab software.

The data treatment for the quantification of enriched DGM is based on the same principle described Chapter 2.1. The total isotopic distribution of DGM is originated from the previous addition of isotopically enriched ^{199}Hg(II) and ^{201}MeHg to lake and seawater samples. Then, the Hg isotopic sources contributing to DGM are from the natural abundance (any possible contamination or natural contribution) and the two incubation tracers. As a result, the molar fraction of each contribution can be calculated by IPD (Eq. 2.12).

$$\begin{bmatrix} A^{198}_{mix} \\ A^{199}_{mix} \\ A^{200}_{mix} \\ A^{201}_{mix} \\ A^{202}_{mix} \end{bmatrix} = \begin{bmatrix} A^{198}_{Nat} & A^{198}_{201MeHg} & A^{198}_{199Hg(II)} \\ A^{199}_{Nat} & A^{199}_{201MeHg} & A^{199}_{199Hg(II)} \\ A^{200}_{Nat} & A^{200}_{201MeHg} & A^{200}_{199Hg(II)} \\ A^{201}_{Nat} & A^{201}_{201MeHg} & A^{201}_{199Hg(II)} \\ A^{202}_{Nat} & A^{202}_{201MeHg} & A^{202}_{199Hg(II)} \end{bmatrix} \times \begin{bmatrix} x^{Hg(0)}_{nat} \\ x^{Hg(0)}_{201MeHg} \\ x^{Hg(0)}_{199Hg(II)} \end{bmatrix} \quad (2.12)$$

Where, **xxx** being a isotope,

- A^{xxx}_{mix} is obtained by dividing the peak area obtained at one particular isotope by the sum of all peak areas obtained for all isotopes measured in the sample.
- A^{xxx}_{nat} corresponds to the natural distribution for each isotope.
- $A^{xxx}_{199Hg\ (II)}$ corresponds to the isotopic distribution of the isotopically enriched ^{199}Hg(II).
- $A^{xxx}_{201MeHg}$ corresponds to the isotopic distribution of the isotopically enriched ^{201}MeHg.
- $X^{Hg(0)}_{nat}$, $x^{Hg(0)}_{199Hg(II)}$ and $x^{Hg(0)}_{201MeHg}$ corresponds to the molar fractions calculated.

In this case, IPD was useful to obtain qualitative information for the DGM by obtaining the molar fractions. As a result, the calculation of DGM concentration was performed by combining the molar fractions obtained with an external calibration. For the calculations of the compounds-specific DGM concentration from ^{199}Hg(II) and ^{201}MeHg, first (1) we plotted the overall intensity of each Hg isotope measured (^{198}Hg, ^{199}Hg, ^{200}Hg, ^{201}Hg and ^{202}Hg) of the standards measured in CT-GC-ICP-MS against the concentration of Hg(0) in the external calibration

graph. Second (2), the total DGM concentration in the samples was calculated by summing the overall intensity of each Hg isotope measured considering all the contributions (natural, enriched in 199 and 201). At this point, the total concentration of DGM concentration calculated contained the natural, and both enriched isotopic sources, but not the compounds-specific concentration from each isotopically enriched compound. For this reason, the final step was to simply multiply the total DGM concentration by the molar fraction corresponding Hg sources of 199 and 201 (**Figure 2 8**).

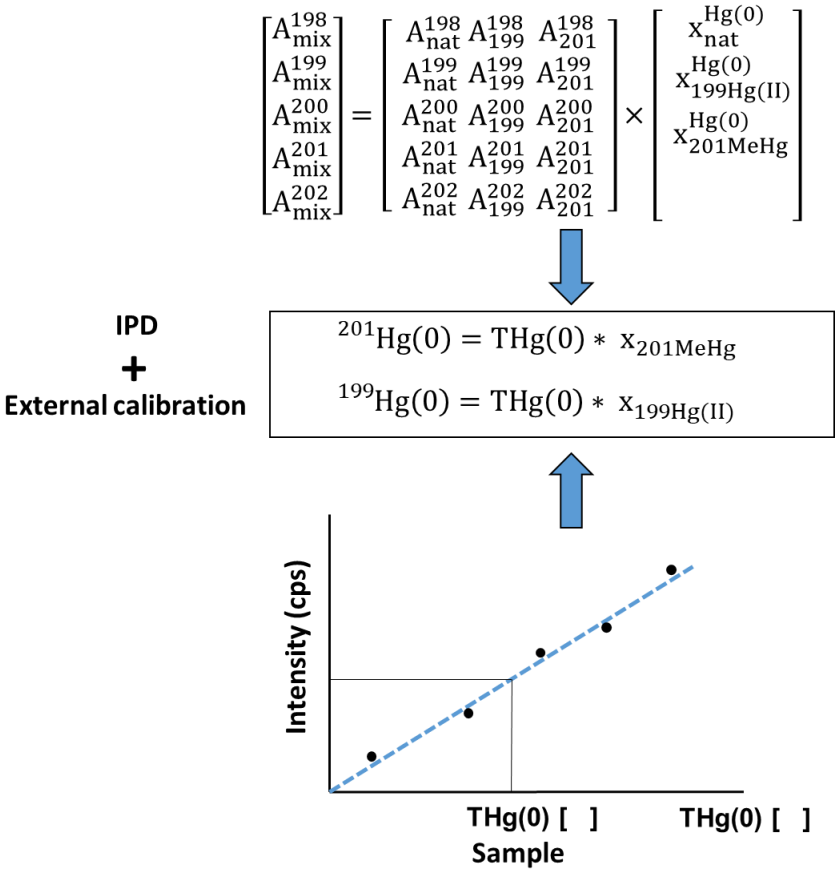

Figure 2 8. Conceptual approach of the combination of IPD with an external calibration for the determination of compounds-specific Hg(0) concentration.

Two main advantages are observed in comparison with the old methodology. The first and most important, IPD has the capability of extension to a higher number isotopically enriched Hg compounds (e.g. ^{198}Hg-DOM complexes, β-^{200}HgS(s), ^{201}Hg-LMW thiol complexes…), leading to investigate the DGM formation in uncountable ways. The second advantage corresponds to the quality of the results. IPD approach provided a more accurate detection since the old methodology does not consider the minor contributions coming from the other isotopes (**Table 2.1**). The old methodology could not be compared with the IPD methodology in the present thesis. This manuscript is still under preparation.

2.2.4. Calculation of ^{199}Hg(II) reduction and reductive ^{201}MeHg demethylation potentials.

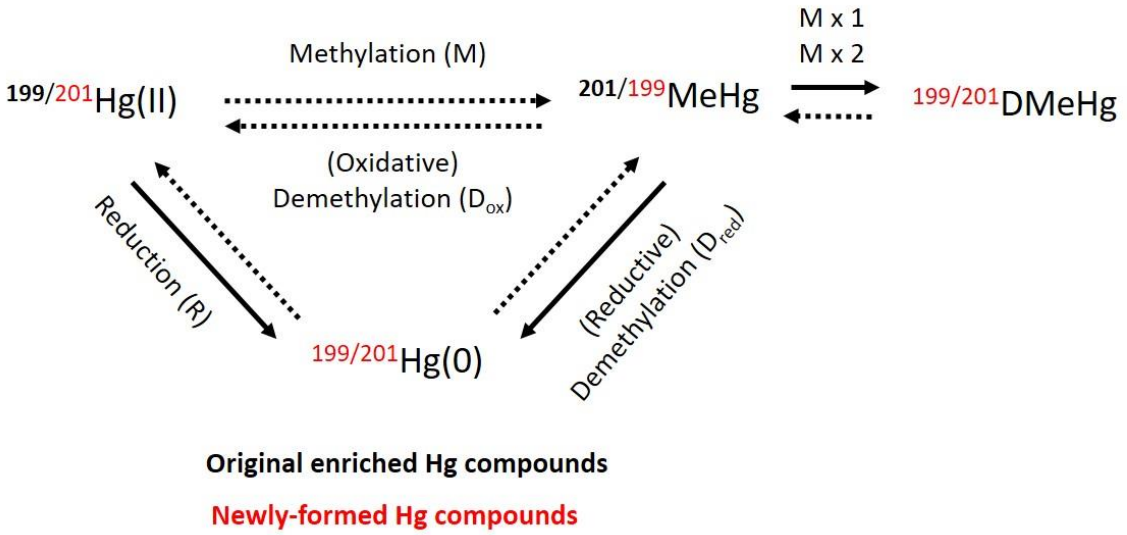

Figure 2.9. Reactivity model of Hg compounds. Solid arrows correspond to the specific reaction pathways that can be calculated combining IPD with an external calibration and dotted arrows correspond the pathway that cannot be determined.

^{199}Hg(II) and ^{201}MeHg reduction potentials (% h^{-1}) were determined by subtracting the concentration of the newly formed DGM at the end of the exposure (t_f) by the t_0 of each contribution (199 or 201) in order to not overestimate the Hg compounds transformation potentials (**Figure 2.9**). Then, the subtracted concentration was divided by the concentration added at the beginning of the incubation for ^{199}Hg (II) and ^{201}MeHg respectively (Eq.2.14 and 2.15), and divide by the incubation time.

$$\%^{199}\text{Hg reduction} = \frac{[^{199}\text{Hg}(0)_{tf}]-[^{199}\text{Hg}(0)_{t0}]}{[^{199}\text{Hg(II)}\ ]\text{initial}} \times \frac{1}{\text{tf(h)}} \times 100 \qquad (2.14)$$

$$\%\ \text{Reductive}^{201}\text{MeHg demethylation} = \frac{[^{201}\text{Hg}(0)_{tf}]-[^{201}\text{Hg}(0)_{t0}]}{[^{201}\text{MeHg}\ ]\text{initial}} \times \frac{1}{\text{tf(h)}} \times 100 \qquad (2.15)$$

2.3. Results and discussion.

The proportion of reduced ^{199}Hg(II) and reductive ^{201}MeHg demethylation from the ^{199}Hg(II) and ^{201}MeHg previously incubated for each incubation time, as well as the percentage of the Hg(II) and MeHg reduction potentials (% h^{-1}) in Lake Gentau (October, 2018 and June 2019), Endoume (October 2020) and Île-Riou (October, 2020), under light and dark conditions is presented in Table 2.6. The highest ^{199}Hg(II) reduction potentials were observed in seawaters of Endoume (4.3±0.7% h^{-1}) and Ile-Riou sites (3.4±0.4% h^{-1}) under light conditions. Under dark conditions, the highest ^{199}Hg(II) reduction potential was found in Endoume (1.2±0.1% h^{-1}).

These reduction potentials are much higher to those found in Lake Gentau under light and dark conditions. Under light conditions, ^{199}Hg reduction potentials were 0.866±0.003% h^{-1} in October 2018, and 0.702±0.001 % h^{-1} in June 2019. Regarding the dark conditions in Lake Gentau, ^{199}Hg reduction potentials differed between sampling campaigns (0.41±0.03% h^{-1}, October 2018 and 0.03±0.01% h^{-1} in June 2019). Concerning the reductive ^{201}MeHg demethylation potentials, the highest values were found in Lake Gentau (0.41±0.04% h^{-1} in October 2018, and 0.29±0.01 % h^{-1}, June 2019). In seawaters, reductive ^{201}MeHg demethylation potentials were 0.21±0.04% h^{-1} in Edoume and 0.15±0.02 % h^{-1} in Île-Riou. Under dark conditions, ^{201}MeHg reduction potentials were detected at lower extents in seawaters (0.041±0.007 % h^{-1} in Edoume and 0.004±0.002 % h^{-1}), whereas no reductive ^{201}MeHg demethylation could be detected in lake waters under dark conditions. In this case, seawater dark incubations were performed over 24 hours, while dark lake water incubations were performed only during 7–9 hours. Therefore, the incubation time was not enough to detect reliable transformations. To sum up, Hg(II) reduction in surface seawater was ten folds greater than those observed in surface lake water, whereas reductive MeHg demethylation in freshwaters was higher than seawaters.

Table 2.6. Proportion (%) of ^{199}Hg(II) and ^{201}MeHg reduced from the total Hg(II) and MeHg incubated during the different incubation times and percentage (%) of $^{199/201}$DGM formation per hours (h^{-1}) under light and dark conditions in Lake Ayous (October, 2018 and June, 2019), Endoume (October, 2020) and Île-Riou (October, 2020).

Matrix	Season	Conditions	Time (h)	Proportion of ^{199}Hg(II) reduced (%)	Proportion of ^{201}MeHg reduced (%)	^{199}Hg reduction (%h^{-1})	^{201}MeHg reduction (%h^{-1})
Lake Gentau	October 2018	Light	7h	6.2 ± 0.1	2.9 ± 0.3	0.866 ± 0.003	0.41 ± 0.04
		Dark	7h	0.5 ± 0.1	< D.L	0.41 ± 0.03	< D.L
Lake Gentau	June 2019	Light	9h	6.09 ± 0.1	2.9 ± 0.3	0.702 ± 0.001	0.29 ± 0.01
		Dark	9h	0.26 ± 0.07	< D.L	0.03 ± 0.01	< D.L
Endoume	October 2020	Light	7h	30.2 ± 4.6	0.9 ± 0.1	4.3 ± 0.7	0.21 ± 0.04
		Dark	24h	28.7± 4.6	1.0 ± 0.1	1.2 ± 0.1	0.041 ± 0.007
Île-Riou	October 2020	Light	7h	23.7± 2.9	0.5± 0.1	3.4 ± 0.4	0.15 ± 0.02
		Dark	24h	3.5± 0.7	0.09± 0.05	0.14 ± 0.03	0.004 ± 0.002

The differences found concerning the reductive MeHg potentials between freshwaters and seawaters can be explained looking at the speciation of MeHg in the corresponding environments. MeHg speciation differs largely in these two aquatic ecosystems because of the ligand competition between Cl^- and organic thiol compounds (e.g., NOM, DOM, LMW thiol compounds). Whereas MeHgCl can be the main specie in coastal marine waters with low DOC

content, freshwater ecosystems contain higher amount of organic ligands (e.g. LMW thiol compounds, DOM or NOM) (Branfireun et al., 2020; Morel et al., 1998). Therefore, the speciation of MeHg in freshwater ecosystems is mainly governed by MeHg binding organic ligands. Indeed, field observations are in agreement with the results presented in this doctoral dissertation showing a greater MeHg photodecomposition in freshwaters than seawaters (Hammerschmidt & Fitzgerald, 2006a; Lehnherr & St. Louis, 2009; Whalin et al., 2007). In laboratory experiments, one study confirmed these observations by determining the photodegration of MeHg complexed with DOM, LMW thiol compounds and Cl^-(Zhang & Hsu-Kim, 2010). In the cited study, results revealed that MeHg photodegradation was enhanced by binding with DOM and LMW thiol compounds, whereas MeHgCl complexes, which can be dominant in seawater, showed to not degrade MeHg as efficiently. In conclusion, the greater reductive MeHg demethylation was confirmed by previous studies suggesting that the methodology proposed in this work can be useful for investigating the MeHg photodegradation between freshwater and seawater ecosystems.

2.4. Conclusions.

In this work, we have shown the potential possibilities of combining IPD with an external calibration for the **simultaneous** determination of ^{199}Hg(II) reduction and reductive ^{201}MeHg demethylation potentials in seawater and freshwater samples. The methodology proposed provided: **(*i*)** higher results accuracy since it considers almost all Hg isotopes for the determination of major Hg compounds reduction pathways, and **(*ii*)** t the possibility of the **extension to higher numbers** isotopically enriched Hg compounds. Overall, the combination of IPD with external calibration provided an **universal approach** to compare compounds-specific Hg reduction pathways between freshwater and seawater ecosystems, bringing new potential possibilities for exploring Hg species potential reduction using different isotopically enriched Hg compounds.

3. Experimental design to determine biotic MeHg demethylation in phytoplankton cells[3].

3.1. Introduction.

Nowadays, MeHg demethylation have been already reported in pure phytoplankton cell cultures (Bravo et al., 2014; Li et al., 2022). However, the determination of MeHg demethylation potentials in phytoplankton can be abiotically or biotically mediated. A recent study added enriched Hg(II) and MeHg to 15 species of marine microalga (^{199}Hg(II):20 ng L^{-1}; ^{201}MeHg:2 ng L^{-1}) with the purpose of determining the potential Hg(II) methylation and MeHg demethylation under environmental relevant concentrations (Li et al., 2022). In the cited study, 6 microalgae species could significantly induce MeHg demethylation, whereas no methylation was observed in none of the phytoplankton species. The comparison of MeHg demethylation rates between microalgae cells and extracellular secretions revealed that, MeHg demethylation was mainly mediated by extracellular polymeric substances (EPS) release by microalgae (Li et al., 2022). In addition to this, higher demethylation rates were correlated with thiol concentrations suggesting that thiol groups of EPS enhance to the photodemethylation of MeHg. Concerning the analytical performance of this previous work, MeHg demethylation rates were calculated by measuring the ^{201}MeHg concentration loss applying the equations of Hintelmann et al., 2000. The quantification of Hg compounds was based on single compounds-specific approach (quantification tracers:^{198}Hg(II) and ^{198}MeHg). As a result, no correction of the methylation/demethylation during the sample preparation could have been considered (remainder in **page 27**). Nowadays, only one study reported the formation of Hg(II) from MeHg in the green alga *Chlamydomonas reinhardtii* (Bravo et al., 2014) under MeHg exposure levels of 800 ng L^{-1} suggesting that the production of Hg(II) was biotically mediated. This suggestion might lead to a misunderstanding. It is true that MeHg can be first internalized within the cell and after demethylated. However, MeHg can also be demethylated in the extracellular medium, and subsequently internalized within the cell. In any case a single MeHg incubation can prove if MeHg was demethylated biotically or abiotically.

In this work, the addition of isotopically enriched Hg compounds in pure phytoplankton cell cultures was performed in two consecutive 48 hours processes. Hg(II) and MeHg were added,

---

[3] *(Manuscript in preparation)*

Authors: Javier Garcia-Calleja, João P. Santos, Zoyne Pedrero Zayas, Vera I. Slaveykova, and David Amouroux.

separately, with concentrations of 200 and 20 ng L^{-1}, respectively. After 48 hours of exposure, cells containing Hg(II) or MeHg were recollected from their respective culture batch, and resuspended in new exposure mediums containing 200 and 20 ng L^{-1} of Hg(II) and MeHg during other 48 hours. The objective of this work was to address the biotic MeHg demethylation potential in phytoplankton cells.

3.2. Experimental design.

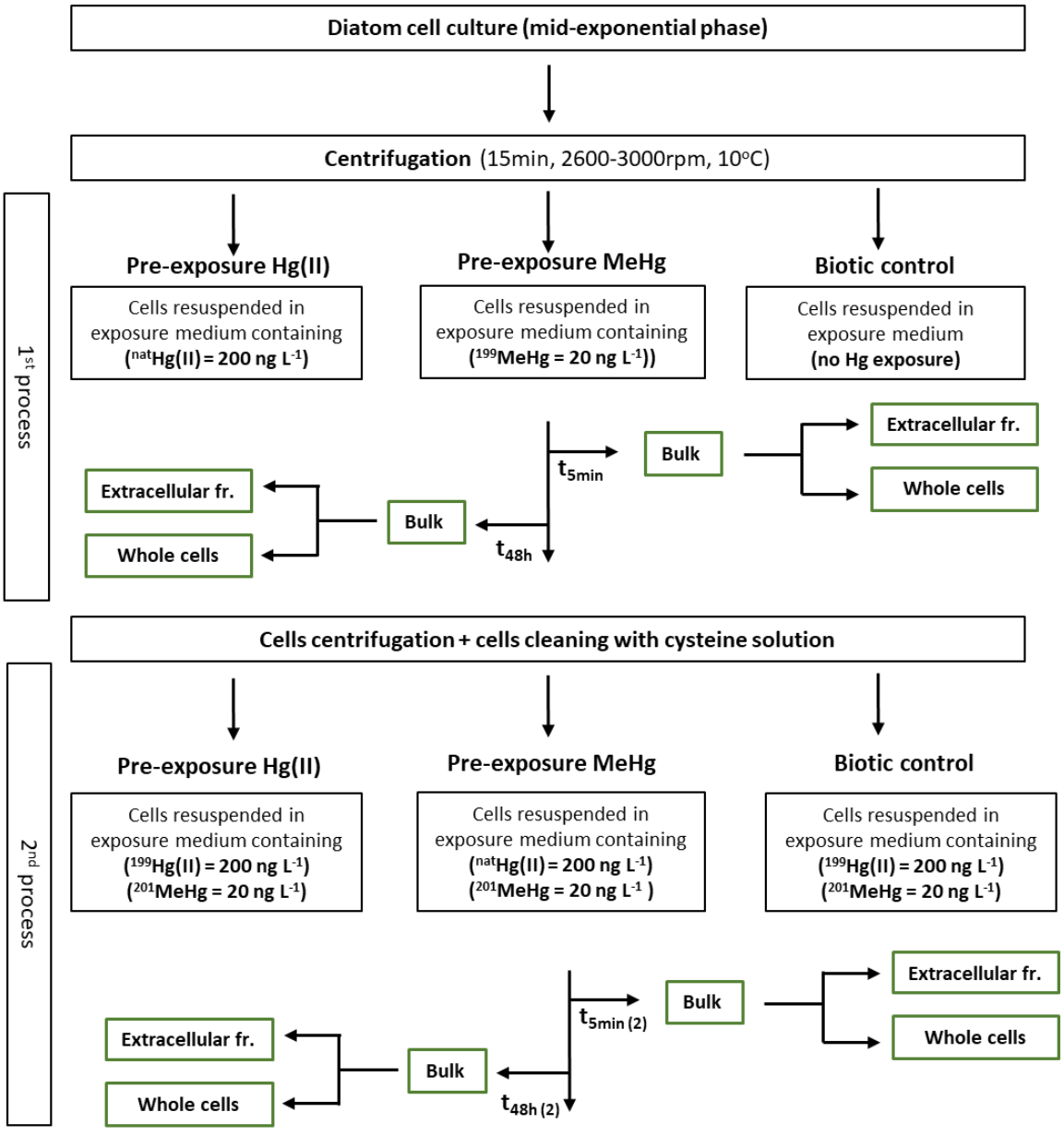

Figure 2.10. Scheme of the experimental approach performed for diatom cell culture in mid-exponential phase in order to obtain samples from the bulk, extracellular fraction, whole cells after 5 minutes and 48 hours in two consecutives processes in Hg(II) and MeHg pre-exposure conditions.

The cell density of *Cyclotella meneghiniana* cell culture was determined by flow cytometry in each growth bottle in order to determine the volume necessary of culture needed for reaching a

concentration of 1 x 10^6 cell mL^{-1} per flask. Then, cells were harvested (15min, 2600-3000rpm, 10°C) and resuspended in the two different exposure medium composed only by major cations (see composition in **Table A3- 2**) containing 420 mL (weighted) of **(1)** 200 ng L^{-1} of natural Hg(II), **(2)** 20 ng L^{-1} of ^{199}MeHg ng L^{-1}. Samples from the bulk, extracellular medium and whole cells were collected after 5 minutes and 48 hours for each condition. After 48 hours of either Hg(II) or MeHg exposure, cell cultures from Hg(II) and MeHg pre-exposures were centrifugated (10min, 4000rpm, 10°C), and cleaned with cysteine solution as performed in Zhong et al., 2009 for removing the potential Hg attachment on the cell wall. Then, cells were resuspended in three exposure mediums containing **(1)** 200 ng L^{-1} of ^{199}Hg (II) and 20 ng L^{-1} of ^{201}MeHg **(2)** 200 ng L^{-1} of natural Hg (II) and 20 ng L^{-1} of ^{201}MeHg and **(3)** 200 ng L^{-1} of ^{199}Hg (II) and 20 ng L^{-1} of ^{201}MeHg. As it was performed in the first step, samples from the bulk, extracellular medium and whole cells were collected after 5 minutes (2) and 48 hours (2) of exposure. Biotic controls (no Hg exposure) were performed throughout the whole experiment in order to check any possible cross Hg contamination between enriched Hg compounds. Different Hg isotopes were incubated for each condition as it can be observed in **Figure 2.10**. Since the isotope 199 was used for MeHg in the first process, natural Hg(II) had to be used in this specific condition (MeHg pre-exposure) during the second process. In order to avoid any cross contamination between flasks, the experimental set-up was carried out by bubbling air in each flask avoiding the entrance of gaseous Hg coming from other flasks (**Figure 2.11**). All conditions were performed in triplicate. The quantification of Hg compounds in the bulk, extracellular medium and whole cells was carried out by adding ^{198}Hg (II) and ^{202}MeHg before the sample preparation as it was described previously in Chapter 2.1.

Figure 2.11. Experiment on-going during the first 48 hours process.

Overall, more detailed information about the sample preparation corresponding to Hg compounds losses due to the centrifugation step in Chapter 3.1 (**Experimental approach**.). This work was mainly focused on determining the potential biotic MeHg demethylation using the quadruple tracer methodology developed.

3.3. Results and discussion.

3.3.1. Biotic oxidative MeHg demethylation.

^{199}MeHg demethylation was observed in the two consecutive 48 hours incubation steps in the bulk (**Table 2.7**). While the concentration of ^{199}MeHg concentration did not significantly change over time, the newly-formed ^{199}Hg(II) concentration increased 0.4 ng L^{-1} from t_{5min} to t_{48h} in both, first and second steps. As a result, no MeHg loss potentials could be obtained. On the other hand, the MeHg demethylation potentials (D_{ox} %) calculated in the first and second steps were 3.5±1.5% and 5.6±1.4%, respectively. Although similar increase in ^{199}Hg(II) concentration was observed in both 48h processes, the differences in D_{ox} potentials between processes were mainly attributed to the initial ^{199}MeHg concentration (see equation 2.10, Chapter 2.1). It is important to point out that the MeHg demethylation potentials were measured in the bulk (whole system) since the centrifugation step for obtaining the extracellular medium and cells might have promoted Hg compound losses, or even, undesirable Hg compounds transformations (more information about the recoveries in Chapter 3.1, **page 105**).

Table 2.7. ^{199}MeHg and newly-formed ^{199}Hg(II) concentration (ng L^{-1}) in the bulk during the first and second process after 5 minutes and 48 hours of Hg exposure. MeHg loss (%) was calculated using eq. 11 and the oxidative demethylation (%) was calculated using eq. 10 (chapter 2.1) changing t_0 by t_{5min}. Standard deviations associated correspond to three independent replicates (n=3). N.D is not determined due to no significant differences.

Bulk		**Original ^{199}MeHg (ng L^{-1})**	**Newly-formed ^{199}Hg(II) (ng L^{-1})**	**D_{ox} (%)**
1st process	t5min	11.6±0.4	0.11±0.07	3.5±1.5%
	t48h	12.1±0.7	0.52±0.19	
2nd process	t5min (2)	7.4±0.1	0.23±0.08	5.6±1.4%
	t48h (2)	7.3±0.4	0.65±0.14	

In order to know if the formation of ^{199}Hg(II) was mainly driven biotically or abiotically, ^{199}MeHg demethylation potentials were linked with the ^{199}MeHg localization between the extracellular fraction and cells during the second process. In **Figure 2.12**, ^{199}MeHg concentration was mainly found in cells within the second 48 hours, and no ^{199}MeHg release into the extracellular medium was observed. Although this previous finding demonstrates that

MeHg demethylation was carried out biotically, it could not be confirmed if the formation of ^{199}Hg(II) was mediated in the intracellular fraction (no cell fractionation in this specific experiment). Bravo et al., 2014 suggested that MeHg demethylation occurred intracellularly in *Chlamydomonas reinhardtii*. In the cited study, no cell fractionation was reported, and it was not clarified if the quantification of ^{199}Hg(II) and ^{201}MeHg by GC-ICP-MS was carried out using the mathematical approach showed in Monperrus et al., 2004 or Rodriguez-Gonzalez et al., 2013. In both cases, the correction of methylation and demethylation processes during the sample preparation was not considered. In this work, we confirm for first time that the formation of ^{199}Hg(II) from ^{199}MeHg was carried out biotically by linking the location of ^{199}MeHg between the extracellular medium and cells with the potential MeHg demethylation observed in the bulk.

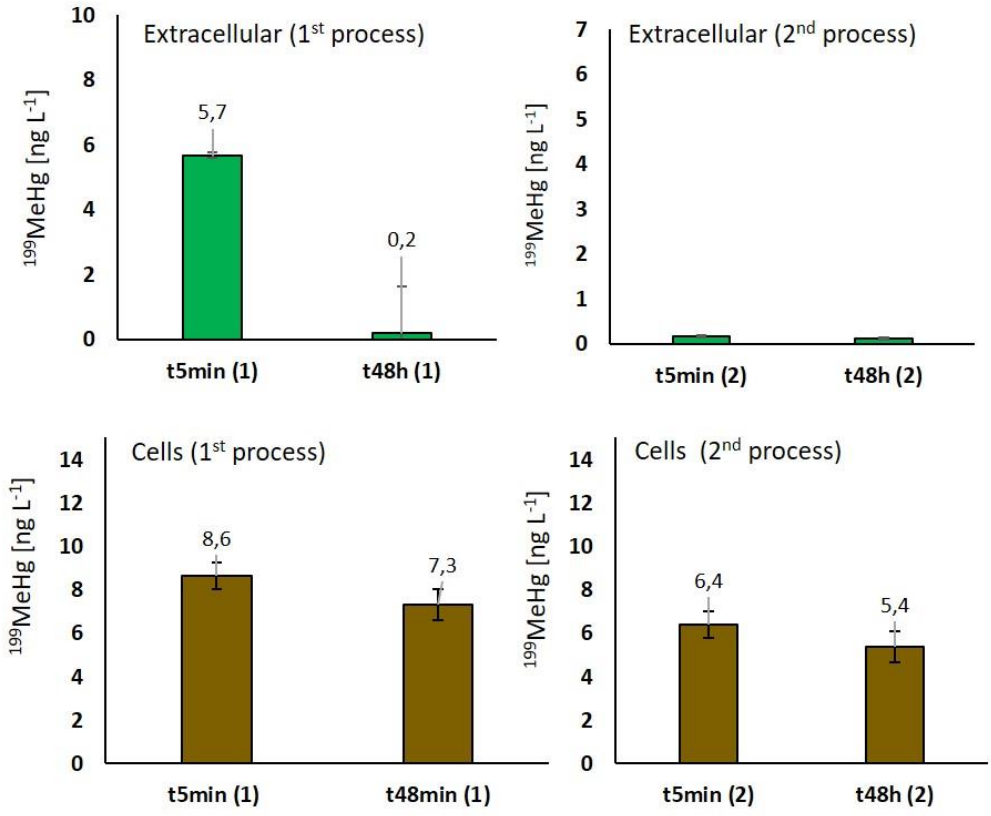

Figure 2.12. ^{199}MeHg concentration (ng L^{-1}) in the extracellular fraction (green) and whole cells (brown) during two consecutive processes at the beginning (t5min) and after 48 hours of Hg exposure. Standard deviations associated correspond to three independent replicates (n=3).

The comparison of ^{201}MeHg demethylation potentials between the Hg(II) and MeHg pre-exposure, and no pre-exposure conditions were also investigated during the second 48h step (**Table 2.8**). Results revealed similar ^{201}MeHg demethylation potentials between non pre-

exposure (2.0±0.3%), Hg(II) (2.6±0.1%), and MeHg pre-exposure conditions (2.5±0.9%) indicating that the previous presence of MeHg or Hg(II) did not influence the formation of ^{201}Hg(II). Furthermore, no differences were observed for the ^{201}MeHg partitioning between the extracellular fraction and whole cells between conditions. The previous exposure of either Hg(II) and MeHg did not influence the Hg(II) produced but also, the potential uptake (**Figure 2.13**).

Table 2.8. ^{201}MeHg and newly-formed ^{201}Hg(II) concentration (ng L^{-1}) in the bulk during the second process after 5 minutes and 48 hours of Hg exposure in Hg(II) and MeHg pre-exposure conditions, and no pre-exposure conditions. ^{201}MeHg loss (%) was calculated using eq. 2.11 and the oxidative demethylation (%) was calculated using eq. 2.10 changing t_0 by t_{5min}. Standard deviations associated correspond to three independent replicates (n=3) D.L corresponds to the detection limit.

Conditions	Time	Original ^{201}MeHg (ng L^{-1})	Newly-formed ^{201}Hg(II) (ng L^{-1})	D_{ox} (%)
Hg (II) pre-exposure	t5min (2)	15.4 ± 0.2	<D.L	2.6 ± 0.1 %
	t48h (2)	15.7 ± 0.3	0.40 ± 0.07	
MeHg pre-exposure	t5min (2)	16.2 ± 0.5	0.23 ± 0.08	2.5 ± 0.9 %
	t48h (2)	16.3 ± 1.0	0.53 ± 0.14	
No pre-exposure	t5min (2)	16.7 ± 1.2	U>X	2.0 ± 0.3 %
	t48h (2)	16.2 ± 0.1	0.38 ± 0.05	

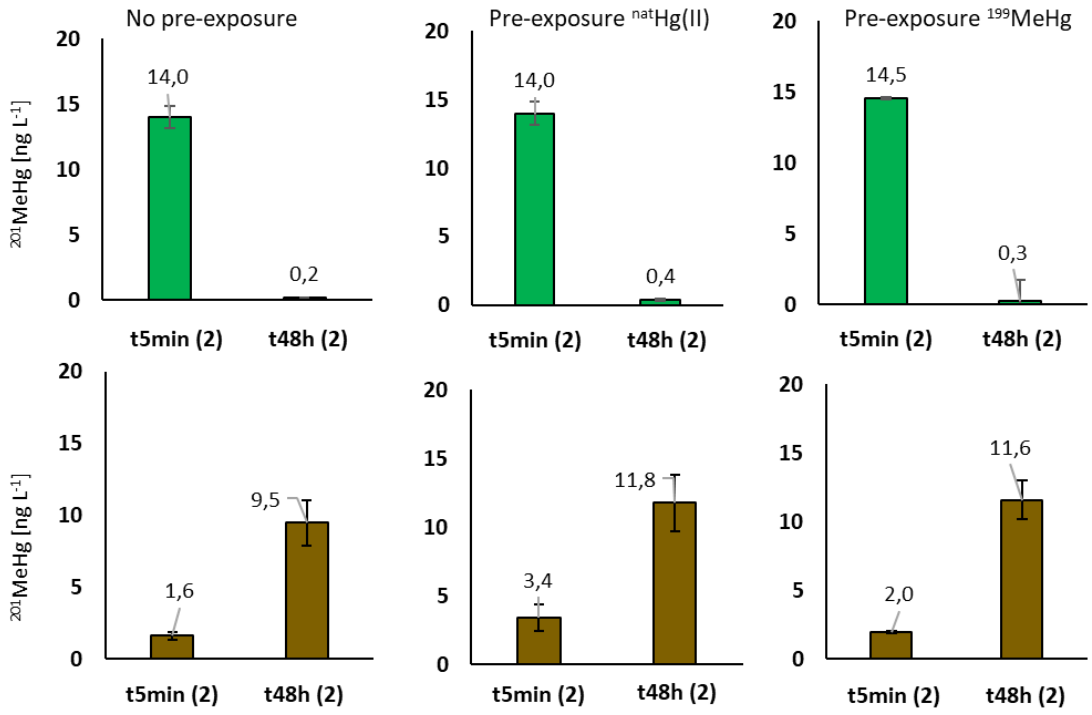

Figure 2.13.^{201}MeHg concentration (ng L^{-1}) in the extracellular fraction (green) and whole cells (brown) during the second process at the beginning (t5min) and after 48 hours of Hg exposure in Hg(II) and MeHg pre-exposure conditions, and no pre-exposure conditions. Standard deviations associated correspond to three independent replicates (n=3).

So far, the use of isotopically enriched Hg isotopes and analysis by GC-ICP-MS allowed to work at environmental relevant concentrations, but also to distinguish between added and background ambient (endogenous) Hg concentrations (Bravo et al., 2014). In the past, the addition of isotopically enriched Hg compounds in sediments (H.Hintelmann et al., 1995; Hintelmann & Evans, 1997) and anaerobic bacteria (Bridou et al., 2011; Pedrero, Bridou, et al., 2012) such as sulfate-reducing bacteria (SRB) has allowed to go a step further in order to elucidate the mechanistic pathways of Hg(II) methylation potentials (Parks et al., 2013). However, a little information is available about the potential Hg(II) methylation and MeHg demethylation in pure phytoplankton cell cultures (Bravo et al., 2014; Li et al., 2022) Furthermore, the cited studies were based on single Hg compounds incubations. Here we showed that, the understanding of isotopic pattern deconvolution (IPD) allowed us to explore new potential possibilities applying the quadruple tracer methodology. The experimental design was based on a double incubation of Hg(II) (^{nat}Hg(II) and ^{199}Hg(II)) and MeHg (^{199}MeHg and ^{201}MeHg) throughout two consecutive 48 hours steps. As a result, the localization of isotopically enriched ^{199}MeHg during both incubation processes confirmed the potential MeHg demethylation by phytoplankton cells. Nevertheless, further investigations are necessary to better understand the metabolic pathways involved in biotic MeHg demethylation in phytoplankton, as it was carried out in the past with the methylation of Hg(II) in anaerobic bacteria.

3.4. Conclusions.

In this work, the versatility of the quadruple tracer methodology has been shown through the addition of different isotopically enriched Hg compounds to phytoplankton cell culture in combination with an experimental design based on two consecutive incubation 48 hours steps. This approach allowed to determine the biotic MeHg demethylation mediated by phytoplankton cells. Although different potential MeHg demethylation (%) were seen between the first and second step, Hg(II) concentration always increased 0.4 ng L^{-1} from 5 minutes to 48 hours of exposure in both processes. Furthermore, the similar increase of the newly-formed Hg(II) concentration in different pre-exposure conditions shows the reproducibility and accuracy of the quadruple tracer methodology for the determination of newly-formed Hg compounds.

Annexes Chapter 2

Annexes Chapter 2.

Common equations for both mathematical models and notation.

Natural abundance Hg(II) and MeHg in the sample (s)

Isotopically enriched incubation tracers: ^{202}Hg (II) & ^{201}MeHg (t1 and t2)

Isotopically enriched quantification tracers: ^{198}Hg (II) & ^{199}MeHg (t3 and t4)

Legend:

A = Hg(II) B = MeHg

$$N_s^A = \text{Hg (II)nat nmol}$$

$$N_s^B = \text{MeHg nat nmol}$$

$$N_{t1}^A = {}^{202}\text{Hg (II) nmol}$$

$$N_{t2}^B = {}^{201}\text{MeHg nmol}$$

$$N_{t3}^A = {}^{198}\text{Hg (II) nmol}$$

$$N_{t4}^B = {}^{199}\text{MeHg nmol}$$

The calculation of the compounds-specific isotope abundances of inorganic mercury (A) and methylmercury (B) in the spiked samples (mixture) is performed by GC-ICP-MS. The isotope abundances in the mixture for inorganic mercury and methylmercury can be calculated from the peak areas measured at each monitored mass (198, 199, 200, 201, 202) divided by the sum of all areas measured for each compound.

It can be assumed that the abundances in the mixture (m) are linear combinations of the individual isotopic sources (s, t1, t2, t3 and t4) present in the system and the molar fraction of each individual source (x_s, x_{t1}, x_{t2}, x_{t3} and x_{t4}). If we assume that the response is first order in all independent variables, we can write the general linear function for each isotope as equations (A1) and (A2) for compound A (Hg(II)):

$$
\begin{aligned}
A_m^{198} &= A_s^{198}.x_{nat}^A + A_{t1}^{198}.x_{t1}^A + A_{t2}^{198}.x_{t2}^A + A_{t3}^{198}.x_{t3}^A + A_{t4}^{198}.x_{t4}^A \\
A_m^{199} &= A_s^{199}.x_{nat}^A + A_{t1}^{199}.x_{t1}^A + A_{t2}^{199}.x_{t2}^A + A_{t3}^{199}.x_{t3}^A + A_{t4}^{199}.x_{t4}^A \\
A_m^{200} &= A_s^{200}.x_{nat}^A + A_{t1}^{200}.x_{t1}^A + A_{t2}^{200}.x_{t2}^A + A_{t3}^{200}.x_{t3}^A + A_{t4}^{200}.x_{t4}^A \\
A_m^{201} &= A_s^{201}.x_{nat}^A + A_{t1}^{201}.x_{t1}^A + A_{t2}^{201}.x_{t2}^A + A_{t3}^{201}.x_{t3}^A + A_{t4}^{201}.x_{t4}^A \\
A_m^{202} &= A_s^{202}.x_{nat}^A + A_{t1}^{202}.x_{t1}^A + A_{t2}^{202}.x_{t2}^A + A_{t3}^{202}.x_{t3}^A + A_{t4}^{202}.x_{t4}^A
\end{aligned}
\qquad \text{(A1)}
$$

$$
\begin{bmatrix} A_m^{198} \\ A_m^{199} \\ A_m^{200} \\ A_m^{201} \\ A_m^{202} \end{bmatrix} = \begin{bmatrix} A_s^{198} & A_{t1}^{198} & A_{t2}^{198} & A_{t3}^{198} & A_{t4}^{198} \\ A_s^{199} & A_{t1}^{199} & A_{t2}^{199} & A_{t3}^{199} & A_{t4}^{199} \\ A_s^{200} & A_{t1}^{200} & A_{t2}^{200} & A_{t3}^{200} & A_{t4}^{200} \\ A_s^{201} & A_{t1}^{201} & A_{t2}^{201} & A_{t3}^{201} & A_{t4}^{201} \\ A_s^{202} & A_{t1}^{202} & A_{t2}^{202} & A_{t3}^{202} & A_{t4}^{202} \end{bmatrix} \times \begin{bmatrix} x_s^A \\ x_{t1}^A \\ x_{t2}^A \\ x_{t3}^A \\ x_{t4}^A \end{bmatrix} \qquad \text{(A2)}
$$

Then, we can calculate the five molar fractions by resolving a multiple linear regression with five equations and five unknowns. It would be the same for B (MeHg) as described in equation (A3).

$$
\begin{bmatrix} A_m^{198} \\ A_m^{199} \\ A_m^{200} \\ A_m^{201} \\ A_m^{202} \end{bmatrix} = \begin{bmatrix} A_s^{198} & A_{t1}^{198} & A_{t2}^{198} & A_{t3}^{198} & A_{t4}^{198} \\ A_s^{199} & A_{t1}^{199} & A_{t2}^{199} & A_{t3}^{199} & A_{t4}^{199} \\ A_s^{200} & A_{t1}^{200} & A_{t2}^{200} & A_{t3}^{200} & A_{t4}^{200} \\ A_s^{201} & A_{t1}^{201} & A_{t2}^{201} & A_{t3}^{201} & A_{t4}^{201} \\ A_s^{202} & A_{t1}^{202} & A_{t2}^{202} & A_{t3}^{202} & A_{t4}^{202} \end{bmatrix} \times \begin{bmatrix} x_s^B \\ x_{t1}^B \\ x_{t2}^B \\ x_{t3}^B \\ x_{t4}^B \end{bmatrix} \qquad \text{(A3)}
$$

The amount of analytical tracers added before sample preparation is known as it is a gravimetrically controlled amount of a previously characterized solution (in terms of concentration and isotopic abundances) so:

$$N_{t3}^A = {}^{198}\text{Hg (II) added} \qquad \text{(A4)}$$

$$N_{t4}^B = {}^{199}\text{MeHg added} \qquad \text{(A5)}$$

If there were no interconversion reactions (methylation/demethylation) the original amounts of the incubation tracers and the natural abundance mercury (^{nc}N) could be calculated based on the measured molar fractions as:

Endogenous Hg compounds

$$^{nc}N_s^A = N_{t3}^A \frac{x_s^A}{x_{t3}^A} \qquad \text{(Natural abundance Hg(II), A6)}$$

$$^{nc}N_s^B = N_{t4}^B \frac{x_s^B}{x_{t4}^B} \qquad \text{(Natural abundance MeHg, A8)}$$

Exogenous Hg compounds

$$^{nc}N_{t1}^A = N_{t3}^A \frac{x_{t1}^A}{x_{t3}^A} \qquad (^{202}\text{Hg enriched Hg(II), A7})$$

$$^{nc}N_{t2}^B = N_{t4}^B \frac{x_{t2}^B}{x_{t4}^B} \qquad (^{201}\text{Hg enriched MeHg, A9})$$

Newly-fomed Hg compounds

$$^{nc}N_{t2}^A = N_{t3}^A \frac{x_{t2}^a}{x_{t3}^A} \qquad (^{201}\text{Hg enriched Hg (II), A10})$$

$$^{nc}N_{t1}^B = N_{t4}^B \frac{x_{t1}^B}{x_{t4}^B} \qquad (^{202}\text{MeHg enriched Hg (II), A11})$$

Thus, using the molar fractions obtained from equations (A2) and (A3) we can calculate the amounts of each tracer and natural abundance species at the end of the sample preparation procedure using equations from A6 to A11. The concentrations in the sample are then calculated based on the mass taken and the atomic weight of mercury in each isotopic form. These concentrations calculated (eq. A6 to A11) are indicated as “non-corrected” concentrations throughout the manuscript.

However, interconversion reactions do occur both during incubation and sample preparation and have to be calculated to gain knowledge of the incubation process and to correct for losses during sample preparation. The following two models take into account these side reactions.

2. Equations for the "step by step" model for quadruple tracer isotope dilution based on isotopic pattern deconvolution.

In a similar way to eq. A6 to A11 we can calculate the amount of analytical tracer transformed by methylation or demethylation during the sample preparation procedure using the molar fractions obtained for t3 and t4:

$$N_{t3}^{B} = {}^{198}\text{MeHg formed by methylation} = N_{t4}^{B} \frac{x_{t3}^{B}}{x_{t4}^{B}} \qquad \text{(A12)}$$

$$N_{t4}^{A} = {}^{199}\text{Hg (II) formed by demethylation} = N_{t3}^{A} \frac{x_{t4}^{A}}{x_{t3}^{A}} \qquad \text{(A13)}$$

Then, we can calculate the interconversion factors that have occurred during sample preparation: M_2 (analytical tracer methylation) and D_2 (analytical tracer demethylation) as the ratio of the amount of tracer found (methylated or demethylated) divided by the total amount of quantification tracer added.

$$M_2 = \frac{N_{t3}^{B}}{N_{t3}^{A}} \qquad \text{(A12)}$$

$$D_2 = \frac{N_{t4}^{A}}{N_{t4}^{B}} \qquad \text{(A13)}$$

The amounts of the incubation tracers found at the end of the sample preparation procedure can be also calculated in the same way as with equations (A12) and (A13) for the quantification tracers:

$${}^{nc}N_{t1}^{B} = {}^{202}\text{MeHg formed by methylation} = N_{t4}^{B} \frac{x_{t1}^{B}}{x_{t4}^{B}} \qquad \text{(A14)}$$

$${}^{nc}N_{t2}^{A} = {}^{201}\text{Hg (II) formed by demethylation} = N_{t3}^{A} \frac{x_{t2}^{A}}{x_{t3}^{A}} \qquad \text{(A15)}$$

Exogenous Hg compounds correction.

These amounts calculated with eq. (A14) and (A15) for the incubation tracers are affected by the analytical methylation/demethylation factors M_2/D_2 previously calculated. We need first to calculate the M_2/D_2 corrected amounts of the incubation tracers to be able to compute the methylation/demethylation factors during incubation (M_1/D_1). So, after incubation and before sample preparation we can calculate the corrected amounts (^{c}N) using the interconversion factors M_2 and D_2 and simple mass balances. For t1 we can establish a system of 2 equations and 2 unknowns (${}^{c}N_{t1}^{B} + {}^{c}N_{t1}^{A}$) and the same for t2 (with ${}^{c}N_{t2}^{B} + {}^{c}N_{t2}^{A}$ as unknowns):

$$^{nc}N_{t1}^{B} = {}^{c}N_{t1}^{B} + {}^{c}N_{t1}^{A}M_2 \qquad \text{(A16)}$$

$$^{nc}N_{t1}^{A} = {}^{c}N_{t1}^{A} + {}^{c}N_{t1}^{B}D_2 \qquad \text{(A17)}$$

$$^{nc}N_{t2}^{B} = {}^{c}N_{t2}^{B} + {}^{c}N_{t2}^{A}M_2 \qquad \text{(A18)}$$

$$^{nc}N_{t2}^{A} = {}^{c}N_{t2}^{A} + {}^{c}N_{t2}^{B}D_2 \qquad \text{(A19)}$$

Once we obtain the corrected concentrations ($^{c}N_{t1}^{B}$, $^{c}N_{t1}^{A}$, $^{c}N_{t2}^{B}$, $^{c}N_{t2}^{A}$) we can calculate now the interconversion factors M_1 and D_1 during the incubation process by dividing the amounts found for the methylated/demethylated incubation tracers by the total amount of that tracer found (the original form plus the methylated/demethylated form).

$$M_1 = \frac{^{c}N_{t1}^{B}}{(\,^{c}N_{t1}^{A} + {}^{c}N_{t1}^{B})} \qquad \text{(A20)}$$

$$D_1 = \frac{^{c}N_{t2}^{A}}{(\,^{c}N_{t2}^{B} + {}^{c}N_{t2}^{A})} \qquad \text{(A21)}$$

Once the incubation factors M_1 and D_1 are calculated we can establish two mass balance equations for the incubation tracers t1 and t2 to calculate the original amounts (^{o}N) of those incubation tracers in the spiked sample:

$$^{c}N_{t1}^{A} = {}^{o}N_{t1}^{A}(1 - M_1) + {}^{o}N_{t1}^{B}D_1 \qquad \text{(A22)}$$

$$^{c}N_{t2}^{B} = {}^{o}N_{t2}^{B}(1 - D_1) + {}^{o}N_{t2}^{A}M_1 \qquad \text{(A23)}$$

Note that the nanomoles of $^{o}N_{t1}^{B}$ and $^{o}N_{t2}^{A}$ are expected to be zero as it was not added before incubation. Any value different from zero would be due to an impurity of the initial spike. So another way of calculation would be assuming that these values are zero:

$$^{o}N_{t1}^{A} = \frac{^{c}N_{t1}^{A}}{(1-M_1)} \qquad \text{(A24)}$$

$$^{o}N_{t2}^{B} = \frac{^{c}N_{t2}^{B}}{(1-D_1)} \qquad \text{(A25)}$$

These initial amounts found for the incubation tracers can be compared with the amounts added to check for loses in the system via volatilization, precipitation, adsorption on container walls or other factors.

Endogenous Hg compounds correction.

Finally, the original amounts of the endogenous natural abundance compounds (${}^{o}N_s$) can be calculated after correction first for M_2, D_2 and then for M_1, D_1 in a similar way as for the tracers. The amounts of the natural abundance compounds found at the end of the sample preparation procedure can be calculated as:

$$ {}^{nc}N_s^A = \text{Hg (II) natural abundance} = N_{t3}^A \frac{x_s^A}{x_{t3}^A} $$

$$ {}^{nc}N_s^B = \text{MeHg natural abundance} = N_{t4}^B \frac{x_s^B}{x_{t4}^B} $$

First, we establish mass balances for the corrected concentrations before sample preparation:

$$ {}^{nc}N_s^B = {}^{c}N_s^B(1 - D_2) + {}^{c}N_s^A M_2 \qquad \text{(A26)} $$

$$ {}^{nc}N_s^A = {}^{c}N_s^A(1 - M_2) + {}^{c}N_s^B D_2 \qquad \text{(A27)} $$

And then, after computation of ${}^{c}N_s^B$ and ${}^{c}N_s^A$, the original amounts of the natural abundance compounds before the incubation, ${}^{o}N_s^A$ and ${}^{o}N_s^B$, can be obtained solving the following system of 2 equations and 2 unknowns correcting for the incubation factors:

$$ {}^{c}N_s^A = {}^{o}N_s^A(1 - M_1) + {}^{o}N_s^B D_1 \qquad \text{(A28)} $$

$$ {}^{c}N_s^B = {}^{o}N_s^B(1 - D_1) + {}^{o}N_s^A M_1 \qquad \text{(A29)} $$

Here, we assume that identical reactivity occurred to the exogenous and endogenous Hg compounds, however, it is different in real samples.

3. Equations for the direct model for quadruple tracer isotope dilution based on isotopic pattern deconvolution

For the direct model we establish different mass balances taking into account a first mixture (m1) of natural abundances compounds and incubation tracers t1 and t2 which can be methylated (M_1) and/or demethylated (D_1) during incubation. Then:

$$ N_{m1}^A = \left(N_s^A + N_{t1}^A\right)(1 - M_1) + (N_s^B + N_{t2}^B)D_1 \qquad \text{(A30)} $$

$$ N_{m1}^B = (N_s^B + N_{t2}^B)(1 - D_1) + \left(N_s^A + N_{t1}^A\right)M_1 \qquad \text{(A31)} $$

After incubation we add the analytical tracers t3 and t4 and obtain a new mixture (m2) which is subjected to sample preparation where it can be methylated (M_2) and/or demethylated (D_2). The new mass balances will be:

$$N_{m2}^{A} = \left(N_{m1}^{A} + N_{t3}^{A}\right)(1 - M_2) + (N_{m1}^{B} + N_{t4}^{B})D_2 \quad \text{(A32)}$$

$$N_{m2}^{B} = (N_{m1}^{B} + N_{t4}^{B})(1 - D_2) + \left(N_{m1}^{A} + N_{t3}^{A}\right)M_2 \quad \text{(A33)}$$

By combining eq. (A30 and A31) and (A32 and A33) we obtain two new equations for A and B taking into account all possible interconversion reactions:

$$N_{m2}^{A}=\left(\left(N_{s}^{A}+N_{t1}^{A}\right)(1\text{-}M_1)+\left(N_{s}^{B}+N_{t2}^{B}\right)D_1+N_{t3}^{A}\right)(1\text{-}M_2)+\left(\left(N_{s}^{B}+N_{t2}^{B}\right)(1\text{-}D_1)+\left(N_{s}^{A}+N_{t1}^{A}\right)M_1+N_{t4}^{B}\right)D_2$$

(A34)

$$N_{m2}^{B}=\left(\left(N_{s}^{B}+N_{t2}^{B}\right)(1\text{-}D_1)+\left(N_{s}^{A}+N_{t1}^{A}\right)M_1+N_{t4}^{B}\right)(1\text{-}D_2)+\left(\left(N_{s}^{A}+N_{t1}^{A}\right)(1\text{-}M_1)+\left(N_{s}^{B}+N_{t2}^{B}\right)D_1+N_{t3}^{A}\right)M_2$$

(A35)

By development of eq. (A34) for component A and separating the terms corresponding to s, t1, t2, t3 and t4 we get:

$$N_{m2}^{A} = N_{s}^{A}(1 - M_1 - M_2 + M_1M_2 + M_1D_2) + N_{s}^{B}(D_1 + D_2 - D_1D_2 - D_1M_2) + N_{t1}^{A}(1 - M_1 - M_2 + M_1M_2 + M_1D_2) + N_{t2}^{B}(D_1 + D_2 - D_1D_2 - D_1M_2) + N_{t3}^{A}(1 - M_2) + N_{t4}^{B}D_2$$

(36)

The different terms in eq. (A36) for each isotopic profile can be related to the molar fractions experimentally obtained in eq. (2) as:

$$x_{s}^{A} = \frac{N_{s}^{A}(1 - M_1 - M_2 + M_1M_2 + M_1D_2) + N_{s}^{B}(D_1 + D_2 - D_1D_2 - D_1M_2)}{N_{m2}^{A}} \quad \text{(A37)}$$

$$x_{t1}^{A} = \frac{N_{t1}^{A}(1 - M_1 - M_2 + M_1M_2 + M_1D_2)}{N_{m2}^{A}} \quad \text{(A38)}$$

$$x_{t2}^{A} = \frac{N_{t2}^{B}(D_1 + D_2 - D_1D_2 - D_1M_2)}{N_{m2}^{A}} \quad \text{(A39)}$$

$$x_{t3}^{A} = \frac{N_{t3}^{A}(1 - M_2)}{N_{m2}^{A}} \quad \text{(A40)}$$

$$x_{t4}^{A} = \frac{N_{t4}^{B} D_2}{N_{m2}^{A}} \quad \text{(A41)}$$

In the same way by development of eq. (A35) for component B and separating the terms corresponding to s, t1, t2, t3 and t4 we get:

$$N_{m2}^{B} = N_{s}^{B}(1 - D_1 - D_2 + D_1D_2 + D_1M_2) + N_{s}^{A}(M_1 + M_2 - M_1M_2 - M_1D_2) + N_{t1}^{A}(M_1 + M_2 - M_1M_2 - M_1D_2) + N_{t2}^{B}(1 - D_1 - D_2 + D_1D_2 + D_1M_2) + N_{t3}^{A}(M_2) + N_{t4}^{B}(1 - D_2) \quad \text{(A42)}$$

The different terms in eq. (A42) for each isotopic profile can be related to the molar fractions experimentally obtained in eq. (A3) as:

$$x_{s}^{B} = \frac{N_{s}^{B}(1 - D_1 - D_2 + D_1D_2 + D_1M_2) + N_{s}^{A}(M_1 + M_2 - M_1M_2 - M_1D_2)}{N_{m2}^{B}} \quad \text{(A43)}$$

$$x_{t1}^{B} = \frac{N_{t1}^{A}(M_1 + M_2 - M_1M_2 - M_1D_2)}{N_{m2}^{B}} \quad \text{(A44)}$$

$$x_{t2}^{B} = \frac{N_{t2}^{B}(1 - D_1 - D_2 + D_1D_2 + D_1M_2)}{N_{m2}^{B}} \quad \text{(A45)}$$

$$x_{t3}^{B} = \frac{N_{t3}^{A}(M_2)}{N_{m2}^{B}} \quad \text{(A46)}$$

$$x_{t4}^{B} = \frac{N_{t4}^{B}(1 - D_2)}{N_{m2}^{B}} \quad \text{(A47)}$$

Now, using equations (A37) to (A41) and (A43) to (A47), we can calculate the methylation and demethylation factors, M_1, D_1, M_2 and D_2, and the original concentrations $({}^{o}N_{s}^{A},\ {}^{o}N_{s}^{B},\ {}^{o}N_{t1}^{A},\ {}^{o}N_{t2}^{B})$.

By dividing eq. (A40) by (A41) and (A46) by (A47), we obtain two new equations where the only unknowns are M_2 and D_2:

$$\frac{x_{t3}^{A}}{x_{t4}^{A}} = \frac{N_{t3}^{A}(1 - M_2)}{N_{t4}^{B}(D_2)} \quad \text{(A48)}$$

$$\frac{x_{t3}^{B}}{x_{t4}^{B}} = \frac{N_{t3}^{A}(M_2)}{N_{t4}^{B}(1 - D_2)} \quad \text{(A49)}$$

And finally, M_2 and D_2 can be determined by solving the following 2 equations with 2 unknowns:

$$x_{t4}^{A} N_{t3}^{A} M_2 + x_{t3}^{A} N_{t4}^{B} D_2 = x_{t4}^{A} N_{t3}^{A} \quad \text{(A50)}$$

$$x_{t4}^{B} N_{t3}^{A} M_2 + x_{t3}^{B} N_{t4}^{B} D_2 = x_{t3}^{B} N_{t4}^{B} \quad \text{(A51)}$$

By dividing the equations (A38) to (A40) and (A44) to (A47), and subsequently dividing both resulting equations we can calculate M_1.

$$\frac{\frac{x_{t1}^{A}}{x_{t3}^{A}}(1 - M_2)N_{t3}^{A}}{\frac{x_{t1}^{B}}{x_{t4}^{B}}(1 - D_2)N_{t4}^{B}} = \frac{(1 - M_1 - M_2 + M_1 M_2 + M_1 D_2)}{(M_1 + M_2 - M_1 M_2 - M_1 D_2)} \quad \text{(A52)}$$

To simplify the calculations we define two new variables: R_A^1 and R_B^1:

$$\frac{x_{t1}^{A}}{x_{t3}^{A}}(1 - M_2)N_{t3}^{A} = R_A^1$$

$$\frac{x_{t1}^{B}}{x_{t4}^{B}}(1 - D_2)N_{t4}^{B} = R_B^1$$

And finally:

$$M_1 = \frac{(R_B^1 - M_2(R_A^1 + R_B^1))}{(R_A^1 + R_B^1)(1 - M_2 - D_2)} \quad \text{(A53)}$$

On the other hand, by dividing equations (A39) to (A40) and (A45) to (A47), and subsequently dividing both resulting equations we can calculate D_1.

$$\frac{\frac{x_{t2}^{A}}{x_{t3}^{A}}(1-M_2)N_{t3}^{A}}{\frac{x_{t2}^{B}}{x_{t4}^{B}}(1-D_2)N_{t4}^{B}} = \frac{(D_1+D_2-D_1D_2-D_1M_2)}{(1-D_1-D_2+D_1D_2+D_1M_2)} \quad \text{(A54)}$$

The same as before, to simplify the calculations we define two new variables: R_A^2 and R_B^2:

$$\frac{x_{t2}^{A}}{x_{t3}^{A}}(1-M_2)N_{t3}^{A} = R_A^2$$

$$\frac{x_{t2}^{B}}{x_{t4}^{B}}(1-D_2)N_{t4}^{B} = R_B^2$$

And finally:

$$D_1 = \frac{\left(R_A^2 - D_2(R_A^2+R_B^2)\right)}{(R_A^2+R_B^2)(1-D_2-M_2)} \quad \text{(A55)}$$

Once the methylation/demethylation factors are calculated the determination of the original concentrations of the incubation tracers ${}^{o}N_{t1}^{A}$ and ${}^{o}N_{t2}^{B}$ is straight forward. By dividing equations (A38) and (A40), we obtain:

$$\frac{x_{t1}^{A}}{x_{t3}^{A}} = \frac{{}^{o}N_{t1}^{A}(1-M_1-M_2+M_1M_2+M_1D_2)}{N_{t3}^{A}(1-M_2)}$$

$$ {}^{o}N_{t1}^{A} = \frac{x_{t1}^{A}N_{t3}^{A}(1-M_2)}{x_{t3}^{A}(1-M_1-M_2+M_1M_2+M_1D_2)} \quad \text{(A56)}$$

In the same way, by dividing the equations (A45) and (A47), we obtain:

$$\frac{x_{t2}^{B}}{x_{t4}^{B}} = \frac{{}^{o}N_{t2}^{B}((1-D_1-D_2+D_1D_2+D_1M_2)}{N_{t4}^{B}(1-D_2)}$$

$$ {}^{o}N_{t2}^{B} = \frac{x_{t2}^{B} N_{t4}^{B} (1 - D_2)}{x_{t4}^{B}((1 - D_1 - D_2 + D_1 D_2 + D_1 M_2)} \qquad \text{(A57)} $$

The determination of the original concentrations ${}^{o}N_s^A$ and ${}^{o}N_s^B$ can be performed by dividing eq. (37) to (40) and (43) to (47). We obtain two equations with two unknowns:

$$ \frac{x_s^A}{x_{t3}^A} = \frac{{}^{o}N_s^A(1 - M_1 - M_2 + M_1 M_2 + M_1 D_2) + {}^{o}N_s^B(D_1 + D_2 - D_1 D_2 - D_1 M_2)}{N_{t3}^A(1 - M_2)} \qquad \text{(A58)} $$

$$ \frac{x_s^B}{x_{t4}^B} = \frac{{}^{o}N_s^B((1 - D_1 - D_2 + D_1 D_2 + D_1 M_2) + {}^{o}N_s^A(M_1 + M_2 - M_1 M_2 - M_1 D_2)}{N_{t4}^B(1 - D_2)} \qquad \text{(A59)} $$

Which can be transformed into:

$$ \frac{x_s^A}{x_{t3}^A}\left(N_{t3}^A(1 - M_2)\right) = {}^{o}N_s^A(1 - M_1 - M_2 + M_1 M_2 + M_1 D_2) + {}^{o}N_s^B(D_1 + D_2 - D_1 D_2 - D_1 M_2) $$

(A60) and,

$$ \frac{x_s^B}{x_{t4}^B}\left(N_{t4}^B(1 - D_2)\right) = {}^{o}N_s^A(M_1 + M_2 - M_1 M_2 - M_1 D_2) + {}^{o}N_s^B((1 - D_1 - D_2 + D_1 D_2 + D_1 M_2) $$

(A61)

Equations (A60) and (A61) can be solved for ${}^{o}N_s^A$ and ${}^{o}N_s^B$ allowing the determination of the endogenous amounts of natural abundance inorganic mercury and methylmercury. Please note that, if all factors (M_1, D_1, M_2, D_2) are zero eq. (A60) and (A61) reduce to the basic IDMS eq. (A6) and (A8), respectively. The same could be said for equations (A56) and (A57) and eq. (A7) and (A9) in the determination of the incubation tracers t1 and t2.

Table A2- 1. Non-corrected endogenous and exogenous Hg (II) and MeHg concentration (ng g^{-1}) in the model incubation experiments with a MeHg: Hg (II) ratio of 1:1, 3:1 and 10:1. Standard deviations associated corresponds to the overall analytical uncertainties calculated by Kragten approach.

Samples	**Endogenous**		**Exogenous**			
	Hg (II) nat (ng g^{-1})	**MeHg nat (ng g^{-1})**	**^{202}Hg (II) (ng g^{-1})**	**Newly formed ^{202}MeHg (ng g^{-1})**	**^{201}MeHg (ng g^{-1}))**	**Newly formed ^{201}Hg (II) (ng g^{-1})**
Ratio 1:1 (1)	655.5 ± 13.6	485.3 ± 10.1	1376.0 ± 17.4	5.5 ± 5.0	1328.7 ± 5.7	291.6 ± 6.6
Ratio 1:1 (2)	880.7 ± 13.4	542.4 ± 11.3	1615.2 ± 18.0	4.2 ± 5.2	1286.1 ± 12.4	316.4 ± 4.4
Ratio 1:1 (3)	992.8 ± 16.7	456.6 ± 9.5	1682.9 ± 21.5	17.4 ± 4.7	1128.3 ± 8.0	523.3 ± 7.4
Ratio 3:1 (1)	434.1 ± 7.5	393.0 ± 13.9	1061.6 ± 12.2	37.2 ± 5.3	2491.2 ± 15.7	304.8 ± 3.7
Ratio 3:1 (2)	447.2 ± 9.2	380.0 ± 12.4	900.1 ± 11.4	25.7 ± 4.9	2301.4 ± 12.0	315.1 ± 5.4
Ratio 3:1 (3)	529.8 ± 10.3	370.3 ± 15.0	1042.6 ± 11.9	35.0 ± 3.6	2294.8 ± 33.5	482.5 ± 6.7
Ratio 10:1 (1)	445.8 ± 12.2	407.2 ± 15.4	454.7 ± 10.3	88.8 ± 5.8	2593.8 ± 16.7	446.8 ± 16.6
Ratio 10:1 (2)	609.4 ± 13.0	393.2 ± 16.2	609.5 ± 8.2	84.9 ± 6.1	2547.9 ± 21.2	753.8 ± 10.7
Ratio 10:1 (3)	415.5 ± 6.3	444.9 ± 16.8	412.0 ± 5.4	105.0 ± 6.5	2855.5 ± 15.2	424.8 ± 5.8

Table A2- 2. Corrected endogenous and exogenous Hg (II) and MeHg concentration (ng g^{-1}) after the correction of the analytical methylation and demethylation yields and the different interconversion reactions due to the analytical procedure (M_2 (%) and D_2 (%)) in the model incubation experiments with a MeHg: Hg (II) ratio of 1:1, 3:1 and 10:1. Standard deviations associated corresponds to the overall analytical uncertainties calculated by Kragten approach.

Samples	**Endogenous**		**Exogenous**				**Interconversion processes**	
	Hg (II) nat (ng g^{-1})	**MeHg nat (ng g^{-1})**	**^{202}Hg (II) (ng g^{-1})**	**Newly formed ^{202}MeHg (ng g^{-1})**	**^{201}MeHg (ng g^{-1})**	**Newly formed ^{201}Hg (II) (ng g^{-1})**	**M_2 (%)**	**D_2 (%)**
Ratio 1:1 (1)	557.5 ± 13.4	483.5 ± 10.4	1375.8 ± 17.4	1.0 ± 4.9	1328.6 ± 5.7	22.4 ± 6.7	0.3 ± 0.1	20.3 ± 0.4
Ratio 1:1 (2)	755.5 ± 12.9	540.2 ± 11.7	1615.3 ± 18.0	-0.4 ± 5.0	1286.0 ± 12.4	18.4 ± 4.5	0.3 ± 0.1	23.2 ± 0.3
Ratio 1:1 (3)	796.4 ± 15.1	450.9 ± 10.0	1680.6 ± 21.4	5.3 ± 4.6	1128.1 ± 8.0	31.9 ± 5.6	0.7 ± 0.1	43.6 ± 0.7
Ratio 3:1 (1)	398.4 ± 7.4	387.1 ± 14.5	1059.7 ± 12.2	21.4 ± 5.6	2490.1 ± 15.7	78.4 ± 4.4	1.5 ± 0.4	9.1 ± 0.2
Ratio 3:1 (2)	403.9 ± 9.1	374.0 ± 13.1	898.6 ± 11.3	12.4 ± 5.2	2300.7 ± 12.1	49.1 ± 6.3	1.5 ± 0.4	11.6 ± 0.3
Ratio 3:1 (3)	466.7 ± 10.1	361.6 ± 15.7	1039.8 ± 11.8	15.7 ± 6.1	2293.3 ± 33.6	82.3 ± 8.2	1.9 ± 0.4	17.4 ± 0.3
Ratio 10:1 (1)	406.5 ± 12.0	394.9 ± 16.6	447.2 ± 10.1	75.2 ± 5.6	2588.0 ± 16.8	189.1 ± 15.8	3.0± 0.6	10.0 ± 0.3
Ratio 10:1 (2)	524.5 ± 12.6	386.5 ± 17.1	592.5 ± 7.8	77.3 ± 5.8	2545.4 ± 21.3	194.8 ± 13.9	1.3 ± 0.4	22.0 ± 0.6
Ratio 10:1 (3)	378.3 ± 5.7	423.9 ± 17.9	404.8 ± 5.3	82.6 ± 6.3	2845.8 ± 15.4	175.5 ± 5.6	5.5 ± 0.7	8.8 ± 0.2

Table A2- 3. Endogenous and exogenous Hg (II) and MeHg concentration (ng g^{-1}) after the correction of both analytical and incubation methylation and demethylation yields and the different interconversion reactions due to the incubation process (M_1 (%) and D_1 (%)) in the model incubation experiments with a MeHg: Hg (II) ratio of 1:1, 3:1 and 10:1. Standard deviations associated corresponds to the overall analytical uncertainties calculated by Kragten approach.

Samples	**Endogenous**		**Exogenous**				**Interconversion processes**	
	Hg (II) nat (ng g^{-1})	**MeHg nat (ng g^{-1})**	**^{202}Hg (II) (ng g^{-1})**	**Newly formed ^{202}MeHg (ng g^{-1})**	**^{201}MeHg (ng g^{-1})**	**Newly formed ^{201}Hg (II) (ng g^{-1})**	**M_1 (%)**	**D_1 (%)**
Ratio 1:1 (1)	549.8 ± 13.5	491.3± 11.6	1376.8 ± 18.0	-	1351.0 ± 8.7	-	0.1 ± 0.4	1.7 ± 0.5
Ratio 1:1 (2)	747.6 ± 12.9	548.2 ± 12.6	1614.9 ± 18.6	-	1304.5 ± 10.8	-	0.0 ± 0.3	1.4 ± 0.3
Ratio 1:1 (3)	786.1 ± 15.1	461.1 ± 11.0	1685.8 ± 21.8	-	1160.0 ± 7.8	-	0.3 ± 0.3	2.8± 0.5
Ratio 3:1 (1)	394.8 ± 7.5	391.2 ± 15.7	1081.1 ± 13.4	-	2568.5 ± 16.0	-	2.0 ± 0.5	3.1 ± 0.2
Ratio 3:1 (2)	401.5 ± 9.1	376.4 ± 14.3	911.1 ± 12.4	-	2349.8 ± 13.6	-	1.4 ± 0.6	2.1 ± 0.3
Ratio 3:1 (3)	460.8 ± 10.2	367.5 ± 16.9	1055.5 ± 13.2	-	2375.6 ± 29.2	-	1.5 ± 0.6	3.5 ± 0.4
Ratio 10:1 (1)	446.6 ± 14.5	354.7 ± 20.8	522.4 ± 11.5	-	2777.1 ± 22.4	-	14.4 ± 1.0	6.8 ± 0.5
Ratio 10:1 (2)	565.2± 14.8	345.8 ± 21.7	669.9 ± 9.7	-	2740.2 ± 22.8	-	11.5 ± 0.8	7.1 ± 0.5
Ratio 10:1 (3)	487.4 ± 8.3	372.8 ± 22.5	487.4 ± 8.3	-	3021.3 ± 16.4	-	16.9± 1.1	5.8 ± 0.2

Table A2- 4. . Corrected endogenous and exogenous Hg(II) and MeHg concentration after the correction of the methylation and demethylation yields during the sample preparation in biofilms (µg L^{-1}), sediments (µg L^{-1}), phytoplankton cell culture (ng L^{-1}) and freshwater incubations (ng L^{-1})at t_0/tinitial and at the end of the incubation (tf) under light (l) and dark(d) conditions. Hg transformation potentials (%) corresponding to the ^{199}Hg(II) Methylation (M), ^{201}MeHg demethylation (D_{ox}) and ^{201}MeHg loss. Standard deviations associated correspond to duplicates of independent samples. N.D refers to no determined because concentrations were under the detection limit or negative values close to zero (<D.L).

Corrected from interconversion processes (CIP)	**Endogenous Hg compounds**		**Exogenous Hg compounds**				**Exogenous Hg compounds transformation potentials**		
Matrices (concentration)	**nat Hg (II)**	**nat MeHg**	**^{199}Hg (II)**	**Newly formed ^{199}MeHg**	**^{201}MeHg**	**Newly formed ^{201}Hg (II)**	**M (%)**	**D_{ox} (%)**	**^{201}MeHg loss (%)**
Biofilms t0 (µg L^{-1})	133.7±21.6	2.2±0.6	93.9±3.0	0.2±0.1	9.0±0.9	0.07±0.01	**d:16.3±4.7 l: 15.0±1.6**	**d:5.7±1.1 l: 15.7±3.8**	**d:10.2±2.7 l: 16.4±1.2**
Biofilms tf-Dark (µg L^{-1})	119.1±25.5	3.4±1.2	82.9±4.9	15.5±4.4	8.1±2.1	0.6±0.1			
Biofilms tf Light (µg L^{-1})	125.3±2.3	3.3±0.4	84.8±8.2	14.3±1.4	7.5±0.1	1.5±0.4			
Sediments t0 (µg L^{-1})	293.1±7.6	0.8±0.1	57.7±6.4	0.1±0.1	4.8±0.2	0.2±0.2	**d:1.6±0.4**	**d:12.3±5.1**	**d:10.9±1.8**
Sediments tf Dark (µg L^{-1})	308.2±10.5	1.0±0.2	54.3±8.4	0.9±0.2	4.3±0.2	0.8±0.1			
Phytoplankton cell culture ti (ng L^{-1})	< D.L	< D.L	657.7±29.5	< D.L	67.9±3.0	0.2±0.2	N.D	**5.5±0.4**	**8.4±0.4**
Phytoplankton cell culture tf (ng L^{-1})	< D.L	< D.L	476.0±7.4	< D.L	62.2±1.6	3.9±0.3			
Freshwater t0 (ng L^{-1})	1.14±0.02	0.07±0.03	1.48±0.05	< D.L	0.16±0.01	0.001±0.001	**d:** N.D **l:** N.D	**d:1.8±0.5 l: 5.0±0.4**	**d:3.0±0.8 l:15.5±2.1**
Freshwater tf Dark (ng L^{-1})	0.66±0.03	0.07±0.00	1.49 ±0.01	< D.L	0.15±0.02	0.004±0.001			
Freshwater tf Light (ng L^{-1})	0.71±0.09	0.08±0.00	1.43±0.05	< D.L	0.13±0.01	0.009±0.002			

Table A2- 5. Non-corrected endogenous and exogenous Hg (II) and MeHg concentration after the correction of the methylation and demethylation yields during the sample preparation in biofilms (µg L^{-1}), sediments (µg L^{-1}), phytoplankton cell culture (ng L^{-1})and freshwater incubations (ng L^{-1})at t0/tinitial and at the end of the incubation (tf) under light (l) and dark(d) conditions. Hg transformation potentials (%) corresponding to the ^{199}Hg(II) Methylation (M), ^{201}MeHg demethylation (D_{OX}) and ^{201}MeHg loss. Standard deviations associated correspond to duplicates of independent samples. N.D refers to no determined because concentrations were under the detection limit (<D.L).

Non-corrected from the interconversion processes (NC)	**Endogenous Hg compounds**		**Exogenous Hg compounds**				**Exogenous Hg compounds transformation potentials**		
Matrices (concentration)	**nat Hg (II)**	**nat MeHg**	**^{199}Hg (II)**	**Newly formed ^{199}MeHg**	**^{201}MeHg**	**Newly formed ^{201}Hg (II)**	**M (%)**	**D_{ox} (%)**	**^{201}MeHg loss (%)**
Biofilms t0 (ng g^{-1})	134.7±24.6	2.2±0.6	93.9±3.0	0.2±0.1	9.0±0.9	0.50±0.03	**d:16.5±4.5 l: 15.1±1.7**	**d:3.3±0.7 l: 18.0±3.5**	**d:10.3±2.7 l: 16.3±1.3**
Biofilms tf-Dark (ng g^{-1})	119.2±25.6	3.2±1.3	83.9±4.9	15.8±4.3	8.1±2.1	0.8±0.2			
Biofilms tf Light (ng g^{-1})	125.3±2.3	3.4±0.6	86.1±8.4	14.4±1.6	7.5±0.1	2.1±0.4			
Sediments t0 (ng g^{-1})	294.1±7.6	0.5 ± 0.3	57.7±6.4	0.1±0.1	4.8±0.2	0.6±0.2	**1.5±0.5**	**d:25.2±6.8**	**d:10.4±1.8**
Sediments tf Dark (ng g^{-1})	308.2±14.0	0.8 ± 0.3	54.3±8.4	0.9±0.2	4.3±0.2	1.8±0.4			
Phytoplankton cell culture ti (pg g^{-1})	< D.L	< D.L	656.7±28.5	< D.L	67.9±3.0	2.2±0.9	N.D	**3.3±0.2**	**8.1±0.6**
Phytoplankton cell culture tf (pg g^{-1})	< D.L	< D.L	475.1±7.4	< D.L	62.2±1.6	4.5±0.7			
Freshwater t0	1.14±0.05	0.07±0.03	1.48±0.05	< D.L	0.16±0.01	0.011±0.004	**d:** N.D	**D:1.0±0.4**	**D:3.0±0.2**
Freshwater tf Dark (pg g^{-1})	0.66±0.03	0.07±0.00	1.49±0.01	< D.L	0.15±0.01	0.012±0.001	**d:** N.D	**L: 5.5±0.6**	**L:15.5±2.1**
Freshwater tf Light (pg g^{-1})	0.71±0.09	0.08±0.00	1.43±0.05	< D.L	0.13±0.02	0.020±0.001			

Methylation and demethylation yields during the sample preparation and incubation process in biofilms, sediments, freshwaters and phytoplankton.

Hg(II) and MeHg methylation and demethylation (D_2 and M_2) during the analytical procedure and incubation process (M_1 and D_1) in biofilms, sediments, freshwaters and phytoplankton.

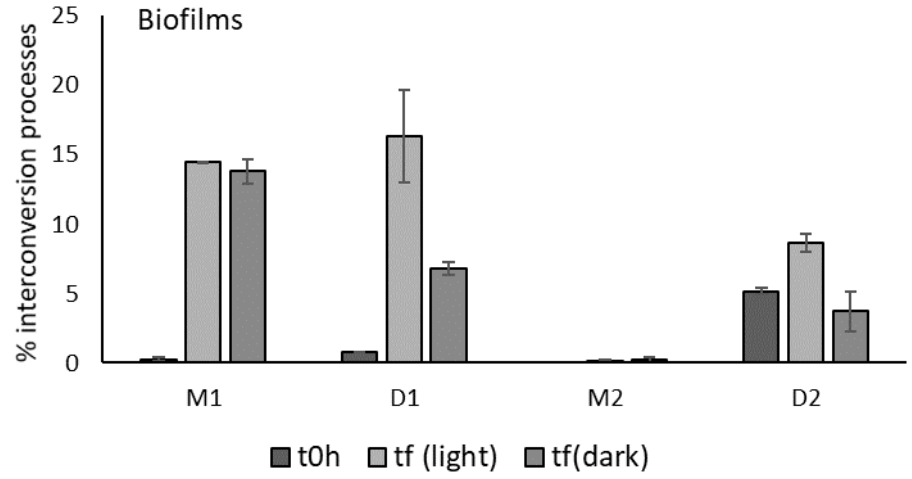

Figure A2- 1. Methylation and demethylation yields corresponding to the sample preparation (M_2 and D_2) and incubation process (M_1 and D_1) for biofilms at t0, tf (light) and tf (dark). Standard deviations correspond to triplicates for each condition (n=2).

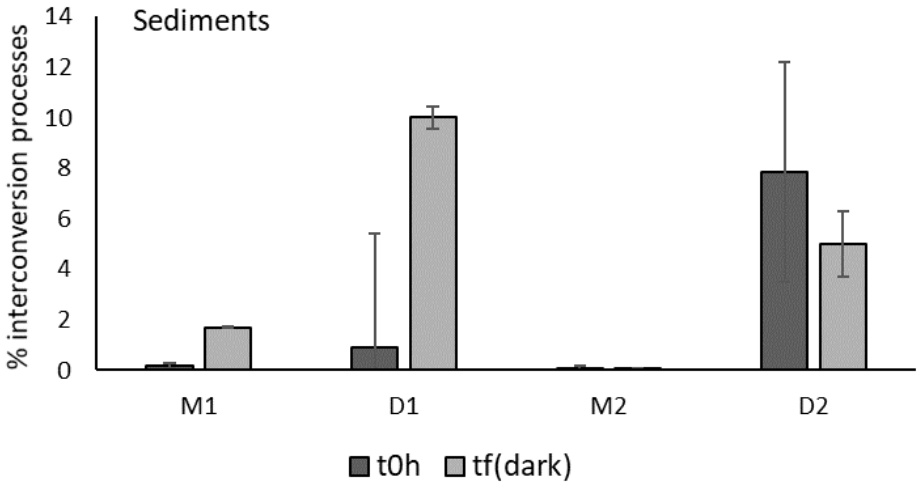

Figure A2- 2. Methylation and demethylation yields corresponding to the sample preparation (M_2 and D_2) and incubation process (M_1 and D_1) for sediments at t0) and tf (dark). Standard deviations correspond to triplicates for each condition (n=2).

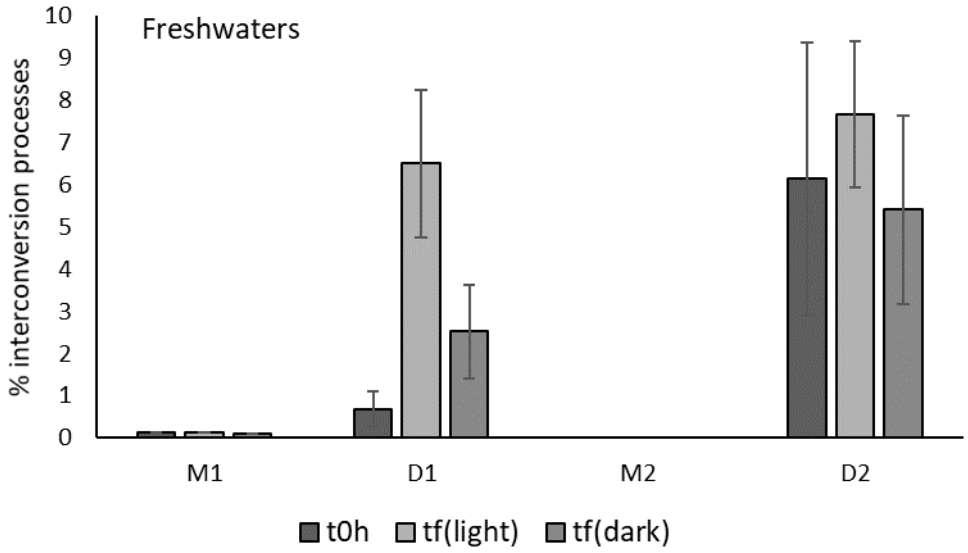

Figure A2- 3. Methylation and demethylation yields corresponding to the sample preparation (M_2 and D_2) and incubation process (M_1 and D_1) for freshwaters at t0, tf (light) and tf (dark). Standard deviations correspond to triplicates for each condition (n=2).

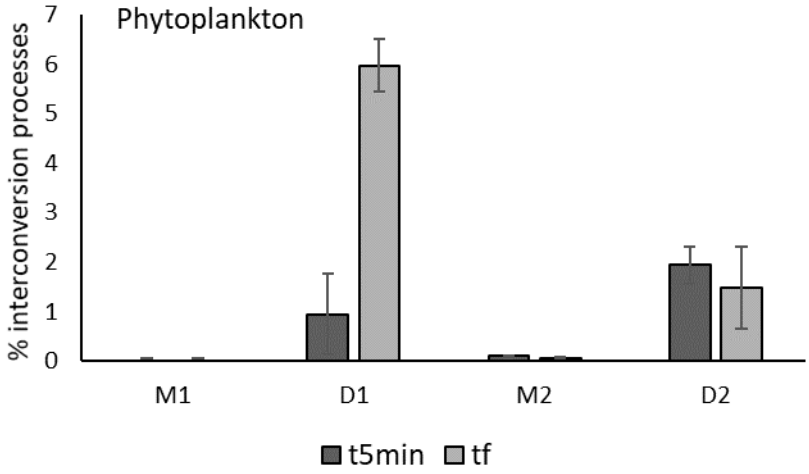

Figure A2- 4. Methylation and demethylation yields corresponding to the sample preparation (M_2 and D_2) and incubation process (M_1 and D_1) for phytoplankton at t5min, tf (96 hours). Standard deviations correspond to triplicates for each condition (n=2).

Relative standard uncertainty (RSD) of natural and enriched Hg compounds.

Figure 4A represents the average of the RSD (%) of the concentration of natural and enriched Hg(II) and MeHg compounds in the three model incubation experiments. The RSD % of the results presented comes from the overall of the analytical uncertainties calculated by Kragten divided by the main value. Enriched ^{201}MeHg RSD (%) displayed the lowest RSD values ranged from 0.5 – 1 % whereas, enriched ^{202}Hg (II) values were between 1–2 %. The highest RSD of endogenous Hg species corresponds to the natural MeHg. In this case, the RSD was increasing with the ratio of enriched ^{201}MeHg added suggesting that same behaviour might occur for the ^{nat}Hg (II) when an excess of enriched Hg(II) is incubated. Normally, the use of multiple isotopically enriched species increase the uncertainty of the analytical results for both species (around 3 %) while the addition of a single enriched specie is typically 1–2 %(Monperrus et al., 2004). These values falls in agreement with the values reported by Monperrus et al. 2008. In this previous work, the evaluation of the quantification of natural Hg (II) and MeHg using isotopically enriched Hg species was based on the classical equation for IDA for with. RSD values of 2 and 3 % for ^{nat}MeHg and ^{nat}Hg(II), respectively (**Figure A2- 5**).

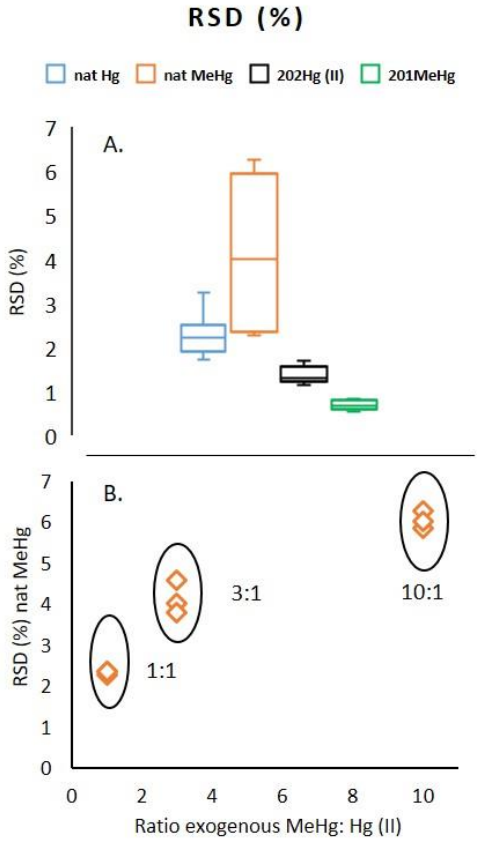

Figure A2- 5. **A)** Average of the relative standard uncertainties (RSD %) concerning to both natural and enriched Hg compounds from all samples measured from model incubation experiments. N = 9. **(B)** RSD % of nat MeHg in function of the theoretical ratio of the isotopically enriched Hg species (MeHg: Hg (II)).

Methylation and demethylation yields correlation with the newly-formed Hg compounds during the incubation process.

In figure 5, the relative error between CI and NC concentration for all Hg compounds was plotted against the methylation and demethylation yields (M_1 and D_1, incubation process). Results show the relative error between Hg compounds concentrations increased when higher methylation and demethylation yields. Particularly, the analysis based on a linear calibration showed that the relative error of enriched ^{202}Hg (II) was directly proportional to the methylation yields with a slope of 1 and an intercept value close to 0. Equal behaviour was observed comparing the relative error of enriched ^{201}MeHg and the demethylation yields in the incubation process. This shows that the determination of newly-formed enriched Hg compounds is directly correlated with the methylation and demethylation yields during the incubation process (M_1 and D_1) and demonstrates that the "step by step" model developed work properly.

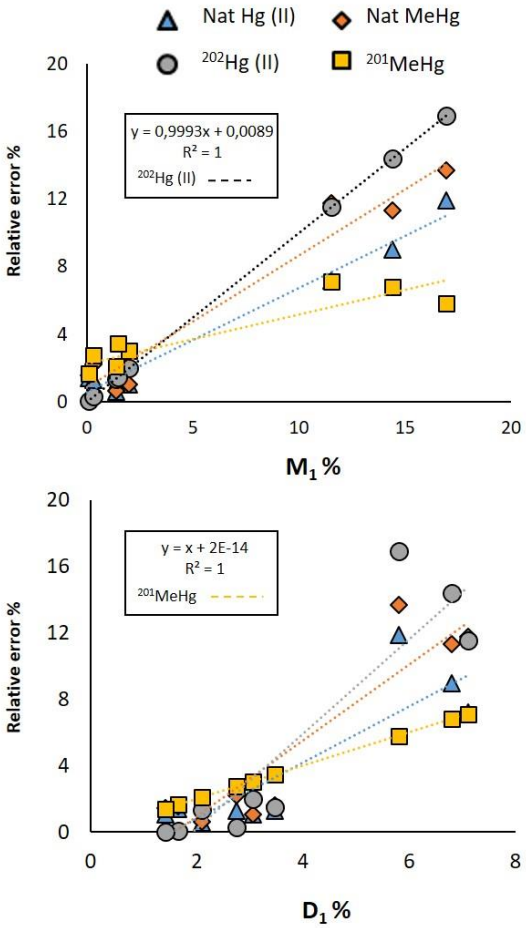

Figure A2- 6. Relative error (%) of the endogenous and exogenous Hg(II) and MeHg compounds concentration measured with and without correction from the interconversion processes in function of the methylation (M_1 %) and demethylation (D_1 %) due to the incubation process (n= 9).

Sources of uncertainty: Kragten approach.

An additional advantage of the methodology proposed is the application of the Kragten approach (Kragten, 1994). This approach consists to distinguish and estimate the degree in which the individual uncertainties of each parameter involved in the calculation contributed to the overall analytical uncertainty of the methylation and demethylation yields and Hg compounds concentrations (**Figure A2- 7**). In this case, the quadruple tracer methodology developed in this work involves forty parameters (see Figure 2.4, k1-k40) with the individual uncertainties corresponding to:

- The weights of the sample and quantification tracers (k1-k3).
- The quantification tracers concentration (k4 and k5).
- The Hg (II) and MeHg peak integration for each Hg isotope involved in IPD calculations (k6-k15).
- The isotopic abundances of the natural and isotopically enriched spikes (k16-k40).

In function of mathematical model applied for obtaining the concentration of newly-formed Hg compounds, the total uncertainty associated depend on the uncertainty propagation during the calculation. ¡Error! No se encuentra el origen de la referencia. shows that the most important contributor to the total uncertainty of the ^{199}MeHg in biofilms was the peak integration of ^{202}Hg isotope in MeHg, with a contribution of 94%. For ^{201}Hg(II), the isotopic abundances of the incubation tracer ^{199}Hg(II) are the major contributors to the overall analytical uncertainty (^{200}Hg: 18%; ^{201}Hg: 20%; ^{202}Hg: 26%). Also, the peak integration of ^{201}Hg (7%) and ^{202}Hg (16%) isotopes for MeHg contributed to the overall analytical uncertainty of ^{201}Hg(II) concentration in biofilms. Concerning to phytoplankton, the ^{202}Hg and ^{201}Hg abundances of the incubation tracer ^{199}Hg(II) contributed to the overall analytical uncertainty of ^{201}Hg(II) concentration in phytoplankton. Indeed, the small variations in the isotopic abundances of exogenous ^{199}Hg (II) tracer can modify the molar fractions of ^{201}Hg(II) (values in the IPD matrix). Similar outcomes were observed in freshwaters in which the major contributors were the ^{202}Hg (27%) and ^{201}Hg (45%) abundances of the incubation tracer ^{199}Hg(II) but also, the concentration of ^{198}Hg(II) (7%) indicating that, the characterization of ^{198}Hg(II) quantification tracer might play an important role in the determination of ^{201}Hg(II) concentration.

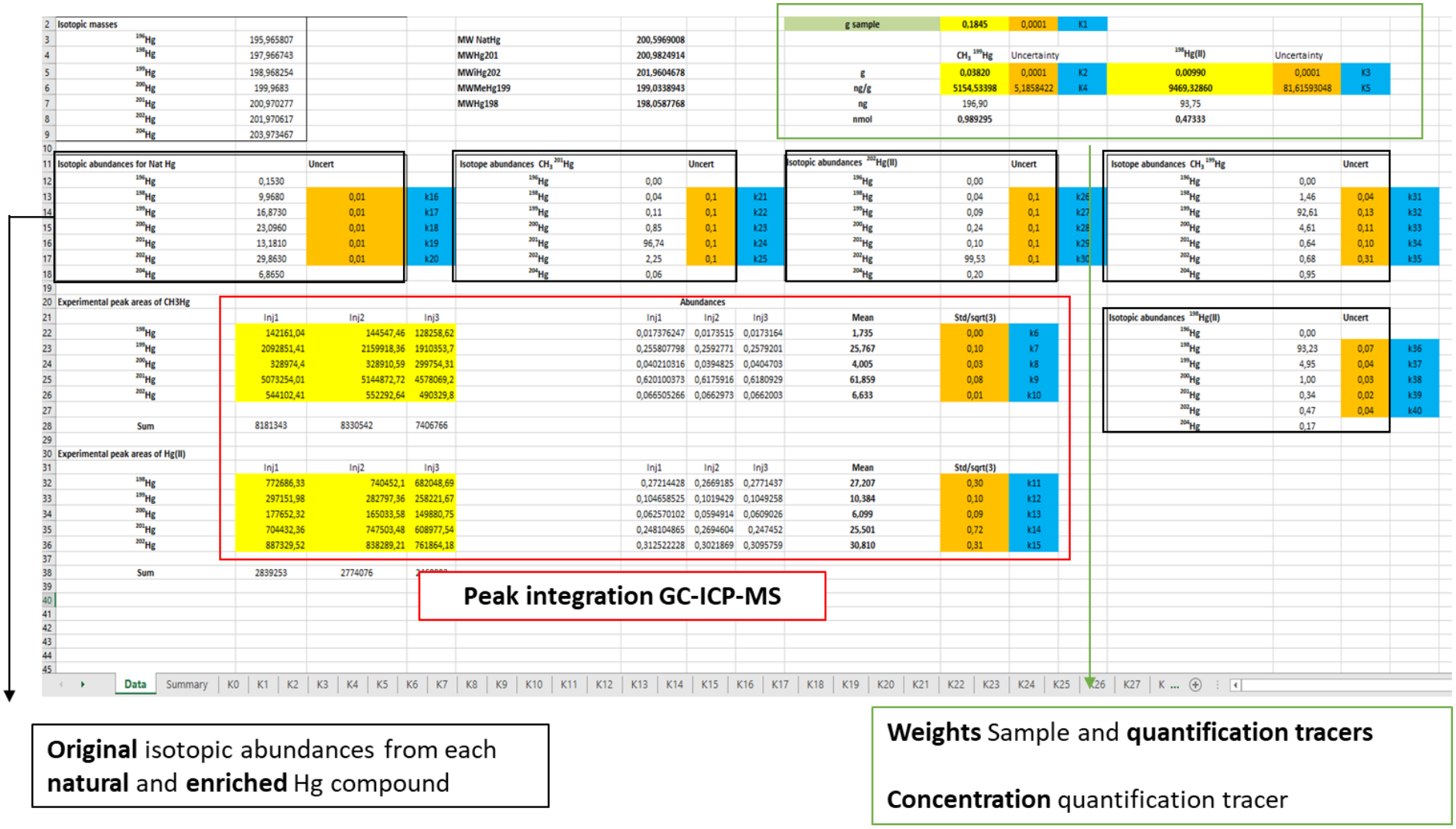

Figure A2- 7. Screenshot of the excel spreadsheet showing the 40 factors and their individual uncertainties corresponding to: the weights for the sample and quantification tracers (k1-k3), the concentration of the quantification tracers (k4 and k5), the peak integration (triplicate injection) for Hg (II) and MeHg for each isotope (k6-k15) and the abundances of natural and isotopically enriched spikes (k16-k40).

Biofilms t_f Light ^{199}MeHg

Code	Meaning	%
K10 (a)	^{202}Hg experimental peak integration MeHg	94 %
K4 (b)	Concentration ^{202}MeHg	1%
K6 (c)	^{198}Hg experimental peak integration MeHg	2 %
K8 (d)	^{200}Hg experimental peak integration MeHg	2 %

Biofilms t_f Light ^{201}Hg(II)

Code	Meaning	%
K9 (a)	^{201}Hg experimental peak integration MeHg	7 %
K10 (b)	^{202}Hg experimental peak integration MeHg	16%
K28 (c)	^{198}Hg experimental peak integration MeHg	2 %
K29 (d)	^{200}Hg experimental peak integration MeHg	2 %

Phytoplankton tf-1 ^{201}Hg(II)

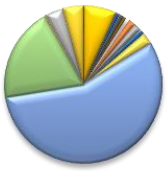

Code	Meaning	%
K29 (a)	^{201}Hg experimental peak integration ^{199}Hg(II)	61 %
K30 (b)	^{202}Hg experimental peak integration ^{199}Hg(II)	22%
K39 (c)	^{201}Hg experimental peak integration ^{198}Hg(II)	5 %
K40 (d)	^{202}Hg experimental peak integration ^{198}Hg(II)	4 %

Lake waters tf L-1 ^{201}Hg(II)

Code	Meaning	%
K5 (a)	Concentration ^{198}Hg(II)	7 %
K28 (b)	^{200}Hg experimental peak integration ^{199}Hg(II)	9%
K29 (c)	^{201}Hg experimental peak integration ^{199}Hg(II)	45 %
K30 (d)	^{202}Hg experimental peak integration ^{199}Hg(II)	27 %

Figure A2- 8. Major contributions of individual uncertainties to the total uncertainty calculated for the concentration of newly-formed Hg compounds (^{199}MeHg and ^{201}Hg(II)) under light conditions in biofilms, sediments, phytoplankton and lake waters samples.

Chapter 3

Hg-phytoplankton interactions: investigation of the intracellular Hg(II) and MeHg binding bioligands in phytoplankton.

Chapter 3: Hg-phytoplankton interactions: investigation of intracellular Hg(II) and MeHg binding bioligands in phytoplankton.

Summary.

In natural waters, the complexation of Hg compounds with different inorganic and organic ligands is well known. However, the complexation of Hg compounds with intracellular bioligands is not well documented. In this chapter, we combine the use of isotopically enriched Hg compounds with hyphenated techniques based on gas and liquid chromatography coupled to elemental and molecular mass spectrometry to explore; the role biogenic ligands involved in Hg intracellular handling in three model phytoplankton microorganisms: the cyanobacterium *Synechocystis* sp. PCC 6803, the diatom *Cyclotella meneghinianna* and green alga *Chlamydomonas reinhardtii*. In *C.meneghiniana*, MeHg binding GSH was identified in the biotic control since the release of Hg compounds into the extracellular fraction after 72 hours of exposure did not allow us to detect any intracellular bioligand bound to Hg in the intracellular fraction. Thanks to other complementary findings in our work, we could hypothesize that GSH might be involved in the specific excretion of MeHg into the extracellular fraction due to stress induced by MeHg, rather than the metabolic excretion of EPS mediated by passive diffusion of living cells. In *Synechocystis*, Hg(II) and MeHg were sequestrated in the intracellular fraction by GSH and other unidentified intracellular bioligands. Whereas GSH seems to play an important role controlling the intracellular Hg speciation, it was suggested that one or several unknown intracellular bioligands bound specifically to Hg(II) might act as an electron acceptor reducing and maintaining Hg(II) intracellular levels in *Synechocystis*. In *C.reinhardtii*, the sequestration of MeHg strongly supported previous studies about the tolerance of *C.reinhardtii* to MeHg exposure. In contrast, Hg(II) was released into the extracellular fraction after 96 hours of exposure. Overall, specific pathways involving sequestration and release of Hg compounds were investigated in three model phytoplankton species representatives from phytoplankton communities.

1. Material and methods.

1.1. Choice and description of the phytoplankton species studied.

In this work, the cyanobacterium *Synechocystis* sp. PCC 6803, the diatom *Cyclotella meneghiniana* and the green alga *Chlamydomonas reinhardtii* were studied since: ***i.*** they represent the major groups of phototrophs in freshwater phytoplankton; ***ii***. they have a sequenced genome, which facilitates their study; ***iii***. their inter-comparison is interesting since cyanobacteria are prokaryotes, while diatom and green alga are eukaryotes; ***iv.*** they are characterized by having different cell wall composition and intracellular structure (**Figure 3.1**).

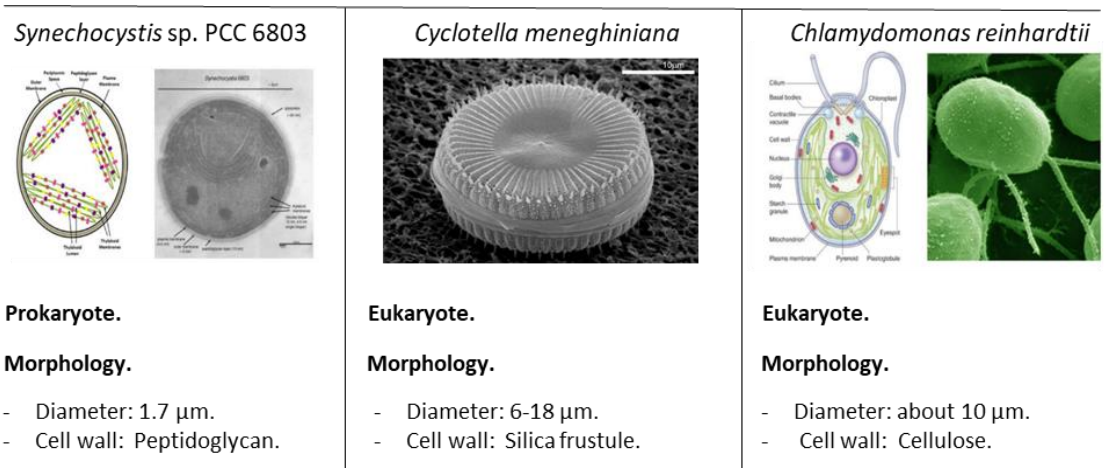

Figure 3.1. Images and main characteristics of the different phytoplanktonic species studied in this work corresponding to cyanobacterium *Synechocystis* sp. PCC 6803, diatom *Cyclotella meneghiniana* and green alga *Chlamydomonas reinhardtii*.

1.2. Experimental approach.

1.2.1. Culture medium conditions.

Phytoplankton cell cultures of the diatom, *Cyclotella meneghiniana*, cyanobacterium, *Synechocystis* sp. PCC 6803 and green alga *Chlamydomonas reinhardtii* were cultivated in SFM medium, BG11 medium modified (sodium nitrate replaced by ammonium nitrate), and TAP medium diluted 4 times (Annexes C3, **page 142**), respectively with an illumination value of 130 µE m^{-2} s^{-1} and an illumination regime of 14:10 hours (light:dark) (Stanier et al., 1979). The cell density was determined by flow cytometry (Accuri C6, BD Biosciences, Switzerland) before the cell resuspension in the exposure medium to reach the cell density desired. Cells were harvested by centrifugation (2600-3000rpm, 15min, 10°C) and resuspended in their respective exposure medium composed by only major cations. After the exposure of cells, cell cultures were divided in two equal parts. While one of them was used as biotic control to check

any possible Hg contamination in the biological system, the other was incubated with enriched ^{199}Hg(II) and ^{201}MeHg reaching a concentration of 600 ng and 60 ng of per L of exposure media, respectively (3 nM ^{199}Hg (II) & 0.3 nM ^{201}MeHg) (**Table 3.1**). Isotopically enriched ^{199}Hg(II) and ^{201}MeHg intermediate solutions (200 ng·L^{-1} / 1 µM) were prepared in the exposure medium on the week of the experiment, where an aliquot was collected for the characterization of the isotopic abundances by reverse isotope dilution analysis. The incubation of the enriched Hg compounds was performed by weighting the exact amount needed in function of cell culture volume in an Eppendorf. After the addition, the Eppendorf was washed 3 times with the medium to be sure that all Hg present in the Eppendorf was added to the cell culture. The cell density of *Synechocystis* sp. and *C. reinhardtii* was measured at the initial point before the spike addition, whereas *C. meneghiniana* cell density was measured at each sampling collection point throughout the whole experiment. Three independent cell cultures were carried out and incubated, simultaneously, with isotopically enriched Hg compounds. The medium was sterile and no contamination occurred with other organisms. An accidental contamination of ^{nat}Hg(II) in *C.meneghiniana* during the cell growth allowed us to compare it with the mercury free growth conditions (MFG) (**Chapter 3.2**). *C.reinhardtii* results are shown in Annexes C.3 (page **147**) since it suffered an accidental ^{nat}Hg(II) contamination and not clean exposure could be provided in this work.

Table 3.1. Initial cell density and Hg exposure level per cell (amol·cell^{-1}) in *Synechocystis* sp. 6803, *Cyclotella meneghiniana* and *Chlamydomonas reinhardtii*.

Phytoplankton strains	Initial cell density (cell·mL^{-1})	Initial / Theoretical Hg exposure level per cell (amol·cell^{-1})
Synechocystis sp. PCC 6803	3.5 x 10^{6}	^{199}Hg(II) = 9 x 10^{-1} ^{201}MeHg = 9 x 10^{-2}
Cyclotella meneghiniana	9.6 x 10^{5}	^{199}Hg(II) = 3.0 ^{201}MeHg = 3.0 x 10^{-1}
Chlamydomonas reinhardtii	7 x 10^{7}	^{199}Hg(II) = 4.2 x 10^{-2} ^{201}MeHg = 4.2 x 10^{-3}

1.2.2. Sample collection.

Aliquots/samples were collected after 5 minutes, 24 hours and 72/96 hours of Hg exposure in parallel to the biotic control (no Hg exposure). 4mL of the bulk were collected and transferred into free metal tubes. Subsequently, an aliquot of 45mL was taken and centrifuged (4000rpm, 10min, 10°C) to separately collect the extracellular medium (supernatant) and whole cells (pellet) fraction. In addition, another 45mL were collected from the cell culture with the purpose of fractionating the cells (see schema of the cell fractionation in ¡Error! No se encuentra el

origen de la referencia.). Particularly in *Synechocystis*, an additional experiment was performed by pre-concentrating one time, 2L of the cell culture only after 96 hours of exposure for the screening of Hg binding bioligands.

1.2.3. Cell fractionation procedure.

After discarding the extracellular medium, the pellet was flash frozen in liquid nitrogen to stop the metabolic activity. Subsequently, 1.5mL of Milli-Q water were added to the pellet and an ultra-sonication (Sonics Vibra-cell, 130W, 20kHz) step was performed for 1 minute at 50% amplitude to break the cells. The separation of the supernatant and solid residue was performed through a centrifugation (10000g, 6min) in a centrifuge 5417R (Eppendorf). The supernatant or soluble fraction corresponds to the cytosolic fraction, composed by heat stable proteins (HSP) and heat denatured proteins (HDP), whereas the solid residue or insoluble fraction corresponds to the granules and membranes with cells debris (Lavoie et al., 2009), but also, any insoluble compound / artifact that might have formed within the cells during the experiment or due to the ultra-sonication. Organelles disruption was only verified in *Synechocystis* sp. Samples from the cytosolic fraction were divided in aliquots and stored at – 80°C to avoid any possible protein degradation for Hg bioligands analysis. The other fractions were acidified with HNO_3 (3N) and stored at 4°C for the quantification of Hg compounds (**Table 3.4**). The scheme of the experimental procedure performed for Hg compounds quantification and the investigation of Hg biocomplexes is displayed in ¡Error! No se encuentra el origen de la referencia.. For the additional experiment pre-concentrating 2L in *Synechocystis*, 10mL Milli-Q water were added to the pellet before breaking the cells.

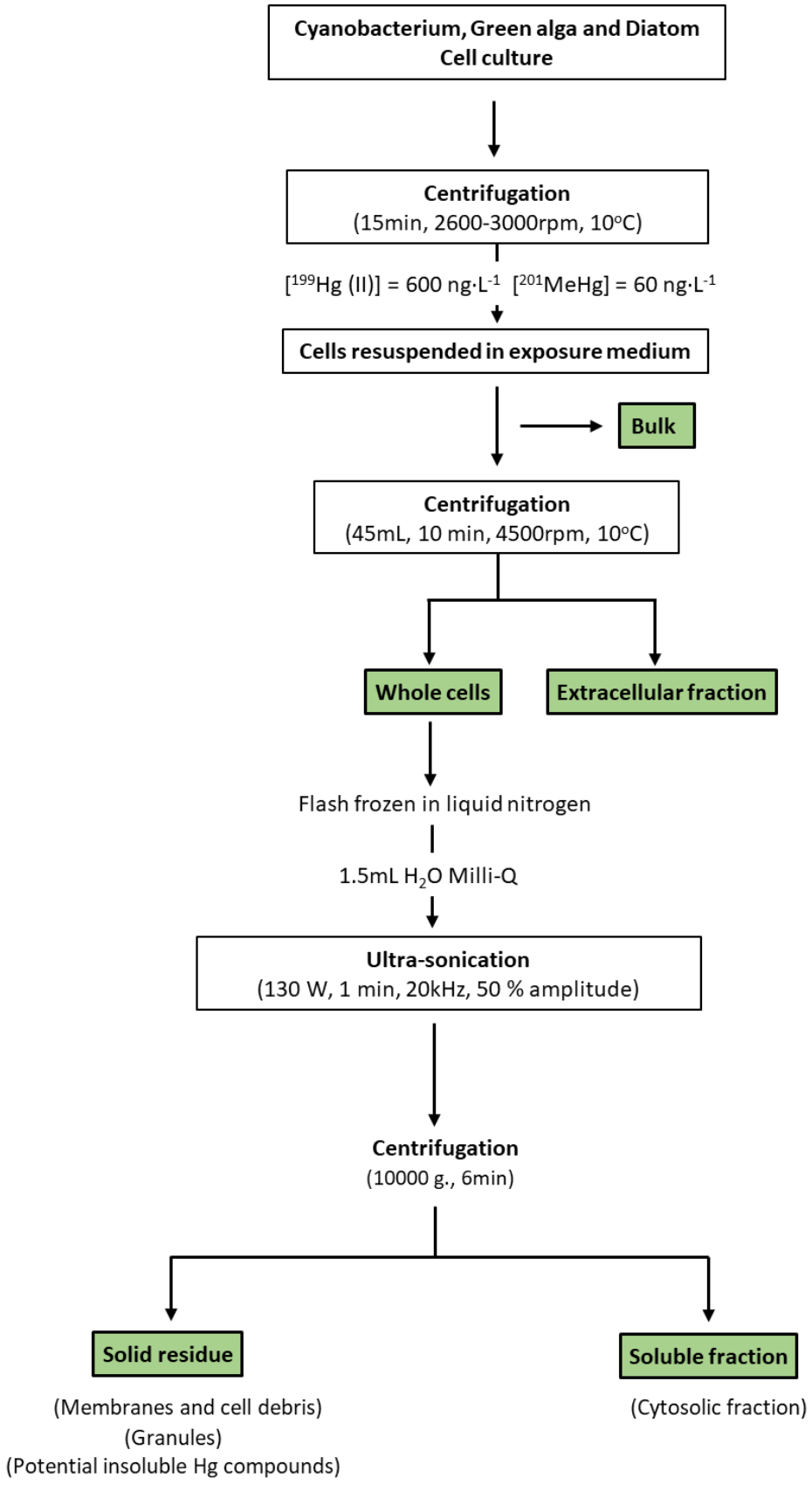

Figure 3.2. Scheme of the experimental approach performed for the three phytoplanktonic species for obtaining the samples from the bulk, extracellular fraction, whole cells, cytosolic fraction and, solid residue (membranes and cell debris + granules + insoluble Hg compounds) at t_{5min}, t_{24h} and $t_{72h/96h}$ for the biotic control and Hg incubation experiments with *Synechocystis* sp. PCC 6803, *Cyclotella meneghiniana* and *Clamydomonas reinhardtii*.

1.2.4. Hg compounds losses throughout the experimental procedure.

In **Table 3.2**, the recoveries of ^{199}Hg(II) and ^{201}MeHg initially added to the cell culture have been obtained to track any potential Hg compounds losses during the first centrifugation step (collection of extracellular and whole cells fraction). On the other hand, Hg compounds losses due to the cell fractionation and subsequent second centrifugation step (cytosolic fraction and membranes and cell debris) are observed in **Table 3.3**. The values correspond to the average obtained with the equations below for t_{5min}, t_{24h} and t_{96h}.

Table 3.2. Percentages (%) of ^{199}Hg(II) and ^{201}MeHg losses due to the centrifugation step to obtain the extracellular fraction and whole cells for the three phytoplankton species

Phytoplankton species	^{199}Hg(II) losses	^{201}MeHg losses
Synechocystis sp. 6803	7.9 ± 7.7%	19.0 ± 6.0%
Cyclotella meneghiniana	34.4 ± 17.2%	9.3 ± 6.4%
Chlamydomonas reinhardtii	10.5 ± 8.4%	1.3 ± 1.8%

$$(1)\ \text{Hg losses}\ (\%) = \frac{[\text{Hg bulk (whole system)}] - ([\text{Hg extracellular}] + [\text{Hg whole cells}])}{[\text{Hg bulk (whole system)}]} \text{x } 100 \qquad (3.1)$$

Table 3.3. Percentages (%) of ^{199}Hg(II) and ^{201}MeHg losses due to the cell fractionation procedure (Ultrasonication + centrifugation) for obtaining the insoluble and soluble cell fraction for the three phytoplankton species.

Phytoplankton species	^{199}Hg(II) losses	^{201}MeHg losses
Synechocystis sp. 6803	32.7 ± 10.9%	21.4 ± 13.3%
Cyclotella meneghiniana	25.0 ± 14.6%	20.0 ± 18.6%
Chlamydomonas reinhardtii	45.3 ± 9.4%	21.8 ± 7.0%

$$(2)\ \text{Hg losses}\ (\%) = \frac{[\text{Hg whole cells}] - ([\text{Hg cytosolic fr.}] + [\text{Hg membranes}])}{[\text{Hg whole cells}]} \text{x } 100 \qquad (3.2)$$

1.3. Analytical approach.

1.3.1. Hg compounds quantification analysis.

The quantification of Hg compounds has been carried out by gas chromatography coupled to inductively coupled plasma (GC-ICP-MS). Samples displayed in **Table 3.4** were digested with 3N HNO_3 under an analytical microwave (Discover and Explorer SP-D 80 system, CEM, NC USA) previously optimized in our laboratory in the past (Clémens et al., 2011; Navarro et al., 2011) to avoid any Hg compounds losses during the digestion process. After, isotopically

enriched ^{198}Hg(II) and ^{202}MeHg were added before the sample preparation (procedure described in Chapter 2.1, **page 44**).

Table 3.4. Description of all the types of samples collected during the experimental procedure.

Analysis	Sample type	Volume sample (weighted)	Volume HNO_3 (50% v/v) (weighted)	Store conditions (°C)
GC-ICP-MS	Bulk	4mL	1mL	4
	Extracellular fr.	9mL	1mL	4
	Whole cells	≈ 300mg	3mL	4
	Cytosolic fr.	500µL	3.5mL	4
	Membranes with cell debris	≈ 40mg (pellet)	1mL	4

1.3.2. Screening of Hg binding bioligands in the cytosolic fraction.

In this work, the screening of Hg binding bioligands of cytosolic fraction was performed by the direct injection of 100µL in the Superdex 200 HR HPLC column with an operation range from 10 to 600 kDa and in the Superdex TM Peptide HPLC column with a separation range from 0.1–7 kDa coupled to ICP-MS. The low Hg compounds binding bioligands concentration in the extracellular fraction did not allow us to detect any bioligand bound to Hg in the extracellular medium. No preconcentration was performed in this work in order to avoid further potential Hg losses and Hg binding bioligands degradation. The operating parameters for size exclusion chromatography (SEC) coupled to ICP-MS are shown in **Table 3.5**.

Table 3.5. Operating parameters for Size Exclusion Chromatography (SEC) coupled to ICP-MS.

Parameters	HPLC column Superdex 200	HPLC column Superdex Peptide
Type of column	Superdex TM 200 Increase 10/300 GL	Superdex TM Peptide Increase 10/300 GL
Mobile phase	A: 100 mM Ammonium Acetate H_2O Milli-Q pH:7.4	A: 100 mM Ammonium Acetate H_2O Milli-Q pH:7.4
Mode	Isocratic	Isocratic
Flow rate	100mL/min	100mL/min
Range	600-10kDa	7-0.1kDa
Injection volume	100µL	100µL
Ionization source	ICP	ICP
Mass analyzer	Quadrupole	Quadrupole

The recoveries of ^{199}Hg(II) and ^{201}MeHg in the HPLC column Superdex 200 HR have been carried out in triplicate (only for *Synechocystis*) by collecting 30mL of the mobile phase at the SEC column outlet after 100µL injection (weighted). The concentration of Hg compounds was compared with the corresponding samples without injection considering the dilution step in the

SEC column. Isotopically enriched Hg compounds have been quantified by isotope dilution analysis GC-ICP-MS adding ^{198}Hg(II) and ^{202}MeHg before the sample preparation. The Hg losses from SEC column for ^{199}Hg(II) and ^{201}MeHg were 40±12% and 20±8%, respectively.

1.3.3. Identification of LMW Hg binding biomolecules.

The identification of Hg compounds binding LMW thiol bioligands was performed by adding 30µL of ACN to 15µL of cytosolic fraction (1:2 v/v) in order to make precipitating the high molecular weight proteins (Klein et al., 2011; Pedrero Zayas et al., 2014). Due to this dilution step, the enriched Hg compounds previously exposed could not be detected bound to any LMW bioligands. For this reason, 250 µg of natural inorganic and methylated Hg per L had to be added to the sample to identify the potential LMW bioligands capable of binding Hg contained in the LMW fraction (> 10kDa) of SEC profiles. After 10min of incubation, 7µL of the cytosolic fraction were injected in the HILIC column TSK gel amide 80 coupled to ICP-MS and ESI-MS. The operating parameters for hydrophilic interaction liquid chromatography (HILIC) coupled to ICP-MS and ESI-MS analysis are shown in **Table 3.6**.

Table 3.6. Operation parameters for hydrophilic interaction liquid chromatography (HILIC) coupled to ICP-MS and ESI-MS

Parameters	HILIC column
Type of column	TSK gel amide 80 column (250 mm×1 mm i.d., 5 µm)
Mobile phase	A: ACN B: 10 mM Ammonium Formate pH:5
Mode	Gradient
Flow rate	50 µL/min
Separation	Polar biomolecules separation
Injection volume	7 µL
Ionization source	ICP / ESI
Mass analyzer	Quadrupole/ Orbitrap

2. Hg compounds release in the diatom *Cyclotella meneghiniana*: a metal-sensitive phytoplankton species.[4]

2.1. Introduction.

When Hg compounds are taken up by phytoplanktonic cells, they will bind to intracellular bioligands (e.g. proteins, small peptides, enzymes, DNA or RNA), which are extremely variable in form and cellular location (Wu & Wang, 2014). Knowing to which intracellular bioligands Hg is binding and in which form is found, will answer several unknown questions about Hg intracellular handling by phytoplankton and Hg bioavailability in the aquatic food chain. On the other hand, the presence of Hg compounds induces oxidative stress by blocking the functional groups (normally thiol groups, S-H) of essential biomolecules, by displacing essential element or disrupting the proteins structure and finally, causing impairment of the biological cell function (see more information in General Introduction **Hg within the phytoplanktonic cells., page 19**).

The diatom *Cyclotella meneghiniana* has been frequently observed as dominant phytoplanktonic specie in oligotrophic waters (Finlay, 2002). So far, only two studies have reported the exposure of Hg(II) and MeHg to the diatom *C.meneghiniana* (Luengen et al., 2012; Pickhardt & Fisher, 2007). In both studies, Hg compounds uptake was investigated by comparing the bioaccumulation between living and dead diatom cells. Results revealed that Hg(II) and MeHg were mainly attached to the cell debris when Hg was exposed to dead cells, whereas Hg compounds were bioaccumulated in the intracellular fraction of living cells (Pickhardt & Fisher, 2007). In other toxicological studies, the investigation of the changes in abundance and diversity of phytoplankton communities showed that, *C.meneghiniana* proportion disappeared in the phytoplankton assemblage due to the stress induced by toxic concentrations of nitrogen species (Zhang et al., 2013), chromium (Lazinsky & Sicko-Goad, 1990) or copper and zinc (Pandey et al., 2015). Indeed, earliest studies described *C.meneghiniana* as metal-sensitive phytoplankton species (Ruggiu et al., 1998; Shehata et al., 1999). In the laboratory, *C.meneghiniana* was accidentally exposed during the cell growth to small quantities of ^{nat}Hg(II) for at least three weeks. Then, we have used it as a reference control

---

[4] *(Manuscript in preparation)*

Authors: Javier Garcia-Calleja, João P. Santos, Zoyne Pedrero Zayas, Laurent Ouerdane, Vera I. Slaveykova, and David Amouroux.

to investigate the isotopically enriched Hg compounds bioaccumulation, (sub–) cellular distribution, screening of newly formed cytosolic Hg binding biomolecules in *C. meneghiniana* under mercury free growth (MFG) and mercury exposure growth (MEG) conditions.

2.2. Results.

2.2.1. Initial conditions between mercury exposure growth (MEG) and mercury free growth (MFG).

Mercury exposure growth (MEG) corresponds to the cell culture that was previously exposed to ^{nat}Hg(II), whereas mercury free growth (MFG) was not previously exposed to Hg(II). In **Figure 3.3**, the total Hg (II) concentration was two folds higher in MEG (THg(II): 926.0±11.9 ng·L^{-1}) than MFG (THg(II): 437.3±6.2 ng·L^{-1}) in the whole system (Bulk) after 5 minutes of exposure. Indeed, the contribution of MEG ^{nat}Hg(II) and ^{199}Hg(II) to the THg(II) was 32% and 68%, respectively, whereas almost all MFG THg(II) was enriched in 199. In the extracellular medium, the initial THg(II) concentration between MEG and MFG was 302±6.9 ng L^{-1} (^{199}Hg(II) 94%) and 111.3±17.0 ng L^{-1} (^{199}Hg(II) 98%), respectively (**Figure 3.3**).

For MEG, the initial THg(II) concentration in the whole cells was 143±4.3 ng L^{-1}, in which ^{nat}Hg(II) contributed 71% of the THg(II). On the other hand, MFG THg(II) concentration in the whole cells was 86.5±10.0 ng L^{-1} (^{199}Hg(II) 98%). In the cytosolic fraction, 65% of the THg(II) was composed by ^{nat}Hg(II) ([THg(II)]= 119.7±47.1 ng L^{-1}), whereas MFG THg(II) concentration was 33.4±13.3 ng L^{-1} (^{199}Hg(II) 97.6%) (**Figure 3.3**).

Concerning ^{201}MeHg, the initial ^{201}MeHg concentration in the bulk was 63.3±2.5 ng L^{-1} for MEG and 53.3±1.7 ng L^{-1} for MFG. Similar concentrations were found in the extracellular medium (31.3–31.7 ng L^{-1}) and whole cells (18.7–23.8 ng L^{-1}) after 5 minutes of exposure between MEG and MFG. Also, no differences in terms of MeHg bioaccumulation were observed in the cytosolic fraction after 5 minutes of exposure (13.3–15.5 ng L^{-1}) (**Figure 3.3**).

Initial conditions (t5min)	THg (II) (ng L^{-1}) in the culture		^{201}MeHg(ng L^{-1}) in the culture	
	MFG	MEG	MFG	MEG
Bulk	437.3 ± 6.2	926.0 ± 11.9	53.3 ± 1.7	63.3 ± 2.5
Extracellular	111.3 ± 17.0	302.6 ± 6.9	31.7 ± 3.0	31.3 ± 1.4
Whole cells	86.5 ± 10.0	143.0 ± 4.3	18.7 ± 1.8	23.8 ± 2.6
Cytosolic fr.	33.4 ± 13.3	119.7 ± 47.1	13.3 ± 3.7	15.5 ± 3.8

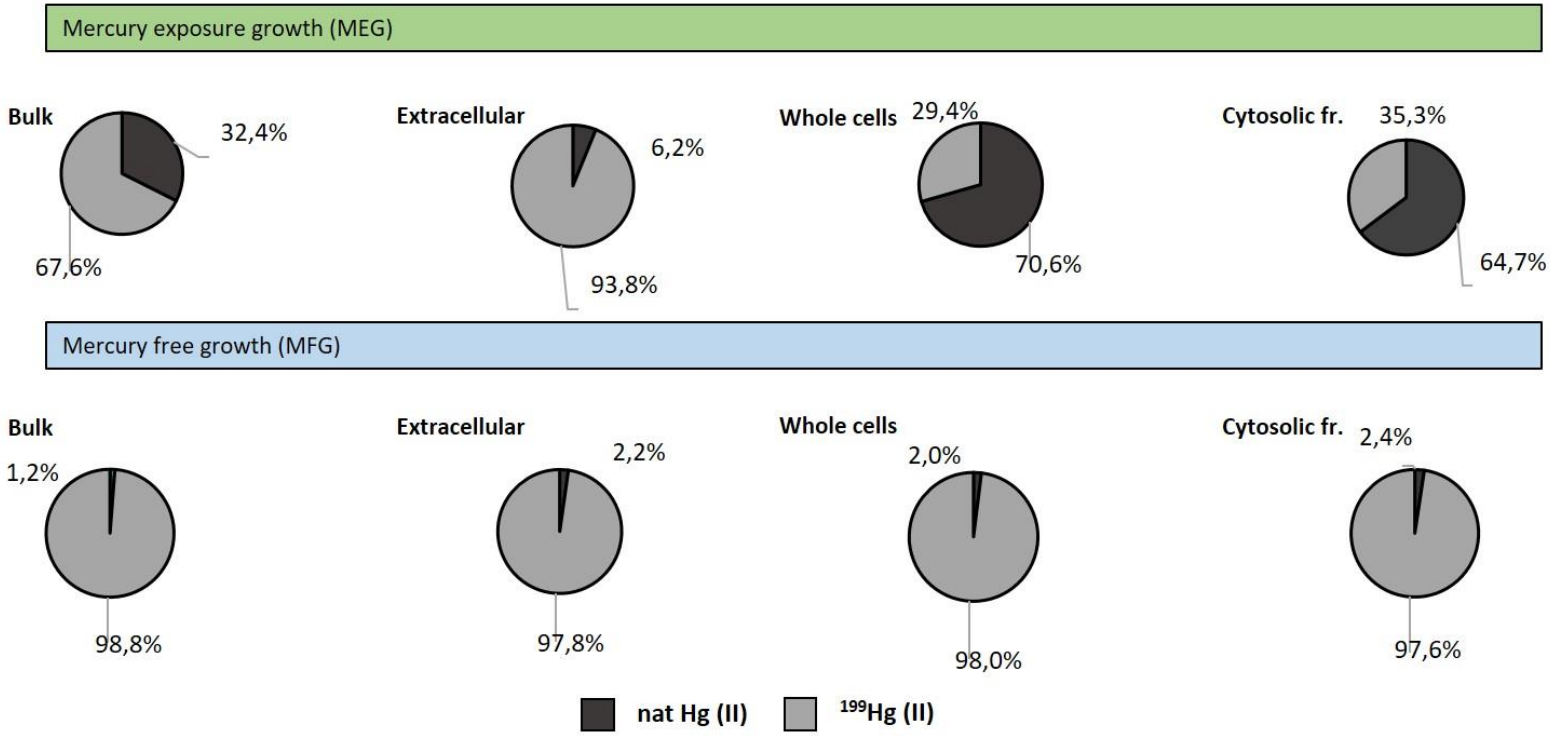

Figure 3.3. THg(II), ^{199}Hg(II) and ^{201}MeHg concentration (ng L^{-1} per exposure media) at the initial conditions (5min) between the mercury exposure growth (MEG) and mercury free growth (MFG) conditions for the different fraction collected (Bulk, extracellular fraction, whole cells and cytosolic fraction) and percentage of ^{nat}Hg(II) and ^{199}Hg(II) in *Cyclotella meneghiniana*.

2.2.2. ^{199}Hg (II) and ^{201}MeHg partitioning between the extracellular fraction and cells over time.

The main difference found between MEG and MFG was referring to the ^{199}Hg(II) concentration in cells. MEG ^{199}Hg(II) concentration ranged from 42.1–51.2 ng L^{-1},whereas MFG ^{199}Hg(II) concentration was between 84.8–139.4 ng L^{-1} due to the previous presence of ^{nat}Hg(II) on the cell surface. Only 13–22% of ^{199}Hg(II) was found in the cells in comparison with MFG (44–60%). In accordance to this, higher MEG ^{199}Hg(II) remained in the extracellular fraction over time (MEG: 78–87%) in comparison with MFG (40–56%). Regarding the evolution of ^{199}Hg(II) over time, MFG ^{199}Hg(II) concentration in cells increased from 84.8±10.2 up to 139.4±37.8 ng L^{-1} after 24 hours of exposure with a subsequent decrease until 108.3±8.0 ng L^{-1} at the end of the exposure. In contrast, MEG ^{199}Hg(II) concentration remained constant over time (42.1–50.9 ng L^{-1}) (**Figure 3.4** and **Figure 3.5**).

Concerning ^{201}MeHg, MEG and MFG revealed similar trends over time. ^{201}MeHg concentration in cells increased from 5min (MFG: 13.7±1.8 ngL^{-1}; MEG: 23.8±2.6 ng L^{-1}) to 24h (MFG: 21.4±1.5 ng L^{-1}; MEG: 39.3±1.5 ng L^{-1}) with a parallel decrease in the extracellular fraction from 5min (MFG: 31.7±1.3 ng L^{-1}; MEG: 31.3±1.4 ng L^{-1}) to 24h (MFG: 9.2±0.3 ng L^{-1}; MEG: 10.8±0.7 ng L^{-1}). The main difference was observed in the extracellular fraction at the end of the sampling point (t_{72h}/t_{96h}). MFG ^{201}MeHg concentration found in the extracellular medium increased up to 46.1±2.8 ng L^{-1} while MEG ^{201}MeHg concentration increased until 25.1±2.0 ng L^{-1}. Consequently, the MeHg concentration found in the cells at the end of the exposure decreased until 7.6±0.3 ng L^{-1} for MFG, and 28.2±4.4 ng L^{-1} for MEG (**Figure 3.4** and **Figure 3.5**).

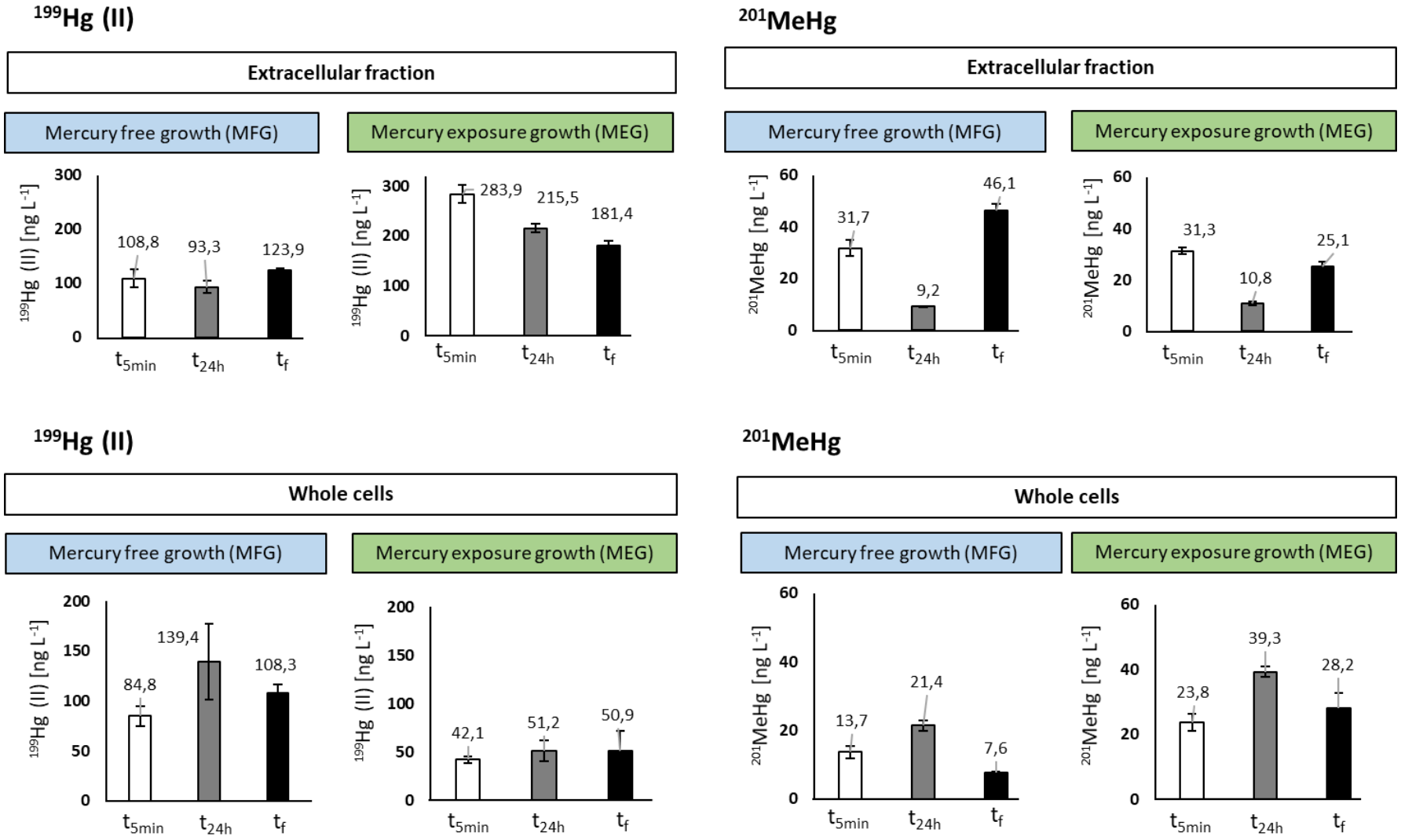

Figure 3.4. ^{199}Hg (II) and ^{201}MeHg concentration (ng L^{-1} per exposure media) in the extracellular fraction and whole cells at the beginning (5min), after 24 hours and at the end of the exposure (t_f = 72h/96h) in *Cyclotella meneghiniana* for mercury free growth (MFG) and mercury exposure growth (MEG) conditions.

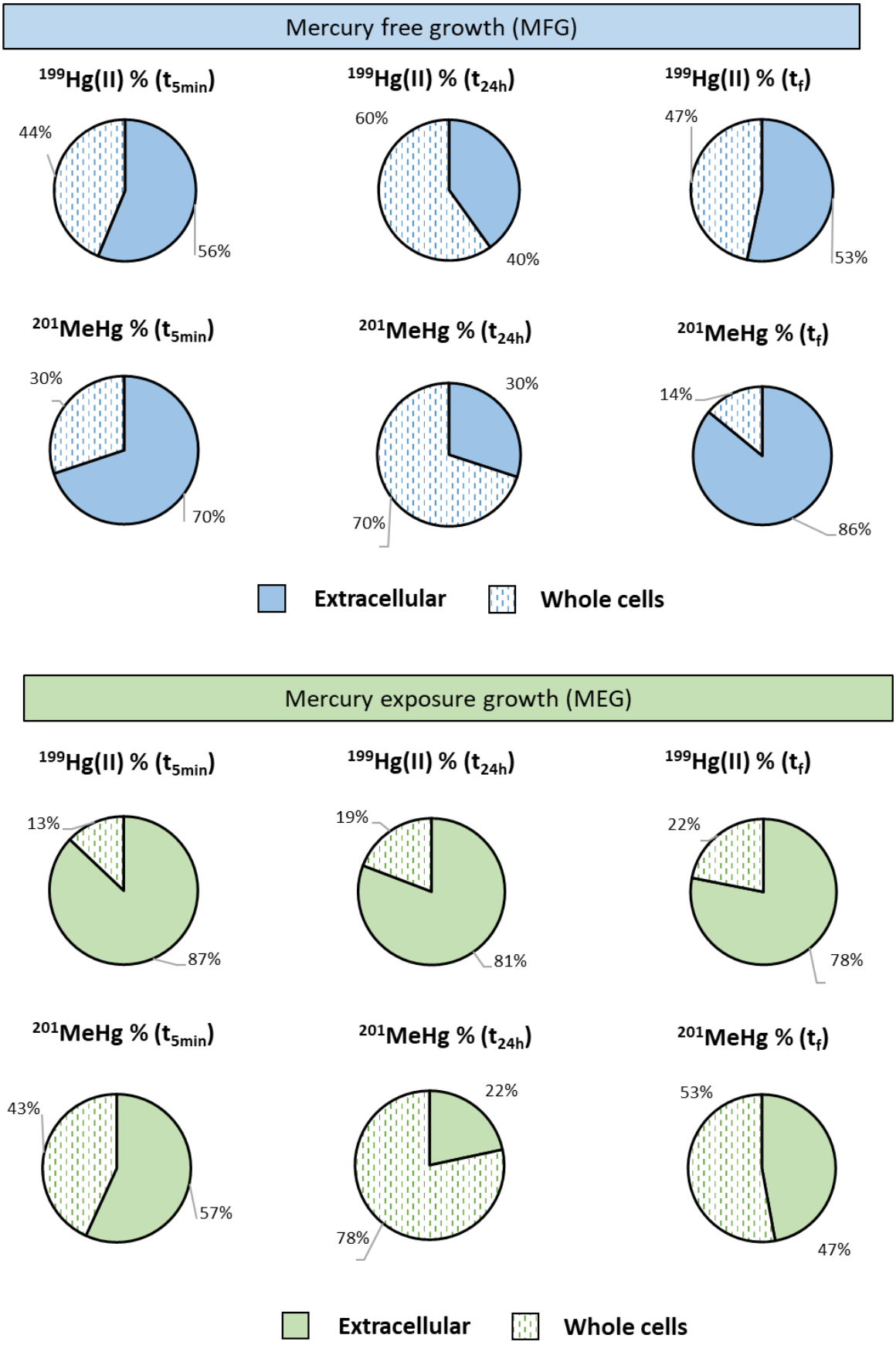

Figure 3.5. Partitioning (%) of ^{199}Hg (II) and ^{201}MeHg in the extracellular fraction and whole cells at t_{5min}, t_{24h} and t_f in *Cyclotella meneghiniana* for mercury free growth (MFG) and mercury exposure growth (MEG) conditions.

2.2.3. Hg (II) and MeHg concentration in the intracellular fraction.

At the beginning of the exposure (5min), MEG and MFG ^{199}Hg(II) concentration in the cytosolic fraction was 42.4±20.5 and 32.6±13.3 ng L^{-1}, respectively in which the concentration remained constant in both conditions after 24h of exposure (MEG: 46.4±19.4 ng L^{-1}; MFG: 33.4±4.5 ng L^{-1}). The main difference between MEG and MFG was observed at the end of the Hg exposure, whereas MEG ^{199}Hg(II) concentration seemed to remain constant (30.5±6.2 ng L^{-1}), a great decrease in MFG ^{199}Hg(II) concentration was observed after 72 hours of exposure (3.1±2.3 ng L^{-1}). In agreement with this observations, the percentage of ^{199}Hg(II) in the cytosolic fraction decreased from 39% (t_{5min}) to 3% (t_f) in MFG (**Figure 3.6** and **Figure 3.7**).

On the other hand, MEG and MFG ^{201}MeHg concentrations in the cytosolic fraction after 5 minutes of Hg exposure were 15.5±3.8 and 13.3±3.7 ng L^{-1}, respectively. After 72h (MFG) and 96h (MEG), a great decrease in ^{201}MeHg concentration was found in both conditions in which the concentration in MFG (0.4±0.2 ng L^{-1}) was ten times lower than MEG (4.9±1.2 ng L^{-1}). According to this, the percentage of ^{201}MeHg in the cytosolic fraction for MFG decreased drastically from 98% (5min) to 6% (tf= 72h) (**Figure 3.6** and **Figure 3.7**).

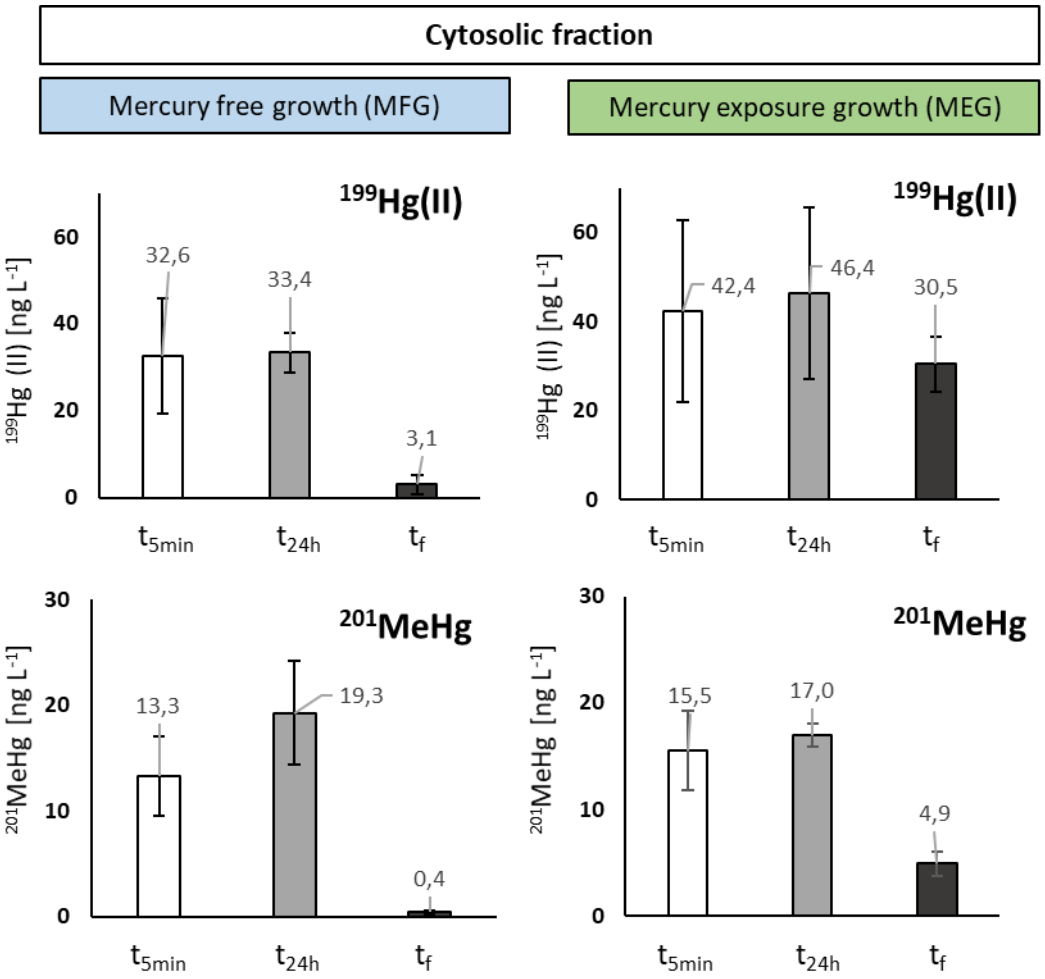

Figure 3.6. ^{199}Hg(II) and ^{201}MeHg concentration (ng·L^{-1}) in the cytosolic fraction at the beginning (5min), after 24 hours and at the end of the exposure (tf = 72h/96h) in *Cyclotella meneghiniana* in mercury free growth (MFG) and mercury exposure growth (MEG) conditions.

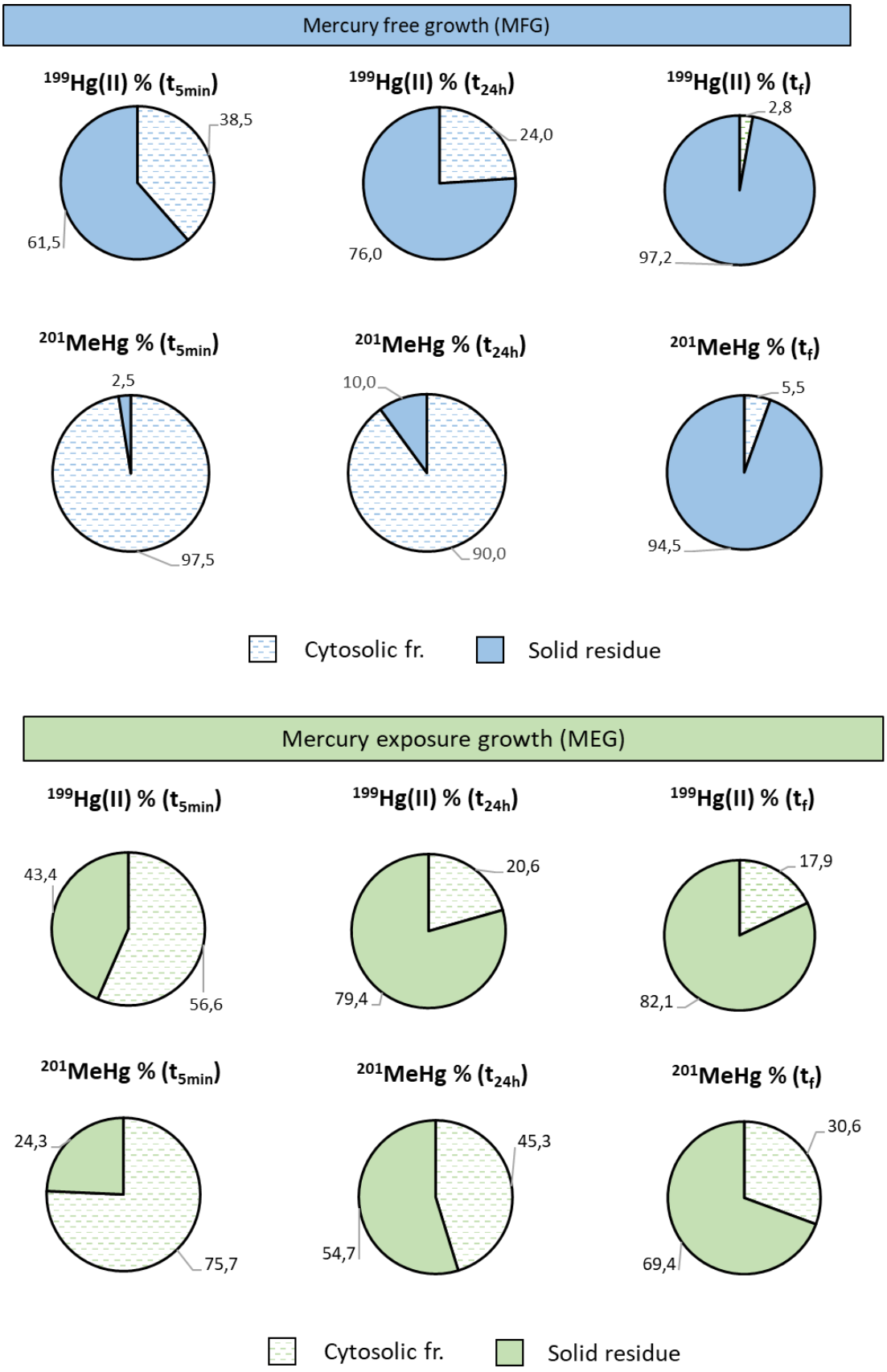

Figure 3.7. Percentage of ^{199}Hg (II) and ^{201}MeHg in the soluble (cytosolic fraction) and solid residue (cell wall, membranes, granules and other potential insoluble Hg compounds) at each sampling point (t_{5min}, t_{24h} and t_f) in *Cyclotella meneghiniana* for mercury free growth (MFG) and mercury exposure growth (MEG) conditions.

2.2.4. Screening of Hg binding intracellular bioligands in the cytosolic fraction.

Regarding the screening of intracellular Hg binding bioligands **(Figure 3.8**), the analysis by SEC-ICP-MS revealed the presence of two main ^{199}Hg containing fractions at 10–13 (void volume) and 22–23 minutes for MFG (a1) and MEG (a2). SEC profiles of ^{nat}Hg(II) previously present (b2) matched with ^{199}Hg(II), except for the fraction that eluted at 28–31 min (LMW fraction, <10kDa). At the end of the Hg exposure (tf= t72h and t96h), a remarkable decrease was observed for both MFG and MEG in all fractions. In contrast, ^{201}MeHg (c1, c2) was found at 10–13min and 28–31 min in MFG and MEG conditions after 5 minutes of exposure matching with the ^{nat}Hg(II) in MEG conditions (b2). Following the same trend as Hg(II), ^{201}MeHg containing in all fractions could not be observed anymore at the end of the exposure in agreement with the depletion of Hg compounds concentration observed in the cytosol (**Figure 3.6**).

In order to obtain further information about the specific affinity of intracellular bioligands, the exogenous addition of other two different enriched Hg compounds (^{198}Hg(II) and ^{202}MeHg) to the cytosolic fraction was performed in MFG conditions and the biotic control (No Hg exposure). This approach revealed the potential biomolecules capable of binding ^{198}Hg(II) and ^{202}MeHg after 5min, 24h and 72h (**Figure 3.9**). Results showed that ^{202}MeHg was specifically binding at 28–31 min in the biotic control and MFG at the beginning of the exposure. However, no ^{202}MeHg was found in the fraction eluting at 28–31 min when the alga was previously exposed to Hg (MFG) after 72 hours, whereas ^{202}MeHg in the biotic control was able of binding potential LMW bioligands (Figure 3.9, a2, b2).

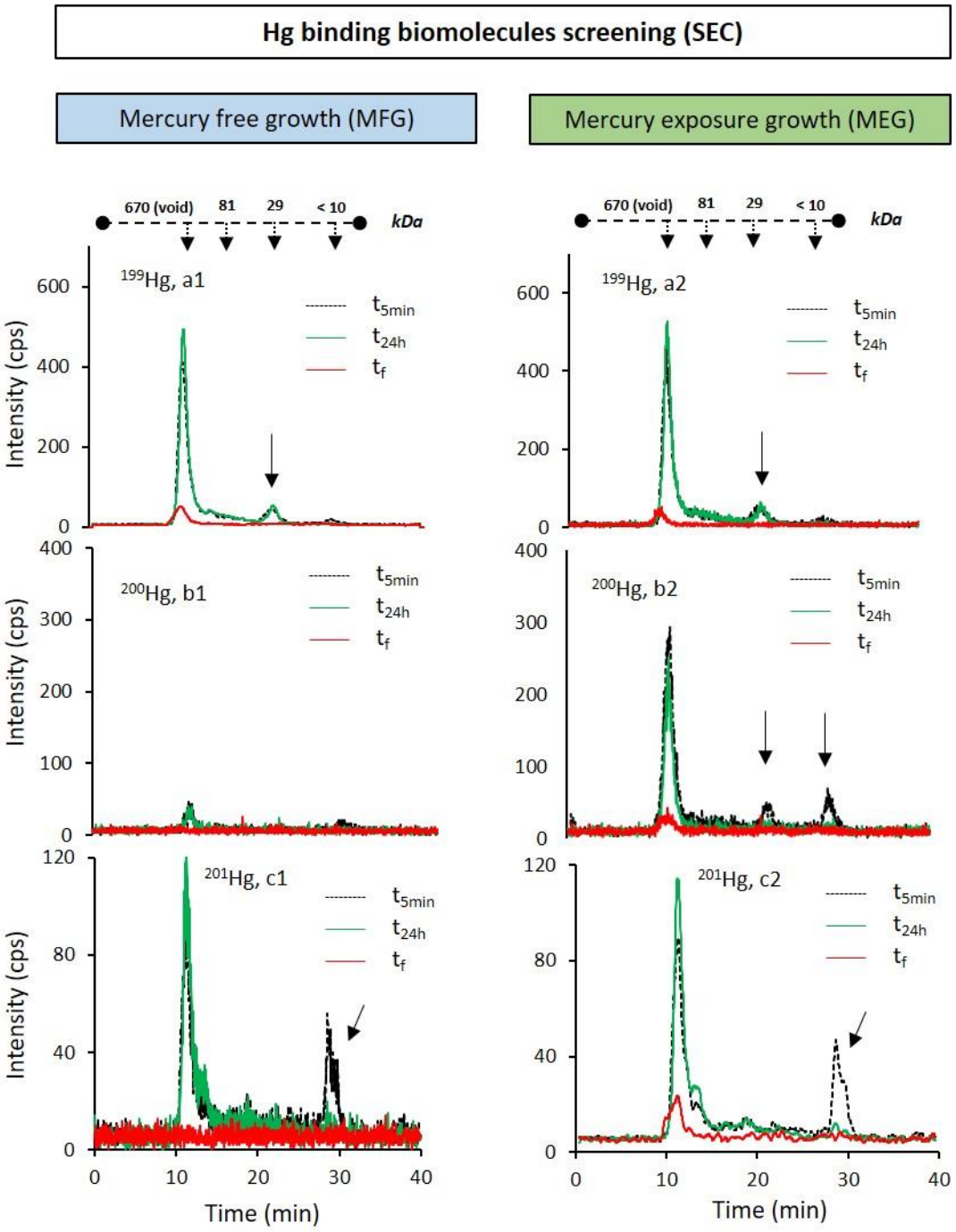

Figure 3.8. Size exclusion chromatograms (Superdex 200 (range: 600-10 kDa)) in the cytosolic fraction of *Cyclotella meneghiniana* for mercury free growth (MFG) and mercury exposure growth (MEG) by ICP-MS detection of (a1,a2) ^{199}Hg corresponding to ^{199}Hg (II) isotopic tracer. (b1,b2) ^{200}Hg corresponding to the ^{nat}Hg (II). (c1,c2) ^{201}Hg corresponding to ^{201}MeHg isotopic tracer at t_{5min}, t_{24h} and tf (72h/96h) of Hg exposure.

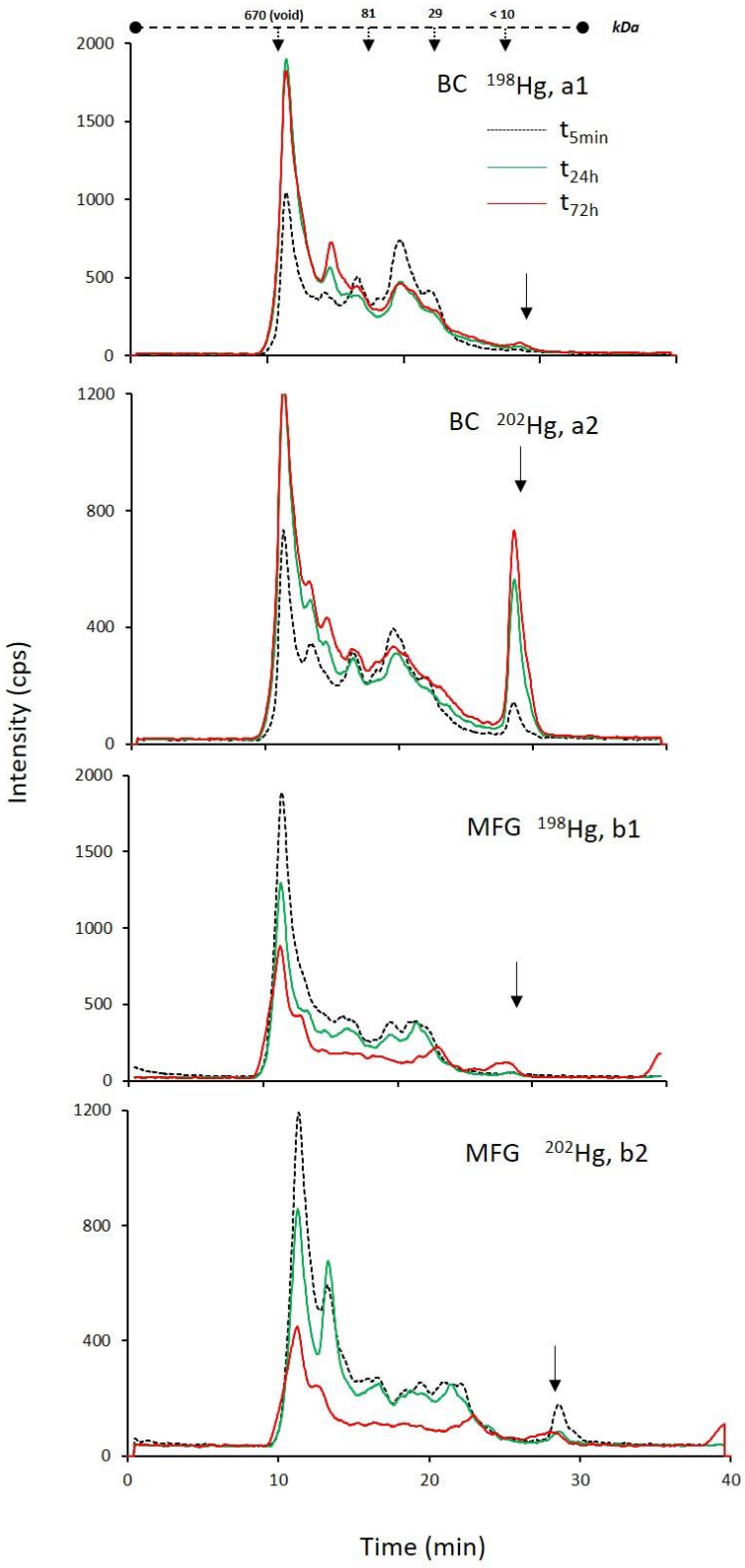

Figure 3.9. Size exclusion chromatograms (Superdex 200 (range: 600-10 kDa)) in the cytosolic fraction of *Cyclotella meneghiniana* (MFG) in the biotic control (A) and Hg exposure (B) by ICP-MS detection of ^{198}Hg (a1, b1) and ^{202}Hg (a2,b2) corresponding to the addition (5 µg L^{-1}) of ^{198}Hg(II) and ^{202}MeHg after 5 minutes, 24 and 72 hours of Hg exposure of both isotopic tracers (^{199}Hg(II) and ^{201}MeHg).

2.2.5. Identification of LMW bioligands binding MeHg.

After the precipitation of HMW proteins by adding ACN, the resulting fraction was injected in the HILIC column coupled to ICP-MS. The incubation of MeHg was carried out in the biotic control and MFG conditions after 72 hours of exposure. But also, to investigate the differences observed in the fraction eluted at 28–31 min between MFG and the biotic control (**Figure 3.9**). HILIC chromatograms revealed only one peak binding MeHg in the biotic control. This peak was not present, or was negligible, when *C.meneghiniana* was exposed to Hg (MFG) (**Figure 3.10**). Therefore, the bioligand present in the cytosolic fraction capable of binding MeHg in the biotic control might have a potential role in MeHg intracellular handling. The injection of the biotic control carrying out the same chromatographic settings (leading to matching retention times) was performed in HILIC-ESI-MS to identify the unknown MeHg-complex. Results showed one ion with the isotopic pattern of mercury (Figure 3.10A) at m/z = 524.08. This mass to charge ratio corresponded to MeHg binding one glutathione (GS-MeHg, $C_{11}H_{20}HgN_3O_6S^+$).

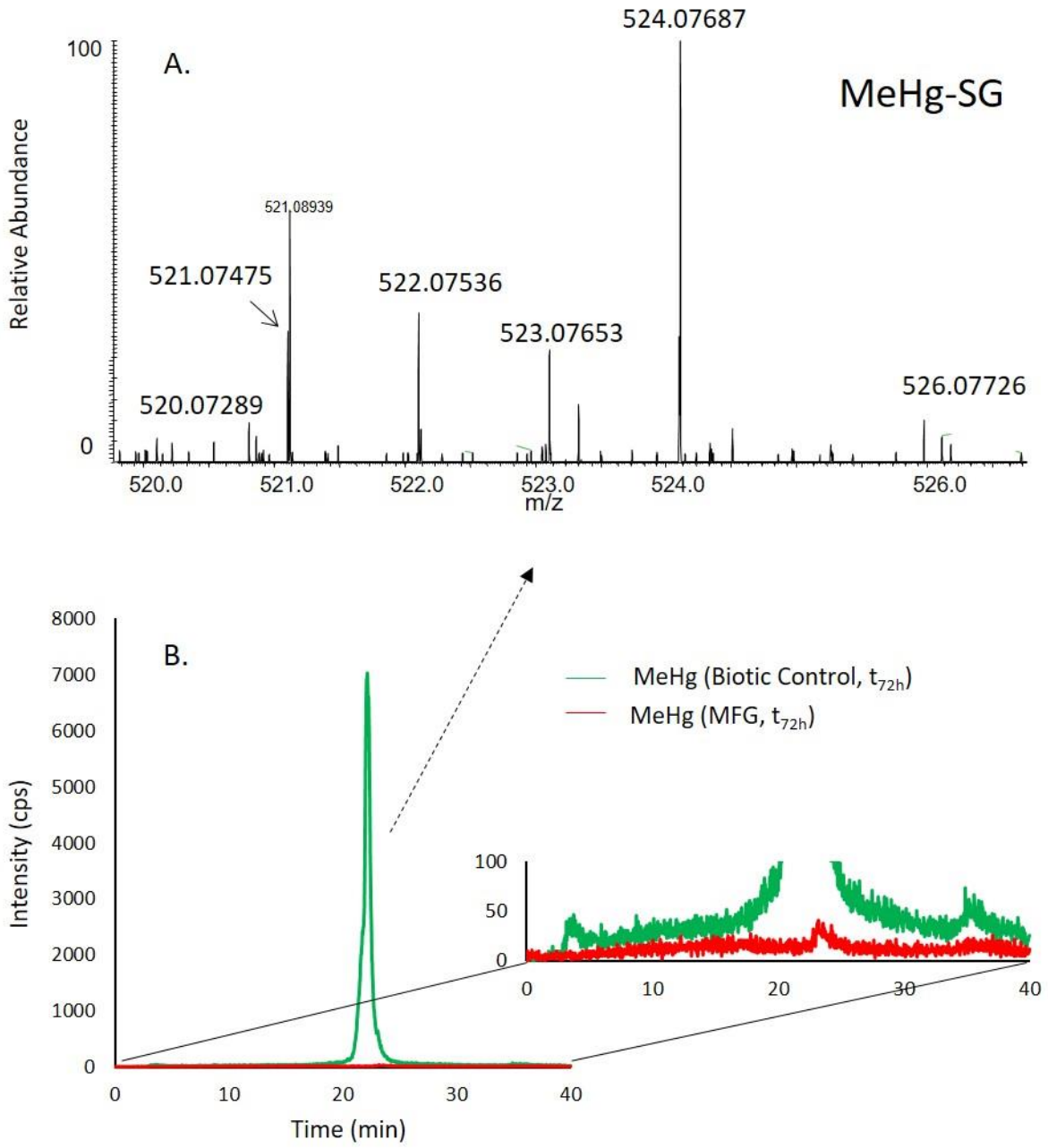

Figure 3.10. (A) Zoom of the mass spectra obtained at 21.4 min demonstrates the presence of MeHg binding one glutathione with its specific isotopic pattern. (B) HILIC chromatogram of the cytosolic fraction by ICP-MS detection of ^{202}Hg in the biotic control and mercury free growth (MFG) conditions after 72 hours of exposure.

2.3. Discussion.

2.3.1. Passive /Active Hg compounds release in *Cyclotella meneghiniana*.

Theoretically, the release of Hg compounds might have been mediated by cellular responses due to the potential toxicity induced by Hg compounds. However, no biomarkers (e.g., ROS concentration, photosynthetic activity...) were determined to address the Hg toxicity towards *C. meneghiniana*. Consequently, two potential possibilities are proposed to explain the release of Hg compounds shown at the end of the exposure:

(1) The passive Hg compounds release was non-specific mediated.

(2) The active Hg compounds excretion was mediated by cellular responses induced by Hg exposure.

The release of both Hg compounds might have occurred: (***i***) passively through the diffusion of Hg compounds outside the cell; (***ii***) accidentally through the excretion of extrapolymeric substances (EPS); or even (***iii***) through insoluble Hg compounds formation due to unintentional precipitation reactions. EPS contains several potential functional groups (e.g. -SH, -NH_2, -COOH) capable of binding Hg (Naveed et al., 2019; Seymour et al., 2017). Indeed, diatoms are the most abundant polysaccharide producers among microalgae (Xiao & Zheng, 2016). EPS production is known to be enhanced under metal stress in response to potentially toxic elements through several metabolic processes (Naveed et al., 2019). However, EPS production is thought to act mostly as a barrier against new potential inputs, rather than as a potential release of toxic compounds (Cassier-Chauvat, 2014). On the other hand, the excretion or precipitation of potential insoluble Hg compounds such as β-HgS (s) have been always associated to cellular responses against Hg exposure (Kelly et al., 2006; Lefebvre et al., 2007). Similar detoxification mechanisms have been also reported through the formation of polyphosphate granules under toxic Cd concentrations (Aguilera & Amils, 2005; Lavoie et al., 2016). Consequently, the non-specific release of Hg compounds is not expected to be mediated by EPS or potential insoluble Hg compounds formation at this Hg concentration levels.

The active excretion of Hg compounds as a detoxification mechanism have been never reported in pure phytoplankton cell cultures. However, no MeHg was found to into the extracellular medium when *C.meneghiniana* was exposed to three times lower MeHg concentrations (Chapter 2.2, ^{199}MeHg 2nd process, **Figure 2.12**). As a result, the excretion of Hg compounds might have been actively mediated by specific biomolecules in charge of reducing the stress

inside the cells. In our work, the exogenous addition of Hg compounds (^{198}Hg(II) and ^{202}MeHg) showed that MeHg was found in the LMW fraction after 72 hours in the biotic control (MFG, **Figure 3.9**), but not in MFG. After the precipitation of HMW bioligands, MeHg binding GSH was identified in the biotic control, but any MeHg binding bioligand was found in MFG conditions (**Figure 3.10**). These previous results suggest that, **(1)** GSH might be involved in the excretion of Hg compounds, (**2**) the remaining intracellular GSH content is oxidized (GS-SG) or, **(3)** the release of the intracellular bioligands bound to Hg compounds into the extracellular medium was mediated by cell disruption or cell lysis.

MeHg was specifically found in the extracellular fraction in MEG (**Figure 3.4**), while Hg(II) remained in the cytosolic fraction (**Figure 3.6**). Therefore, the excretion of Hg compounds by cell lysis or cellular disruption is not a consistent hypothesis since both Hg compounds should have been found in the extracellular medium. Consequently, the specific excretion of MeHg suggests that MeHg might have induced high oxidative stress within the cell as it was already reported for other phytoplankton species (Beauvais-Flück et al., 2017, 2018). Although no studies have ever demonstrated the active MeHg excretion by GSH, Skrobonja et al., 2019 reported an increase in the extracellular GSH concentration in the freshwater microalga *Selenastrum capricornutum* under Hg exposure. Furthermore, the increase in extracellular GSH concentration was also shown under toxic Cu exposure levels in phytoplankton and particularly, in diatoms (Navarrete et al., 2019; Tang et al., 2005; Vasconcelos et al., 2002). Based on these findings and our results, we hypothesized that the excretion of MeHg by GSH could be driven by an active effort by the alga to detoxify preferentially MeHg into the extracellular medium. Nevertheless, further investigations will be needed to confirm the potential role of GSH in Hg intracellular handling in *Cyclotella meneghiniana*.

2.3.2. Comparison between mercury free growth (MFG) and mercury exposure growth (MEG) conditions in *Cyclotella meneghiniana*.

Phytoplankton communities growing under stressful conditions may become more resistant to the effects of Hg toxicity (Val et al., 2016). This resistance is based on the Pollution-Induced Tolerance Concept (PICT), which indicates the phenotypic adaptation of individuals resulting in a higher tolerant specie towards toxic compounds (Blanck, 2002). Field observations in phytoplankton communities revealed the adapting capacity of phytoplankton to toxic chemical compounds (Echeveste et al., 2014). In our work, MEG MeHg concentration was ten folds higher after 96 hours than MFG after 72 hours of exposure (**Figure 3.6**). Furthermore, MFG Hg(II) concentration was found in the extracellular medium after 72 hours, whereas MEG

Hg(II) remained in the cytosolic fraction after 96 hours of exposure. The variability observed between conditions suggests that the previous exposure of ^{nat}Hg(II) could have induced higher tolerance against Hg exposure; being translated in lower cellular responses. Our results are in agreement with laboratory experiments which showed that pre-exposure of Hg(II) and MeHg induce an acclimation and enhanced a greater tolerance towards Hg(II) and MeHg exposure in the marine diatom *Thalassiosira weissflogii* (Wu & Wang, 2013, 2014).

2.3.3. Comparison between our work and other studies in *Cyclotella meneghiniana*.

Concerning *C. meneghiniana*, only two articles reported the Hg compounds exposure in this specific phytoplankton strain (Luengen et al., 2012; Pickhardt & Fisher, 2007). In these previous studies, 60–70% of MeHg remained constant over 80 hours within the cells, even if the MeHg exposure level per cell at the beginning of the exposure was up to 20 times higher than our conditions. The differences in terms of MeHg bioaccumulation between the cited studies and the excretion of MeHg found in our work might be explained by the batch solution where cells were exposed. As previously described, the exposure medium used in our work (SFM medium) was based on only major cations (no nutrients), whereas cells in the cited studies were exposed to filtered freshwater river. The different chemical composition of the medium was evidenced to alter Hg toxicity in freshwater algal communities, where EC_{50} values in river waters were lower than in MOPS artificial exposure medium (Gorski et al., 2008; Le Faucheur et al., 2011; Val et al., 2016). Consequently, the nutrient concentrations between exposure mediums might influence the metabolic activity of *C.meneghiniana*. Pickhardt & Fisher, 2007 reported an increase in the cell density from 5 x 10^3 cell mL^{-1} up to 1 x 10^5 cell mL^{-1} after 80 hours of MeHg exposure, whereas a decrease from 1 x 10^6 cell mL^{-1} to 6 x 10^5 cell mL^{-1} after 72 hours was observed in our work (**Figure A3- 3**). Consequently, the biodilution of Hg compounds concentration by the cell growth might have also mitigated the potential Hg toxicity. In summary, the experimental conditions such as the biodilution of Hg compounds concentration by the cell growth in combination with the potential nutrients present in filtered freshwaters might have influenced in the metabolic activity and the harmful effects of MeHg on *Cyclotella meneghiniana*; leading to explain the differences in MeHg intracellular handling between our work and previous studies.

2.4. Conclusions.

In conclusion, the comparison between mercury exposure growth (MEG) and mercury free growth (MFG) allowed to evaluate the influence of previous presence of Hg(II) during the cell growth. GSH was identified in the biotic control, but this LMW-thiol compound could not be identified in MFG after 72 hours of exposure. Moreover, the release of Hg compounds into the extracellular fraction in MFG, and the specific release of MeHg after 96 hours in MEG could suggest that, GSH preferentially excreted MeHg into the extracellular fraction in order to reduce the potential oxidative stress. In addition, the remaining intracellular MeHg and Hg(II) concentration after 96 hours in MEG in comparison with the Hg compounds depletion observed after 72 hours in MFG can only mean that the previous exposure of Hg(II) during the cell growth induced higher tolerance against Hg exposure in *C.meneghiniana*, as previously reported. Finally, the differences in MeHg intracellular handling between our work and previous studies carried out with *C.meneghiniana* indicated that the exposure medium could probably have a strong influence on the metabolic activity of *C.meneghiniana* to handle MeHg.

3. Potential intracellular sequestration of Hg compounds in the cyanobacterium *Synechocystis sp*. PCC 6803.

3.1. Introduction.

In this work, the study of intracellular complexation of Hg compounds was carried out by taking advantage of the tracking with isotopically enriched isotopes. The enriched isotopic tracers (^{199}Hg (II) and Me^{201}Hg) were added after cells resuspension in the exposure medium with the purpose of tracing and investigating the original enriched Hg compounds and the newly formed Hg biocomplexes in the cytosolic fraction. The main aim of this work was to characterize Hg-biocomplexes involved in Hg speciation and to study different Hg compounds specific biding affinities in the intracellular fraction of the cyanobacterium *Synechocystis* sp. PCC 6803. This model cyanobacterium is representative from freshwater ecosystems, a prokaryotic cell with a single chromosome free in cytoplasm and capable of growth by oxygenic photosynthesis or by glycolysis and oxidative phosphorylation in dark conditions. A phytoplankton microorganism structurally and metabolically more similar to bacteria than an eukaryotic cell that can be found in microbial and phytoplankton communities (Liberton et al., 2013; Sarma, 2012). The combination of complementary information obtained by hyphenated analytical techniques such as GC-ICP-MS, SEC-ICP-MS and HILIC-ICP/ESI-MS provide new insights on the role of intracellular ligands in Hg speciation and intracellular handling in photosynthetic cyanobacteria.

3.2. Results.

3.2.1. ^{199}Hg (II) and ^{201}MeHg in cellular and sub-cellular fractions.

In **Figure 3.11**, the concentration of ^{199}Hg(II) and ^{201}MeHg (ng·L^{-1}) after 5min, 24h and 96h is observed in the extracellular medium, whole cells, and cytosolic fraction, as well as the percentage of Hg compounds internalized in the cytosol. In the extracellular fraction, ^{199}Hg (II) concentration decreased significantly from 445.0±19.2 to 34.7±9.4 ng L^{-1} within the first 24 hours, while the entire ^{201}MeHg exposed in the culture was already found in the whole cells after 5min of exposure (51.2±4.1 ng L^{-1}) (**Figure 3.11A**). The concentration of ^{199}Hg (II) in the whole cells increased from 115.3±2.6 to 218.8±30.9 ng L^{-1} after 24 hours of exposure (**Figure 3.11B**). No release of Hg compounds was observed after 96 hours of exposure. ^{199}Hg(II) concentration in the cytosolic fraction increased from 15.4±2.4 to 30.9±4.8 ng L^{-1} the first 24 hours, whereas ^{201}MeHg concentration was constant (16.7–20.3 ng L^{-1}) over 96 hours (**Figure 3.11C**). Furthermore, the percentage (%) of ^{201}MeHg and ^{199}Hg(II) internalized in the cytosolic fraction did not reveal significant differences over time (MeHg:32.9–46.2% ;Hg(II):15.7–16.3%) (**Figure 3.11D**).

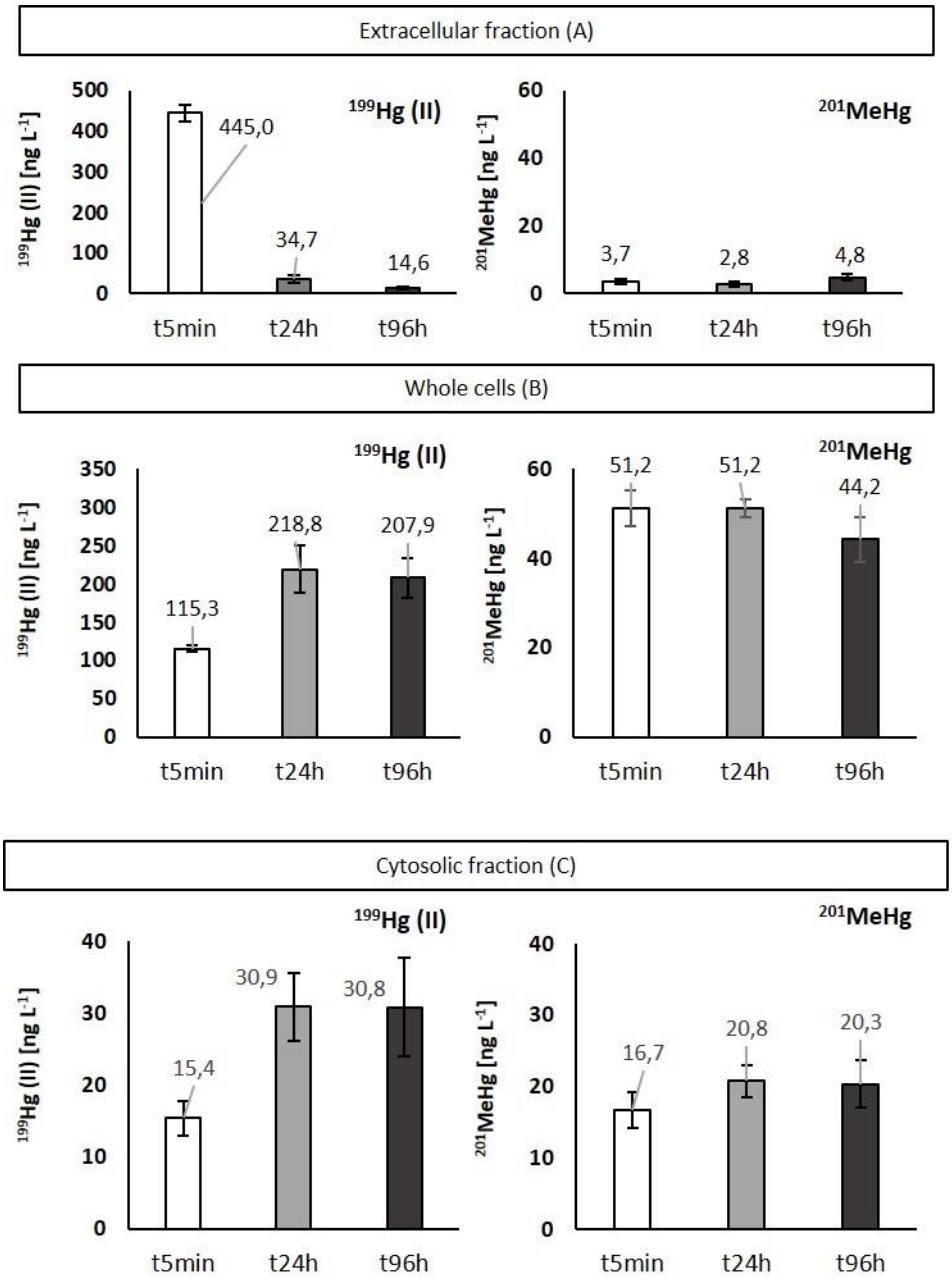

% ^{199}Hg (II) and ^{201}MeHg internalized in the cytosolic fraction (D)

Time	% of Hg compounds internalized	
	^{199}Hg (II)	^{201}MeHg
t_{5min} (%)	15.7 ± 2.4	32.9 ± 5.6
t_{24h} (%)	15.2 ± 3.3	40.3 ± 4.6
t_{96h} (%)	16.3 ± 7.5	46.2 ± 9.1

Figure 3.11. ^{199}Hg(II) and ^{201}MeHg concentration (ng L^{-1} exposure media) in (A) the extracellular fraction and (B) whole cells, (C) cytosolic fraction and, (D) percentage of Hg compounds internalized at the beginning (5min), after 24 hours and 96 hours of Hg exposure in *Synechocystis* sp. PCC 6803

3.2.2. Screening of Hg binding bioligands in *Synechocystis* sp.

Regarding ^{199}Hg(II) and ^{201}MeHg binding intracellular bioligands, SEC-ICP-MS analysis revealed a distribution of Hg associated to several fractions in a wide range of molecular weight (600–10 kDa) (**Figure 3.12**). Overall, different SEC profiles are shown for the detection of ^{199}Hg and ^{201}Hg isotopes, except for the match in the fraction eluting at 28–31 min. After 5 minutes of exposure, ^{199}Hg(II) was preferentially found in fractions eluting at 10–15 min, whereas ^{201}MeHg was mainly binding to intracellular bioligands containing in the fractions that eluted between 17–27 min and 28–31 min . Looking at the evolution of Hg compounds associated with size fractions, a remarkable increase was observed for ^{201}MeHg and ^{199}Hg(II) in the LMW fraction (28–31 min) the first 24 hours with a subsequent decrease after 96 hours. On the other hand, the fractions that eluted between 15–27 min containing both ^{199}Hg(II) and ^{201}MeHg increased from 5 min to 96 hours. The preconcentation of 2L of cell culture in 10mL of Milli-Q water allowed a clearer illustration (Figure 3.12C) about the Hg compounds-specific binding affinities with the fractions that eluted between 10–15 min and 15–27 min in comparison with the preconcentration of 45 mL in 1.5mL (Figure 3.12A and Figure 3.12B). Furthermore, the injection of the cytosolic fraction after 24 hours of exposure in the SEC peptide (7–0.1 kDa) revealed a match with a standard of GSH previously incubated with ^{199}Hg(II) and ^{201}MeHg (**Figure 3.13**).

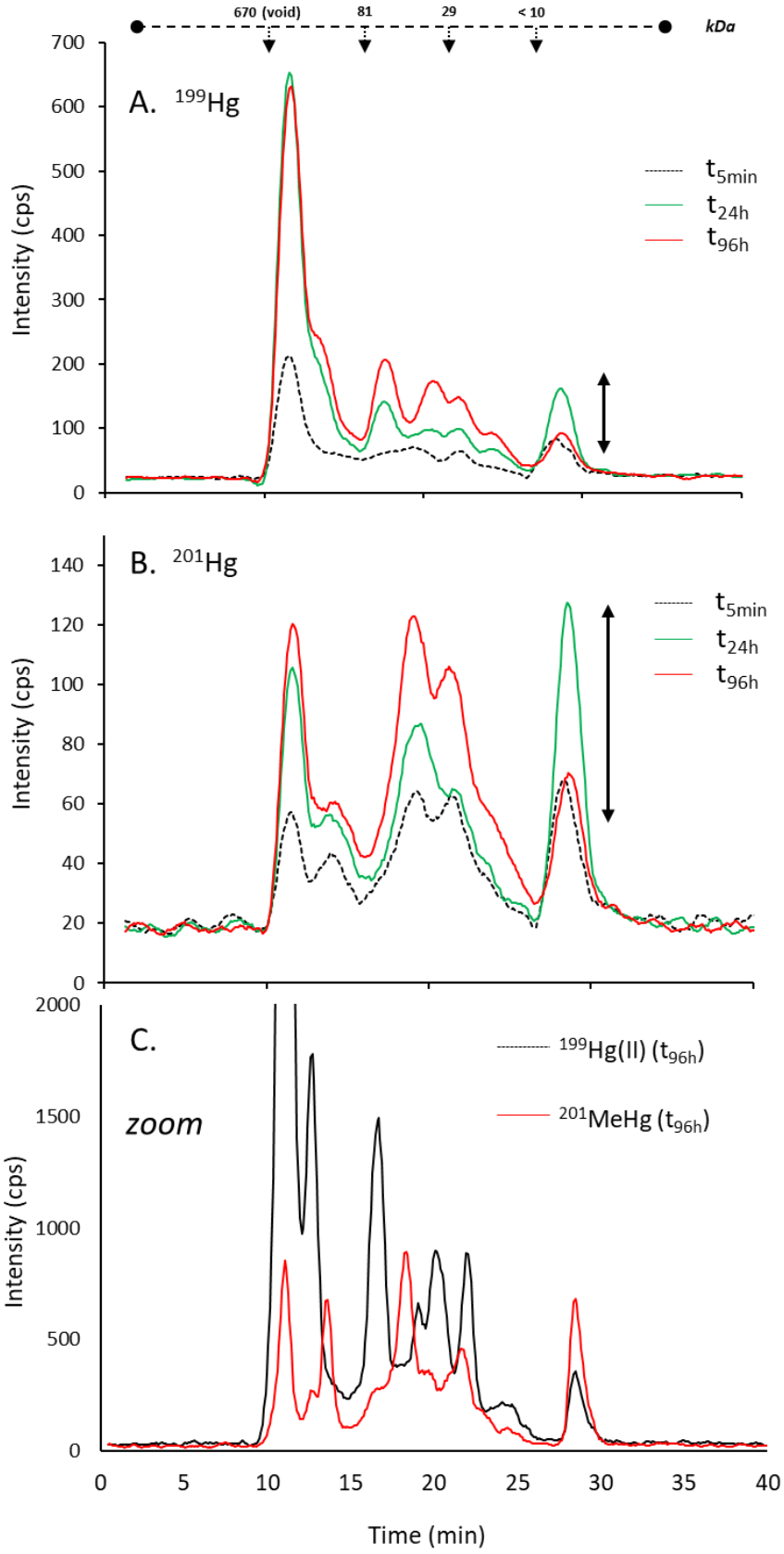

Figure 3.12. Size exclusion chromatograms (Superdex 200 (range: 600-10 kDa)) by ICP-MS detection of (A) ^{199}Hg and (B) ^{201}Hg corresponding to ^{199}Hg (II) and ^{201}MeHg isotopic tracer in the cytosolic fraction of *Synechocystis* sp.at the beginning (5min), after 24 hours and after 96h of Hg exposure. (C) SEC profile of the cytosolic fraction corresponding to the preconcentration of 2L of cell culture in 10 mL after 96 hours of ^{199}Hg(II) and ^{201}MeHg exposure.

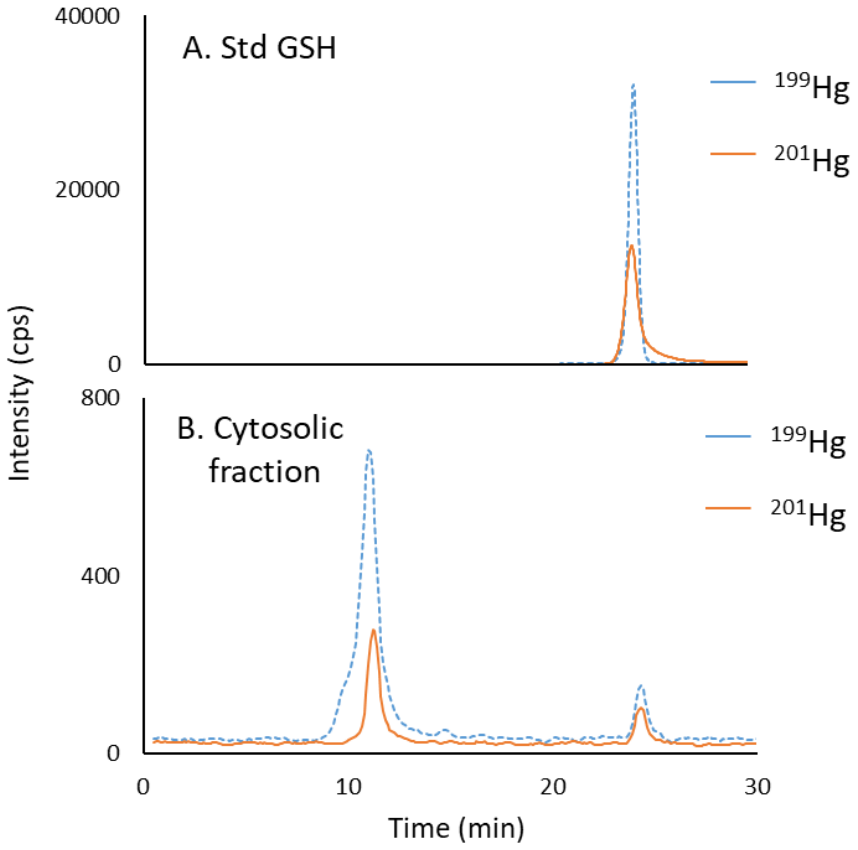

Figure 3.13. Size exclusion chromatograms (Range: 7-0.1 kDa) by ICP-MS detection of (A) standard of glutathione (GSH) binding ^{199}Hg(II) and ^{201}MeHg. (B) the cytosolic fraction of *Synechocystis* sp. PCC 6803 corresponding to both Hg isotopic tracers (^{199}Hg (II) and ^{201}MeHg) after 24 hours of exposure.

3.2.3. Identification of GSH binding Hg(II) and MeHg in *Synechocystis* sp.

Both Hg compounds were coeluting at the same retention time in SEC peptide column. Then, the exogenous incubation of ^{nat}Hg(II) and ^{nat}MeHg was carried out in the cytosolic fraction for the analysis by HILIC-ICP-MS. HILIC chromatograms based on ^{202}Hg isotope monitoring revealed two Hg binding fractions at 21.0 min and 23.7 min (Figure 3.14A). For the identification of both Hg binding fractions, the injection of the same cytosolic fraction carrying out the same chromatographic settings (leading to matching retention times) was done by coupling to an electrospray ionization mass spectrometer, that provides structural information about the compounds previously detected (Figure 3.14, B). Firstly, the Hg natural isotopic pattern was investigated in the full scan spectra at both retention times. Electrospray MS at the retention time of 21.2 min revealed one ion with the isotopic pattern of mercury (Figure 3.15A) at m/z = 524.08 (m/z corresponding to the most abundant isotope in the isotopic distribution) corresponding to Hg methylated binding one glutathione (GS-MeHg, $C_{11}H_{20}HgN_3O_6S^+$). Regarding the electrospray MS at the retention time of 23.5 min, the Hg isotopic pattern was observed (Figure 3.15, B) at m/z = 815.14, corresponding to Hg(II) binding two glutathione ($(GS)_2$-Hg), $C_{20}H_{33}HgN_6O_{12}S_2^+$). Even if the theoretical natural isotopic pattern for Hg(II) and MeHg binding GSH did not match in all isotopes in comparison with the experimental Hg isotopic patterns the experimental masses agreed with the theoretical ones.

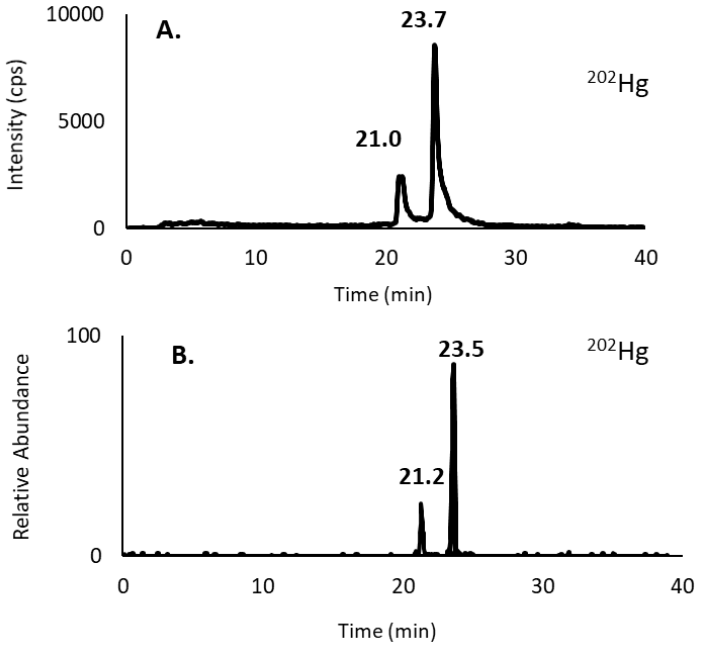

Figure 3.14. HILIC chromatogram of the cytosolic fraction by (A) ICP-MS detection of ^{202}Hg and (B) ESI-LTQ Orbitrap MS detection.

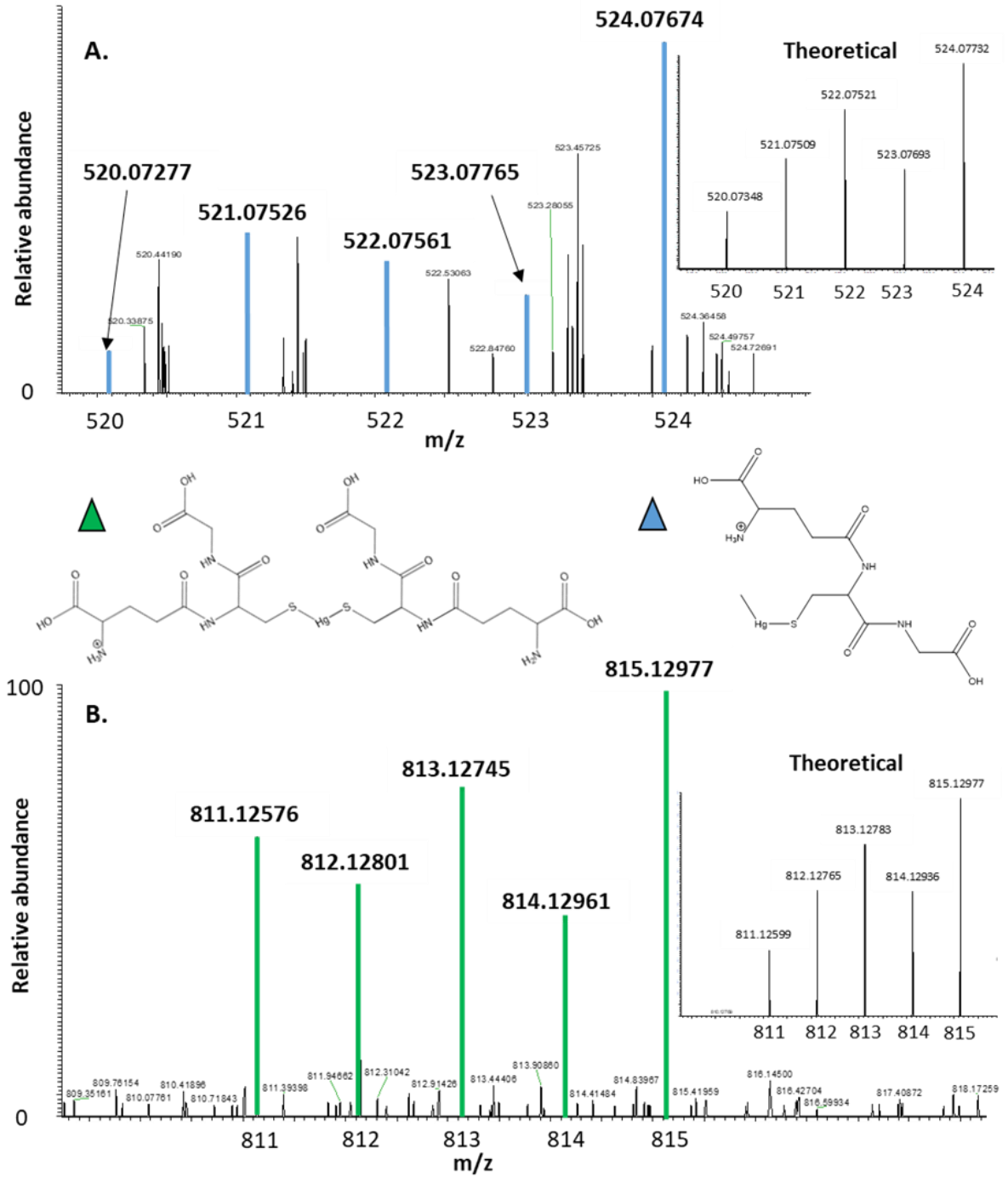

Figure 3.15. (A) Zoom of the mass spectra obtained at 21.2 min demonstrates the presence of MeHg binding one glutathione with its specific isotopic pattern. (B). Zoom of the mass spectra obtained at 23.5 min demonstrate the presence of Hg binding two glutathione with its specific isotopic pattern.

3.3. Discussion.

3.3.1. Role of GSH in *Synechocystis* sp.

Particularly in cyanobacteria, GSH plays a central role in redox control of protein thiols and disulfide bonds, including protection against toxic metabolites, xenobiotic, and oxidative stress (Narainsamy et al., 2013, 2016). Hg exposure is well known to induce accumulation of ROS and peroxidation products in phytoplankton (Elbaz et al., 2010). Under oxidative stress, glutathione acts as a protein reductant against highly reactive oxidants such as singlet oxygen, superoxide and hydroxyl radicals forming GS-SG (Sarma, 2012). The reduction of GS-SG (S-S) to two GSH is normally mediated by the enzyme glutathione reductase being a critical process for its regeneration. Other studies reported that exposure of green alga *Chlamydomonas reinhardtii* to sub-toxic concentrations of Hg(II) and MeHg resulted in a significant increase of reduced GSH after Hg-treatments (Slaveykova et al., 2021). GSH is known to be a precursor of phytochelatins synthesis, which can be activated following the exposure to different toxic metals including Hg. The cyanobacterial phytochelatin synthesis was shown to be close functionally to that of plants. However, no PCs induction was observed. The increase of Hg(II) and MeHg containing in the LMW fraction (≤ 10 kDa) after 24 hours with the subsequent decrease observed in this specific fraction after 96 hours (**Figure 3.12**) might be related with the role of GSH to control the intracellular Hg speciation as it was previously demonstrated by Morelli et al., 2009; Wu & Wang, 2012, 2014 in eukaryotic microalgae. In these previous studies, Hg compounds amol per cell was 100-1000 times higher than our conditions.

3.3.1. Uncharacterized Hg(II) binding intracellular bioligands in *Synechocystis* sp.

Regarding the concentration of ^{199}Hg(II), a huge decrease in the extracellular fraction was observed after 24 hours of Hg exposure (**Figure 3.11A**) which was not related to the potential Hg(II) losses due to the centrifugation step (Chapter 3.1 **page 105**). Certainly, this previous finding was observed due to the ability of *Synechocystis* to reduce Hg(II) into Hg(0) by MerA-like enzymes, already demonstrated by Marteyn et al., 2013. On the other hand, ^{199}Hg(II) concentration in the cytosolic fraction increased two folds after 24 hours (**Figure 3.11C**). Furthermore, SEC profiles also revealed an increase of several fractions containing specifically ^{199}Hg(II) eluting between 17–27 min after 24 hours and 96 hours of exposure (**Figure 3.12**), even if the percentage of Hg(II) internalized during 96 hours was constant (**Figure 3.11D)**. Although the simultaneous Hg(II) reduction and Hg(II) sequestration may be contradictory, a recent study suggested that phototrophic bacteria use Hg(II) as an electron sink reducing and

maintaining Hg(II) intracellular levels and redox homeostasis (Grégoire & Poulain, 2016). In the cited study, Hg(0) production decreased when alternative electron acceptors such as dimethylsulphoxide (DMSO) were added to the culture. On the other hand, Hg(0) production increased when bacteria grew phototrophically and when enzyme cofactors signalled the existence of an intracellular redox imbalance. In our work, the results mentioned before in combination with the studies cited in this section suggests that the one or several unknown intracellular bioligands containing in the fractions eluting between 17–27 min might play important roles acting as an electron acceptor and maintaining Hg(II) intracellular levels within the cell. On the other hand, MeHg was also specifically found in several fractions that increased with the exposure time but the potential role of these uncharacterized bioligands could not be hypothesized.

3.4. Conclusions.

In this work, the identification of glutathione binding to Hg(II) ($(GS)_2$-Hg) and MeHg (GS-MeHg) in cyanobacterium *Synechocystis* sp. PCC 6803 in turns with the changes in the LMW fraction over time confirm that GSH plays an important role in controlling Hg speciation within the cell. On the other hand, one or more specific unknown Hg(II) binding bioligands containing in the fractions eluting between 17–27 min were hypothesized to act as an electron sink reducing and maintaining the Hg(II) constant intracellular levels based on two main studies found in the literature (Grégoire & Poulain, 2016; Marteyn et al., 2013). However, further studies will be needed for the identification of these unknown intracellular bioligands with the purporse of elucidating or confirming their specific role in Hg intracellular handling.

4. Comparison of Hg-phytoplankton interactions in three different phytoplankton species: Green alga, diatom and cyanobacterium.

4.1. Hg compounds concentration in ng L^{-1} vs amol $cell^{-1}$.

Although the concentration of Hg(II) and MeHg given in ng per L of exposure media was at the same range (0–60 ng L^{-1}) between the three phytoplankton species, the Hg content (amol) per cell varied significantly (**Table 3.7**). The highest Hg(II) concentration (60.3±10.6 ng L^{-1}) found in the cytosolic fraction after 24 hours of exposure in *C.reinhardtii* might be related to the high cell density (7x 10^7 cell mL^{-1}) since more cells were able to taken up Hg(II). Consequently, Hg(II) amol per cell in *C.reinhardtii* was 10 and 20 folds lower than in *Synechocystis* and *C.meneghiniana*, respectively. On the other hand, the concentration of Hg(II) and MeHg per cell in *C.meneghiniana* after 24 hours of exposure was 10 and 20 times higher than *Synechocystis* and *C.reinhardtii*, respectively (initial cell density in **Table 3.1**).

Table 3.7. Hg(II) and MeHg concentration in amol $cell^{-1}$ and ng L^{-1} after 5 minutes and 24 hours of exposure in *Synechocystis* sp., *Cyclotella meneghiniana* and *Chlamydomonas reinhardtii.*

	^{199}Hg (II) (ng L^{-1})			**^{201}MeHg (ng L^{-1})**		
Time	***Synechocystis***	***C.meneghiniana***	***C.reinhardtii***	***Synechocystis***	***C.meneghiniana***	***C.reinhardtii***
t_{5min}	15.4±2.4	32.6±13.3	28.9±3.6	16.7±2.5	13.3±3.7	8.5±0.6
t_{24h}	30.9±4.8	33.4±4.8	63.8±10.6	20.8±2.2	19.2±4.9	30.5±1.3
	^{199}Hg (II) (amol $cell^{-1}$)			**^{201}MeHg (amol $cell^{-1}$)**		
Time	***Synechocystis***	***C.meneghiniana***	***C.reinhardtii***	***Synechocystis***	***C.meneghiniana***	***C.reinhardtii***
t_{5min}	2.1±0.2 $x10^{-2}$	2.2±0.2 $x10^{-1}$	2.2±0.3 $x10^{-3}$	2.8±0.4 $x10^{-2}$	9.1±0.5 $x10^{-2}$	6.4±0.4 $x10^{-4}$
t_{24h}	4.3±0.7 $x10^{-2}$	2.2±0.2 $x10^{-1}$	5.1±0.8 $x10^{-3}$	3.1±0.3 $x10^{-2}$	1.0±0.3 $x10^{-1}$	2.2±0.3 $x10^{-3}$

4.2. Sequestration and release of Hg compounds.

Figure 3.16 shows the evolution of ^{199}Hg(II) and ^{201}MeHg concentration in the cytosolic fraction over time for *Synechocytis* sp. *C.meneghiniana* and *C.reinhardtii*. Concerning *C.reinhardtii*, Hg(II) concentration increased two fold within the first 24 hours, whereas a decrease was observed after 96 hours of exposure (see extracellular fraction **Figure A3- 1**). In *Synechocystis*, Hg(II) concentration increased up to 30.9 ng L^{-1} and remained constant after 96 hours. On the other hand, a fast Hg(II) bioaccumulation was observed after 5 minutes in *C.meneghiniana*, in which Hg(II) concentration remained constant within the first 24 hours. In this specific phytoplankton microorganism, a huge depletion was shown after 72 hours of exposure for both Hg(II) and MeHg. In *C.reinhardtii*, MeHg concentration increased three folds within the first 24 hours, and remained constant over time. On the other hand, a fast MeHg bioaccumulation was observed after 5 minutes of exposure in *Synechocystis*.

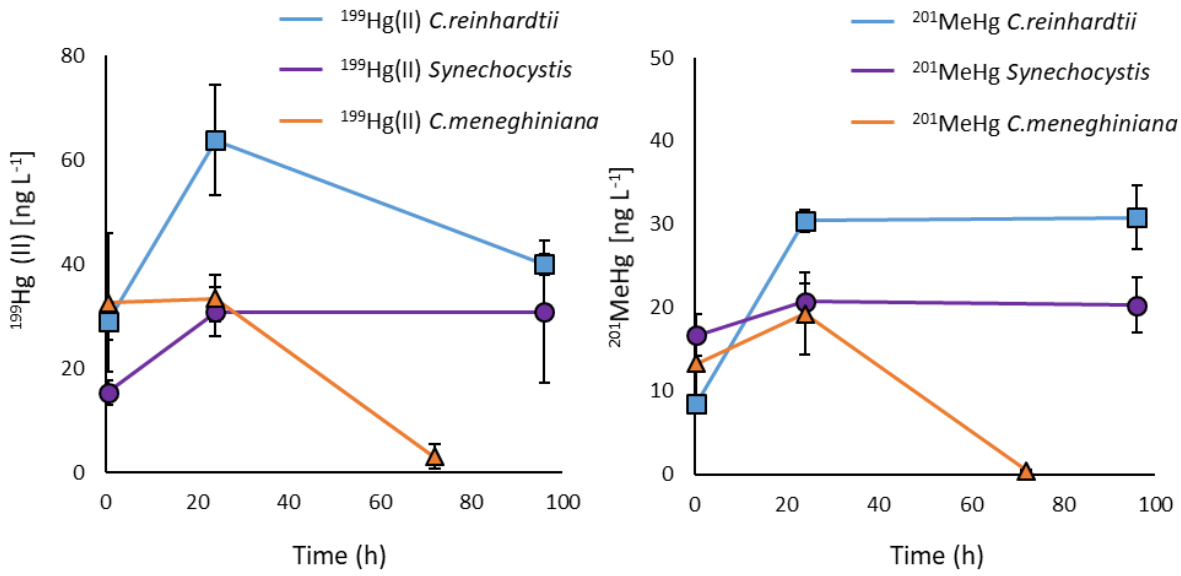

Figure 3.16. ^{199}Hg (II) and ^{201}MeHg concentration (ng L^{-1}) in the cytosolic fraction after 5 minutes, 24 hours and 72/96 hours of Hg exposure in *Synechocystis* sp., *Cyclotella meneghiniana* and *Chlamydomonas reinhardtii*.

4.3. Hg compounds bioaccumulation and removal capacity.

The volume concentration factor (VCF) is a good approach to address the Hg compounds enrichment in cells relative to the surrounding waters. It is normally used to compare the Hg bioaccumulation on cells and removal capacity of Hg compounds from the extracellular medium between different phytoplankton species. It is obtained by dividing the concentration in whole cells and extracellular fraction (Luengen et al., 2012). In our work, the VCF was obtained using the Eq. 3.3. The VCF using Eq. 3.3 could not be compared with other studies. It is important to point out that, VCF increases with the Hg concentration in cells due to: (1) the attachment of Hg compounds on the cell wall surface, (2) internalization in the intracellular fraction and, (3) the reduction and/or precipitation of Hg compounds in the extracellular medium.

$$\mathrm{VCF} = \frac{[\text{Hg concentration (ng Hg L exposure media)}]_{\text{cells}}}{[\text{Hg concentration (ng L exposure media)}]_{\text{extracellular}}} \qquad (3.3)$$

Results revealed that *Synechocystis* possess the highest bioaccumulation and removal capacity for Hg(II) (**Figure 3.17A**) with VCF four times higher than *C.meneghiniana* and *C.reinhardtii*. In contrast, VCF in *C.reinhardtii* was 2 times higher *Synechocystis* and 60 times higher than *C.meneghiniana* (**Figure 3.17B**).

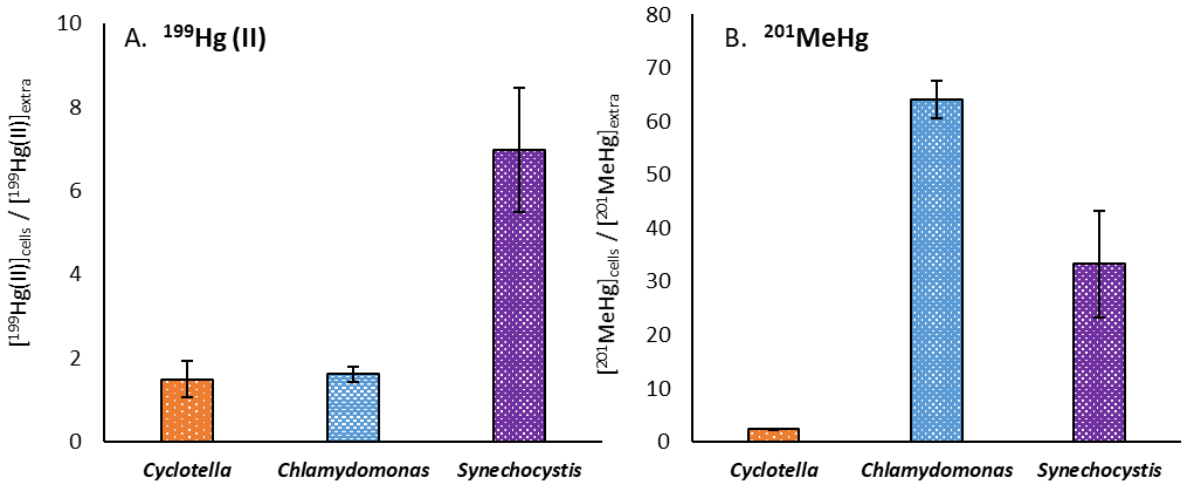

Figure 3.17. .(A) ^{199}Hg(II) and (B) ^{201}MeHg volume concentration factor (VCF) in the cytosolic fraction after 24 hours of exposure in *Synechocystis* sp., *Cyclotella meneghiniana* and *Chlamydomonas reinhardtii*.

4.4. Comparison of the screening of intracellular Hg binding bioligands.

The use of SEC coupled to ICP-MS have been useful to investigate the progressive changes of intracellular biomolecules binding ^{199}Hg(II) and ^{201}MeHg in the cytosolic fraction of three different phytoplankton species but also, the potential specific binding affinities of both Hg compounds (**Figure 3.18**). Since low Hg interconversion reactions occurred in phytoplankton cell culture during the incubation process and no potential Hg compounds interconversion processes were tested due to the cell fractionation, it is assumed that the isotope 199 corresponds to Hg(II) and the isotope 201 to MeHg. As a remainder, *Synechocystis* showed an increase of Hg(II) concentration by two folds after 24 hours in agreement with the appearance of several MMW fractions (81-29 kDa) binding specifically ^{199}Hg (II) after 24 hours and 96 hours of exposure. Furthermore, fluctuations in the LMW fraction containing ^{199}Hg(II) and ^{201}MeHg were observed over time. In *C.meneghiniana*, the concentration of ^{199}Hg(II) and ^{201}MeHg remained constant within the first 24 hours where ^{201}MeHg was only found in the LMW fraction (≤10 kDa, 28–31 min) after 5 minutes. In contrast, ^{199}Hg(II) was found in the MMW fraction (≈ 29 kDa, 22–23 min) within the first 24 hours of exposure. In *C.reinhardtii*, no Hg compounds containing in the LMW fraction were detected. The increase of ^{199}Hg(II) and ^{201}MeHg concentration after 24 hours could not be correlated to any SEC fraction however; a MMW fraction (20–23 min) was observed after 96 hours of exposure when Hg(II) was released to the extracellular medium.

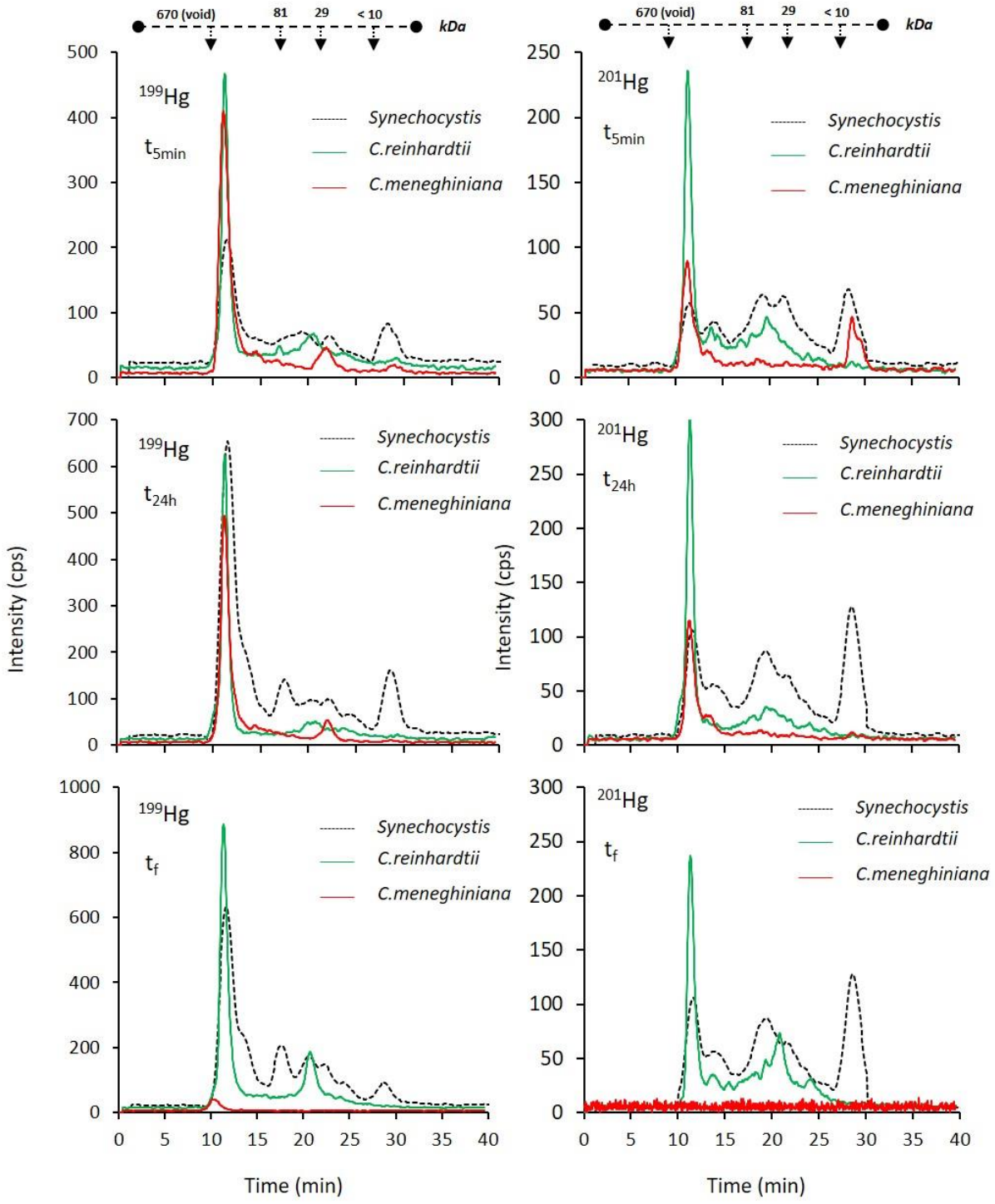

Figure 3.18. Size exclusion chromatograms (Superdex 200 (range: 600-10 kDa)) in the cytosolic fraction of *Synechocystis* sp., *Chlamydomonas reinhardtii* and *Cyclotella meneghiniana* by ICP-MS detection of ^{199}Hg and ^{201}Hg corresponding to the incubation spikes after 5 minutes, 24 hours and 72/96 hours of exposure.

Annexes Chapter 3

Annexes Chapter 3.

Composition of the growth medium.

Synechocystis sp. PCC 6803.

Table A3- 1. Growth medium composition (BG11 medium).

Composition	Concentration (g L^{-1})
H_3BO_3	2.9
$MnCl_2.4H_2O$	1.8
$ZnSO_4.7H_2O$	0.2
$Na_2MoBO_4.2H_2O$	0.4
$CuSO_4.5H_2O$	0.079
$Co(NO_3)_2.6H_2O$	49.4
K_2HPO_4	4.0
$MgSO_4.7H_2O$	7.5
$CaCl_2.2H_2O$	3.6
Citric acid ($C_6H_8O_7$)	6.0
$Na_2EDTA.2H_2O$	0.1
Ferric ammonium citrate ($C_6H_8FeNO_7$)	6.0
Na_2CO_3	2.0

Exposure medium composition: Same composition as growth medium except for the trace elements stock solution, acids and EDTA.

Cyclotella meneghiniana.

Table A3- 2. Growth medium composition (SFM medium)

Composition	Concentration (nM)
HEPES	1 nM
$Ca(NO_3)_2.4H_2O$	0.21 mM
$ZnSO_4.\ 7H_2O$	0.2 mM
$MgSO_4.7H_2O$	0.2 mM
$K_2HPO_4.3H_2O$	13 µM
Na_2CO_3	0.2 mM
$NaNO_3$	0.35 mM
H_2BO_3	16 µM
Vitamin B12	0.15 mM
Biotin	4.1 nM
Thiamine-HCl	0.30 µM
Niacinamide	0.8 nM
$Na_2EDTA.2H_2O$	-
Other trace metals	-
$Na_2SiO_3.7H_2O$	0.5 mM

Exposure medium has the same composition than the growth medium (SFM) except for:

- HEPES buffer.
- Trace metals solution.
- Vitamins solution.

Chlamydomonas reinhardtii.

Table A3- 3. Growth medium composition (TAP medium).

Composition	Concentration (g L^{-1})
KH_2PO_4	13.7
KH_2PO_4	26.0
NH_4NO_3	26.9
CH_3COONa	10
$MgSO_4.7H_2O$	5
$CaCl_2.2H_2O$	2.5
H_2BO_3	2.4
$MnCl_2.4H_2O$	12.4
$ZnSO_4.\ 7H_2O$	5.5
$Na_2EDTA.2H_2O$	12.5
$CoCl_2.4H_2O$	0.4
$CuSO_4.5H_2O$	0.4

Exposure medium has the same composition than the growth medium except for the trace elements stock solution, acids and EDTA.

Results *Chlamydomonas reinhardtii*.

In **Figure A3- 1**, ^{199}Hg (II) was taken up by the cells during the first 24 hours. At t5min, the concentration of ^{199}Hg (II) in the extracellular fraction and whole cells was 455.4 and 132.9 ng L^{-1} respectively. After 24 hours, the concentration of ^{199}Hg (II) in the extracellular fraction decreased until 132.6 ng L^{-1} while the concentration in the whole cells increased up to 214.4 ng L^{-1}. From 24 to 96 hours, results showed the release of ^{199}Hg (II) from the cells to the extracellular fraction. At 96h, the concentration in the extracellular fraction increased until 266.6 ng L^{-1}, whereas the concentration in the whole cells decreased up to 144.0 ng L^{-1}. On the other hand, all ^{201}MeHg was taken up by the cells after 24 hours. From 5 minutes to 24 hours, the concentration in the extracellular medium decreased from 41.1 to 0.8 ng L^{-1} whereas the concentration in whole cells increased from 13.0 until 51.1 ng L^{-1}. After 96h, ^{201}MeHg was sequestrated by the cells since ^{201}MeHg concentration remained constant in both fractions.

Figure A3- 2 shows the Hg compounds concentration, the percentage internalized and the screening of Hg binding bioligands from 600 to 10 kDa of the isotopically enriched ^{199}Hg (II) and ^{201}MeHg incubated in the cytosolic fraction at t_{5min}, t_{24h} and t_{96h}. Overall, the percentage of ^{199}Hg (II) and ^{201}MeHg internalized was around 21.8-27.8 and 65.8-57.8 %. From 5 minutes to 24 hours, the ^{199}Hg (II) concentration increased from 28.9±3.8 to 63.8±10.6 ng L^{-1} whereas, as it was seen for the whole fraction, ^{199}Hg (II) concentration decreased until 40.0±2.0 ng L^{-1} after 96 hours. For ^{201}MeHg, the concentration increased from 8.5±0.6 to 30.5±1.3 ng L^{-1} within the first 24 hours and remained constant over 96 hours.

For ^{199}Hg (II), size exclusion chromatogram profile reveals two main fractions at HMW (($\geq$ 600 kDa, 10-13 min) and MMW (29 kDa, 20-23 min) where an increase in this last fraction was seen after 96 hours. On the other hand, ^{201}MeHg was binding to similar fractions. In order to observe the potential bioligands capable of binding Hg in the cytosolic fraction, the exogenous addition of ^{198}Hg (II) and ^{202}MeHg was performed. However, SEC profiles did not reveal any specific binding affinity. Furthermore, no LMW bioligands were capable of binding endogenous (^{199}Hg (II) & ^{201}MeHg) or exogenous (^{198}Hg (II) & ^{202}MeHg) Hg.

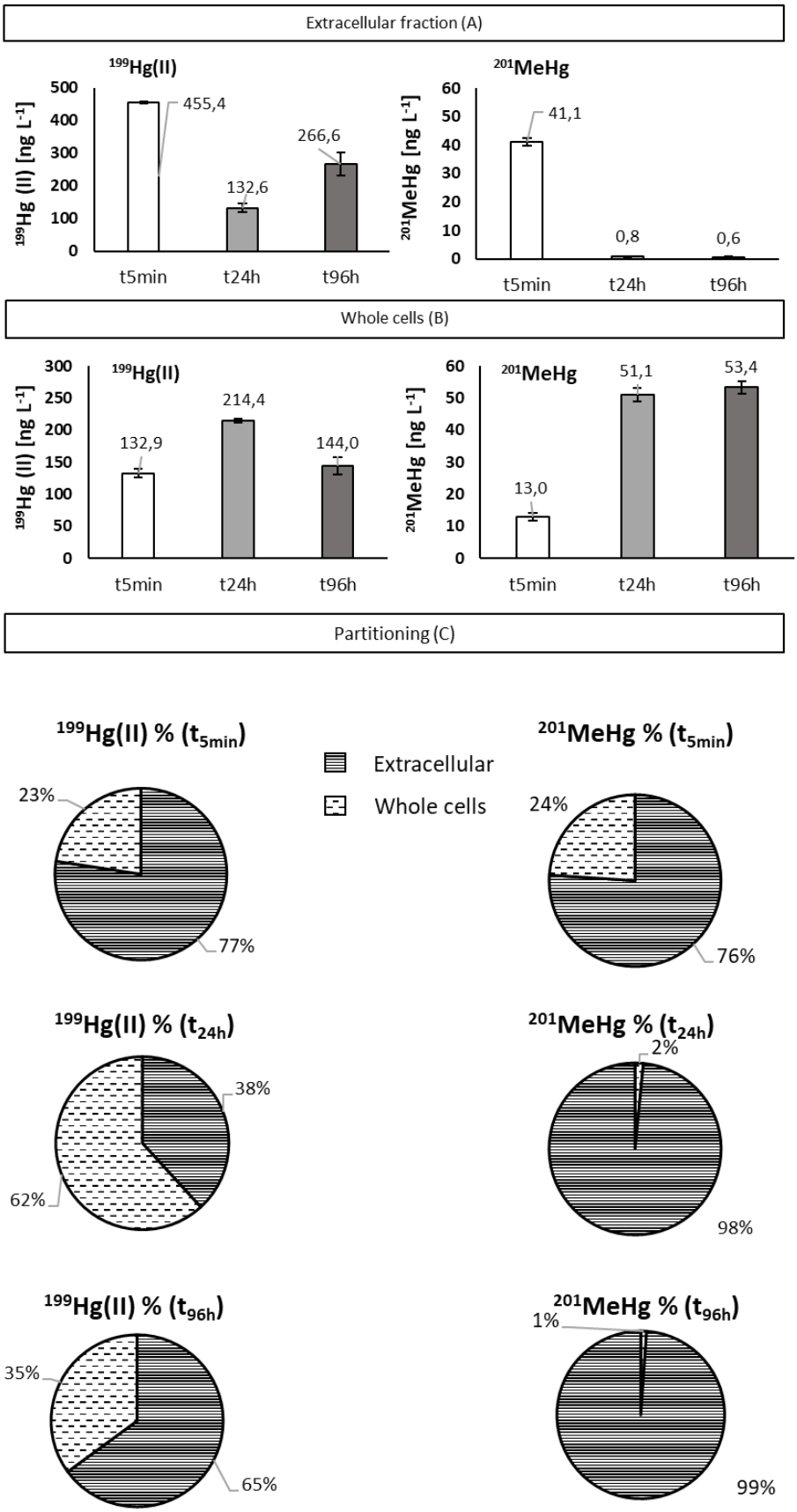

Figure A3- 1. ^{199}Hg (II) and ^{201}MeHg concentration (ng L^{-1} exposure media) in (A) the extracellular fraction and (B) whole cells and (C) partitioning between the extracellular medium and whole cells at the beginning (5min), after 24 hours and 96h of Hg exposure in *Chlamydomonas reinhardtii*.

Cytosolic fraction (A)

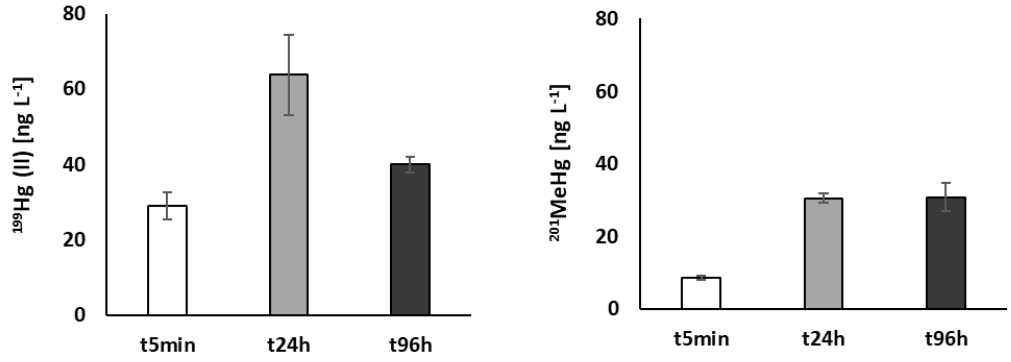

% ^{199}Hg (II) and ^{201}MeHg internalized in the cytosolic fr. (B)

Time	% of Hg species internalized	
	^{199}Hg (II)	^{201}MeHg
t_{5min} (%)	21.8 ± 3.0	65.8 ± 5.9
t_{24h} (%)	29.7 ± 5.0	59.7 ± 3.6
t_{96h} (%)	27,8. ± 3.0	57.8 ± 7.4

Size exclusion chromatography (600-10 kDa) in the cytosolic fr. (C)

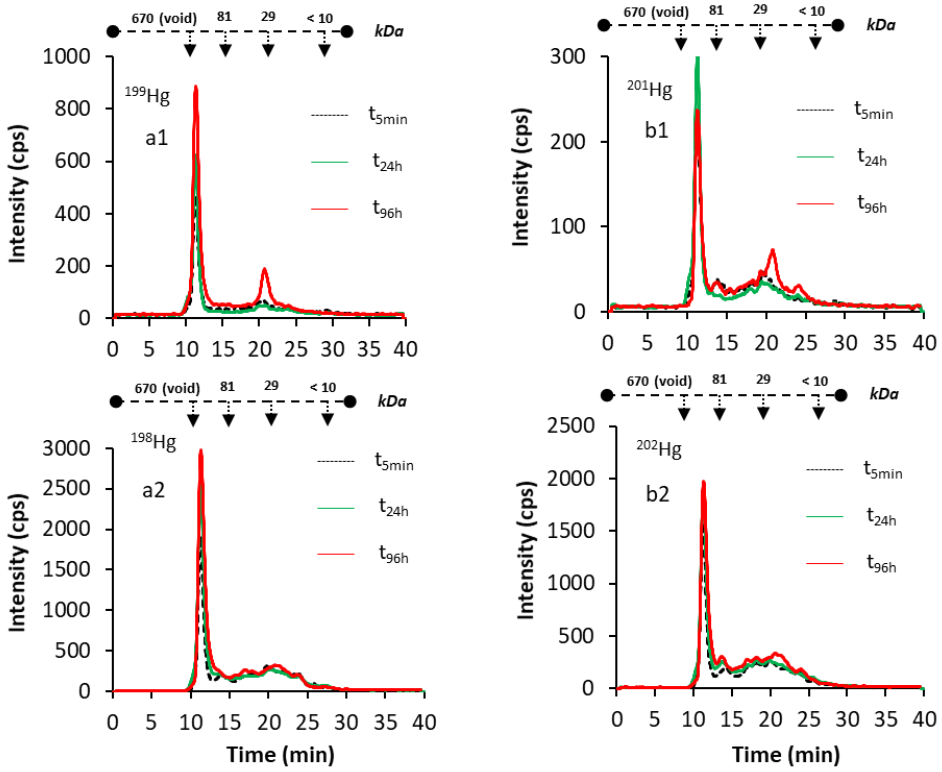

Figure A3- 2. (A) ^{199}Hg (II) and ^{201}MeHg concentration (ng L^{-1} exposure media) in the cytosolic fraction at the beginning (t5min), after 24 hours and after 96h of Hg exposure. (B) Percentage of Hg compounds internalized at the beginning (5min), after 24 hours and 96 hours of Hg exposure. (C) Size exclusion chromatograms (Superdex 200 (range: 600-10 kDa)) by ICP-MS detection of (a1) ^{199}Hg and (b1) ^{201}Hg corresponding to ^{199}Hg (II) and ^{201}MeHg isotopic tracer, (a2) ^{198}Hg and (b2) ^{202}Hg corresponding to the exogenous addition in the cytosolic fraction of *Chlamydomonas reinhardtii* at the beginning (5min), after 24 hours and after 96h of Hg exposure.

Cell density *Cyclotella meneghiniana*: MFG vs biotic control.

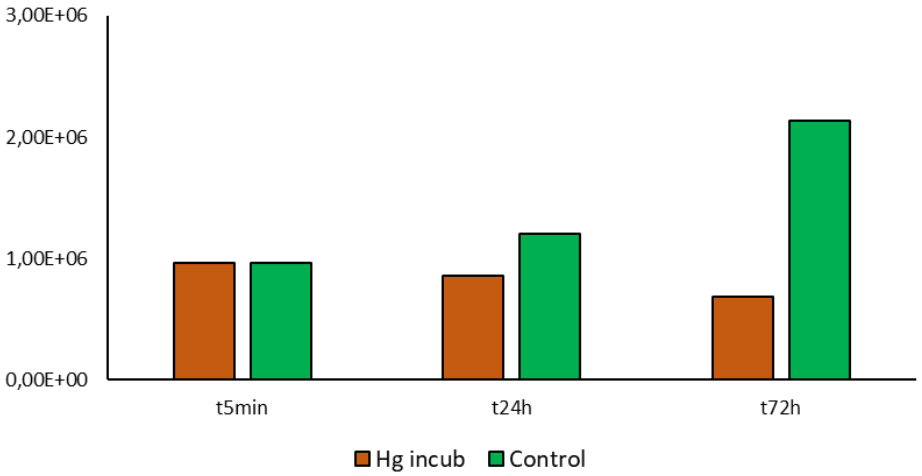

Figure A3- 3. Cell density between the biotic control and mercury free growth (MFG) after 5 minutes, 24 hours and 72 hours in *Cyclotella meneghiniana*.

Chapter 4

Conclusions and perspectives

Chapter 4. Conclusions and perspectives.

The analytical approach carried out during the present doctoral dissertation was based on the incubation of isotopically enriched ^{199}Hg(II) and ^{201}MeHg. Hyphenated techniques based on elemental and molecular mass spectrometry were used to track (1) the simultaneous Hg compounds-specific transformation pathways, and (2) the Hg compounds-specific intracellular complexation with bioligands in three different model phytoplankton microorganisms (**Figure 4.1**).

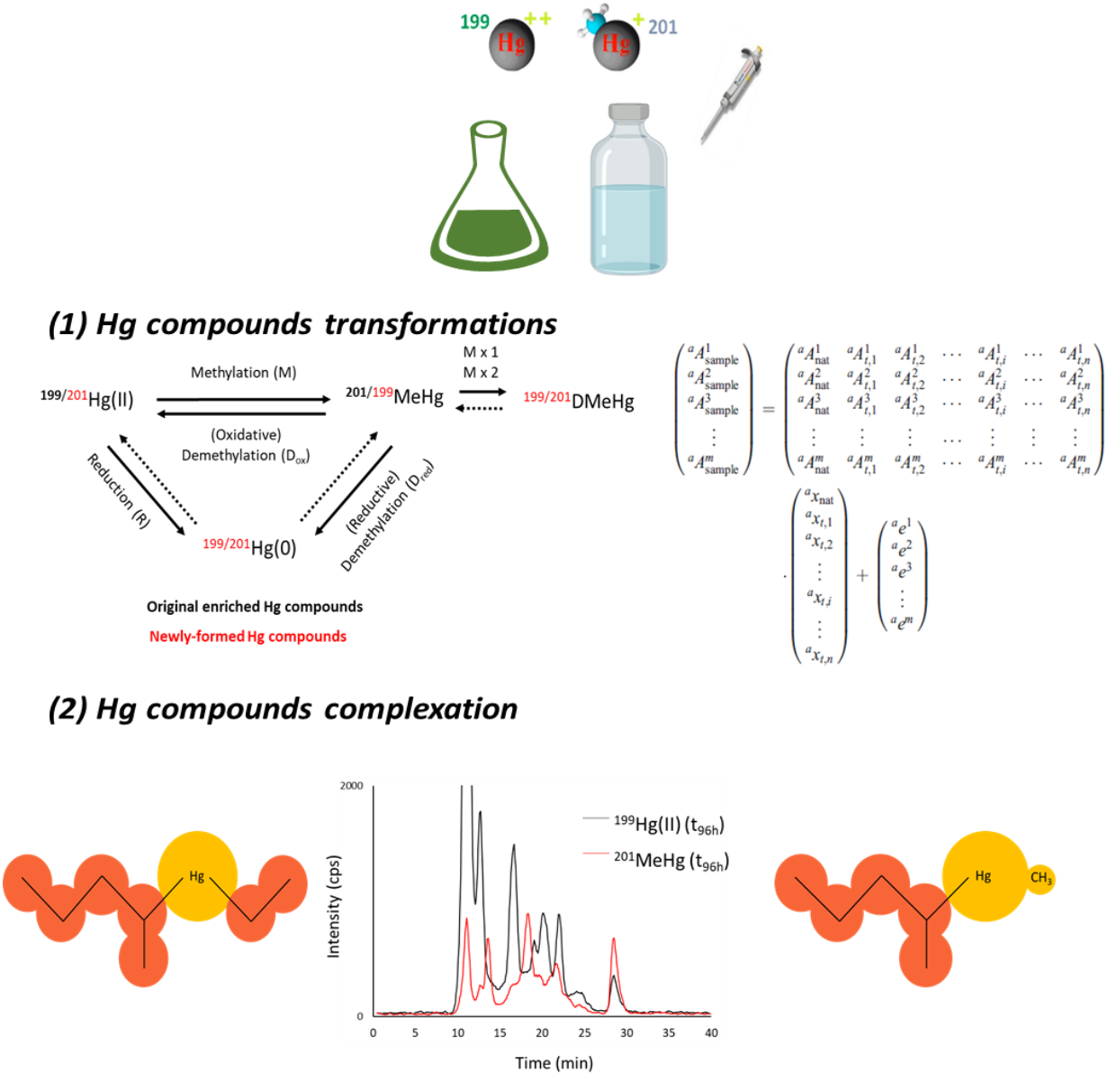

Figure 4.1. Overview about the analytical approach applied in this doctoral work.

First, the evaluation of the quadruple tracer methodology allowed the **distinction of methylation and demethylation yields** during the incubation process and sample preparation; being successfully applied in Hg incubation experiments with different **environmental matrices and phytoplankton cell cultures**. Furthermore, it allowed the distinction of MeHg loss and MeHg demethylation in biofilms, sediments, freshwaters and phytoplankton. The versatility of IPD was combined with an external calibration with the purpose of **distinguishing the dissolved gaseous mercury isotopic signatures**. This approach allowed us determining and comparing the Hg(II) reduction and reductive MeHg demethylation potentials between unfiltered surface freshwater and seawater samples. Overall, IPD has proved to be a suitable, universal and versatile tool for the determination of **Hg compounds transformations (Figure 4.1)**. Finally, the quadruple tracer methodology also allowed us to determine, for first time, the biotic MeHg demethylation potentials in *Cyclotella meneghiniana* thanks to the application of an experimental design based on the double incubation of Hg compounds in two consecutives 48 hours processes.

Second, the investigation of the major bioligands involved in Hg speciation and Hg intracellular handling in two main phytoplankton species was achieved at low Hg exposure levels. The quantification of isotopically enriched Hg compounds in the different (sub-) cellular fractions give us the location of enriched Hg compounds over time. The screening of Hg binding bioligands and the identification of Hg(II) and MeHg binding glutathione in the cytosolic fraction allowed us hypothesized their potential role in Hg intracellular handling. In *Cyclotella meneghiniana*, **GSH could be involved in the active excretion of MeHg** in order to reduce the potential oxidative stress within the cells. The main findings supporting this hypothesis are: **(1)** the release of Hg compounds in mercury free growth (MFG); **(2)** the preferential MeHg release in mercury exposure growth conditions (MEG); and **(3)** the identification of GSH in the biotic control, but not in MFG.

In *Synechocystis* sp. PCC 6803, GSH is suggested to play a major role controlling the intracellular Hg speciation. The main results supporting this hypothesis are: **(1)** the sequestration of MeHg and Hg(II) in the cytosolic fraction over 96 hours; (**2**) the identification of GSH binding Hg(II) and MeHg; **(3)** the changes in the screening of Hg binding bioligands, particularly, the increase of the LMW fraction (28–31 min), mainly composed by GSH, within the first 24 hours and the decrease after 96 hours; and **(4)** the previous studies reporting the role of GSH in eukaryotic algae under Hg exposure (Morelli et al., 2009; Wu & Wang, 2012, 2014). In addition, one or more bioligands bound specifically to Hg(II) containing in the size fractions

might act as a sink reducing and maintaining Hg(II) intracellular levels. This hypothesis is based on: **(1)** evidences found in phototrophic bacteria, in which Hg(II) was used as an electron acceptor controlling Hg(II) intracellular levels and redox homeostasis (Grégoire & Poulain, 2016); (**2**) the potential capacity of *Synechocystis* sp. PCC 6803 to reduce Hg(II) into Hg(0) (Marteyn et al., 2013); (**3**) the constant percentage of Hg(II) internalized over 96 hours and **(4)** the increase of size fractions containing bioligands bound specifically to Hg(II) over 96 hours. In *Chlamydomonas reinhardtii*, MeHg was sequestrated inside the cells over 96 hours. In contrast, Hg(II) was released into the extracellular medium after 96 hours of exposure. To sum up, the potential multifunctionality of GSH to handle Hg compounds has been shown in the cyanobacterium *Synechocystis* sp. PCC 6803 and the diatom *Cyclotella meneghiniana*. Moreover, different compounds-specific sequestration and release pathways have been observed in the three phytoplankton species showing the importance of each photosynthetic microorganisms in the Hg compounds fate (**Figure 4.2**).

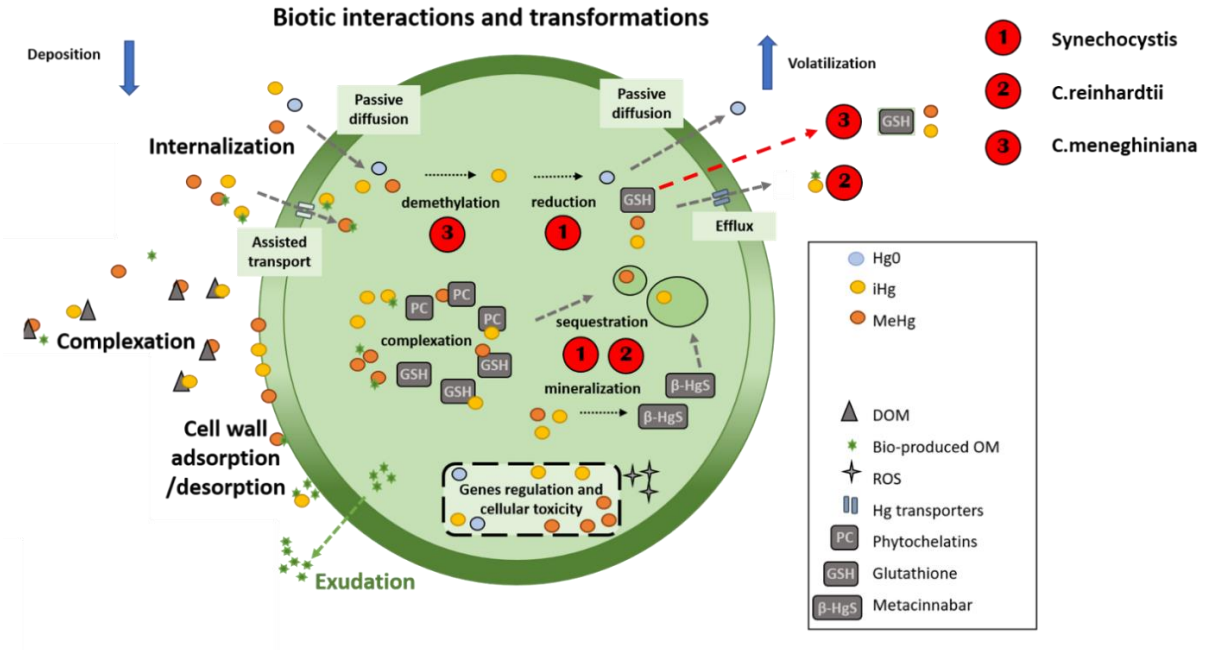

Figure 4.2. Conceptual scheme of the different processes (elucidated and/or speculated) affecting Hg(II) and MeHg in phytoplankton cells (Cossart, Thibaut & Garcia-Calleja, Javier & Santos P. Joao et al., 2022).

Potential role (s) of GSH in phytoplankton.

Although GSH counteract the oxidative stress induced by high Hg exposure by increasing cellular GSH levels (Morelli et al., 2009; Wu & Wang, 2012) or promoting PCs formation (García-Sevillano et al., 2014; Wu & Wang, 2012), the role of GSH in Hg intracellular handling had not yet been addressed. In this work, GSH was observed to sequestrate MeHg and Hg(II)

over 96 hours in *Synechocystis* sp. On the other hand, GSH was hypothesized to be potentially involved in the excretion process of MeHg into the extracellular medium in *C.meneghiniana* manifesting its potential multifunctionality to handle Hg in different phytoplankton species. The main explanation about these two contrasting mechanisms to handle Hg compounds might be associated to the tolerance of both phytoplankton species towards Hg exposure. Cyanobacteria are more resistant to pollutant exposure, high temperatures, and eutrophication events and therefore, oxidative stress (Chapra et al., 2017; Paerl & Paul, 2012).On the other hand, several studies described *C.meneghiniana* as a metal sensitive microalga showing its disappearance from phytoplankton assemblages due to the exposure of toxic chemical compounds (Pandey et al., 2015). Although GSH concentration was not measured in both photosynthetic microorganisms, the differences observed might be also related to the GSH load capacity to handle Hg directly as well as the potential oxidative stress induced by Hg. Reduced GSH concentrations reported in cyanobacteria were at the milimolar levels (3-5 mM) (Cameron & Pakrasi, 2010; Tel-or et al., 1986), whereas the intracellular GSH concentration determined in diatoms were approximately at the micromolar levels (0.5-12 µM) (Kawakami et al., 2006a, 2006b; Morelli et al., 2009; Wu & Wang, 2012). Based on the reported values and our results, the intracellular GSH content and the phytoplankton capacity to cope the potential oxidative stress are the main factors controlling the cellular handling of Hg compounds in phytoplankton. Whereas the most sensitive phytoplankton species might excrete MeHg about the impossibility to cope MeHg stress within the cell, the most tolerant phytoplankton species such as cyanobacteria could sequestrate and handle MeHg inside the cell.

Environmental implications.

Freshwater phytoplankton communities are composed by several phytoplankton species such as cyanobacteria, diatoms and green algae, among others (Reynolds, 2006). The diversity and abundance of phytoplankton communities is affected by environmental factors such as seasonal variations and eutrophication status (Bouraï et al., 2020). Eutrophication events or alga blooms consist in an excessive growth of microorganisms due to the increased availability of one or more limiting growth factors needed for photosynthesis such as sunlight or nutrients fertilizers. On the other hand, seasonal variations also influence the eutrophication status of freshwaters ecosystems due to the sunlight intensity and water temperature, having a direct effect on the metabolic activity of aquatic microorganisms.

Eutrophication events also enhance the MeHg production in freshwaters ecosystems due to alga decomposition and organic matter production, which act as a fuel for microbial methylators

(Branfireun et al., 2020). A recent study showed that the activities of methanogens were significantly promoted during alga decomposition in eutrophic shallow lakes (Lei et al., 2021). Cyanobacteria enhanced MeHg production in periphyton by releasing high amount of DOM into water (Lázaro et al., 2019). Although the increase of cell density is thought to reduce Hg concentration per cell (biodilution) (Pickhardt et al., 2002), fields observations in the Baltic sea showed that eutrophication events increased MeHg content in phytoplankton (Soerensen et al., 2016). Consequently, the eutrophication status of freshwater systems have a major role on the MeHg production and its potential transfer through the trophic chain.

Eutrophication events not only affect higher consumers through the MeHg production, but also induces potential oxidative stress affecting the composition and diversity of phytoplankton communities. The increase of both nutrient and water temperature was observed to enhance cyanobacteria composition in alga blooms, in which environmental models suggest that cyanobacteria will increase their dominance caused by climate change (Chapra et al., 2017; Paerl & Paul, 2012). In addition, blooms of Chlamydomonas have been observed in eutrophic Antarctic lakes (Hawes, 1990; Mataloni et al., 2000). These findings are thought to be correlated with the high tolerance of *Synechocystis* and *C.reinhardtii* to cope the potential stress induced by anthropogenic, natural disturbances, and MeHg. Therefore, we expect that both phytoplankton species have major role in MeHg sequestration and potential trophic transfer in eutrophic freshwater ecosystems. On the other hand, we hypothesize that *C.meneghiniana* will disappear from the phytoplankton assessable caused by the toxicity induced by MeHg production, nutrients enrichment or rising water temperatures.

Perspectives.

Hg-phytoplankton interactions.

The understanding of Hg-phytoplankton interactions is of great importance for the improvement of mitigation strategies, Hg biogeochemical modelling, and rational environmental risk assessments in changing aquatic ecosystems. Several questions remain open concerning the Hg compounds uptake mechanisms, Hg compounds transformations, cellular handling, and the role of biomolecules released by phytoplankton.

Several potential experiments could be carried out to better understand the MeHg hot spots production and better predict the long-term changes in Hg bioavailability to food web in these specific spots. The main experiments would be:

(1) The identification of the major phytoplankton and zooplankton species in two different eutrophic freshwater and seawater MeHg hot spots production ecosystems.

(2) The incubation of isotopically enriched Hg compounds separately and together with the phytoplankton and zooplankton assemblage collected from those freshwater and seawater environments.

(3) The incubation of isotopically enriched Hg compounds in isolate phytoplankton strains and zooplankton species representatives from these particular freshwater and seawater ecosystems.

(4) The incubation of Hg compounds in the phytoplankton assemblage and subsequent the exposure of zooplankton in the same culture batch to address the potential trophic transfer in both studied freshwater and seawater ecosystems.

The final goal of this approach would be to correlate the findings by the combination of *in situ* field sampling campaigns, and laboratory experiments. Moreover, several climate change scenarios at a global scale can be carried out in the laboratory by changing the temperature, nutrients, and other potential physicochemical parameters in order to understand the potential long-term changes in Hg bioavailability to food webs in freshwater and seawater ecosystems. Given the interconnection between biogeochemical Hg cycle and global change, the combination of *in situ* field sampling campaigns and laboratory experiments are crucial for a better understanding of the Hg compounds bioaccumulation and transformation processes in combination with the development of mechanistic models coupling Hg transport, primary production under various climate change scenarios at a global scale.

Application to other field of research: metabolic studies.

The uptake, distribution, and elimination of other essential and toxic elements (e.g., metals, inorganic compounds or organic compounds labelled in ^{2}H, ^{13}C ^{34}S, ^{18}O or ^{15}N among others) in living organisms can be investigated using isotopically enriched tracers. As opposed to radioactive tracers, stable tracers can be administered safely to any subject including living organisms in which the isotope composition of the element or organic compounds is determined by mass spectrometric techniques. Additionally, single, and double incubations can be carried out. As a result, more meaningful results could be achieved using double or triple incubations approach as it was performed in **Chapter 2.3**.

Whatever the application field and the method selected for the incorporation of the tracer to the organisms, samples must be collected at regular intervals (time scale) to study the isotope composition of the element. This allows assessing two important parameters: the evolution of

the total concentration of the element and the ratio between the enriched isotope and natural abundance element. In case, several species of the same element are quantified, and potential interconversion processes might have occurred, a chromatography separation before the detection must be performed to determine the species-specific concentration of the element. Therefore, the sample must be spiked with other enriched isotopes (corresponding to each species) to perform isotope dilution analysis based on IPD as described in **Chapter 2.1**. If no interconversion processes or incomplete recoveries were demonstrated to occur during the same preparation, the determination of species-specific concentration (enriched + natural) can be obtained by applying IPD in combination with a methodological calibration as described in **Chapter 2.2**. The number of isotopes and number of species of the element limit these potential approaches.

References.

Abad, S. Q. (2019). DETERMINACIÓN DE LA CONCENTRACIÓN Y EL FRACCIONAMIENTO ISOTÓPICO DE ESPECIES DE MERCURIO EN MUESTRAS BIOLÓGICAS MEDIANTE EL ACOPLAMIENTO DE LA CROMATOGRAFÍA DE GASES A DISTINTOS ESPECTRÓMETROS DE MASAS.

Achá, D., Pabón, C. A., & Hintelmann, H. (2012). Mercury methylation and hydrogen sulfide production among unexpected strains isolated from periphyton of two macrophytes of the Amazon. FEMS Microbiology Ecology, 80(3), 637–645. https://doi.org/10.1111/j.1574-6941.2012.01333.x

Adediran, G. A., Liem-Nguyen, V., Song, Y., Schaefer, J. K., Skyllberg, U., & Björn, E. (2019). Microbial Biosynthesis of Thiol Compounds: Implications for Speciation, Cellular Uptake, and Methylation of Hg(II). Environmental Science & Technology, 53(14), 8187–8196. https://doi.org/10.1021/acs.est.9b01502

Aguilera, A., & Amils, R. (2005). Tolerance to cadmium in sp. (Chlorophyta) strains isolated from an extreme acidic environment, the Tinto River (SW, Spain). Aquatic Toxicology, 75(4), 316–329. https://doi.org/10.1016/j.aquatox.2005.09.002

Ahner, B., Wei, L., Oleson, J., & Ogura, N. (2002). Glutathione and other low molecular weight thiols in marine phytoplankton under metal stress. Marine Ecology Progress Series, 232, 93–103. https://doi.org/10.3354/meps232093

Alanoca, L., Amouroux, D., Monperrus, M., Tessier, E., Goni, M., Guyoneaud, R., Acha, D., Gassie, C., Audry, S., Garcia, M. E., Quintanilla, J., & Point, D. (2016). Diurnal variability and biogeochemical reactivity of mercury species in an extreme high-altitude lake ecosystem of the Bolivian Altiplano. Environmental Science and Pollution Research, 23(7), 6919–6933. https://doi.org/10.1007/s11356-015-5917-1

AlChoubassi, G., Aszyk, J., Pisarek, P., Bierla, K., Ouerdane, L., Szpunar, J., & Lobinski, R. (2018). Advances in mass spectrometry for iron speciation in plants. TrAC Trends in Analytical Chemistry, 104, 77–86. https://doi.org/10.1016/j.trac.2017.11.006

Alonso, J. I. G., & Rodriguez-González, P. (2013). Isotope Dilution Mass Spectrometry. Royal Society of Chemistry. https://books.google.fr/books?id=6LM1DQUnf4wC

Amos, H. M., Jacob, D. J., Streets, D. G., & Sunderland, E. M. (2013). Legacy impacts of all-time anthropogenic emissions on the global mercury cycle: GLOBAL IMPACTS OF LEGACY MERCURY. Global Biogeochemical Cycles, 27(2), 410–421. https://doi.org/10.1002/gbc.20040

Amyot, M., Gill, G. A., & Morel, F. M. M. (1997). Production and Loss of Dissolved Gaseous Mercury in Coastal Seawater. Environmental Science & Technology, 31(12), 3606–3611. https://doi.org/10.1021/es9703685

Bank, M.S. (2012). Mercury in the Environment: Pattern and Process. University of California Press. 10.1525/california/9780520271630.001.0001

Barkay, T., & Gu, B. (2021). Demethylation–The Other Side of the Mercury Methylation Coin: A Critical Review. ACS Environmental Au, acsenvironau.1c00022. https://doi.org/10.1021/acsenvironau.1c00022

Barkay, T., & Wagner-Döbler, I. (2005). Microbial Transformations of Mercury: Potentials, Challenges, and Achievements in Controlling Mercury Toxicity in the Environment. In Advances in Applied Microbiology (Vol. 57, pp. 1–52). Elsevier. https://doi.org/10.1016/S0065-2164(05)57001-1

Beauvais-Flück, R., Slaveykova, V., & Cosio, C. (2018). Molecular Effects of Inorganic and Methyl Mercury in Aquatic Primary Producers: Comparing Impact to A Macrophyte and A Green Microalga in Controlled Conditions. Geosciences, 8(11), 393. https://doi.org/10.3390/geosciences8110393

Beauvais-Flück, R., Slaveykova, V. I., & Cosio, C. (2016). Transcriptomic and Physiological Responses of the Green Microalga Chlamydomonas reinhardtii during Short-Term Exposure to Subnanomolar Methylmercury Concentrations. Environmental Science & Technology, 50(13), 7126–7134. https://doi.org/10.1021/acs.est.6b00403

Beauvais-Flück, R., Slaveykova, V. I., & Cosio, C. (2017). Cellular toxicity pathways of inorganic and methyl mercury in the green microalga Chlamydomonas reinhardtii. Scientific Reports, 7(1), 8034. https://doi.org/10.1038/s41598-017-08515-8

Bellini, E., Varotto, C., Borsò, M., Rugnini, L., Bruno, L., & Sanità di Toppi, L. (2020). Eukaryotic and Prokaryotic Phytochelatin Synthases Differ Less in Functional Terms Than Previously Thought: A Comparative Analysis of Marchantia polymorpha and Geitlerinema sp. PCC 7407. Plants, 9(7), 914. https://doi.org/10.3390/plants9070914

Bishop, K., Shanley, J. B., Riscassi, A., de Wit, H. A., Eklöf, K., Meng, B., Mitchell, C., Osterwalder, S., Schuster, P. F., Webster, J., & Zhu, W. (2020). Recent advances in understanding and measurement of mercury in the environment: Terrestrial Hg cycling. Science of The Total Environment, 721, 137647. https://doi.org/10.1016/j.scitotenv.2020.137647

Björn, E., Larsson, T., Lambertsson, L., Skyllberg, U., & Frech, W. (2007). Recent Advances in Mercury Speciation Analysis with Focus on Spectrometric Methods and Enriched Stable Isotope Applications. Ambio, 36(6,), 443–451. http://www.jstor.org/stable/25547793

Blanck, H. (2002). A Critical Review of Procedures and Approaches Used for Assessing Pollution-Induced Community Tolerance (PICT) in Biotic Communities. Human and Ecological Risk Assessment: An International Journal, 8(5), 1003–1034. https://doi.org/10.1080/1080-700291905792

Blum, J. D., Sherman, L. S., & Johnson, M. W. (2014). Mercury Isotopes in Earth and Environmental Sciences. Annual Review of Earth and Planetary Sciences, 42(1), 249–269. https://doi.org/10.1146/annurev-earth-050212-124107

Bouchet, S., & Björn, E. (2014). Analytical developments for the determination of monomethylmercury complexes with low molecular mass thiols by reverse phase liquid chromatography hyphenated to inductively coupled plasma mass spectrometry. Journal of Chromatography A, 1339, 50–58. https://doi.org/10.1016/j.chroma.2014.02.045

Bouchet, S., Goñi-Urriza, M., Monperrus, M., Guyoneaud, R., Fernandez, P., Heredia, C., Tessier, E., Gassie, C., Point, D., Guédron, S., Achá, D., & Amouroux, D. (2018). Linking Microbial Activities and Low-Molecular-Weight Thiols to Hg Methylation in Biofilms and Periphyton from High-Altitude Tropical Lakes in the Bolivian Altiplano. Environmental Science & Technology, 52(17), 9758–9767. https://doi.org/10.1021/acs.est.8b01885

Bouchet, S., Rodriguez-Gonzalez, P., Bridou, R., Monperrus, M., Tessier, E., Anschutz, P., Guyoneaud, R., & Amouroux, D. (2013). Investigations into the differential reactivity of endogenous and exogenous mercury species in coastal sediments. Environmental Science and Pollution Research, 20(3), 1292–1301. https://doi.org/10.1007/s11356-012-1068-9

Bouchet, S., Tessier, E., Masbou, J., Point, D., Lazzaro, X., Monperrus, M., Guédron, S., Acha, D., & Amouroux, D. (2022). In Situ Photochemical Transformation of Hg Species and Associated Isotopic Fractionation in the Water Column of High-Altitude Lakes from the Bolivian Altiplano. Environmental Science & Technology, 56(4), 2258–2268. https://doi.org/10.1021/acs.est.1c04704

Bouraï, L., Logez, M., Laplace-Treyture, C., & Argillier, C. (2020). How Do Eutrophication and Temperature Interact to Shape the Community Structures of Phytoplankton and Fish in Lakes? Water, 12(3), 779. https://doi.org/10.3390/w12030779

Boyd, E. S., & Barkay, T. (2012). The Mercury Resistance Operon: From an Origin in a Geothermal Environment to an Efficient Detoxification Machine. Frontiers in Microbiology, 3. https://doi.org/10.3389/fmicb.2012.00349

Branfireun, B. A., Cosio, C., Poulain, A. J., Riise, G., & Bravo, A. G. (2020). Mercury cycling in freshwater systems—An updated conceptual model. Science of The Total Environment, 745, 140906. https://doi.org/10.1016/j.scitotenv.2020.140906

Bravo, A. G., Bouchet, S., Tolu, J., Björn, E., Mateos-Rivera, A., & Bertilsson, S. (2017). Molecular composition of organic matter controls methylmercury formation in boreal lakes. Nature Communications, 8(1), 14255. https://doi.org/10.1038/ncomms14255

Bravo, A. G., Le Faucheur, S., Monperrus, M., Amouroux, D., & Slaveykova, V. I. (2014). Species-specific isotope tracers to study the accumulation and biotransformation of mixtures of inorganic and methyl mercury by the microalga Chlamydomonas reinhardtii. Environmental Pollution, 192, 212–215. https://doi.org/10.1016/j.envpol.2014.05.013

Bridou, R., Monperrus, M., Gonzalez, P. R., Guyoneaud, R., & Amouroux, D. (2011). Simultaneous determination of mercury methylation and demethylation capacities of various sulfate-reducing bacteria using species-specific isotopic tracers. Environmental Toxicology and Chemistry, 30(2), 337–344. https://doi.org/10.1002/etc.395

Cameron, J. C., & Pakrasi, H. B. (2010). Essential Role of Glutathione in Acclimation to Environmental and Redox Perturbations in the Cyanobacterium Synechocystis sp. PCC 6803. Plant Physiology, 154(4), 1672–1685. https://doi.org/10.1104/pp.110.162990

Campbell, P. G. C., Errécalde, O., Fortin, C., Hiriart-Baer, V. P., & Vigneault, B. (2002). Metal bioavailability to phytoplankton—Applicability of the biotic ligand model. Comparative Biochemistry and Physiology Part C: Toxicology & Pharmacology, 133(1–2), 189–206. https://doi.org/10.1016/S1532-0456(02)00104-7

Cassier-Chauvat, C. (2014). Responses to Oxidative and Heavy Metal Stresses in Cyanobacteria: Recent Advances. International Journal of Molecular Sciences, 16(1), 871–886. https://doi.org/10.3390/ijms16010871

Castillo, Á., Rodríguez-González, P., Centineo, G., Roig-Navarro, A. F., & Alonso, J. I. G. (2010). Multiple Spiking Species-Specific Isotope Dilution Analysis by Molecular Mass Spectrometry: Simultaneous Determination of Inorganic Mercury and Methylmercury in Fish Tissues. Analytical Chemistry, 82(7), 2773–2783. https://doi.org/10.1021/ac9027033

Chapra, S. C., Boehlert, B., Fant, C., Bierman, V. J., Henderson, J., Mills, D., Mas, D. M. L., Rennels, L., Jantarasami, L., Martinich, J., Strzepek, K. M., & Paerl, H. W. (2017). Climate Change Impacts on Harmful Algal Blooms in U.S. Freshwaters: A Screening-Level Assessment. Environmental Science & Technology, 51(16), 8933–8943. https://doi.org/10.1021/acs.est.7b01498

Chen, B., Wang, T., Yin, Y., He, B., & Jiang, G. (2007). Methylation of inorganic mercury by methylcobalamin in aquatic systems. Applied Organometallic Chemistry, 21(6), 462–467. https://doi.org/10.1002/aoc.1221

Chen, C. Y., & Folt, C. L. (2005). High Plankton Densities Reduce Mercury Biomagnification. Environmental Science & Technology, 39(1), 115–121. https://doi.org/10.1021/es0403007

Chen, L., Yang, L., & Wang, Q. (2009). In vivo phytochelatins and Hg–phytochelatin complexes in Hg-stressed Brassica chinensis L. Metallomics, 1(1), 101–106. https://doi.org/10.1039/B815477E

Chételat, J., Ackerman, J. T., Eagles-Smith, C. A., & Hebert, C. E. (2020). Methylmercury exposure in wildlife: A review of the ecological and physiological processes affecting contaminant concentrations and their interpretation. Science of The Total Environment, 711, 135117. https://doi.org/10.1016/j.scitotenv.2019.135117

Clarkson, T. W., & Magos, L. (2006). The Toxicology of Mercury and Its Chemical Compounds. Critical Reviews in Toxicology, 36(8), 609–662. https://doi.org/10.1080/10408440600845619

Clémens, S., Monperrus, M., Donard, O. F. X., Amouroux, D., & Guérin, T. (2011). Mercury speciation analysis in seafood by species-specific isotope dilution: Method validation and occurrence data. Analytical and Bioanalytical Chemistry, 401(9), 2699–2711. https://doi.org/10.1007/s00216-011-5040-1

Clémens, S., Monperrus, M., Donard, O. F. X., Amouroux, D., & Guérin, T. (2012). Mercury speciation in seafood using isotope dilution analysis: A review. Talanta, 89, 12–20. https://doi.org/10.1016/j.talanta.2011.12.064

Colombo, M. J., Ha, J., Reinfelder, J. R., Barkay, T., & Yee, N. (2014). Oxidation of Hg(0) to Hg(II) by diverse anaerobic bacteria. Chemical Geology, 363, 334–340. https://doi.org/10.1016/j.chemgeo.2013.11.020

Cossa, D., Averty, B., & Pirrone, N. (2009). The origin of methylmercury in open Mediterranean waters. Limnology and Oceanography, 54(3), 837–844. https://doi.org/10.4319/lo.2009.54.3.0837

Cossart, T., Garcia-Calleja, J., Worms, I. A. M., Tessier, E., Kavanagh, K., Pedrero, Z., Amouroux, D., & Slaveykova, V. I. (2021). Species-specific isotope tracking of mercury uptake and transformations by pico-nanoplankton in an eutrophic lake. Environmental Pollution, 288, 117771. https://doi.org/10.1016/j.envpol.2021.117771

Cossart, Thibaut & Garcia-Calleja, Javier & Santos P. Joao, Lotfti Kalahroodi, Elaheh, Worms, Isabelle, Pedrero Zayas, Zoyne, Amouroux, David, & Slaveykova Vera. (2022). Role of phytoplankton in aquatic mercury speciation and transformations. Environmental Chemistry.

Craig, P. J. (Ed.). (1986). Organometallic compounds in the environment: Principles and reactions (1. publ). Longman.

Dranguet, P., Flück, R., Regier, N., Cosio, C., Le Faucheur, S., & Slaveykova, V. I. (2014). Towards Mechanistic Understanding of Mercury Availability and Toxicity to Aquatic Primary Producers. CHIMIA International Journal for Chemistry, 68(11), 799–805. https://doi.org/10.2533/chimia.2014.799

Drott, A., Lambertsson, L., Björn, E., & Skyllberg, U. (2008a). Do Potential Methylation Rates Reflect Accumulated Methyl Mercury in Contaminated Sediments? Environmental Science & Technology, 42(1), 153–158. https://doi.org/10.1021/es0715851

Drott, A., Lambertsson, L., Björn, E., & Skyllberg, U. (2008b). Potential demethylation rate determinations in relation to concentrations of MeHg, Hg and pore water speciation of MeHg in contaminated sediments. Marine Chemistry, 112(1–2), 93–101. https://doi.org/10.1016/j.marchem.2008.07.002

Duval, B. D. Y. (2021). Ecodynamics of metals and metalloids in Pyrenean lakes in relation to climate change and anthropogenic pressure.

Echeveste, P., Tovar-Sánchez, A., & Agustí, S. (2014). Tolerance of polar phytoplankton communities to metals. Environmental Pollution, 185, 188–195. https://doi.org/10.1016/j.envpol.2013.10.029

Elbaz, A., Wei, Y. Y., Meng, Q., Zheng, Q., & Yang, Z. M. (2010). Mercury-induced oxidative stress and impact on antioxidant enzymes in Chlamydomonas reinhardtii. Ecotoxicology, 19(7), 1285–1293. https://doi.org/10.1007/s10646-010-0514-z

Finlay, B. (2002). Hypothesis: The Rate and Scale of Dispersal of Freshwater Diatom Species is a Function of their Global Abundance. Protist, 153(3), 261–273. https://doi.org/10.1078/1434-4610-00103

Fitzgerald, W. F., Lamborg, C. H., & Hammerschmidt, C. R. (2007). Marine Biogeochemical Cycling of Mercury. Chemical Reviews, 107(2), 641–662. https://doi.org/10.1021/cr050353m

Freire-Nordi, C. S., Vieira, A. A. H., & Nascimento, O. R. (2005). The metal binding capacity of Anabaena spiroides extracellular polysaccharide: An EPR study. Process Biochemistry, 40(6), 2215–2224. https://doi.org/10.1016/j.procbio.2004.09.003

Gaffney, J., & Marley, N. (2014). In-depth review of atmospheric mercury: Sources, transformations, and potential sinks. Energy and Emission Control Technologies, 1. https://doi.org/10.2147/EECT.S37038

Garcia-Calleja, J., Cossart, T., Pedrero, Z., Santos, J. P., Ouerdane, L., Tessier, E., Slaveykova, V. I., & Amouroux, D. (2021). Determination of the Intracellular Complexation of Inorganic and Methylmercury in Cyanobacterium Synechocystis sp. PCC 6803. Environmental Science, 9.

García-Sevillano, M. Á., García-Barrera, T., Navarro, F., Gailer, J., & Gómez-Ariza, J. L. (2014). Use of elemental and molecular-mass spectrometry to assess the toxicological effects of inorganic mercury in the mouse Mus musculus. Analytical and Bioanalytical Chemistry, 406(24), 5853–5865. https://doi.org/10.1007/s00216-014-8010-6

Gascón Díez, E., Loizeau, J.-L., Cosio, C., Bouchet, S., Adatte, T., Amouroux, D., & Bravo, A. G. (2016). Role of Settling Particles on Mercury Methylation in the Oxic Water Column of Freshwater Systems. Environmental Science & Technology, 50(21), 11672–11679. https://doi.org/10.1021/acs.est.6b03260

Gechev, T. S., Van Breusegem, F., Stone, J. M., Denev, I., & Laloi, C. (2006). Reactive oxygen species as signals that modulate plant stress responses and programmed cell death. BioEssays, 28(11), 1091–1101. https://doi.org/10.1002/bies.20493

Gilmour, C. C., Bullock, A. L., McBurney, A., Podar, M., & Elias, D. A. (2018). Robust Mercury Methylation across Diverse Methanogenic Archaea. MBio, 9(2). https://doi.org/10.1128/mBio.02403-17

Gilmour, C. C., Elias, D. A., Kucken, A. M., Brown, S. D., Palumbo, A. V., Schadt, C. W., & Wall, J. D. (2011). Sulfate-Reducing Bacterium Desulfovibrio desulfuricans ND132 as a Model for Understanding Bacterial Mercury Methylation. Applied and Environmental Microbiology, 77(12), 3938–3951. https://doi.org/10.1128/AEM.02993-10

Gilmour, C. C., Henry, E. A., & Mitchell, R. (1992). Sulfate stimulation of mercury methylation in freshwater sediments. Environmental Science & Technology, 26(11), 2281–2287. https://doi.org/10.1021/es00035a029

Gómez-Jacinto, V., García-Barrera, T., Gómez-Ariza, J. L., Garbayo-Nores, I., & Vílchez-Lobato, C. (2015). Elucidation of the defence mechanism in microalgae Chlorella sorokiniana under mercury exposure. Identification of Hg–phytochelatins. Chemico-Biological Interactions, 238, 82–90. https://doi.org/10.1016/j.cbi.2015.06.013

Gorski, P. R., Armstrong, D. E., Hurley, J. P., & Krabbenhoft, D. P. (2008). Influence of natural dissolved organic carbon on the bioavailability of mercury to a freshwater alga. Environmental Pollution, 154(1), 116–123. https://doi.org/10.1016/j.envpol.2007.12.004

Gosnell, K. J., Dam, H. G., & Mason, R. P. (2021). Mercury and methylmercury uptake and trophic transfer from marine diatoms to copepods and field collected zooplankton. Marine Environmental Research, 170, 105446. https://doi.org/10.1016/j.marenvres.2021.105446

Graham, A. M., Aiken, G. R., & Gilmour, C. C. (2012). Dissolved Organic Matter Enhances Microbial Mercury Methylation Under Sulfidic Conditions. Environmental Science & Technology, 46(5), 2715–2723. https://doi.org/10.1021/es203658f

Graham, A. M., Aiken, G. R., & Gilmour, C. C. (2013). Effect of Dissolved Organic Matter Source and Character on Microbial Hg Methylation in Hg–S–DOM Solutions. Environmental Science & Technology, 47(11), 5746–5754. https://doi.org/10.1021/es400414a

Grégoire, D. S., & Poulain, A. J. (2014). A little bit of light goes a long way: The role of phototrophs on mercury cycling. Metallomics, 6(3), 396. https://doi.org/10.1039/c3mt00312d

Grégoire, D. S., & Poulain, A. J. (2016). A physiological role for HgII during phototrophic growth. Nature Geoscience, 9(2), 121–125. https://doi.org/10.1038/ngeo2629

Gworek, B., Dmuchowski, W., & Baczewska-Dąbrowska, A. H. (2020). Mercury in the terrestrial environment: A review. Environmental Sciences Europe, 32(1), 128. https://doi.org/10.1186/s12302-020-00401-x

Hall, J. L. (2002). Cellular mechanisms for heavy metal detoxification and tolerance. Journal of Experimental Botany, 53(366), 1–11. http://www.jstor.org/stable/23697260

Hamelin, S., Amyot, M., Barkay, T., Wang, Y., & Planas, D. (2011). Methanogens: Principal Methylators of Mercury in Lake Periphyton. Environmental Science & Technology, 45(18), 7693–7700. https://doi.org/10.1021/es2010072

Hamelin, S., Planas, D., & Amyot, M. (2015). Mercury methylation and demethylation by periphyton biofilms and their host in a fluvial wetland of the St. Lawrence River (QC, Canada). Science of The Total Environment, 512–513, 464–471. https://doi.org/10.1016/j.scitotenv.2015.01.040

Hammerschmidt, C. R., & Fitzgerald, W. F. (2006a). Photodecomposition of Methylmercury in an Arctic Alaskan Lake. Environmental Science & Technology, 40(4), 1212–1216. https://doi.org/10.1021/es0513234

Hammerschmidt, C. R., & Fitzgerald, W. F. (2006b). Bioaccumulation and Trophic Transfer of Methylmercury in Long Island Sound. Archives of Environmental Contamination and Toxicology, 51(3), 416–424. https://doi.org/10.1007/s00244-005-0265-7

Harada, M. (1995). Minamata Disease: Methylmercury Poisoning in Japan Caused by Environmental Pollution. Critical Reviews in Toxicology, 25(1), 1–24. https://doi.org/10.3109/10408449509089885

Hawes, I. (1990). Eutrophication and Vegetation Development in Maritime Antarctic Lakes. In K. R. Kerry & G. Hempel (Eds.), Antarctic Ecosystems (pp. 83–90). Springer Berlin Heidelberg. https://doi.org/10.1007/978-3-642-84074-6_8

He, F., Zheng, W., Liang, L., & Gu, B. (2012). Mercury photolytic transformation affected by low-molecular-weight natural organics in water. Science of The Total Environment, 416, 429–435. https://doi.org/10.1016/j.scitotenv.2011.11.081

H.Hintelmann, R . D O U G L A S EVANS, & A N I C E Y . V I L L E N E U V E. (1995). Measurement of Mercury Methylation in Sediments by Using Enriched Stable Mercury Isotopes Combined with Methy mercury Determinat ion by Gas Chromatography-Inductively Coupled Plasma Mass Spectrometry.

Hintelmann, H., & Evans, R. D. (1997). Application of stable isotopes in environmental tracer studies—Measurement of monomethylmercury (CH 3 Hg +) by isotope dilution ICP-MS and detection of species transformation. Fresenius' Journal of Analytical Chemistry, 358(3), 378–385. https://doi.org/10.1007/s002160050433

Hintelmann, H., Keppel-Jones, K., & Evans, R. D. (2000). Constants of mercury methylation and demethylation rates in sediments and comparison of tracer and ambient mercury availability. Environmental Toxicology and Chemistry, 19(9), 2204–2211. https://doi.org/10.1002/etc.5620190909

Holmes, C. D., Jacob, D. J., Corbitt, E. S., Mao, J., Yang, X., Talbot, R., & Slemr, F. (2010). Global atmospheric model for mercury including oxidation by bromine atoms. Atmospheric Chemistry and Physics, 10(24), 12037–12057. https://doi.org/10.5194/acp-10-12037-2010

Huo, D. & H.M. Kingston. (2000). Correction of Species Transformations in the Analysis of Cr(VI) in Solid Environmental Samples Using Speciated Isotope Dilution Mass Spectrometry. 8.

Iglesia-Turiño, S., Febrero, A., Jauregui, O., Caldelas, C., Araus, J. L., & Bort, J. (2006). Detection and Quantification of Unbound Phytochelatin 2 in Plant Extracts of Brassica napus Grown with Different Levels of Mercury. Plant Physiology, 142(2), 742–749. https://doi.org/10.1104/pp.106.085068

Imlay, J. A. (2013). The molecular mechanisms and physiological consequences of oxidative stress: Lessons from a model bacterium. Nature Reviews Microbiology, 11(7), 443–454. https://doi.org/10.1038/nrmicro3032

Jerry M. Parks, Alexander Johs, Mircea Podar, Romain Bridou, Richard A. Hurt, Steven D. Smith, Stephen J. Tomanicek, Yun Qian, Steven D. Brown, Craig C. Brandt, Anthony V. Palumbo, Jeremy C. Smith, Judy D. Wall, Dwayne A. Elias, & Liyuan Liang. (2013). The Genetic Basis for Bacterial Mercury Methylation. Sciencexpress.

Jones, D. S., Walker, G. M., Johnson, N. W., Mitchell, C. P. J., Coleman Wasik, J. K., & Bailey, J. V. (2019). Molecular evidence for novel mercury methylating microorganisms in sulfate-impacted lakes. The ISME Journal, 13(7), 1659–1675. https://doi.org/10.1038/s41396-019-0376-1

Jonsson, S., Skyllberg, U., Nilsson, M. B., Lundberg, E., Andersson, A., & Björn, E. (2014). Differentiated availability of geochemical mercury pools controls methylmercury levels in estuarine sediment and biota. Nature Communications, 5(1), 4624. https://doi.org/10.1038/ncomms5624

Karimi, R., Chen, C. Y., Pickhardt, P. C., Fisher, N. S., & Folt, C. L. (2007). Stoichiometric controls of mercury dilution by growth. Proceedings of the National Academy of Sciences, 104(18), 7477–7482. https://doi.org/10.1073/pnas.0611261104

Kawakami, S. K., Gledhill, M., & Achterberg, E. P. (2006a). Effects of Metal Combinations on the Production of Phytochelatins and Glutathione by the Marine Diatom Phaeodactylum tricornutum. BioMetals, 19(1), 51–60. https://doi.org/10.1007/s10534-005-5115-6

Kawakami, S. K., Gledhill, M., & Achterberg, E. P. (2006b). PRODUCTION OF PHYTOCHELATINS AND GLUTATHIONE BY MARINE PHYTOPLANKTON IN RESPONSE TO METAL STRESS. Journal of Phycology, 42(5), 975–989. https://doi.org/10.1111/j.1529-8817.2006.00265.x

Kelly, D. J. A., Budd, K., & Lefebvre, D. D. (2006). Biotransformation of mercury in pH-stat cultures of eukaryotic freshwater algae. Archives of Microbiology, 187(1), 45–53. https://doi.org/10.1007/s00203-006-0170-0

Klapstein, S. J., & O'Driscoll, N. J. (2018). Methylmercury Biogeochemistry in Freshwater Ecosystems: A Review Focusing on DOM and Photodemethylation. Bulletin of Environmental Contamination and Toxicology, 100(1), 14–25. https://doi.org/10.1007/s00128-017-2236-x

Klein, M., Ouerdane, L., Bueno, M., & Pannier, F. (2011). Identification in human urine and blood of a novel selenium metabolite, Se-methylselenoneine, a potential biomarker of metabolization in mammals of the naturally occurring selenoneine, by HPLC coupled to electrospray hybrid linear ion trap-orbital ion trap MS. Metallomics, 3(5), 513. https://doi.org/10.1039/c0mt00060d

Kováčik, J., Rotková, G., Bujdoš, M., Babula, P., Peterková, V., & Matúš, P. (2017). Ascorbic acid protects Coccomyxa subellipsoidea against metal toxicity through modulation of ROS/NO balance and metal uptake. Journal of Hazardous Materials, 339, 200–207. https://doi.org/10.1016/j.jhazmat.2017.06.035

Kragten, J. (1994). Tutorial review. Calculating standard deviations and confidence intervals with a universally applicable spreadsheet technique. The Analyst, 119(10), 2161. https://doi.org/10.1039/an9941902161

Krupp, E. M., Mestrot, A., Wielgus, J., Meharg, A. A., & Feldmann, J. (2009). The molecular form of mercury in biota: Identification of novel mercury peptide complexes in plants. Chemical Communications, 28, 4257. https://doi.org/10.1039/b823121d

Lalonde, J. D., Amyot, M., Kraepiel, A. M. L., & Morel, F. M. M. (2001). Photooxidation of Hg(0) in Artificial and Natural Waters. Environmental Science & Technology, 35(7), 1367–1372. https://doi.org/10.1021/es001408z

Lambertsson, L., Lundberg, E., Nilsson, M., & Frech, W. (2001). Applications of enriched stable isotope tracers in combination with isotope dilution GC-ICP-MS to study mercury species

transformation in sea sediments during in situ ethylation and determination. Journal of Analytical Atomic Spectrometry, 16(11), 1296–1301. https://doi.org/10.1039/b106878b

Lamborg, C. H., Hammerschmidt, C. R., Bowman, K. L., Swarr, G. J., Munson, K. M., Ohnemus, D. C., Lam, P. J., Heimbürger, L.-E., Rijkenberg, M. J. A., & Saito, M. A. (2014). A global ocean inventory of anthropogenic mercury based on water column measurements. Nature, 512(7512), 65–68. https://doi.org/10.1038/nature13563

Lanzillotta, E., Ceccarini, C., Ferrara, R., Dini, F., Frontini, F. P., & Banchetti, R. (2004). Importance of the biogenic organic matter in photo-formation of dissolved gaseous mercury in a culture of the marine diatom Chaetoceros sp. Science of The Total Environment, 318(1–3), 211–221. https://doi.org/10.1016/S0048-9697(03)00400-5

Latch, D. E., & McNeill, K. (2006). Microheterogeneity of Singlet Oxygen Distributions in Irradiated Humic Acid Solutions. Science, 311(5768), 1743–1747. https://doi.org/10.1126/science.1121636

Lavoie, M., Le Faucheur, S., Boullemant, A., Fortin, C., & Campbell, P. G. C. (2012). THE INFLUENCE OF pH ON ALGAL CELL MEMBRANE PERMEABILITY AND ITS IMPLICATIONS FOR THE UPTAKE OF LIPOPHILIC METAL COMPLEXES1: PH AND MEMBRANE PERMEABILITY. Journal of Phycology, 48(2), 293–302. https://doi.org/10.1111/j.1529-8817.2012.01126.x

Lavoie, M., Le Faucheur, S., Fortin, C., & Campbell, P. G. C. (2009). Cadmium detoxification strategies in two phytoplankton species: Metal binding by newly synthesized thiolated peptides and metal sequestration in granules. Aquatic Toxicology, 92(2), 65–75. https://doi.org/10.1016/j.aquatox.2008.12.007

Lavoie, M., Raven, J. A., Jones, O. A. H., & Qian, H. (2016). Energy cost of intracellular metal and metalloid detoxification in wild-type eukaryotic phytoplankton. Metallomics, 8(10), 1097–1109. https://doi.org/10.1039/C6MT00049E

Lázaro, W. L., Díez, S., Bravo, A. G., da Silva, C. J., Ignácio, Á. R. A., & Guimaraes, J. R. D. (2019). Cyanobacteria as regulators of methylmercury production in periphyton. Science of The Total Environment, 668, 723–729. https://doi.org/10.1016/j.scitotenv.2019.02.233

Lázaro, W. L., Guimarães, J. R. D., Ignácio, A. R. A., Da Silva, C. J., & Díez, S. (2013). Cyanobacteria enhance methylmercury production: A hypothesis tested in the periphyton of two lakes in the Pantanal floodplain, Brazil. Science of The Total Environment, 456–457, 231–238. https://doi.org/10.1016/j.scitotenv.2013.03.022

Lazinsky, D., & Sicko-Goad, L. (1990). Morphometric analysis of phosphate and chromium interactions in Cyclotella meneghiniana. Aquatic Toxicology, 16(2), 127–139. https://doi.org/10.1016/0166-445X(90)90082-Z

Le Faucheur, S., Campbell, P. G. C., Fortin, C., & Slaveykova, V. I. (2014). Interactions between mercury and phytoplankton: Speciation, bioavailability, and internal handling: Mercury-phytoplankton interactions. Environmental Toxicology and Chemistry, 33(6), 1211–1224. https://doi.org/10.1002/etc.2424

Le Faucheur, S., Tremblay, Y., Fortin, C., & Campbell, P. G. C. (2011). Acidification increases mercury uptake by a freshwater alga, Chlamydomonas reinhardtii. Environmental Chemistry, 8(6), 612. https://doi.org/10.1071/EN11006

Lee, C.-S., & Fisher, N. S. (2016). Methylmercury uptake by diverse marine phytoplankton. Limnology and Oceanography, 61(5), 1626–1639. https://doi.org/10.1002/lno.10318

Lefebvre, D. D., Kelly, D., & Budd, K. (2007). Biotransformation of Hg(II) by Cyanobacteria. Applied and Environmental Microbiology, 73(1), 243–249. https://doi.org/10.1128/AEM.01794-06

Lehnherr, I., & St. Louis, V. L. (2009). Importance of Ultraviolet Radiation in the Photodemethylation of Methylmercury in Freshwater Ecosystems. Environmental Science & Technology, 43(15), 5692–5698. https://doi.org/10.1021/es9002923

Lei, P., Zhang, J., Zhu, J., Tan, Q., Kwong, R. W. M., Pan, K., Jiang, T., Naderi, M., & Zhong, H. (2021). Algal Organic Matter Drives Methanogen-Mediated Methylmercury Production in Water from

Eutrophic Shallow Lakes. Environmental Science & Technology, 55(15), 10811–10820. https://doi.org/10.1021/acs.est.0c08395

Leopold, K., Foulkes, M., & Worsfold, P. (2010). Methods for the determination and speciation of mercury in natural waters—A review. Analytica Chimica Acta, 663(2), 127–138. https://doi.org/10.1016/j.aca.2010.01.048

Li, Y., Li, D., Song, B., & Li, Y. (2022). The potential of mercury methylation and demethylation by 15 species of marine microalgae. Water Research, 215, 118266. https://doi.org/10.1016/j.watres.2022.118266

Liberton, M., Page, L. E., O'Dell, W. B., O'Neill, H., Mamontov, E., Urban, V. S., & Pakrasi, H. B. (2013). Organization and Flexibility of Cyanobacterial Thylakoid Membranes Examined by Neutron Scattering. Journal of Biological Chemistry, 288(5), 3632–3640. https://doi.org/10.1074/jbc.M112.416933

Liem-Nguyen, V., Bouchet, S., & Björn, E. (2015). Determination of Sub-Nanomolar Levels of Low Molecular Mass Thiols in Natural Waters by Liquid Chromatography Tandem Mass Spectrometry after Derivatization with p-(Hydroxymercuri) Benzoate and Online Preconcentration. Analytical Chemistry, 87(2), 1089–1096. https://doi.org/10.1021/ac503679y

Liem-Nguyen, V., Huynh, K., Gallampois, C., & Björn, E. (2019). Determination of picomolar concentrations of thiol compounds in natural waters and biological samples by tandem mass spectrometry with online preconcentration and isotope-labeling derivatization. Analytica Chimica Acta, 1067, 71–78. https://doi.org/10.1016/j.aca.2019.03.035

Liem-Nguyen, V., Nguyen-Ngoc, H.-T., Adediran, G. A., & Björn, E. (2020). Determination of picomolar levels of methylmercury complexes with low molecular mass thiols by liquid chromatography tandem mass spectrometry and online preconcentration. Analytical and Bioanalytical Chemistry. https://doi.org/10.1007/s00216-020-02389-y

Liem-Nguyen, V., Skyllberg, U., & Björn, E. (2017). Thermodynamic Modeling of the Solubility and Chemical Speciation of Mercury and Methylmercury Driven by Organic Thiols and Micromolar Sulfide Concentrations in Boreal Wetland Soils. Environmental Science & Technology, 51(7), 3678–3686. https://doi.org/10.1021/acs.est.6b04622

Liem-Nguyen, V., Skyllberg, U., & Björn, E. (2021). Methylmercury formation in boreal wetlands in relation to chemical speciation of mercury(II) and concentration of low molecular mass thiols. Science of The Total Environment, 755, 142666. https://doi.org/10.1016/j.scitotenv.2020.142666

Lobinski, R., Becker, J. S., Haraguchi, H., & Sarkar, B. (2010). Metallomics: Guidelines for terminology and critical evaluation of analytical chemistry approaches (IUPAC Technical Report). Pure and Applied Chemistry, 82(2), 493–504. https://doi.org/10.1351/PAC-REP-09-03-04

Luengen, A. C., Fisher, N. S., & Bergamaschi, B. A. (2012). Dissolved organic matter reduces algal accumulation of methylmercury. Environmental Toxicology and Chemistry, 31(8), 1712–1719. https://doi.org/10.1002/etc.1885

Luo, H., Cheng, Q., & Pan, X. (2020). Photochemical behaviors of mercury (Hg) species in aquatic systems: A systematic review on reaction process, mechanism, and influencing factor. Science of The Total Environment, 720, 137540. https://doi.org/10.1016/j.scitotenv.2020.137540

Mangal, V., Phung, T., Nguyen, T. Q., & Guéguen, C. (2019). Molecular Characterization of Mercury Binding Ligands Released by Freshwater Algae Grown at Three Photoperiods. Frontiers in Environmental Science, 6. https://doi.org/10.3389/fenvs.2018.00155

Marteyn, B., Sakr, S., Farci, S., Bedhomme, M., Chardonnet, S., Decottignies, P., Lemaire, S. D., Cassier-Chauvat, C., & Chauvat, F. (2013). The Synechocystis PCC6803 MerA-Like Enzyme Operates in the Reduction of Both Mercury and Uranium under the Control of the Glutaredoxin 1 Enzyme. Journal of Bacteriology, 195(18), 4138–4145. https://doi.org/10.1128/JB.00272-13

Marvin-DiPasquale, M., Agee, J., McGowan, C., Oremland, R. S., Thomas, M., Krabbenhoft, D., & Gilmour, C. C. (2000). Methyl-Mercury Degradation Pathways: A Comparison among Three

Mercury-Impacted Ecosystems. Environmental Science & Technology, 34(23), 4908–4916. https://doi.org/10.1021/es0013125

Mason, R. P., Choi, A. L., Fitzgerald, W. F., Hammerschmidt, C. R., Lamborg, C. H., Soerensen, A. L., & Sunderland, E. M. (2012). Mercury biogeochemical cycling in the ocean and policy implications. Environmental Research, 119, 101–117. https://doi.org/10.1016/j.envres.2012.03.013

Mason, R. P., Reinfelder, J. R., & Morel, F. M. M. (1996). Uptake, Toxicity, and Trophic Transfer of Mercury in a Coastal Diatom. Environmental Science & Technology, 30(6), 1835–1845. https://doi.org/10.1021/es950373d

Mataloni, G., Tesolın, G., Sacullo, F., & Tell, G. (2000). Factors regulating summer phytoplankton in a highly eutrophic Antarctic lake. 8.

Meija, J., Yang, L., Caruso, J. A., & Mester, Z. (2006). Calculations of double spike isotope dilution results revisited. Journal of Analytical Atomic Spectrometry, 21(11), 1294. https://doi.org/10.1039/b607823k

Meister Alton, A. M. E. (1983). Glutathione. 52:711-760. https://doi.org/10.1146/annurev.bi.52.070183.003431

Monperrus, M., Krupp, E., Amouroux, D., Donard, O. F. X., & Rodríguez Martín-Doimeadios, R. C. (2004). Potential and limits of speciated isotope-dilution analysis for metrology and assessing environmental reactivity. TrAC Trends in Analytical Chemistry, 23(3), 261–272. https://doi.org/10.1016/S0165-9936(04)00313-9

Monperrus, M., Rodriguez Gonzalez, P., Amouroux, D., Garcia Alonso, J. I., & Donard, O. F. X. (2008). Evaluating the potential and limitations of double-spiking species-specific isotope dilution analysis for the accurate quantification of mercury species in different environmental matrices. Analytical and Bioanalytical Chemistry, 390(2), 655–666. https://doi.org/10.1007/s00216-007-1598-z

Monperrus, M., Tessier, E., Amouroux, D., Leynaert, A., Huonnic, P., & Donard, O. F. X. (2007). Mercury methylation, demethylation and reduction rates in coastal and marine surface waters of the

Mediterranean Sea. Marine Chemistry, 107(1), 49–63. https://doi.org/10.1016/j.marchem.2007.01.018

Morel, F. M. M., Kraepiel, A. M. L., & work(s):, M. A. R. (1998). The Chemical Cycle and Bioaccumulation of Mercury. Annual Review of Ecology and Systematics, 2, 543–566. http://www.jstor.org/stable/221718

Morelli, E., Ferrara, R., Bellini, B., Dini, F., Di Giuseppe, G., & Fantozzi, L. (2009). Changes in the non-protein thiol pool and production of dissolved gaseous mercury in the marine diatom Thalassiosira weissflogii under mercury exposure. Science of The Total Environment, 408(2), 286–293. https://doi.org/10.1016/j.scitotenv.2009.09.047

Narainsamy, K., Farci, S., Braun, E., Junot, C., Cassier-Chauvat, C., & Chauvat, F. (2016). Oxidative-stress detoxification and signalling in cyanobacteria: The crucial glutathione synthesis pathway supports the production of ergothioneine and ophthalmate: Ophthalmate an evolutionary-conserved stress marker. Molecular Microbiology, 100(1), 15–24. https://doi.org/10.1111/mmi.13296

Narainsamy, K., Marteyn, B., Sakr, S., Cassier-Chauvat, C., & Chauvat, F. (2013). Genomics of the Pleïotropic Glutathione System in Cyanobacteria. In Advances in Botanical Research (Vol. 65, pp. 157–188). Elsevier. https://doi.org/10.1016/B978-0-12-394313-2.00005-6

Navarrete, A., González, A., Gómez, M., Contreras, R. A., Díaz, P., Lobos, G., Brown, M. T., Sáez, C. A., & Moenne, A. (2019). Copper excess detoxification is mediated by a coordinated and complementary induction of glutathione, phytochelatins and metallothioneins in the green seaweed Ulva compressa. Plant Physiology and Biochemistry, 135, 423–431. https://doi.org/10.1016/j.plaphy.2018.11.019

Navarro, P., Clémens, S., Perrot, V., Bolliet, V., Tabouret, H., Guérin, T., Monperrus, M., & Amouroux, D. (2011). Simultaneous determination of mercury and butyltin species using a multiple species-specific isotope dilution methodology on the European, Anguilla anguilla glass eel and yellow eel. 19.

Naveed, S., Li, C., Lu, X., Chen, S., Yin, B., Zhang, C., & Ge, Y. (2019). Microalgal extracellular polymeric substances and their interactions with metal(loid)s: A review. Critical Reviews in Environmental Science and Technology, 49(19), 1769–1802. https://doi.org/10.1080/10643389.2019.1583052

Ndu, U., Mason, R. P., Zhang, H., Lin, S., & Visscher, P. T. (2012). Effect of Inorganic and Organic Ligands on the Bioavailability of Methylmercury as Determined by Using a mer-lux Bioreporter. Applied and Environmental Microbiology, 78(20), 7276–7282. https://doi.org/10.1128/AEM.00362-12

Nowicka, B. (2022). Heavy metal–induced stress in eukaryotic algae—Mechanisms of heavy metal toxicity and tolerance with particular emphasis on oxidative stress in exposed cells and the role of antioxidant response. Environmental Science and Pollution Research. https://doi.org/10.1007/s11356-021-18419-w

Oh, S., Kim, M.-K., Lee, Y.-M., & Zoh, K.-D. (2011). Effect of Abiotic and Biotic Factors on the Photo-Induced Production of Dissolved Gaseous Mercury. Water, Air, & Soil Pollution, 220(1–4), 353–363. https://doi.org/10.1007/s11270-011-0759-z

Ouerdane, L., Mester, Z., & Meija, J. (2009). General Equation for Multiple Spiking Isotope Dilution Mass Spectrometry. Analytical Chemistry, 81(12), 5075–5079. https://doi.org/10.1021/ac900205b

Pablo Rodrıguez-Gonzalez, Andres Rodrıguez-Cea, J. Ignacio Garcıa Alonso, & Alfredo Sanz-Medel. (2006). Species-specific isotope dilution analyisis and isotope pattern deconvolution for butyltincompounds metabolism investigations. 77. https://doi.org/10.1021/ac051091r

Paerl, H. W., & Paul, V. J. (2012). Climate change: Links to global expansion of harmful cyanobacteria. Water Research, 46(5), 1349–1363. https://doi.org/10.1016/j.watres.2011.08.002

Pandey, L. K., Han, T., & Gaur, J. P. (2015). Response of a phytoplanktonic assemblage to copper and zinc enrichment in microcosm. Ecotoxicology, 24(3), 573–582. https://doi.org/10.1007/s10646-014-1405-5

Pedrero, Z., Bridou, R., Mounicou, S., Guyoneaud, R., Monperrus, M., & Amouroux, D. (2012). Transformation, Localization, and Biomolecular Binding of Hg Species at Subcellular Level in Methylating and Nonmethylating Sulfate-Reducing Bacteria. Environmental Science & Technology, 46(21), 11744–11751. https://doi.org/10.1021/es302412q

Pedrero, Z., Mounicou, S., Monperrus, M., & Amouroux, D. (2011). Investigation of Hg species binding biomolecules in dolphin liver combining GC and LC-ICP-MS with isotopic tracers. J. Anal. At. Spectrom., 26(1), 187–194. https://doi.org/10.1039/C0JA00154F

Pedrero, Z., Ouerdane, L., Mounicou, S., Lobinski, R., Monperrus, M., & Amouroux, D. (2012). Identification of mercury and other metals complexes with metallothioneins in dolphin liver by hydrophilic interaction liquid chromatography with the parallel detection by ICP MS and electrospray hybrid linear/orbital trap MS/MS. Metallomics, 4(5), 473. https://doi.org/10.1039/c2mt00006g

Pedrero Zayas, Z., Ouerdane, L., Mounicou, S., Lobinski, R., Monperrus, M., & Amouroux, D. (2014). Hemoglobin as a major binding protein for methylmercury in white-sided dolphin liver. Analytical and Bioanalytical Chemistry, 406(4), 1121–1129. https://doi.org/10.1007/s00216-013-7274-6

Petersen, C. G. J. (1895). The yearly immigration of young plaice in the Limfjord from the German sea. Rept. Danish Biol. Sta., 6, 1–48.

Pickhardt, P. C., & Fisher, N. S. (2007). Accumulation of Inorganic and Methylmercury by Freshwater Phytoplankton in Two Contrasting Water Bodies. Environmental Science & Technology, 41(1), 125–131. https://doi.org/10.1021/es060966w

Pickhardt, P. C., Folt, C. L., Chen, C. Y., Klaue, B., & Blum, J. D. (2002). Algal blooms reduce the uptake of toxic methylmercury in freshwater food webs. Proceedings of the National Academy of Sciences, 99(7), 4419–4423. https://doi.org/10.1073/pnas.072531099

Pickhardt, P. C., Folt, C. L., Chen, C. Y., Klaue, B., & Blum, J. D. (2005). Impacts of zooplankton composition and algal enrichment on the accumulation of mercury in an experimental

freshwater food web. Science of The Total Environment, 339(1–3), 89–101. https://doi.org/10.1016/j.scitotenv.2004.07.025

Pirrone, N., Cinnirella, S., Feng, X., Finkelman, R. B., Friedli, H. R., Leaner, J., Mason, R., Mukherjee, A. B., Stracher, G. B., Streets, D. G., & Telmer, K. (2010). Global mercury emissions to the atmosphere from anthropogenic and natural sources. Atmospheric Chemistry and Physics, 10(13), 5951–5964. https://doi.org/10.5194/acp-10-5951-2010

Poulain, A. J., Amyot, M., Findlay, D., Telor, S., Barkay, T., & Hintelmann, H. (2004). Biological and photochemical production of dissolved gaseous mercury in a boreal lake. Limnology and Oceanography, 49(6), 2265–2275. https://doi.org/10.4319/lo.2004.49.6.2265

Pröfrock, D., & Prange, A. (2012). Inductively Coupled Plasma–Mass Spectrometry (ICP-MS) for Quantitative Analysis in Environmental and Life Sciences: A Review of Challenges, Solutions, and Trends. Applied Spectroscopy, 66(8), 843–868. https://doi.org/10.1366/12-06681

Qian, Y., Yin, X., Lin, H., Rao, B., Brooks, S. C., Liang, L., & Gu, B. (2014). Why Dissolved Organic Matter Enhances Photodegradation of Methylmercury. Environmental Science & Technology Letters, 1(10), 426–431. https://doi.org/10.1021/ez500254z

Quantities, Units and Symbols in Physical Chemistry, Third Edition. (2006). Chemistry International -- Newsmagazine for IUPAC, 28(1). https://doi.org/10.1515/ci.2006.28.1.28a

Rahman, G. M. M., & Kingston, H. M. 'Skip'. (2004). Application of Speciated Isotope Dilution Mass Spectrometry To Evaluate Extraction Methods for Determining Mercury Speciation in Soils and Sediments. Analytical Chemistry, 76(13), 3548–3555. https://doi.org/10.1021/ac030407x

Ranchou-Peyruse, M., Monperrus, M., Bridou, R., Duran, R., Amouroux, D., Salvado, J. C., & Guyoneaud, R. (2009). Overview of Mercury Methylation Capacities among Anaerobic Bacteria Including Representatives of the Sulphate-Reducers: Implications for Environmental Studies. Geomicrobiology Journal, 26(1), 1–8. https://doi.org/10.1080/01490450802599227

Ravichandran, M. (2004). Interactions between mercury and dissolved organic matter—a review. Chemosphere, 55(3), 319–331. https://doi.org/10.1016/j.chemosphere.2003.11.011

Regnell, O., & Watras, Carl. J. (2019). Microbial Mercury Methylation in Aquatic Environments: A Critical Review of Published Field and Laboratory Studies. Environmental Science & Technology, 53(1), 4–19. https://doi.org/10.1021/acs.est.8b02709

Reynolds, C. S. (2006). The Ecology of Phytoplankton. Cambridge University Press.

Rodriguez-Gonzalez, P., Bouchet, S., Monperrus, M., Tessier, E., & Amouroux, D. (2013). In situ experiments for element species-specific environmental reactivity of tin and mercury compounds using isotopic tracers and multiple linear regression. Environmental Science and Pollution Research, 20(3), 1269–1280. https://doi.org/10.1007/s11356-012-1019-5

Rodríguez-González, P., & García Alonso, J. I. (2010). Recent advances in isotope dilution analysis for elemental speciation. Journal of Analytical Atomic Spectrometry, 25(3), 239. https://doi.org/10.1039/b924261a

Rodríguez-González, P., Marchante-Gayón, J. M., García Alonso, J. I., & Sanz-Medel, A. (2005). Isotope dilution analysis for elemental speciation: A tutorial review. Spectrochimica Acta Part B: Atomic Spectroscopy, 60(2), 151–207. https://doi.org/10.1016/j.sab.2005.01.005

Rodríguez-González, P., Monperrus, M., García Alonso, J. I., Amouroux, D., & Donard, O. F. X. (2007). Comparison of different numerical approaches for multiple spiking species-specific isotope dilution analysis exemplified by the determination of butyltin species in sediments. Journal of Analytical Atomic Spectrometry, 22(11), 1373. https://doi.org/10.1039/b706542f

Rodríguez-González, P., Rodríguez-Cea, A., García Alonso, J. I., & Sanz-Medel, A. (2005). Species-Specific Isotope Dilution Analysis and Isotope Pattern Deconvolution for Butyltin Compounds Metabolism Investigations. Analytical Chemistry, 77(23), 7724–7734. https://doi.org/10.1021/ac051091r

Rodríguez Martín-Doimeadios, R. C., Tessier, E., Amouroux, D., Guyoneaud, R., Duran, R., Caumette, P., & Donard, O. F. X. (2004). Mercury methylation/demethylation and volatilization pathways in estuarine sediment slurries using species-specific enriched stable isotopes. Marine Chemistry, 90(1–4), 107–123. https://doi.org/10.1016/j.marchem.2004.02.022

Rodrıguez-Gonzalez, P., Encinar, J. R., Alonso, J. I. G., & Sanz-Medel, A. (2004). Development of a triple spike methodology for validation of butyltin compounds speciation analysis by isotope dilution mass spectrometry. J. Anal. At. Spectrom., 7.

Ruggiu, D., Luglie, A., Cattaneo, A., & Panzani, P. (1998). Paleoecological evidence for diatom response to metal pollution in Lake Orta (N. Italy). 13.

Ruiz Encinar, J., Rodriguez Gonzalez, P., García Alonso, J. I., & Sanz-Medel, A. (2002). Evaluation of Extraction Techniques for the Determination of Butyltin Compounds in Sediments Using Isotope Dilution-GC/ICPMS with ^{118}Sn and ^{119}Sn-Enriched Species. Analytical Chemistry, 74(1), 270–281. https://doi.org/10.1021/ac010551n

Sarma, T. A. (2012). Handbook of Cyanobacteria (0 ed.). CRC Press. https://doi.org/10.1201/b14316

Schaefer, J. K., Rocks, S. S., Zheng, W., Liang, L., Gu, B., & Morel, F. M. M. (2011). Active transport, substrate specificity, and methylation of Hg(II) in anaerobic bacteria. Proceedings of the National Academy of Sciences of the United States of America, 108(21), 8714–8719. Scopus. https://doi.org/10.1073/pnas.1105781108

Scheuhammer, A. M., Meyer, M. W., Sandheinrich, M. B., & Murray, M. W. (2007). Effects of Environmental Methylmercury on the Health of Wild Birds, Mammals, and Fish. AMBIO: A Journal of the Human Environment, 36(1), 12–19. https://doi.org/10.1579/0044-7447(2007)36[12:EOEMOT]2.0.CO;2

Selin, N. E. (2009). Global Biogeochemical Cycling of Mercury: A Review. Annual Review of Environment and Resources, 34(1), 43–63. https://doi.org/10.1146/annurev.environ.051308.084314

Seymour, J. R., Amin, S. A., Raina, J.-B., & Stocker, R. (2017). Zooming in on the phycosphere: The ecological interface for phytoplankton–bacteria relationships. Nature Microbiology, 2(7), 17065. https://doi.org/10.1038/nmicrobiol.2017.65

Sharif, A., Monperrus, M., Tessier, E., Bouchet, S., Pinaly, H., Rodriguez-Gonzalez, P., Maron, P., & Amouroux, D. (2014). Fate of mercury species in the coastal plume of the Adour River estuary

(Bay of Biscay, SW France). Science of The Total Environment, 496, 701–713. https://doi.org/10.1016/j.scitotenv.2014.06.116

Shehata, S. A., Lasheen, M. R., Kobbia, I. A., & Ali, G. H. (1999). Toxic Effect of Certain Metals Mixture on Some Physiological and Morphological Characteristics of Freshwater Algae. 17.

Si, L., & Ariya, P. A. (2011). Aqueous photoreduction of oxidized mercury species in presence of selected alkanethiols. Chemosphere, 84(8), 1079–1084. https://doi.org/10.1016/j.chemosphere.2011.04.061

Si, L., & Ariya, P. A. (2015). Photochemical reactions of divalent mercury with thioglycolic acid: Formation of mercuric sulfide particles. Chemosphere, 119, 467–472. https://doi.org/10.1016/j.chemosphere.2014.07.022

Siciliano, S. D., O'Driscoll, N. J., Tordon, R., Hill, J., Beauchamp, S., & Lean, D. R. S. (2005). Abiotic Production of Methylmercury by Solar Radiation. Environmental Science & Technology, 39(4), 1071–1077. https://doi.org/10.1021/es048707z

Singh, D. K., Lingaswamy, B., Koduru, T. N., Nagu, P. P., & Jogadhenu, P. S. S. (2019). A putative merR family transcription factor Slr0701 regulates mercury inducible expression of MerA in the cyanobacterium Synechocystis sp. PCC6803. MicrobiologyOpen, 8(9). https://doi.org/10.1002/mbo3.838

Skrobonja, A., Gojkovic, Z., Soerensen, A. L., Westlund, P.-O., Funk, C., & Björn, E. (2019). Uptake Kinetics of Methylmercury in a Freshwater Alga Exposed to Methylmercury Complexes with Environmentally Relevant Thiols. Environmental Science & Technology, acs.est.9b05164. https://doi.org/10.1021/acs.est.9b05164

Slaveykova, V. I., Majumdar, S., Regier, N., Li, W., & Keller, A. A. (2021). Metabolomic Responses of Green Alga Chlamydomonas reinhardtii Exposed to Sublethal Concentrations of Inorganic and Methylmercury. Environmental Science & Technology, acs.est.0c08416. https://doi.org/10.1021/acs.est.0c08416

Soerensen, A. L., Mason, R. P., Balcom, P. H., Jacob, D. J., Zhang, Y., Kuss, J., & Sunderland, E. M. (2014). Elemental Mercury Concentrations and Fluxes in the Tropical Atmosphere and Ocean. Environmental Science & Technology, 48(19), 11312–11319. https://doi.org/10.1021/es503109p

Soerensen, Anne. L., Schartup, A. T., Gustafsson, E., Gustafsson, B. G., Undeman, E., & Björn, E. (2016). Eutrophication Increases Phytoplankton Methylmercury Concentrations in a Coastal Sea—A Baltic Sea Case Study. Environmental Science & Technology, 50(21), 11787–11796. https://doi.org/10.1021/acs.est.6b02717

Song, Y., Adediran, G. A., Jiang, T., Hayama, S., Björn, E., & Skyllberg, U. (2020). Toward an Internally Consistent Model for Hg(II) Chemical Speciation Calculations in Bacterium–Natural Organic Matter–Low Molecular Mass Thiol Systems. Environmental Science & Technology, 54(13), 8094–8103. https://doi.org/10.1021/acs.est.0c01751

Song, Y., Jiang, T., Liem-Nguyen, V., Sparrman, T., Björn, E., & Skyllberg, U. (2018). Thermodynamics of Hg(II) Bonding to Thiol Groups in Suwannee River Natural Organic Matter Resolved by Competitive Ligand Exchange, Hg L_{III} -Edge EXAFS and ^{1}H NMR Spectroscopy. Environmental Science & Technology, 52(15), 8292–8301. https://doi.org/10.1021/acs.est.8b00919

Stanier, R. Y., Deruelles, J., Rippka, R., Herdman, M., & Waterbury, J. B. (1979). Generic Assignments, Strain Histories and Properties of Pure Cultures of Cyanobacteria. Journal of General Microbiology, 111(1), 1–61. https://doi.org/10.1099/00221287-111-1-1

Stein, E. D., Cohen, Y., & Winer, A. M. (1996). Environmental distribution and transformation of mercury compounds. Critical Reviews in Environmental Science and Technology, 26(1), 1–43. https://doi.org/10.1080/10643389609388485

Strickman, R. J., & Mitchell, C. P. J. (2017). Accumulation and translocation of methylmercury and inorganic mercury in Oryza sativa: An enriched isotope tracer study. Science of The Total Environment, 574, 1415–1423. https://doi.org/10.1016/j.scitotenv.2016.08.068

Sunda, W. G., & Huntsman, S. A. (1998). Processes regulating cellular metal accumulation and physiological effects: Phytoplankton as model systems. Science of The Total Environment, 219(2–3), 165–181. https://doi.org/10.1016/S0048-9697(98)00226-5

Sundseth, K., Pacyna, J., Pacyna, E., Pirrone, N., & Thorne, R. (2017). Global Sources and Pathways of Mercury in the Context of Human Health. International Journal of Environmental Research and Public Health, 14(1), 105. https://doi.org/10.3390/ijerph14010105

Tan, S. W., Meiller, J. C., & Mahaffey, K. R. (2009). The endocrine effects of mercury in humans and wildlife. Critical Reviews in Toxicology, 39(3), 228–269. https://doi.org/10.1080/10408440802233259

Tang, D., Shafer, M. M., Karner, D. A., & Armstrong, D. E. (2005). Response of nonprotein thiols to copper stress and extracellular release of glutathione in the diatom Thalassiosira weissflogii. Limnology and Oceanography, 50(2), 516–525. https://doi.org/10.4319/lo.2005.50.2.0516

Tel-or, E., Huflejt, M. E., & Packer, L. (1986). Hydroperoxide metabolism in cyanobacteria. Archives of Biochemistry and Biophysics, 246(1), 396–402. https://doi.org/10.1016/0003-9861(86)90485-6

The role of microorganisms in elemental mercury formation in natural waters. (n.d.). 13.

Tjerngren, I., Karlsson, T., Björn, E., & Skyllberg, U. (2012). Potential Hg methylation and MeHg demethylation rates related to the nutrient status of different boreal wetlands. Biogeochemistry, 108(1–3), 335–350. https://doi.org/10.1007/s10533-011-9603-1

Ugya, A. Y., Imam, T. S., Li, A., Ma, J., & Hua, X. (2020). Antioxidant response mechanism of freshwater microalgae species to reactive oxygen species production: A mini review. Chemistry and Ecology, 36(2), 174–193. https://doi.org/10.1080/02757540.2019.1688308

Ullrich, S. M., Tanton, T. W., & Abdrashitova, S. A. (2001). Mercury in the Aquatic Environment: A Review of Factors Affecting Methylation. Critical Reviews in Environmental Science and Technology, 31(3), 241–293. https://doi.org/10.1080/20016491089226

UNEP. (2018). Global mercury assessment 2018.

Val, J., Muñiz, S., Gomà, J., & Navarro, E. (2016). Influence of global change-related impacts on the mercury toxicity of freshwater algal communities. Science of The Total Environment, 540, 53–62. https://doi.org/10.1016/j.scitotenv.2015.05.042

Van Breusegem, F., Bailey-Serres, J., & Mittler, R. (2008). Unraveling the Tapestry of Networks Involving Reactive Oxygen Species in Plants. Plant Physiology, 147(3), 978–984. https://doi.org/10.1104/pp.108.122325

Vasconcelos, M. T. S. D., Leal, M. F. C., & van den Berg, C. M. G. (2002). Influence of the nature of the exudates released by different marine algae on the growth, trace metal uptake and exudation of Emiliania huxleyi in natural seawater. Marine Chemistry, 77(2–3), 187–210. https://doi.org/10.1016/S0304-4203(01)00087-1

Wang, K., Munson, K. M., Armstrong, D. A., Macdonald, R. W., & Wang, F. (2020). Determining seawater mercury methylation and demethylation rates by the seawater incubation approach: A critique. Marine Chemistry, 219, 103753. https://doi.org/10.1016/j.marchem.2020.103753

Whalin, L., Kim, E.-H., & Mason, R. (2007). Factors influencing the oxidation, reduction, methylation and demethylation of mercury species in coastal waters. Marine Chemistry, 107(3), 278–294. https://doi.org/10.1016/j.marchem.2007.04.002

Wiatrowski, H. A., Ward, P. M., & Barkay, T. (2006). Novel Reduction of Mercury(II) by Mercury-Sensitive Dissimilatory Metal Reducing Bacteria. Environmental Science & Technology, 40(21), 6690–6696. https://doi.org/10.1021/es061046g

Wu, Y., & Wang, W.-X. (2012). Thiol compounds induction kinetics in marine phytoplankton during and after mercury exposure. Journal of Hazardous Materials, 217–218, 271–278. https://doi.org/10.1016/j.jhazmat.2012.03.024

Wu, Y., & Wang, W.-X. (2013). Differential acclimation of a marine diatom to inorganic mercury and methylmercury exposure. Aquatic Toxicology, 138–139, 52–59. https://doi.org/10.1016/j.aquatox.2013.04.012

Wu, Y., & Wang, W.-X. (2014). Intracellular speciation and transformation of inorganic mercury in marine phytoplankton. Aquatic Toxicology, 148, 122–129. https://doi.org/10.1016/j.aquatox.2014.01.005

Wu, Y., Zeng, Y., Qu, J. Y., & Wang, W.-X. (2012). Mercury effects on Thalassiosira weissflogii: Applications of two-photon excitation chlorophyll fluorescence lifetime imaging and flow cytometry. Aquatic Toxicology, 110–111, 133–140. https://doi.org/10.1016/j.aquatox.2012.01.003

Xiao, R., & Zheng, Y. (2016). Overview of microalgal extracellular polymeric substances (EPS) and their applications. Biotechnology Advances, 34(7), 1225–1244. https://doi.org/10.1016/j.biotechadv.2016.08.004

Yorifuji, T., Tsuda, T., Inoue, S., Takao, S., & Harada, M. (2011). Long-term exposure to methylmercury and psychiatric symptoms in residents of Minamata, Japan. Environment International, 37(5), 907–913. https://doi.org/10.1016/j.envint.2011.03.008

Zhang, J., Wang, F., House, J. D., & Page, B. (2004). Thiols in wetland interstitial waters and their role in mercury and methylmercury speciation. Limnology and Oceanography, 49(6), 2276–2286. https://doi.org/10.4319/lo.2004.49.6.2276

Zhang, J. Y., Ni, W. M., Zhu, Y. M., & Pan, Y. D. (2013). Effects of different nitrogen species on sensitivity and photosynthetic stress of three common freshwater diatoms. Aquatic Ecology, 47(1), 25–35. https://doi.org/10.1007/s10452-012-9422-z

Zhang, L., Liang, X., Wang, Q., Zhang, Y., Yin, X., Lu, X., Pierce, E. M., & Gu, B. (2021). Isotope exchange between mercuric [Hg(II)] chloride and Hg(II) bound to minerals and thiolate ligands: Implications for enriched isotope tracer studies. Geochimica et Cosmochimica Acta, 292, 468–481. https://doi.org/10.1016/j.gca.2020.10.013

Zhang, L., Wright, L. P., & Blanchard, P. (2009). A review of current knowledge concerning dry deposition of atmospheric mercury. Atmospheric Environment, 43(37), 5853–5864. https://doi.org/10.1016/j.atmosenv.2009.08.019

Zhang, T., & Hsu-Kim, H. (2010). Photolytic degradation of methylmercury enhanced by binding to natural organic ligands. Nature Geoscience, 3(7), 473–476. https://doi.org/10.1038/ngeo892

Zhang, Y., Soerensen, A. L., Schartup, A. T., & Sunderland, E. M. (2020). A Global Model for Methylmercury Formation and Uptake at the Base of Marine Food Webs. Global Biogeochemical Cycles, 34(2). https://doi.org/10.1029/2019GB006348

Zhong, H., & Wang, W.-X. (2009). Controls of Dissolved Organic Matter and Chloride on Mercury Uptake by a Marine Diatom. Environmental Science & Technology, 43(23), 8998–9003. https://doi.org/10.1021/es901646k

Zhu, W., Song, Y., Adediran, G. A., Jiang, T., Reis, A. T., Pereira, E., Skyllberg, U., & Björn, E. (2018). Mercury transformations in resuspended contaminated sediment controlled by redox conditions, chemical speciation and sources of organic matter. Geochimica et Cosmochimica Acta, 220, 158–179. https://doi.org/10.1016/j.gca.2017.09.045